Universidad Politécnica de Valencia

Departamento de Biotecnología

Regulation of Lysosomal Degradation by Ca^{2+} And Ca^{2+}-Binding Proteins

Dissertation submitted
for obtaining the degree of Doctor in
Biotechnology
Valencia, 2013

by

GHITA GHISLAT

Supervisor

Dr. ERWIN KNECHT

Acknowledgements

First of all, I would like to thank my supervisor, Erwin Knecht, for giving me the opportunity to pursue a PhD in his lab and for the exhaustive scientific guidance throughout all these years. This work would not have been possible without the support of my PhD programme at the CIPF and funding provided by Fundació Marató TV3.

I would like to show my deepest gratitude to Ramon Serrano for his help in the initial steps of my enrolment in the UPV.

Great thanks to Asunción Montaner, not only for your technical support in the lab, but for much more.

To my past and present lab mates from I-11 and I-08 from whom I have learnt a lot and who made the lab life pleasant, thank you for your support along these years.

To my colleagues from other labs, I am glad to have known you, exchanged knowledge and shared great moments.

The daily work of this PhD has been made considerably easier through the labors of many people in the centre. Thank you all so much.

I am also very grateful to Rosario Rizzuto, for welcoming me to his lab in Padua, and to all his group members who have introduced me in the "world of calcium". It has been a pleasure to work with you. This stay would not have been possible without the EMBO and MEC fellowships.

Finally, a deep thanks to my family who has always been there unconditionally.

A maman, pour tout ton sacrifice

ABSTRACT

Macroautophagy and endocytosis are two evolutionarily conserved catabolic processes that comprise vesicle trafficking events for the clearance of the sequestered intracellular and extracellular cargo, respectively. Both start differently: formation of a new organelle, the autophagosome, that engulfs cytoplasmic substrates (macroautophagy) and internalization of extracellular material and plasma membrane components within endocytic vesicles (endocytosis). However, they end in the same compartment, the lysosome.

In a proteomic analysis of purified lysosomal membranes from mouse fibroblasts, three Ca^{2+}-dependent phospholipid-binding proteins were found to increase their levels on these membranes under amino acid starvation, a condition that activates macroautophagy. Prompted by this initial finding and given that Ca^{2+} is an important second messenger, we sought to gain insights into the involvement of Ca^{2+} in the regulation of macroautophagy by amino acid starvation and the role of Ca^{2+}-binding proteins in macroautophagy.

We describe a Ca^{2+}-dependent signalling pathway that triggers the formation of autophagosomes. Thus, withdrawal of essential amino acids leads to an increase in cytosolic Ca^{2+}, arising from both extracellular medium and intracellular stores, which induces, *via* Ca^{2+}/calmodulin-dependent kinase kinase-β, the activation of adenosine monophosphate-activated protein kinase and the inhibition of the mammalian target of rapamycin complex 1. In the final step of this pathway, UNC-51-like kinase, a mammalian autophagy-initiating kinase, is activated and this leads to the formation of autophagosomes.

Annexin A1, annexin A5 and copine 1 are the three Ca^{2+}-dependent phospholipid binding proteins whose levels on lysosomal membranes increased under amino acid starvation in the proteomic analysis. Biochemical and immunofluorescence methods show that starvation causes the Ca^{2+}-dependent translocation of annexin A5 from Golgi complex to

lysosomal membranes and that it also induces the accumulation of annexin A1 and copine 1 in this localization. Using overexpression and silencing experiments, we found that all three proteins induce autophagosome fusion with lysosomes and that copine 1, and to a lesser extent annexin A1, enhance the effect of annexin A5 in this process. Moreover, annexin A5 inhibits endocytosis whereas copine 1 induces it. Thus, annexin A1, annexin A5, and copine 1 emerge as regulators of autophagosome maturation and the last two have opposite roles in endocytic trafficking.

Overall, our results highlight that the activation of autophagosome formation by the starvation of amino acids follows in part a Ca^{2+}-dependent signalling pathway and that this condition also activates the maturation of autophagosomes to autolysosomes through Ca^{2+}-binding proteins.

La macroautofagia y la endocitosis son dos procesos catabólicos conservados evolutivamente en los que, mediante un tráfico vesicular, se degrada el material secuestrado, cuyo origen es intra- y extracelular, respectivamente. Ambos procesos comienzan de manera diferente: mediante la formación de un nuevo orgánulo, el autofagosoma, que secuestra material citoplásmico (macroautofagia), o mediante la internalización de material extracelular y de algunos componentes de la membrana plasmática a través de vesículas endocíticas (endocitosis). Sin embargo, los dos terminan en el mismo compartimiento: el lisosoma.

En un análisis proteómico de membranas lisosomales, purificadas a partir de fibroblastos de ratón, identificamos tres proteínas, que se unen a fosfolípidos de una manera dependiente de calcio, y cuyos niveles en la membrana lisosomal aumentaban en ausencia de aminoácidos, una condición que activa la macroautofagia. Basándonos en esos resultados iniciales, y teniendo en cuenta que el calcio es un segundo mensajero muy importante, decidimos: en primer lugar, abordar el papel del calcio en la activación de la autofagia producida por el ayuno de aminoácidos, y, en segundo lugar, investigar el papel de esas tres proteínas en el mecanismo autofágico.

Como resultado de estos estudios, describimos en primer lugar una nueva vía de señalización dependiente de calcio que activa la formación de autofagosomas por los aminoácidos. Concretamente, hemos encontrado que el ayuno de aminoácidos esenciales produce un aumento en el calcio citosólico, procedente tanto del medio extracelular como de almacenes intracelulares. Como consecuencia de esto, la calmodulina quinasa quinasa-β activa a AMPK y a mTORC1. En la última etapa de esta vía, ULK1, una quinasa responsable de la iniciación de la autofagia, se activa para contribuir a la formación de los autofagosomas.

Las tres proteínas identificadas en el estudio proteómico y cuyos niveles en las membranas lisosomales aumentan en ausencia de

aminoácidos son la anexina A1, la anexina A5 y la copina 1. Empleando métodos bioquímicos y de inmunofluorescencia observamos que el ayuno de aminoácidos causa la translocación de la anexina A5 desde el complejo de Golgi hasta las membranas lisosomales, donde también se acumulan la anexina A1 y la copina 1. Asimismo, demostramos por sobre-expresión y silenciamiento de esas tres proteínas, que las tres inducen la fusión de autofagosomas con lisosomas y que la copina 1, y en menor medida la anexina A1, aumentan el efecto individual de la anexina A5. Finalmente, la anexina A5 inhibe la endocitosis mientras que copina 1 la induce.

En resumen, nuestros resultados ponen de manifiesto que la activación de la formación de autofagosomas por el ayuno de aminoácidos es debida, al menos en parte, a una vía de señalización dependiente de Ca^{2+} y que esta condición también conlleva la aceleración de la maduración de los autofagosomas a autolisosomas a través de proteínas que unen el Ca^{2+} como las anexinas A1 y A5 y la copina 1.

La macroautofagia i la endocitosi son dos processos catabòlics conservats evolutivament en els que, mitjançant processos de tràfic vesicular, es degrada el material segrestrat, d'origen intracel·lular i extracel·lular, respectivament. Ambdós comencen de manera diferent: *via* la formació d'un nou orgànul, l'autofagosoma, que segrestra material citoplàsmic (macroautofagia) o *via* d'internalització de material extracel·lular i d'alguns components de la membrana plasmàtica a traves de vesícules endocítiques (endocitosi). Tanmateix, els dos processos terminen en el mateix compartiment: el lisosoma.

En una anàlisi proteòmica de membranes lisosomals, purificades a partir de fibroblastos de ratolí, identifiquem tres proteïnes, que s'uneixen a fosfolípids d'una manera dependent de calci, i els nivells de les qual en la membrana lisosomal augmentaven en absència d'aminoàcids, una condició que activa la macroautofagia. Basant-nos en aquests resultats preliminars, i tenint en compte que el calci es un segon missatger molt important, decidim: en primer lloc, abordar el paper del calci en l'activació de la macroautofagia produïda pel dejú d'aminoàcids, i, en segon lloc, investigar el paper d'aquestes tres proteïnes en el mecanisme autofagic.

Com a resultat d'aquests estudis, descrivim en primer lloc una nova via de senyalització depenent del calci que activa la formació d'autofagosomes pels aminoàcids. Concretament, hem trobat que el dejú d'aminoàcids essencials incrementa el nivell del calci citosòlic, provenint tant del medi extracel·lular com de magatzems intracel·lulars. Com a conseqüencia, la calmodulina quinasa quinasa-β activa a AMPK y a mTORC1. En l'última etapa d'aquesta via, ULK1, una quinasa responsable de la iniciació de l'autofagia, s'activa per a contribuir a la formació dels autofagosomes.

Les tres proteïnes identificades en l'estudi de proteomica i els nivells de les qual en les membranes lisosomals augmenten en absència d'aminoàcids son la anexina A1, la anexina A5 i la copina 1. Emprant

mètodes bioquímics i d'immunofluorescència observem que el dejú d'aminoàcids causa la translocació de la anexina A5 del complex de Golgi a les membranes lisosomals, a on també migren la anexina A1 i la copina 1. Així mateix, demostrem per sobreexpressió i silenciament d'aquestes proteïnes, que les tres indueixen la fusió d'autofagosomes amb lisosomes i que la copina 1, i en menor mesura la anexina A1, augmenten l'efecte de la anexina A5 en aquest procés. Finalment, la anexina A5 inhibeix l'endocitosi mentre que la copina 1 la indueix.

En resum, els nostres resultats posen en manifest que l'activació de la formació d'autofagosomes pel deju d'aminoàcids es deguda, al menys en part, a una via de senyalització depenent de Ca^{2+} i que aquesta condició també implica l¡acceleració de la maduració dels autofagosomes a autolisosomes a traves de proteïnes que s'uneixen al Ca^{2+} com les anexines A1 i A5 i la copina 1.

ABBREVIATIONS

2-APB	2-aminoethoxydiphenyl borate
2D-DIGE	two-Dimensional DIfferential Gel Electrophoresis
α-SNAP	α-soluble N-ethylmaleimide-sensitive factor attachment protein
AA	KH provided with amino acids (2x)
AAA ATPase SKD	Vacuolar protein sorting 4/suppressor of K^+ transport growth defect 1
ALG-2	Apoptosis-linked gene-2
AMPK	AMP-activated protein kinase
AKT/PKB	Protein kinase B
AMBRA	Activating molecule in BECLIN 1-regulated
ATG	Autophagy-related genes
Av_i	Early autophagic vacuoles
Av_d	late autophagic vacuoles
BAIAP2	Brain specific angiogenesis inhibitor 1-associated protein 2
BAPTA-AM	1,2-bis(o-aminophenoxy)ethane-*N,N,N',N'*-tetraacetic acid, acetoxymethyl ester
BCECF-AM	2',7'-*bis*-(carboxyethyl)-5-(and-6)-carboxyfluorescein, acetoxymethyl ester
BCL-2	B-cell lymphoma/leukemia 2
BNIP3	Adenovirus E1B 19-kDa-interacting protein 3
BSA	Bovine serum albumin
CAMKI	Ca^{2+}/CALMODULIN-dependent protein kinase I
CAMKII	Ca^{2+}/CALMODULIN-dependent kinase II
CAMKK-α	Ca^{2+}/CALMODULIN-dependent kinase kinase-α
CAMKK-β	Ca^{2+}/CALMODULIN-dependent kinase kinase-β
COXII	Mitochondrial complex II (succinate-ubiquinol oxidoreductase)
DAPK	Death-associated protein kinase
DMEM	Dulbecco's modified Eagle's medium
dNTP	Deoxyribonucleotide triphosphate
DTT	Dithiothreitol

EDTA	Ethylenediaminetetraacetic acid
EEA1	Early endosome antigen 1
EF1 α	the translation elongation factor 1α
EGF	Epidermal growth factor
eGFP	Enhanced Green Fluorescent Protein
EGFR	EGF receptor
EGTA	Ethylene glycol tetra acetic acid
ER	Endoplasmic reticulum
ERK	Extracellular signalling-regulated kinase
FACS	Fluorescence-activated cell sorting
FBS	Foetal bovine serum
FCS	Foetal calf serum
FIP 200	Focal adhesion kinase family interacing protein of 200 kDa
FITC	Fluorescein isothiocyanate
GAIP	Gα-interacting protein
GAPDH	Glyceraldehyde-3-phosphate dehydrogenase
GβL	G protein β-subunit-like protein
GTPase	Rag guanosine triphosphatase
Hepes	4-(2-hydroxyethyl)-1-piperazineethanesulfonic acid
HRS	Hepatocyte responsive serum phosphoprotein
IAA	KH provided with insulin (0.1 μM) and amino acids (2x)
IDH	NADP-dependent isocitrate dehydrogenase
IMPases	Inositol monophosphatases
IP	Inositol 4 monophosphate
IP_2	Inositol 4,5 bisphosphate
IP_3	Inositol 1,4,5-trisphosphate
IP_3R	IP_3 receptor
IRS1/2	Insulin receptor substrate 1 and 2
KH	Krebs-Henseleit medium

Lamp1	Lysosomal-associated membrane protein 1
LB	Lurias Broth
LBPA	Lysobisphosphatidic acid
LBT	Lactulose breath test
LC3B	Microtubule-associated protein 1 Light Chain 3 β
Leup	Leupeptin
Li	Llithium
LRS	Leucyl-tRNA synthetase
MDH	NADP-dependent malate dehydrogenase
MEFs	Mouse embryonic fibroblasts
MEK	MAP kinase kinase
MES	2-(N-Morpholino) ethanesulfonic acid
MEM	Minimum essential medium
MS	Mass spectroscopy
mTOR	Mammalian target of rapamycin
mTORC1	Mammalian target of rapamycin complex 1
mTORC2	Mammalian target of rapamycin complex 2
MVB	Multivesicular bodies
NS	No significant difference
p70S6K	ribosomal protein S6 kinase 1
PBS	Phosphate buffered saline
PCR	Polymerase chain reaction
PDH	Pyruvate dehydrogenase
PDP	PDH phosphatase
PDK1	phosphoinositide-dependent kinase 1
PE	Phosphatidylethanolamine
PI_3K	Class I phosphatidylinositol 3-kinase
PI_3KI	Class III phosphatidylinositol 3-kinase complex I
PI_3KII	Class III phosphatidylinositol 3-kinase complex II
PIP_2	Phosphatidylinositol 4,5-bisphosphate
PKC	Protein Kinase C

PLC	Phospholipase C
PRAS40	Proline-rich AKT substrate of 40 kDa
PROTOR	Protein observed with RICTOR
PTEN	Phosphatase and tensin homolog
RAPTOR	Regulatory associated protein of mTOR
RFP	Red Fluorescent Protein
RICTOR	Rapamycin-insensitive companion of mTOR
SDS	Sodium dodecyl sulfate
SEM	Standard error of the mean
SERCA	Sarco/Endoplasmic Reticulum Ca^{2+}-ATPase
SIN1	SAPK-interacting protein 1
siRNAs	small interfering RNAs
SNARE	Soluble NSF attachment protein receptor
TBS	Tris-buffered saline
TCA	Trichloroacetic acid
TPC	Two-pore channel
Tris	Tis(hydroxymethyl)aminomethane
TRPM2	Transient receptor potential cation channel subfamily M member 2
TRPML1	Transient receptor potential cation channel, mucolipin subfamily 1
TRPML2	Transient receptor potential cation channel, mucolipin subfamily 2
TRPML3	Transient receptor potential cation channel, mucolipin subfamily 3
TSC1/2	Tuberous sclerosis complex
ULK1	UNC-51-like kinase 1
UVRAG	Ultraviolet irradiation resistance-associated gene, VPS38
V-ATPase	Vacuolar H^+-ATPase
WT	Wild type

1. INTRODUCTION

1. Regulation of autophagy by insulin and amino acids

Lysosomes are acidic organelles that constitute the main catabolic compartment in eukaryotic cells (Saftig and Klumperman, 2009). The first evidences for the existence of lysosomes date back to 1907, when Élie Metchnikoff (1908 Nobel Prize in Physiology or Medicine, along with Paul Ehrlich) found that particles fed to mammalian phagocytes were digested through acidic reactions occurring in phagosomes (Tauber, 2003). It was until about 1950 that this digestion model was extended to non-phagocytic cells, when Christian de Duve (1974 Nobel Prize in Physiology or Medicine, together with Albert Claude and George E. Palade) found acid phosphatases and other acid hydrolases surrounded by a membrane (De Duve *et al*., 1955). This new organelle, considered since then as a repository of acid hydrolases, was termed by De Duve "lysosome" due to its "lytic" role in the cell. Later, observations by electron microscopy of novel double membrane vacuoles holding cytoplasmic components in different stages of degradation, led to the discovery of the lysosomal degradative pathway coined by De Duve with the term "autophagy" (De Duve and Wattiaux, 1966). This cellular self-digestion process hitherto remains the most prominent for lysosomal degradation, despite that lysosomes degrade cargo collected also from other pathways (endocytosis, crinophagy and other types of autophagy) (Knecht *et al*., 2009). From the 60s until the 80s of the past century, extensive morphological analysis of autophagy allowed the characterization of the successive steps of autophagy. First, the phagophore, a sequestering lipid bilayer, is formed and then expands into an autophagosome that fuses usually first with endocytic vesicles to form amphisomes, and next with lysosomes to form autolysosomes (Fig. 1). Later, a series of studies using autophagy mutants in *Saccharomyces cerevisiae* by different groups allowed the identification of the main proteins involved in autophagic degradation (reviewed in (Mizushima *et al.*, 2011a)).

These efforts culminated in the identification of new genes, the so-called ATG (AuTophaGy-related) genes (Klionsky, 2012), essential for the autophagic machinery. Consequently, autophagy gained prominence in the field of intracellular protein degradation and its initial concept was revolutionized by increasing breakthroughs.

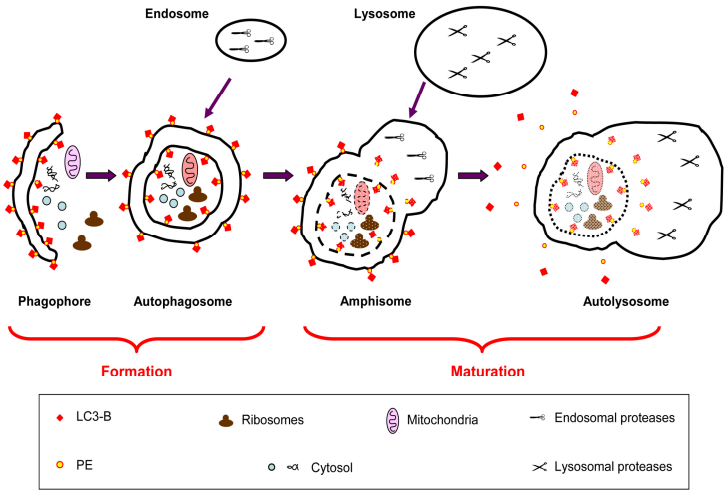

Figure 1. The successive stages of the autophagic degradation pathway. First, a double lipid bilayer, called phagophore, decorated among other proteins with microtubule-associated protein 1 light chain 3 β (LC3-B) that is bound to this membrane through phosphatidylethanolamine (PE), sequesters cytosolic constituents, including ribosomes and mitochondria. Then, this initial isolation membrane expands and closes into an autophagosome. Next, this organelle fuses, usually first with endocytic structures to generate the amphisome, where a slight proteolytic capacity is observed, and then with lysosomes to form autolysosomes, where the final degradation of autophagic cargo occurs. Therefore, this process can be divided into two main steps: formation and maturation of autophagosomes.

Autophagy is physiologically regulated. Whereas in yeast, nutrient starvation, particularly of nitrogen, is the most potent stimulus of autophagy, in mammalian cells both nutritional and hormonal factors regulate it. In fact, early studies showed that autophagy is induced by glucagon and glucose, and is inhibited by vitamins, osmotic stress, various growth factors, insulin and some amino acids (Knecht *et al*., 2009). Amino acids and insulin are the major nutritional and hormonal regulators of autophagy, respectively

(Lavallard *et al*., 2012). Whereas the signalling pathway by which insulin restrains autophagy is well-known, the intracellular amino acid-sensing to control autophagy remains less understood. However, it is well-established now that both regulators converge into the serine-threonine kinase mammalian target of rapamycin (mTOR) to inhibit autophagy.

The kinase mTOR exists in two distinct complexes: the rapamycin-sensitive mTORC1 and the less rapamycin-sensitive mTORC2. In addition to mTOR, the complex mTORC1 contains other proteins: regulatory associated protein of mTOR (RAPTOR), G protein β-subunit-like protein (GβL) and the inhibitory protein proline-rich AKT substrate of 40 kDa (PRAS40). It constitutes the primary complex responsible for assessing the presence of nutrients and hormonal growth factors to control autophagy. The active mTORC1 complex is well-known to inhibit autophagy through its interaction with the UNC-51-like kinase 1 (ULK1) (the homolog of the yeast Atg1) and its inactivation by phosphorylation. The mTORC2 complex, by contrast, is not considered directly involved in autophagy regulation (Ravikumar *et al*., 2010b), except in isolated reports that describe a partial implication (Gurusamy *et al*., 2010). This complex comprises, apart from mTOR, the following proteins: rapamycin-insensitive companion of mTOR (RICTOR), GβL, SAPK-interacting protein 1 (SIN1) and the protein observed with RICTOR (PROTOR).

Here below, we will describe the different signalling pathways triggered by insulin and amino acids for autophagy inhibition by mTORC1 activation.

1.1. Regulation of autophagy by insulin

Insulin is an anabolic hormone that once bound to its tyrosine kinase receptor produces its auto-phosphorylation (see Fig. 2). This leads to the phosphorylation of insulin receptor substrate 1 and 2 (IRS1/2). Class I phosphatidylinositol 3-kinase (PI_3K) is then recruited and generates

phosphatidylinositol 3,4,5-trisphosphate (PIP_3) from phosphatidylinositol 4,5-bisphosphate (PIP_2). In contrast, the phosphatase and tensin homolog (PTEN) inhibits the accumulation of PIP_3 by hydrolysing it to PIP_2, inhibiting in this way the downstream pathway induced by insulin. The availability of PIP_3 at the plasma membrane leads to the activation of protein kinase B (AKT/PKB) *via* phosphorylation by phosphoinositide-dependent kinase 1 (PDK1). Subsequently, AKT/PKB prevents the formation of the tuberous sclerosis complex (TSC1/2) by phosphorylating the TSC2 protein. This heterodimeric complex induces the GTPase activity of RHEB, a Ras-related GTPase, which acts in its GTP-bound form as an activator of mTORC1, a well-known inhibitor of autophagy (Wang and Levine, 2010). Thus, the inhibition of the TSC1/2 complex formation by the insulin-AKT/PKB pathway restrains autophagy *via* mTORC1.

1.2. Regulation of autophagy by amino acids

Although amino acids are the best known nutritional sensors for the stimulation of mTORC1 signalling in autophagy inhibition, the mechanisms involved in this regulation are not yet fully elucidated. Among the various amino acids, the branched ones, such as leucine, are especially active in stimulating mTORC1 and inhibiting autophagy in many cell types (van Sluijters *et al*., 2000). However, the regulatory amino acids of autophagy may vary depending on the cell type (Esteban *et al*., 2007). Their sensing is proposed to be intracellular rather than extracellular (Kim and Guan, 2011). However, an amino acid receptor on the plasma membrane was recently reported (Wauson *et al*., 2012). In contrast to insulin, whose receptor is well-characterized, amino acid sensors were only very recently recognized. Leucyl-tRNA synthetase (LRS) was shown to be an amino acid sensor in mammals (Han *et al*., 2012), and in yeast (Bonfils *et al*., 2012). Another candidate receptor of amino acids is the antiporter that exports glutamine while importing leucine and other branched amino acids (Nicklin *et al*., 2009). Moreover, glutamate dehydrogenase was also proposed to act as an

amino acid sensor for the inhibition of autophagy, since it is activated by leucine, which leads to the activation of mTORC1 (Meijer and Codogno, 2009).

A well-characterized mediator of amino acid availability to mTORC1 activation is the Rag GTPase. In fact, the proposed amino acid sensor LRS activates mTORC1 by activating Rag in a leucine-dependent manner (Han *et al*., 2012) (see Fig. 2). Rag is a heterodimer of RagA/B-GTP with RagC/D-GDP localized in the vicinity of lysosomes. In the presence of amino acids, this heterodimeric complex binds to mTORC1 through RAPTOR in a perilysosomal area that contains the mTORC1 activator RHEB (Sancak *et al*., 2010). Furthermore, ATP hydrolysis by the vacuolar H^+-ATPase (V-ATPase), responsible of proton pumping inside lysosomes, appears to be crucial for the Rag GTPases-mediated activation of mTORC1 by the amino acids present inside the lysosomal lumen (Zoncu *et al*., 2011). In this mechanism, lysosome-derived amino acids are controlled by the lysosomal proton-assisted amino acid transporter PAT1, responsible for the efflux of amino acids from the lysosomes. The activation of mTORC1 by amino acids provided by lysosomes may seem contradictory with the fact that when lysosomes provide amino acids to the cytosol (starvation) autophagy is induced. However, mTORC1 signalling was recently shown to be inhibited during initiation of autophagy, but reactivated by a more prolonged starvation and requires the degradation of autolysosomal products (Yu *et al*., 2010). In summary, while LRS senses cytosolic amino acids, V-ATPase senses the intralysosomal pool of amino acids, and both recruit mTORC1 to the lysosomal surface and activate it through Rag GTPases. However, the precise localization of mTORC1 at the lysosomal membrane and its dynamics are not yet entirely deciphered and remain currently a matter of active investigation.

The amino acid-mediated stimulation of mTORC1 was also proposed to occur *via* the class III PI_3K (Byfield *et al*., 2005; Nobukuni *et al*., 2005).

However, the involvement of class III PI_3K in autophagy inhibition by amino acids is not clear, since this enzyme is also implicated in the initiation of autophagy in an mTOR-independent way. Also, class III PI_3K was recently reported to be activated by AMPK for autophagy induction (Kim *et al*., 2013). Thus, class III PI_3K is presumably part of different protein complexes with distinct functions (Meijer and Codogno, 2009).

Whereas mTORC1 activation is required for amino acid-mediated inhibition of autophagy, amino acid starvation activates autophagy through several mechanisms, including the activation of the Raf kinase signalling pathway (Shaw and Cantley, 2006) (see Fig. 2).

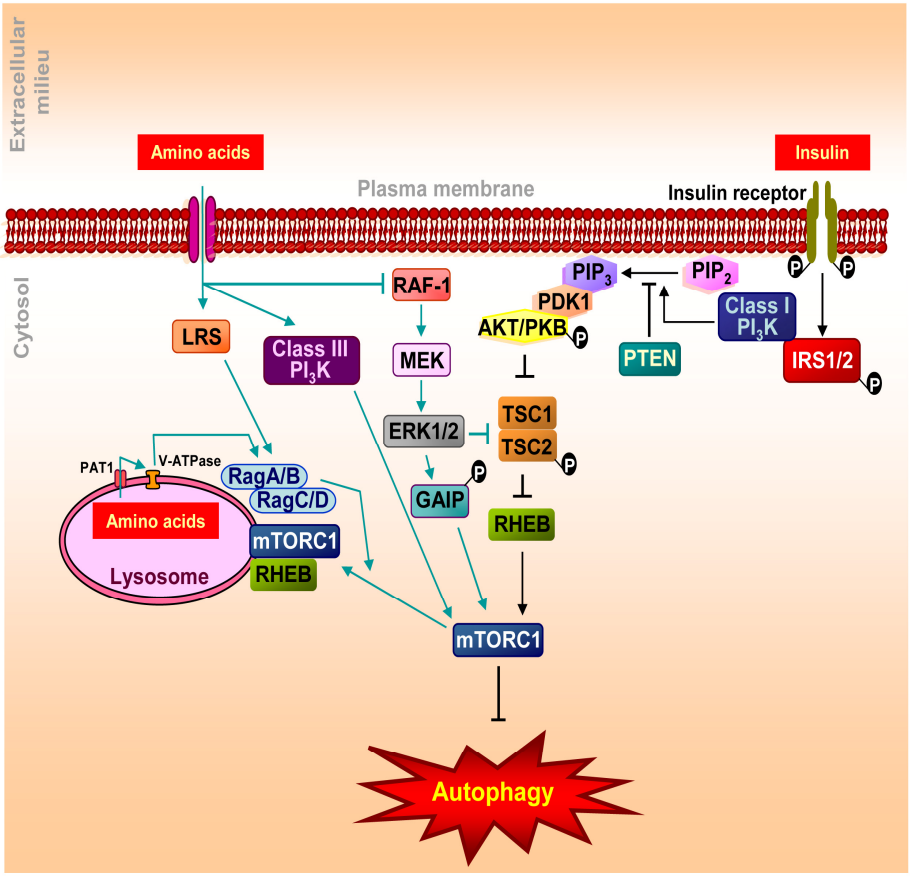

Figure 2. Main signalling pathways regulating autophagy in response to insulin and amino acids. Insulin activates class I PI_3K and AKT/PKB, which inhibits the TSC1/2 complex and activates mTORC1 by RHEB and consequently restrains autophagy. Amino acids inhibit autophagy by activating mTORC1 through class III PI_3K and Rag complex. Withdrawal of amino acids activates extracellular signalling-regulated kinase (ERK) 1/2 through RAF-1 and MEK, leading to a high phosphorylation/activation of the regulator of cytoplasmic heterotrimeric Gi3 protein the Gα-interacting protein (GAIP), which increases autophagic turnover. However, inhibition of ERK 1/2 by amino acids is controversial (Settembre *et al*., 2012). See text for further details.

In general, no consensus exists for the mechanisms by which amino acid availability and starvation regulate autophagy. It is probable that their impact on this lysosomal process is the result of various signalling cascades that are hitherto only partially characterized.

In a preliminary proteomic study, amino acid starvation raised in lysosomal membranes from mouse fibroblasts the levels of a group of Ca^{2+}-binding proteins (see Objectives and Chapter 1 of Results). On the basis of this initial result and given that Ca^{2+} is an important second messenger for several physiological cell functions (Missiaen *et al*., 2000a), this doctoral thesis has been focused on the involvement of Ca^{2+} and the identified Ca^{2+}-binding proteins in autophagy (and also in endocytosis, another important lysosomal degradative process). Thus, the second part of this Introduction is centred on the outcomes from the last years on the involvement of Ca^{2+} on autophagy and endocytosis, whereas the last part is a general overview of the annexin and copine families.

2. Ca^{2+}-sensor proteins in the autophagic and endocytic traffic

Published in Ghislat G, Knecht E (2012). Ca^{2+}-sensor proteins in the autophagic and endocytic traffic. Curr Protein Pept Sci (in press).

As mentioned before, lysosomes are ubiquitous organelles that degrade material sequestered by two main dynamic processes: autophagy and endocytosis. Both processes comprise a complex traffic of vesicles that finally ends with the clearance of their contents by the lysosomal acid hydrolases.

Autophagy is an important pathway responsible for the turnover of intracellular macromolecules and even whole organelles (Knecht *et al*., 2009). At least three different forms of autophagy coexist in the cell (Fig. 3): microautophagy, chaperone-mediated autophagy and macroautophagy. Microautophagy involves the internalization of cytosolic components by various modifications of the lysosomal membrane (Mijaljica *et al*., 2011). It has been mainly characterized in yeast and it is still poorly understood in eukaryotic cells. Chaperone-mediated autophagy is a more selective form of autophagy by which specific amino acid motifs in cytosolic proteins (KFERQ-like) are recognized by a chaperone (HSC70) that binds to isoform A of lysosome-associated membrane protein type 2. This allows, with the help of other chaperones at the lysosome, such as HSP90 and the lysosomal isoform of HSC70, the unfolding and subsequent translocation of the specific substrate proteins into the lysosomal lumen (Cuervo, 2010a). Finally, macroautophagy is the most prominent and best studied of these three forms and hence it will be simply called autophagy. It starts with the formation of a cup-shaped vesicle, called phagophore, whose origin is still a matter of conjecture, that engulfs cytoplasmic material and closes, thus generating a double membrane vacuole, the autophagosome (Levine and Klionsky, 2004). Several compartments, including mitochondria (Hailey *et al*., 2010; Mari *et al*., 2010), plasma membrane (Ravikumar *et al*., 2010a),

Golgi complex (Yamamoto *et al*., 2012) and endosomes (Longatti and Tooze, 2012) appear to contribute proteins and lipids to the phagophore (Cuervo, 2010b), but the most accepted origin of this structure is the endoplasmic reticulum (ER) (Axe *et al*., 2008; Hayashi-Nishino *et al*., 2009; Yla-Anttila *et al*., 2009). Once formed, the autophagosome undergoes a maturation process by fusing with late endosomes/lysosomes to acquire proteolytic competence (Noda *et al*., 2009). Analysis of autophagy in yeast led to the identification of a series of autophagy-related genes (*ATG*s), most of them essential for autophagosome formation and whose mammalian homologues are well-identified (Klionsky *et al*., 2003). Many reviews have already discussed the functions of these genes (e.g. (Klionsky *et al.*, 2003; Knecht *et al.*, 2009; Mizushima *et al.*, 2011b)), and here we will only provide a brief summary of those mentioned here. They include ULK1 (whose yeast homologue is ATG1), ATG13, FIP200 (ATG17) and ATG101, all of which form a complex involved in the initiation of the phagophore, and WIPI1 (ATG18), which is involved in the nucleation of the autophagosomal membrane. In addition, its elongation is controlled by two complexes. The first is formed by the ATG7-mediated binding of ATG12 and ATG5, which later oligomerize with ATG16L (ATG16). The second is formed by BECLIN 1 (ATG6), PI_3K class III (VPS34), p150 (VPS15) and ATG14L (ATG14). BECLIN 1 is a tumour suppressor that under nutrient rich conditions is bound to protein B-cell lymphoma/leukemia 2 (BCL-2). Under starvation, JNK1 phosphorylates BCL-2, from which BECLIN 1 dissociates and interacts with the above mentioned second complex involved in the elongation of the autophagosomal membrane. Other BECLIN 1 partners appear to inhibit, such as BCL-XL, or to activate, such as Activating molecule in BECLIN 1-regulated autophagy (AMBRA), autophagosome formation, and others, such as Bif1 and Ultraviolet irradiation resistance-associated gene, VPS38 (UVRAG), induce the fusion of autophagosomes with lysosomes. Finally, we should also mention here LC3 (ATG8). Its cytosolic form (LC3-I) can covalently bind to phosphatidylethanolamine

under a series of reactions catalyzed by ATG4, ATG7 and ATG3, forming LC3-II that associates to the autophagosomal membrane.

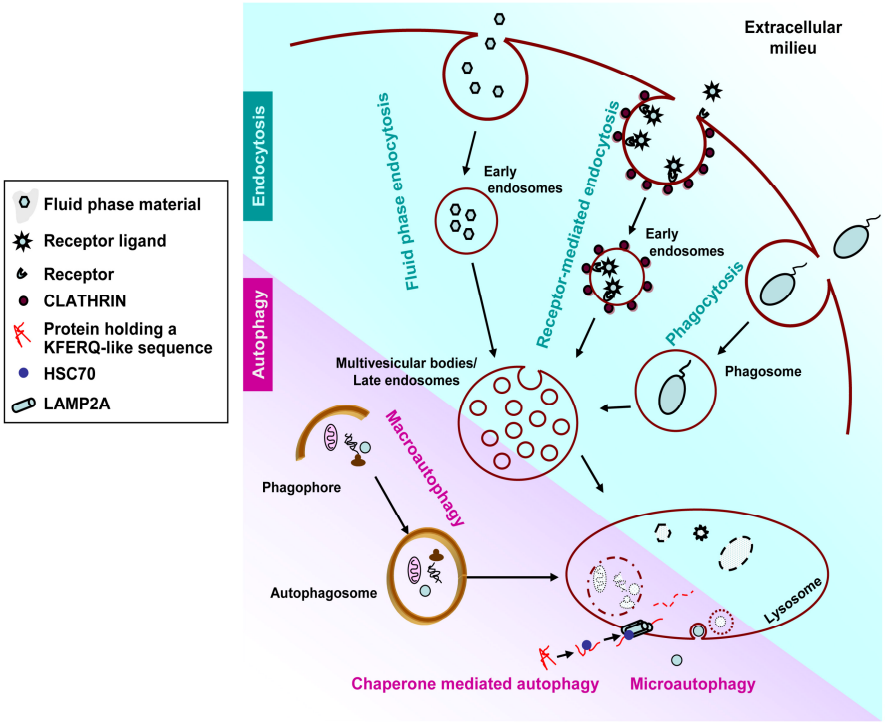

Figure 3. Main endocytic and autophagic pathways. Upper part depicts from left to right: i) fluid phase endocytic uptake of extracellular fluid containing small molecules; ii) receptor-mediated endocytic uptake of specific ligands, generally within CLATHRIN-coated vesicles; and iii) phagocytic uptake of solid particles, such as bacteria. Lower part represents from left to right: i) macroautophagy of cytosolic components including organelles; ii) chaperone-mediated autophagy of proteins harbouring KFERQ-related sequences; iii) microautophagy of cytosolic material. See text for further details.

Endocytosis is the process whereby extracellular and plasma membrane materials are internalized and transported to lysosomes by vesicles (Doherty and McMahon, 2009). During this endocytic traffic, early endosomes undergo maturation and budding/scission events, thereby generating larger and more acidic multivesicular bodies/late endosomes, which are subsequently delivered to lysosomes for the final degradation of the endocytosed cargo (see Fig. 3). One of the best-characterized forms of

endocytosis is receptor-mediated endocytosis, responsible for the selective internalization of specific ligands recognized by their receptors at the cell surface (Doherty and McMahon, 2009). Phagocytosis and fluid phase endocytosis are other forms of endocytosis in which structures and molecules of variable size are engulfed by the cell (Swanson, 2008). Different proteins are involved in all these endocytic processes that together coordinate the specific and non-specific uptake of extracellular material into the cell and their subsequent transport to lysosomes. Therefore, and although their early steps are differently governed, autophagy and endocytosis can converge at a pre-lysosomal step or at the lysosomes to form hybrid organelles called, respectively, amphisomes or amphilysosomes (Doherty and McMahon, 2009; Fader and Colombo, 2009).

Ca^{2+} is a second messenger that is involved in the regulation of several physiological cell functions, such as gene transcription, metabolism, secretion and apoptosis, and perturbations in its homeostasis have been implicated in various pathological processes, such as disorders of the nervous system, cardiac and vascular pathologies and *diabetes mellitus* (Missiaen *et al*., 2000b; Berridge *et al*., 2003). Insights from the last years have deciphered some mechanisms that link Ca^{2+} with signalling and trafficking steps related with autophagy and endocytosis, but several details still remain unknown. In the next paragraphs, we will review, consecutively, the role of Ca^{2+} in the regulation of: i) autophagy, ii) endocytosis, and iii) their final convergence into lysosomes for the degradation of the material taken up by these two processes.

2.1. Involvement of Ca^{2+} in the regulation of autophagy

2.1.1. Cytosolic Ca^{2+} signalling in autophagy

Direct evidence that cytosolic Ca^{2+} signalling activates autophagy was provided in a study performed in MCF-7, NIH3T3 and HeLa cells, where increasing cytosolic Ca^{2+} levels with pharmacological agents, such as

ionomycin, induced autophagy in a BECLIN 1- and ATG7-dependent manner (Hoyer-Hansen *et al*., 2007) (see Fig. 4A). Autophagy was activated by a signalling pathway, involving Ca^{2+}/CALMODULIN-dependent kinase kinase-β (CAMKK-β) and AMP-activated protein kinase (AMPK), which inhibits the serine-threonine kinase mTORC1. This inhibition of mTORC1 can occur directly *via* phosphorylation of raptor (Gwinn *et al.*, 2008) or indirectly *via* TSC1/2 and its substrate, the Ras-family GTP-binding protein RHEB, which directly regulates the activity of mTORC1 (Sarbassov *et al*., 2005). This was also confirmed in HEK293 cells transfected with amyloid-β and using resveratrol, a naturally existing polyphenol that increases cytosolic Ca^{2+}. Under these conditions, the CAMKK-β-AMPK signalling pathway becomes activated and inhibits mTORC1, leading to the autophagic degradation of amyloid-β (Vingtdeux *et al*., 2010). Moreover, activation of autophagy by resveratrol has been reported to occur in MCF-7 cells by a non conventional mechanism that is independent from canonical BECLIN 1 (Scarlatti *et al*., 2008).

However, it has been reported that Ca^{2+} can also induce autophagy *via* WIPI1 by an alternative pathway downstream of CAMKK-β that activates Ca^{2+}/CALMODULIN-dependent protein kinase I (CAMKI) and bypasses AMPK (Pfisterer *et al*., 2011). Further support for the involvement of cytosolic Ca^{2+} in the induction of autophagy was derived from transfection experiments with calcium-phosphate precipitates in which it was observed that these precipitates activate autophagy in a BECLIN 1- and ATG5-dependent way (Gao *et al*., 2008).

However, other results are in conflict with those described above, since they support an inhibitory effect of cytosolic Ca^{2+} on autophagy (see Fig. 4B). Thus, using Ca^{2+} channel antagonists, such as verapamil, which inhibit a family of Ca^{2+}-activated cystein proteases, the CALPAINs, autophagy was activated by a pathway independent of mTOR (Williams *et al*., 2008), whereas Ca^{2+} channel agonists inhibit autophagy *via* the

cleavage of ATG5 by CALPAINs, which in turn decreases the formation of the ATG12-ATG5 conjugate that is indispensable for the formation of autophagosomes (Xia *et al.*, 2010).

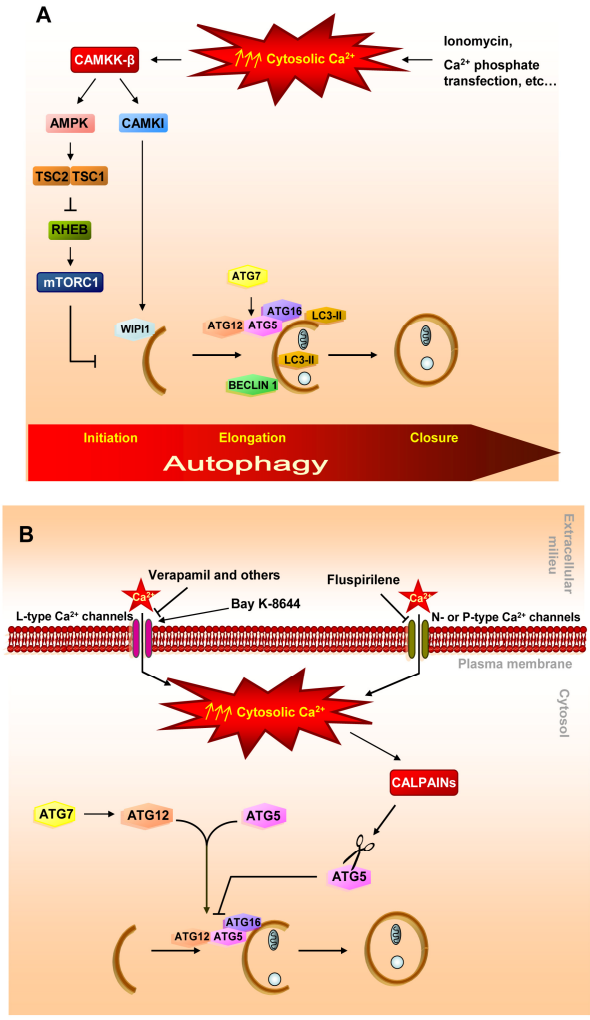

Figure 4. Cytosolic Ca^{2+} effects on autophagy. (**A**) Cytosolic Ca^{2+} induces autophagy in non-excitable cells: rise of cytosolic Ca^{2+}, produced by different drugs and Ca^{2+} phosphate-mediated transient transfections, activate the CAMKK-β-AMPK-mTOR and CAMKK-β-CAMKI signalling pathways that induce autophagy through various protein targets implicated in this process. (**B**) Cytosolic Ca^{2+} inhibits autophagy in excitable cells: antagonists of L-, N- or P-type Ca^{2+} channels (verapamil, fluspirilene etc…), and an agonist of L-type Ca^{2+} channels (Bay K-8644) modify cytosolic Ca^{2+} levels and consequently affect the activity of the Ca^{2+}-dependent proteases CALPAINs, including their *ATG5* cleavage that inhibits autophagy. See text for further details.

Therefore, whether rises in the cytosolic Ca^{2+} activate or inactivate autophagy is still a matter of discussion. Of note, studies supporting inactivation of autophagy by cytosolic Ca^{2+} are based on the modulation of voltage-dependent Ca^{2+} channels (L-, N- or P-type Ca^{2+} channels) that exist only in excitable cells (Williams *et al*., 2008; Xia *et al*., 2010), whereas activation of autophagy by cytosolic Ca^{2+} has been reported in non-excitable cells (Hoyer-Hansen *et al*., 2007; Gao *et al*., 2008; Pfisterer *et al*., 2011). Given that in excitable cells cytosolic Ca^{2+} is mainly provided from the extracellular space by voltage-activated channels, whereas in non-excitable cells it is mainly released from intracellular stores *via* second messengers (such as inositol 1,4,5-trisphosphate (IP_3)) (Pfisterer *et al*., 2011), it is possible that different Ca^{2+}-sensor proteins in both groups of cells activate distinct signalling routes that lead to opposite autophagic responses.

2.1.2. Regulation of autophagy by ER-derived Ca^{2+}

Earlier studies demonstrated a role of Ca^{2+} storage within cell compartments in autophagy stimulation (Gordon *et al*., 1993). In this pioneering study, Ca^{2+} inside the ER lumen was shown to induce autophagy while its release from this organelle to the cytosol would inhibit autophagy. Since then, the importance of ER-derived Ca^{2+} for the autophagic activity has been confirmed by several experimental evidences. The ER lumen constitutes both the main intracellular Ca^{2+} store and the major site in the secretory pathway for the proper folding of proteins, which is carried out by a group of chaperones, most of them Ca^{2+}-dependent (Berridge, 2002; Bernales *et al*., 2006; Momoi, 2006). Therefore, disturbances in Ca^{2+} homeostasis inside the ER cause stress that compromises the functionality of this organelle and of the cell.

2.1.2.1. Autophagic response to the inhibition of ER Ca^{2+}-ATPases by thapsigargin

The first direct evidence of a possible connection between Ca^{2+} efflux from the ER and autophagy came from the observation of an induction of autophagy by thapsigargin (Ogata *et al*., 2006). This compound hampers the Ca^{2+} transport into the ER through Ca^{2+}-ATPase pumps, rendering this store depleted of Ca^{2+} and, subsequently, provokes ER stress (Thastrup *et al*., 1990; Ogata *et al*., 2006). Several evidences indicate that Ca^{2+} rather than ER stress is important for the induction of autophagy by thapsigargin, since this effect is abolished by the potent cell permeant Ca^{2+} chelator BAPTA-AM (1,2-bis(o-aminophenoxy)ethane-*N,N,N',N'*-tetraacetic acid (acetoxy methyl ester)) (Hoyer-Hansen *et al*., 2007; Pfisterer *et al*., 2011) and thapsigargin causes ER stress only after prolonged treatments (reviewed in (Puzianowska-Kuznicka and Kuznicki, 2009)), while autophagy activation is evident at short times. Moreover, thapsigargin is able to induce autophagy in cells deficient in the unfolded protein response (Sakaki *et al*., 2008) and other compounds that deplete Ca^{2+} from the ER induce autophagy without altering the unfolded protein response (Hoyer-Hansen and Jaattela, 2007). All these data support the contribution of ER-derived Ca^{2+} to the activation of autophagy independently of ER stress.

The Ca^{2+}-dependent activation of autophagy by thapsigargin has been reported to occur in simple eukaryotes, such as *Dictyostelium* (Lam *et al*., 2008), as well as in a wide range of mammalian cells (lymphocytes, hepatocytes and fibroblasts are some examples) (Hoyer-Hansen *et al*., 2007; Sakaki *et al*., 2008; Grotemeier *et al*., 2010; Pfisterer *et al*., 2011). In *Dictyostelium*, ATG1 is shown to be required (Lam *et al*., 2008), whereas in mammalian cells this Ca^{2+}-dependent activation of autophagy has been described to occur either *via* CAMKK-β-AMPK-mTOR signalling (Hoyer-Hansen *et al*., 2007) that activates the mammalian homologue of ATG1, ULK1 (according to (Kim *et al*., 2011) and Chapter 2 of Results (Ghislat *et al*., 2012a)). Other possibilities for this autophagy activation include the participation of CAMKK-β-CAMKI (Grotemeier *et al*., 2010; Pfisterer *et al*., 2011) or a Ca^{2+}-dependent phosphorylation of protein kinase C (PKC) θ that

recruits this PKC isoform to the autophagic vesicles (Sakaki *et al*., 2008) (see Fig. 5A).

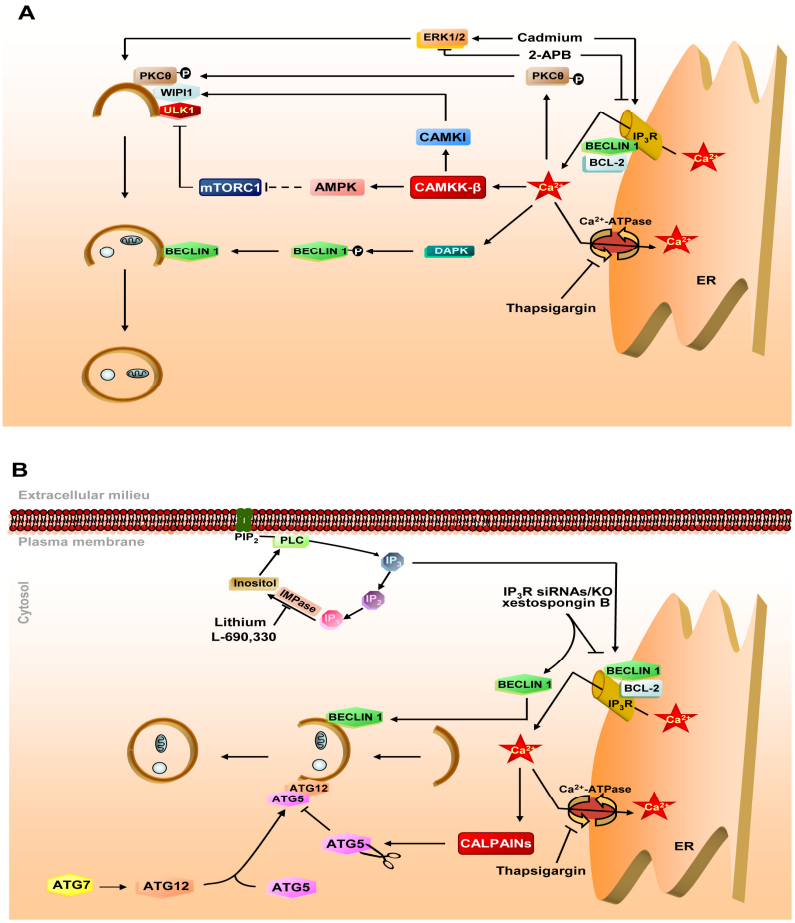

Figure 5. ER-derived Ca^{2+} effects on autophagy. (**A**) Under starvation conditions, Ca^{2+} derived from the ER activates autophagy: ER depletion of Ca^{2+} by thapsigargin induces autophagy *via* the same signalling pathways as from Fig. 2A, and by a Ca^{2+}-dependent phosphorylation of PKCθ that directs this kinase to autophagosomes. Ca^{2+} release from the ER through the IP_3R is inhibited with 2-aminoethoxydiphenyl borate (2-APB) and induced with Cd and this inhibits and activates, respectively, autophagy *via* ERK 1/2 signalling. Ca^{2+}-dependent phosphorylation of BECLIN 1 by DAPK also induces autophagy. (**B**) Under full nutrient conditions, Ca^{2+} derived from the ER restrains autophagy: thapsigargin inhibits autophagy *via* ATG5 cleavage by CALPAINs. As regards IP_3R function, inhibitors of inositol monophosphatases (IMPases), such as lithium (Li) and L-690,330, which prevent Ca^{2+} release through IP_3R by inhibiting IP_3 generation, induce autophagy. Also the inhibition of IP_3R function with xestospongin B and knockdown/knockout of IP_3R dissociates BECLIN 1 from BCL-2-IP_3R complex and stimulates autophagy. IP: inositol 4 monophosphate; IP_2: inositol 4,5 bisphosphate. See text for further details.

However, other studies have shown the opposite effect of thapsigargin (Gordon *et al*., 1993; Yitzhaki *et al*., 2007; Williams *et al*., 2008; Ganley *et al*., 2011), and, as mentioned before, one of these studies ascribed this inhibition of autophagy to the Ca^{2+}-dependent activation of CALPAINs (Williams *et al*., 2008). It seems that, in general and in accordance with what it was indicated in the previous section, in excitable cells autophagy is inhibited by thapsigargin, suggesting a negative role of ER-derived Ca^{2+} and hence of the Ca^{2+} supplied to the cytosol in this process. However, examples of non-excitable cells where autophagy is inhibited (Gordon *et al*., 1993; Williams *et al*., 2008) or activated (Hoyer-Hansen *et al*., 2007; Sakaki *et al*., 2008; Grotemeier *et al*., 2010; Pfisterer *et al*., 2011) are also observed. Given the diversity of the experimental conditions employed (0.01 to 5 μM of thapsigargin, for 15 min to 24 h), these differences could be due to side effects unrelated with the ER-derived Ca^{2+}, since, for example, possible disturbances in ATP levels caused by thapsigargin have not been investigated and also the use of BAPTA-AM in some of these studies does not rule out the involvement of Ca^{2+} present in other organelles. In fact, thapsigargin treatments at high concentrations and/or during prolonged times inhibit for example Ca^{2+}-ATPase pumps at the Golgi complex (Dode *et al*., 2006). Therefore, whether the Ca^{2+} released by thapsigargin from the ER activates or inhibits autophagy in non-excitable cells is still under debate.

Apart from Ca^{2+}-ATPase pumps that control Ca^{2+} entry to the ER lumen, Ca^{2+} homeostasis in this organelle is also affected by Ca^{2+} release through the IP_3 receptor (IP_3R), an aspect that we discuss below.

2.1.2.2. Regulation of autophagy by IP_3R-dependent Ca^{2+} release from the ER

Efflux of Ca^{2+} from the ER is mainly regulated by interaction of the second messenger IP_3 with IP_3R, resulting in the formation of a Ca^{2+} release channel at the ER (Patterson *et al*., 2004). IP_3 is generated through the

cleavage of PIP_2 by phospholipase C (PLC), which can be activated by inositol recycled from inositol monophosphate by dephosphorylation (Brandt *et al*., 2005) (see Fig. 5B). Inhibitors of this inositol monophosphatase, such as lithium, induce autophagy, suggesting a negative role of IP_3 in the regulation of autophagy (Sarkar *et al*., 2005; Criollo *et al*., 2007). In accordance with this observation, various reports suggest that Ca^{2+} release through IP_3R prevents autophagy, since inhibitors of this receptor, such as xestospongin B or dexamethasone, or the knockdown/knockout of all three IP_3R isoforms induce autophagy (Criollo *et al*., 2007; Cardenas *et al*., 2010; Harr *et al*., 2010; Khan and Joseph, 2010). This negative effect on autophagy of the Ca^{2+} released to the cytosol through IP_3R appears to be only relevant under nutrient rich conditions, because in this situation, but not under starvation (Cardenas *et al*., 2010), the knockout of the three IP_3R isoforms decreases mTOR activity and results in an increase of basal autophagy (Khan and Joseph, 2010).

Moreover, this channel has been associated with two autophagy-related proteins, BCL-2 and BECLIN 1, which interact with IP_3R forming a complex. Although BCL-2 is not necessary for the *in vitro* binding of BECLIN 1 to IP_3R, it is indispensable for the complex formation in a cellular context and under full nutrient conditions (Decuypere *et al*., 2011). However, starvation releases BECLIN 1 from the complex with IP_3R/BCL-2 (Vicencio *et al*., 2009; Decuypere *et al*., 2011) and this dissociation, which is a basic condition to activate autophagy, occurs when BECLIN 1 is phosphorylated by the death-associated protein kinase (DAPK) (see Fig. 5A) (Zalckvar *et al*., 2009b). Of note, interactors of BECLIN 1, such as BCL-XL and the nutrient deprivation factor NaF-1, are also part of this complex and are released from BECLIN 1 and IP_3R under starvation conditions (Feng *et al*., 2007; Oberstein *et al*., 2007; Zalckvar *et al*., 2009a; Chang *et al*., 2010). Also, inhibition of IP_3R by its knockdown or by xestospongin B disrupts the complex and leads to autophagy activation (Criollo *et al*., 2007; Vicencio *et*

al., 2009). Thus, IP_3R probably acts as a scaffold to recruit proteins of the autophagic machinery under nutrient rich conditions.

As for the role of these autophagy-related proteins in IP_3R function as a Ca^{2+} channel, it also seems to be dependent on the nutritional state of the cell, at least for the autophagy inducer BECLIN 1. Under full nutrient conditions this protein does not affect Ca^{2+} release through IP_3R (Vicencio *et al*., 2009), whereas under starvation BECLIN 1 enhances the release of Ca^{2+} from the ER by IP_3R in response to IP_3 (Decuypere *et al*., 2011). Moreover, BCL-2, which inhibits autophagy by recruiting BECLIN 1 to IP_3R, reduces Ca^{2+} release through IP_3R by a still unknown mechanism (Chen *et al*., 2004; Palmer *et al*., 2004; Hanson *et al*., 2008; Rong *et al*., 2008).

In conclusion, the impact of Ca^{2+} discharge from the ER through IP_3R on autophagy appears to depend on two factors: the nutritional state of the cell and the scaffold properties of this channel to recruit autophagy-related proteins. Under full nutrient conditions, IP_3R sequesters proteins essential for autophagy activation that do not affect Ca^{2+} release through this channel, whereas under starvation conditions these proteins are liberated and this increases both autophagy and Ca^{2+} release.

Other drugs that increase (Cadmium) or inhibit (2-aminoethoxydiphenyl borate) Ca^{2+} efflux from the ER *via* IP_3R, produce a similar effect (activation or inhibition, respectively) on autophagy *via* ERK1/2 (Wang *et al*., 2008) (see Fig. 5A). However, these chemicals are not necessarily specific for IP_3R. For example, 2-aminoethoxydiphenyl borate is not a selective inhibitor of IP_3R, because it also alters the activity of store-operated Ca^{2+} channels and Sarco/Endoplasmic Reticulum Ca^{2+}-ATPase (SERCA) pumps at the plasma membrane (Missiaen *et al*., 2001; Bilmen *et al*., 2002) and activates mTORC1 and AMPK in a CAMKK-β–independent manner (our unpublished results). Thus, probably the effect of these drugs on autophagy may not be exclusively due to the Ca^{2+} derived from the ER through IP_3R.

Overall, Ca^{2+} release from the ER through this channel appears to induce autophagy in starved cells, but to inhibit it under full nutrient conditions. As all these studies have been performed in non-excitable cells, this conclusion, at least under starvation conditions, is in agreement with the studies that proposed a role of cytosolic Ca^{2+} inducing autophagy in these cells.

2.1.3. Mitochondrial link between ER-derived Ca^{2+} and autophagy

IP_3R is also found at ER-mitochondrial contact sites, since these two organelles are often found in close connection (Criollo *et al*., 2007). Thus, a blockage in Ca^{2+} release from the ER also alters Ca^{2+} homeostasis in mitochondria. The close proximity of ER and mitochondria is essential for an efficient transport of Ca^{2+} from the ER to mitochondria and the subsequent activation of Ca^{2+}-dependent mitochondrial enzymes that participate in ATP production, such as pyruvate dehydrogenase (PDH), two enzymes of the Krebs cycle (isocitrate dehydrogenase and ketoglutarate dehydrogenase), and the F_1F_0 ATPase. Activation of PDH occurs by its dephosphorylation produced by the Ca^{2+}-dependent stimulation of the PDH phosphatase (PDP). Although some cells, such as hepatocytes, express a PDP isoform whose activity is Ca^{2+}-independent (Sugden and Holness, 2003), the Ca^{2+}-dependent activation of PDH by PDP seems to be a key step in many cells to supply them with NADH and ATP (Duchen, 2004; Spat *et al*., 2008; Szabadkai and Duchen, 2008; Balaban, 2009). Thus, in HEK-293 cells that express PDP with Ca^{2+}-dependent activity, when a moderate extent of Ca^{2+} (in the low micromolar range) is delivered to mitochondria, ATP increases, AMPK is inhibited and this restrains autophagy by an mTOR-independent signalling pathway (Cardenas *et al*., 2010) (see Fig. 6A).

On the contrary, under situations that may induce cell death, such as oxidative stress, a massive entry of Ca^{2+} (in the millimolar range) into mitochondria occurs as a consequence of its depolarization. This provokes

the disruption of the integrity of the mitochondrial outer membrane and a rise in mitochondrial permeability (Rasola and Bernardi, 2007; Decuypere *et al*., 2010). In most cells, these stress events provoke a specific autophagy (called mitophagy), which selectively degrades damaged mitochondria to preserve a healthy mitochondrial pool (Elmore *et al*., 2001; Twig *et al*., 2008) (see Fig. 6B).

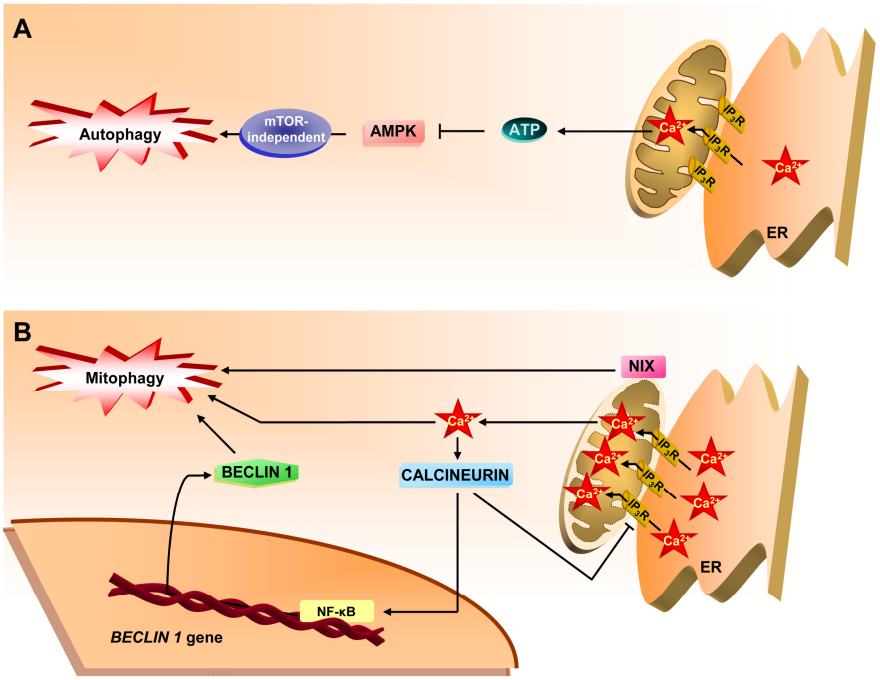

Figure 6. Effects of mitochondrial Ca^{2+} on autophagy. (**A**) Mitochondrial Ca^{2+} inhibits autophagy: a moderate transfer of Ca^{2+} from the ER to mitochondria through IP_3R, triggers ATP production that subsequently inactivates AMPK-dependent autophagy. (**B**) Under stress, mitochondrial Ca^{2+} can activate autophagy: mitochondria overloaded with Ca^{2+} are permeabilized and damaged. This promotes mitophagy and also activates CALCINEURIN, which enhances NF-κB-mediated transcription of *BECLIN 1.* Also, NIX buried in the outer mitochondrial membrane induces Ca^{2+} transfer from the ER to mitochondria and activates mitophagy. See text for further details.

Indirect links between mitochondrial Ca^{2+} overload and autophagy are provided by some proteins. The proapoptotic proteins adenovirus E1B 19-kDa-interacting protein 3 (BNIP3) and BNIP3-like, also known as NIX, participate in mitophagy induction in various cell types, including tumours,

and localize on the outer mitochondrial membrane (Zhang and Ney, 2009). As NIX has been reported to trigger Ca^{2+} transfer from the ER to mitochondria, in cardiac cells under stress conditions that may induce cell death (Diwan *et al*., 2009), it is possible that this BNIP3-like protein uses this action to activate autophagy. However, further experiments are needed to confirm whether autophagy induction by these two proteins is due to an effect of NIX on mitochondrial Ca^{2+} overload and to generalize these observations to other cell types.

Moreover, permeabilization of mitochondrial membranes under Ca^{2+} overload inside this organelle activates the cytosolic Ca^{2+}-dependent phosphatase CALCINEURIN (Cereghetti *et al*., 2008), which further promotes autophagy (see Fig. 6B) by dephosphorylation and inhibition of IP_3R, constituting in this way a negative feedback to control Ca^{2+} release and to preserve mitochondrial homeostasis (Bultynck *et al*., 2003; Wang *et al*., 2008). Since CALCINEURIN has been reported to be essential for the activation of NF-κB (Kanno and Siebenlist, 1996), a nuclear factor that, among other effects, enhances the transcription of BECLIN 1 and induces autophagy (Copetti *et al*., 2009), it is possible that this effect also contributes to the activation of autophagy observed in the mitochondrial Ca^{2+}-mediated activation of CALCINEURIN (see Fig. 6B).

In summary, mitochondrial Ca^{2+} regulates autophagy in two opposite ways. Moderate Ca^{2+} levels provided from the ER within mitochondria produce ATP that represses autophagy *via* inhibition of AMPK. Otherwise, when cells run into stress conditions, an excessive mitochondrial Ca^{2+} upload occurs, which activates mitophagy by mechanisms involving pro-apoptotic proteins and probably CALCINEURIN.

Taken together the different Ca^{2+} stores in non-excitable cells, it seems that this cation and its sensor proteins in the cytosol induce autophagy when cells encounter conditions that require this process. Ca^{2+} release from the ER and mitochondria to the cytosol activates autophagy

under stress conditions, whereas in healthy state, the storage of this cation inside these two organelles maintains low levels of autophagy. Thus, Ca^{2+} seems to participate in the adaptation of the autophagic level of the cells to their physiological state. As for excitable cells, although less attention has been paid to the Ca^{2+} impact on their autophagy, cytosolic Ca^{2+} seems to have the opposite effect on autophagy, probably because, as pointed above, the characteristics of the Ca^{2+}-sensor proteins implicated in autophagy in these cells are different from the corresponding proteins in non-excitable cells.

2.2. Involvement of Ca^{2+} in endocytosis

During endocytosis, Ca^{2+} appears to be relevant in fusion events (Pryor *et al.*, 2000; Luzio *et al.*, 2007b). There are two different types of fusion: homotypic (early endosomes) and heterotypic (late endosomes-lysosomes), and their basic steps comprise: tethering, docking and, finally, blending of the membrane bilayers (see Fig. 7). Tethering starts with the binding of a complex of proteins including RABs and HOPS to the target membrane. Subsequently, membrane docking is promoted by the phosphoinositide (PIP)-dependent association of soluble NSF attachment protein receptors (SNAREs) to the two opposite membranes (v- for vesicle and t- for target) that finally culminate their fusion (Pryor *et al*., 2004; Jahn and Scheller, 2006; Malsam *et al*., 2008; Martens and McMahon, 2008). In spite of their differences, fission and fusion events share several biochemical similarities and, for instance, RAB proteins and PIPs regulate both processes (Roth, 2004). After docking, a release of luminal Ca^{2+} from endolysosomal compartments is thought to trigger fusion/fission events near Ca^{2+} release sites (Pryor *et al.*, 2000; Hay, 2007; Luzio *et al.*, 2007b; Luzio *et al.*, 2007a). This concept was evidenced for the first time using the intracellular Ca^{2+} chelators BAPTA and ethylene glycol tetraacetic (EGTA). In membrane fusion assays, BAPTA but not EGTA inhibits the fusion of late endosomes with early endosomes (Mills *et al*., 2001), lysosomes (Peters

and Mayer, 1998) or yeast vacuoles (Pryor *et al*., 2000). As at their maximal concentrations (10 mM), BAPTA binds Ca^{2+} in less time (0.3 µs) than EGTA (1.2 ms) (Adler *et al*., 1991), and since the Ca^{2+} diffusion rate in the cytosol is 20 nm/ms (Burgoyne and Clague, 2003), this selective inhibition leads to postulate that the Ca^{2+} release source is situated at 20 nm or less from the site where fusion occurs, a reasonable distance to consider the lumen of vesicles committed to a fusion event as the source of this Ca^{2+}. In fact, the depletion of luminal Ca^{2+} from these vesicles has the same effect on their fusion as BAPTA (Peters and Mayer, 1998; Holroyd *et al*., 1999).

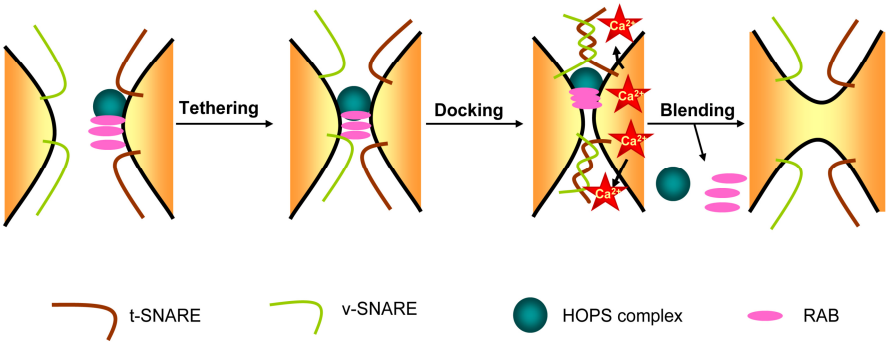

Figure 7. Main steps in the fusion of endocytic vesicles. First, the HOPs complex, RABs and other proteins are recruited to the target vesicle in order to allow tethering with the other vesicle. Subsequently, v- and t-SNAREs interact to allow the appropriate docking of the two opposite membranes. Ca^{2+} release from the target vesicle occurs at this stage to facilitate the blending of the two membranes. See text for further details.

It is believed that specific endolysosomal Ca^{2+}-sensors transduce these Ca^{2+} signalling into a fusion response. The best studied sensor is CALMODULIN, which has been shown to be crucial in homotypic (Colombo *et al*., 1997; Mills *et al*., 2001) and heterotypic (Pryor *et al*., 2000) fusions. Ca^{2+}-binding to CALMODULIN leads to interactions between this protein and specific targets, such as CALMODULIN-dependent kinase II (CAMKII) (Colombo *et al*., 1997) or a complex formed by early endosome antigen 1 (EEA1) (Mills *et al*., 2001) and the SNARE protein SYNTAXIN 13 (McBride *et al*., 1999), to promote early endosome fusions. Moreover, CALMODULIN

has the ability to dislocate EEA1 from early endosomal membranes (Mills *et al*., 2001). Thus, Ca^{2+}/CALMODULIN may not only play the role of recruiting fusion effectors to early endosomes, but it can also recycle tethering molecules, such as EEA1.

Apoptosis-linked gene-2 (ALG-2), has been also proposed as a Ca^{2+}-sensor for later fusion events in the endolysosomal system through its Ca^{2+}-dependent interaction with the transient receptor potential cation channel, mucolipin subfamily 1 (TRPML1) (Vergarajauregui *et al*., 2009), a putative endolysosomal ion channel involved in the transport of Ca^{2+} and other ions from the lysosomal lumen to the cytosol (LaPlante *et al*., 2002; LaPlante *et al*., 2004; Xu *et al*., 2007). Since the release of Ca^{2+} from the lumen of vesicles is essential for their fusion, this channel may provide Ca^{2+} from endolysosomes for their fusion with endosomes and autophagic vacuoles (LaPlante *et al*., 2004; Treusch *et al*., 2004; Dong *et al*., 2010; Zeevi *et al*., 2010; Grimm *et al*., 2012), hence the importance of lysosomal Ca^{2+} in these processes that we will discuss in the following section.

2.3. Role of endolysosomal Ca^{2+} in autophagy and endocytosis

Fusion of autophagosomes and endosomes with lysosomes to deliver their respective cargo constitutes a late step in autophagy and endocytosis. Both groups of fusions share certain features, such as the involvement of RAB7 and the AAA ATPase SKD (Vacuolar protein sorting 4/suppressor of K^+ transport growth defect 1) in their regulation (Nara *et al*., 2002; Jager *et al*., 2004). Although in comparison to the early stages of autophagy and endocytosis these late steps remain poorly understood, it is known that Ca^{2+} is a key player (Pryor *et al.*, 2000; Luzio *et al.*, 2007b). Here below, we will review recent advances focused on the involvement of Ca^{2+} derived from lysosomes in the fusion of these organelles with autophagosomes and endosomes.

2.3.1. Endolysosomal Ca^{2+} channels

The best characterized Ca^{2+} channels present in lysosomal and late endosomal membranes are TRPMLs (LaPlante *et al*., 2002; LaPlante *et al*., 2004; Puertollano and Kiselyov, 2009; Grimm *et al*., 2012). Three isoforms (1, 2 and 3) have been identified in database searches (Puertollano and Kiselyov, 2009), and mutations in the gene encoding TRPML1 provoke type IV mucolipidosis (Bargal *et al*., 2009), a lysosomal storage disease. Although TRPML1 showed Ca^{2+}-related features in endolysosomal compartments, such as Ca^{2+} permeability (LaPlante *et al*., 2002; Xu *et al*., 2007), its consideration as a reliable Ca^{2+} channel is still under debate (Cantiello *et al*., 2005; Soyombo *et al*., 2006; Miedel *et al*., 2008). However, TRPML1, and TRPML2 as well, have been reported to heteromultimerize with TRPML3, which is the most accepted isoform to function as a Ca^{2+} channel (Grimm *et al*., 2007; Kim *et al*., 2007; Xu *et al*., 2007; Nagata *et al*., 2008), and to control its lysosomal localization (Venkatachalam *et al*., 2006).

While there is no experimental evidence for a direct involvement of the two other isoforms in autophagy, recent data have shown that TRPML3 is localized in autophagosomal membranes, where it induces autophagy under stress conditions (Kim *et al*., 2009; Zeevi *et al*., 2010), and also at the plasma membrane and early endosomal membranes, where it inhibits endocytosis (Kim *et al*., 2009; Martina *et al*., 2009).

Two other candidates to function as lysosomal/endosomal Ca^{2+} release channels have recently emerged: transient receptor potential cation channel subfamily M member 2 (TRPM2) and two-pore channels (TPCs). TRPM2, whose expression is restricted to specific cells, like pancreatic β cells, is mainly expressed at the plasma membrane, but it has been also localized in lysosomes, where it has been proposed to regulate luminal Ca^{2+}

release (Lange *et al*., 2009). TPC1 and TPC2 appear to be exclusively localized in early/late endosomes and lysosomes, respectively (Brailoiu *et al*., 2009; Calcraft *et al*., 2009; Galione *et al*., 2010). Both TRPM2 and TPCs are reported to be regulated by NAADP, a well-known endogenous second messenger that releases Ca^{2+} from acidic compartments (Beck *et al*., 2006; Brailoiu *et al*., 2009; Zong *et al*., 2009).

Although NAADP-regulated TRPM/TPCs channels can release Ca^{2+} from endolysosomal compartments, knowledge on their specific role in autophagy and endocytosis remains rudimentary. In this regard, it has been suggested that Ca^{2+} release through NAADP-sensitive channels contributes, at least, to fusions between lysosomes and endosomes, since these channels are localized in these organelles (Brailoiu *et al*., 2009; Calcraft *et al*., 2009; Galione *et al*., 2010).

Lysosomal Ca^{2+} is also regulated by pH. In fact, disruption of lysosomal pH by lysosomotropic agents, like bafilomycin A1, chloroquine diphosphate or nigericin, prevents Ca^{2+} storage in the lysosomal lumen and arrests the fusion of lysosomes with autophagosomes (Churchill *et al*., 2002). Therefore, an acidic pH is crucial to maintain high levels of Ca^{2+} in the lysosomal lumen, a requirement to induce fusions between lysosomes and endosomes or autophagosomes upon Ca^{2+} release from the lumen of these vesicles. In accordance with this concept, an *in vitro* study with isolated autophagosomes and lysosomes revealed that fusion between both organelles requires a minimum of 250 μM of calcium chloride (Koga *et al*., 2010).

2.3.2. Ca^{2+}-dependent effectors of endolysosomal fusions

Another physiological feature of Ca^{2+} that is relevant in autophagy and endocytosis consists in its ability to promote the fusion of vesicles by inducing local segregations of specific lipids, such as phosphatidic acid (Swairjo *et al*., 1994; Geng *et al*., 1998). Several *in vivo* and *in vitro* data

support that these lipid domains are stabilized by proteins that bind to the membranes (Buser *et al*., 1995; Rytomaa and Kinnunen, 1996; Denisov *et al*., 1998). The best studied of these proteins belong to the SNARE machinery. First, this protein complex triggers docking of vesicles, which provokes a quick luminal Ca^{2+} release. Subsequently, Ca^{2+}-binding proteins (that we will discuss below; see Table 1) are activated, probably by organizing a scaffold upon the membranes that initiates the fusion processes. Finally, after dissipation of the Ca^{2+} gradient, these proteins remain activated until fusion is accomplished (Hay, 2007).

A peculiar protein from the SNARE complex is hepatocyte responsive serum phosphoprotein (HRS), a Ca^{2+}-sensitive protein associated to early endosomes. When bound to a still undefined SNARE protein on the membrane of early endosomes, HRS prevents homotypic membrane fusions, thus negatively regulating the fusogenic function of SNAREs (Sun *et al*., 2003). Ca^{2+} release from the endosomal lumen dissociates HRS from the SNARE complex and abolishes this effect, enabling in this way endocytic fusion (Yan *et al*., 2004).

On the other hand, this protein has been also shown to partially colocalize with autophagosomes and to promote their maturation (Tamai *et al*., 2007).

CALMODULIN has been also proposed to be a Ca^{2+}-sensor of SNAREs. The first evidences of this role were obtained in yeast, where CALMODULIN was identified within a protein complex involved in homotypic vacuole fusion (Peters and Mayer, 1998; Peters *et al*., 1999). In mammalian cells, an implication of CALMODULIN in homotypic and heterotypic fusions was also proposed (Colombo *et al*., 1997; Huber *et al*., 2000; Pryor *et al*., 2000; Mills *et al*., 2001; De Haro *et al*., 2003)

Moreover, some members of the annexin family of Ca^{2+}-binding proteins are associated with fusion events in the endolysosomal system. *In vitro* studies showed the requirement of annexin A1 in fusions between early

endosomes in a Ca^{2+}-dependent manner (Raynal and Pollard, 1994), whereas *in vivo* analysis attributed to annexin A2, annexin A5 and annexin A6 the abilities to mediate the fusions of early endosomes (Emans *et al*., 1993), autophagosomes/lysosomes (Chapter 3 of Results (Ghislat *et al*., 2012b)), and late endosomes/lysosomes (Futter and White, 2007), respectively.

Table 1. Ca^{2+}-dependent effectors involved in the fusions between lysosomes, autophagosomes and/or endosomes.

Ca^{2+}-dependent effectors	**Organelles participating in the fusion event**	**Molecular details of their role**	**References**
ALG-2	Late endosomes and lysosomes	Interacts with TRPML1 channel	(Vergarajauregui *et al*., 2009)
Annexin A1	Early endosomes	Requires Ca^{2+} to induce fusion *in vitro*	(Raynal and Pollard, 1994)
Annexin A2	Early endosomes	Mediates membrane interactions between early endosomes	(Emans *et al*., 1993)
Annexin A6	Late endosomes and lysosomes	Requires Ca^{2+} and CALPAINs for fusion	(Futter and White, 2007)
CALMODULIN	Late endosomes and lysosomes Early endosomes	Binds to Ca^{2+} and leads to interactions with specific targets	(Pryor *et al*., 2000)
CAMKII	Early endosomes	Is a CALMODULIN target	(Colombo *et al*., 1997)
EEA1	Early endosomes	Interacts with CALMODULIN and SYNTAXIN 13	(Mills *et al*., 2001)
HRS	Early endosomes Autophagosomes and lysosomes	Inhibits fusion when Ca^{2+} release abolishes its interaction with SNAREs	(Yan *et al*., 2004) (Sun *et al*., 2003) (McBride *et al*., 1999)
SYNTAXIN 13	Early endosomes	Interacts with Ca^{2+}/CALMODULIN to promote early endosome fusions	(McBride *et al*., 1999)

Overall, Ca^{2+}-dependent effectors of fusions between autophagosomes, endosomes and lysosomes belong to a wide range of subgroups, such as SNAREs, EF-hand proteins and annexins, with some common characteristics, including the requirement of Ca^{2+}-binding. However, the molecular mechanisms by which they control these events are still poorly understood.

Conclusions

Growing evidences support that Ca^{2+} controls endocytosis and autophagy. Its effect on autophagy occurs both at the level of the signalling pathways that initiate it or, later, when autophagosomes fuse with endolysosomal compartments.

The effect of Ca^{2+} on autophagy depends on the cell type, since excitable and non-excitable cells exhibit opposite autophagic responses (inhibition or activation, respectively) to this cation. Although less attention has been paid to excitable cells, Ca^{2+} rise within them restrains autophagy and this effect is mainly due to the activation of CALPAINs that cleave proteins essential for autophagy. To decide whether other Ca^{2+}-sensor proteins, specific or not for these cells, are also involved in this effect requires further work that would help to better understand the autophagic behaviour of these cells.

In non-excitable cells, the effect of Ca^{2+} on autophagy depends on the nutritional state of the cells and, probably, on the Ca^{2+} levels within the cytosol. Under full nutrient conditions, Ca^{2+} levels in the cytosol are low and maintain a basal autophagy. Starvation and stress conditions induce a rise of cytosolic Ca^{2+} originated, respectively, from the ER and mitochondria overloaded with Ca^{2+}. Consequently, these conditions trigger autophagy *via* various pathways that depend on Ca^{2+}-sensor proteins (Fig. 8). Thus, in non-excitable cells, Ca^{2+} seems to play a protective role by adapting the autophagic activity to extracellular conditions. Therefore, manipulation of

intracellular Ca^{2+} levels in situations of defective autophagy may be useful to recuperate cellular homeostasis.

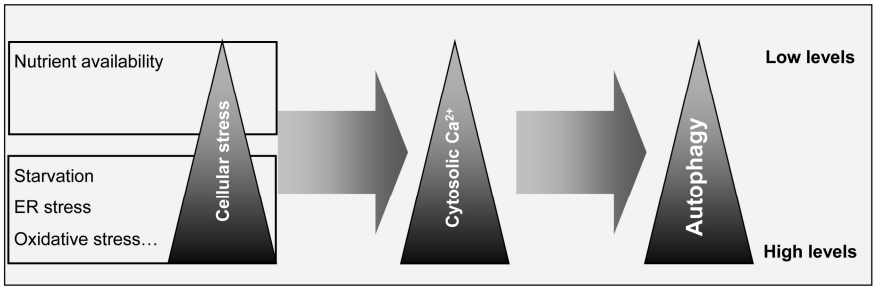

Figure 8. Possible relationships between nutrient availability, cell stress, cytosolic Ca^{2+} levels and autophagy. Starvation and an increased cell stress correlate with a high level of cytosolic Ca^{2+} generated from the ER and/or mitochondria and this induces autophagy. On the other hand, when nutrients are available to cells and no stress occurs, cytosolic Ca^{2+} remains at a low level and, consequently, basal autophagic activity is maintained.

Concerning endocytosis, the traffic of endocytic vesicles is controlled by Ca^{2+} derived from their lumen and, subsequently, Ca^{2+}-sensor proteins transduce this Ca^{2+} signalling into fusion events.

Finally, the convergence of the autophagic and endocytic vesicles to lysosomes shares several features that depend on Ca^{2+} originated from lysosomes/late endosomes and on proteins that are subsequently activated by this cation. However, the involvement of Ca^{2+} and its effects on sensor proteins in these final autophagic and endocytic stages remain poorly understood. Although various members of these proteins have been identified, further investigations are needed to identify new Ca^{2+}-effectors and their role in the regulation of the different steps of autophagy and endocytosis.

3. The annexin and copine families

Ca^{2+}-binding proteins play a crucial role in the transfer of the Ca^{2+} signal for a wide variety of cellular activities, such as cytoskeletal organization, motility and differentiation, cell cycle regulation and modulation of the activity of various enzymes. They bind to membrane phospholipids in a Ca^{2+}-dependent manner and most of them are expressed in a cell-specific fashion. Ca^{2+}-binding proteins can be classified into two main groups, depending on the presence or not of a structural motif, the EF-hand, which selectively binds Ca^{2+} with high affinity at a loop surrounded by two (E and F) helix regions (Yanez *et al*., 2012). Annexins and copines are Ca^{2+}-binding proteins that belong to the group that lacks this domain.

3.1. The annexins

3.1.1. The origins of the family

The first annexin was identified in 1978 (Creutz *et al*., 1978) and initially it was named “synexin” (from the greek noun “synexis”, which means “meeting”), but later it was known as annexin A7 (Creutz and Sterner, 1983). Afterwards, two other members of the family (lipocortin and calpactin, now known as annexins A1 and A2) were identified as substrates of the epidermal growth factor receptor (EGFR) kinase and the proto-oncogene tyrosine-protein kinase, respectively (Huang *et al*., 1986; Saris *et al*., 1986). Soon, an interaction was described between annexin A2 and a member of the S100 proteins, S100A10, which are dimeric Ca^{2+}-binding proteins holding an EF-hand motif (Saris *et al*., 1987), and today all annexins are known to share this property (Rintala-Dempsey *et al*., 2008; Yanez *et al*., 2012). In order to unify the nomenclature, the name “annexins” was attributed to this family in 1988, referring to the ability of the proteins to “annex” to acidic phospholipids of membranes in a Ca^{2+}-dependent manner (Crompton *et al*., 1988). As annexins have been subsequently identified in a wide range of organisms, they have been classified into 5 groups according

to their origin: A (vertebrate annexins: annexins A1-A11 and A13, A12 is unassigned), B (invertebrates), C (fungi and unicellular eukaryotes), D (plants) and E (protists) (Moss and Morgan, 2004).

3.1.2. Structure and function of annexins

One of the most important features of these proteins that justify their inclusion into a new family is their high similarity (~50%) in both amino acid and nucleotide sequences. A conserved C-terminal core domain (Fig. 9A) exists in all annexins, composed of a sequence of four (eight in the case of annexin A6) tandem repeats of nearly 70 amino acids, forming five α helices connected by short loops that contain the Ca^{2+}-binding sites and the sites responsible for the interaction with negatively charged phospholipids. In contrast, the N-terminal domains of annexins are variable, and confer to each family member its own identity (Gerke and Moss, 2002).

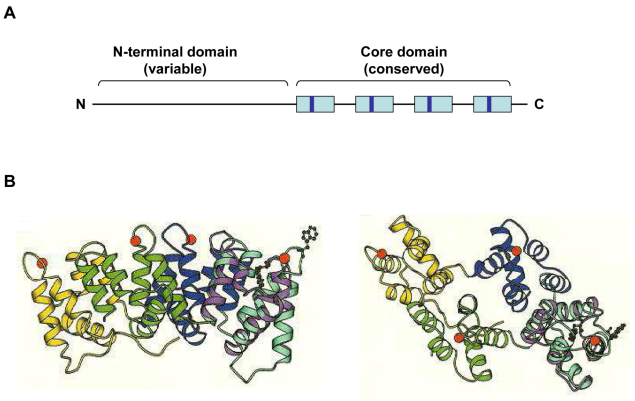

Figure 9. Representations of the domains of annexins. (**A**) Schematic representation of the four tandem repeats in the conserved C-terminal domain (eight in the case of annexin A6) and the variable N-terminal domain in the structure of annexins. Each repeat contains a conserved 17 amino acid long consensus called the endonexin fold. (**B**) Three-dimensional structure of human annexin A5, according to (Liemann and Lewit-Bentley, 1995) that represents the conformational changes that occur in repeat III under high and low Ca^{2+} concentrations. The four tandem repeats within the core domain are exposed in different colours. Repeat I is shown in yellow, repeat II in blue, repeat IV in green and repeat III in cyan or violet under high or low Ca^{2+} binding, respectively. Ca^{2+} ions are indicated by orange spheres. The N-terminal domain extends from repeat I along the concave side of the molecule. The side chain of tryptophan187 (shown in ball-and-stick illustration) is exposed on the surface upon the Ca^{2+}-induced conformational change. The structure is visualized from above (right) and from the side (left).

The C-terminal core domain of annexins is characterized by the presence of a conserved Ca^{2+}-binding domain (type II), which is different from the EF-hand domain (type I) of the majority of proteins that selectively bind Ca^{2+} with high affinity. It contains an ultraconserved region, named "endonexin" (KGhGTDExxLIpILApR, being h an hydrophobic residue, p a polar residue and x a variable residue), which is thought to be crucial for Ca^{2+}-binding (Gerke and Moss, 2002). Crystal structures of annexins have been resolved for their core domains and for those annexins with short N-termini (Concha *et al*., 1993; Luecke *et al*., 1995; Favier-Perron *et al*., 1996; Rety *et al*., 2005; Butsushita *et al*., 2009). The core domain has the shape of a slightly curved disc, with lipid-binding sites and Ca^{2+} positioned at the convex face of the molecule. Once bound, this cation bridges carbonyl/carboxyl groups (such as a tryptophan residue in the case of annexin A5; see Fig. 9B) of the protein to phosphoryl groups at the glycerol backbone of the membrane phospholipids (Swairjo *et al*., 1995). Consequently, this binding leads to a conformational change in the core domain, particularly in its third repeat (Concha *et al*., 1993; Ayala-Sanmartin *et al*., 2000; Babiychuk and Draeger, 2000).

The variability in the N-termini affects the affinity of annexins for Ca^{2+} and, consequently, their lipid-binding capacity (Sopkova *et al*., 2002). This domain harbours sites for post-translational modifications, such as phosphorylation, and for the interaction with lipids (Gerke, 2001; Gerke and Moss, 2002). In fact, besides that annexins bind membrane phospholipids through their core domain in a Ca^{2+}-dependent way (Fig. 10A), they also can bind through their N-terminal domain to a second membrane (either by one annexin alone (Fig. 10B), or by forming a dimer (Fig. 10C)), thereby acting as a bridge that allows the association of membranes to vesicles (Nakata *et al*., 1990). Annexin N-termini also allow their binding with other proteins, including members of the S100 family (Miwa *et al*., 2008). After binding to Ca^{2+}, S100 homodimers undergo significant conformational

changes by exposing hydrophobic residues on their two opposite surfaces, which allows them to bind to the N-terminal region of annexins. This heterotetrameric interaction brings in close proximity two annexins, each one bound to a membrane (Fig. 10D). By this way, annexins lead to the aggregation of membranes (Miwa *et al*., 2008; Rescher and Gerke, 2008), or even the association of membranes to the actin cytoskeleton (Hayes *et al*., 2004). In fact, various annexins (A1, A2, A5, A6 and A8) have been reported to associate, in a Ca^{2+}-dependent manner, to actin (monomeric and in microfilaments) at membrane contact sites, forming an interface for a dynamic membrane-associated actin cytoskeleton (Monastyrskaya *et al*., 2009).

In summary, both the N- and C-terminal domains of annexins are crucial for their function in the traffic of vesicular membranes and organization of lipid microdomains.

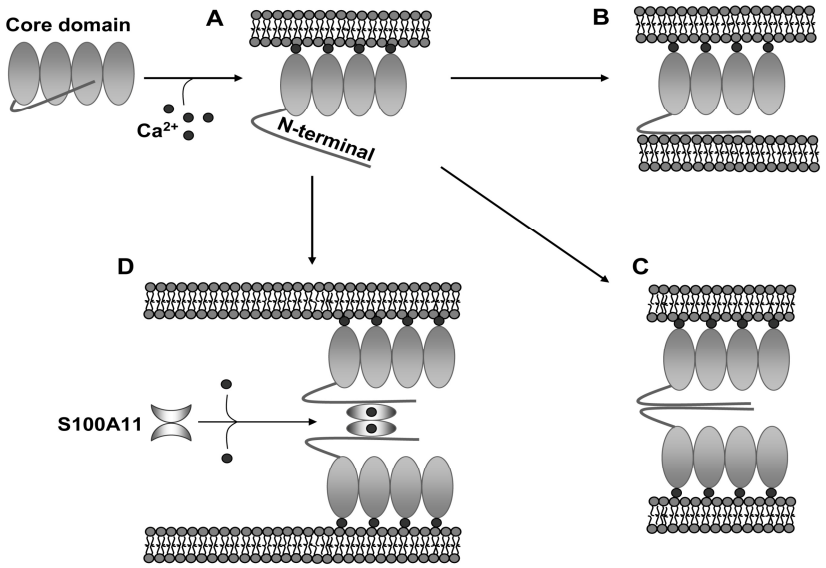

Figure 10. Interactions of annexin A1 with cell membranes. The four repeats of the core domain bind to membranes upon sequestering Ca^{2+} (**A**). This renders the N-terminal motif accessible to a membrane surface (**B**), to another N-terminal motif of a membrane bound annexin A1 (**C**) or to a S100A11 dimer previously bound to Ca^{2+} that allows the formation of an annexin A1/S100A11 heterotetramer and brings two membranes closer (**D**).

3.1.3. Tissue distribution and intracellular localization of annexins

The expression levels and tissue distribution of annexins span a broad range from abundant and ubiquitous, like annexins A1, A2, A4, A5, A6, A7 and A11 (Raynal *et al*., 1993; Babiychuk and Draeger, 2000; Camors *et al*., 2005; Draeger *et al*., 2005), to annexins with a more selective localization, such as A3 in neutrophils and placenta (Le Cabec *et al*., 1992), A8 in skin, eye and tongue (Runkel *et al*., 2006) and A9 in tongue, spleen and liver (Goebeler *et al*., 2003; Moss and Morgan, 2004). There are even annexins with a quite restrictive distribution, such as annexin A10 in the stomach and annexin A13 in the small intestine (Iglesias *et al*., 2002). In any case, the presence of various annexins in the same cell, despite of their high similarity in molecular structure, also points to specific functions of the different annexins, including the ubiquitous ones.

The expression level and intracellular distribution of annexins are altered in some diseases. For example, most forms of human cancer are associated with significant disturbances in gene expression and intracellular localization of annexins, consistent with the role of these proteins in vesicle trafficking, cell division, apoptosis and Ca^{2+} signalling (Mussunoor and Murray, 2008).

Because compiling all the available information about the twelve members of the annexin family would be very extensive, a brief summary of their localization and of the proposed biological functions is given below (see also Table 2).

Annexin A1 is a ubiquitous protein, especially abundant in smooth muscle and endothelial cells (Monastyrskaya *et al*., 2009). It is predominantly cytosolic, however it has been also found associated with: i) the plasma membrane, where it has been reported to regulate its lipid architecture by binding to ceramide platforms in a Ca^{2+}-dependent way (Babiychuk *et al*., 2008), ii) early endosomes and, upon epidermal growth

factor (EGF) stimulation, multivesicular bodies (MVB), where the protein has been reported to inactivate the EGFR and iii) phagosomes, annexin A1 was shown to participate in their inward vesiculation (Gerke *et al*., 2005; Futter and White, 2007), and to induce their interaction with actin, promoting in this way phagocytosis (Patel *et al*., 2011). Annexin A1 was also shown to induce autophagy, probably by controlling amphisome formation (Kang *et al*., 2011).

Annexin A2 is also ubiquitous and especially abundant in endothelial and smooth muscle cells, where it has been shown to act as an intracellular sensor of Ca^{2+} during muscle contraction (Monastyrskaya *et al*., 2009). It belongs to the network of membrane-cytoskeleton linkages (Chasserot-Golaz *et al*., 1996) and is also associated to CLATHRIN coated vesicles (Creutz and Snyder, 2005) and to early and late endosomes, where it appears to be involved in intracellular vesicle movement and MVB formation (Merrifield *et al*., 1999; Mayran *et al*., 2003).

Annexin A3 is mainly located at the plasma membrane and at the membranes of intracellular granules in human neutrophils (Ernst *et al*., 1990). Its expression is decreased in prostate cancer cells, which makes it a useful marker of the disease (Kollermann *et al*., 2008), and it has been reported to regulate hepatocyte regeneration (Harashima *et al*., 2008).

Annexin A4 is abundant in smooth muscle cells and cardiomyocytes (Monastyrskaya *et al*., 2009). In addition to its association to endosomes in hepatocytes (Pol *et al*., 1997), it has been mainly found at the plasma membrane and, depending on the tissue, on its apical or basolateral surfaces in polarized cells (Massey *et al*., 1991; Kojima *et al*., 1994). This annexin is known to be involved in apoptosis, cell cycling and anticoagulation. It is overexpressed in cancers of various origins, including gastric tumours, where it seems to regulate the expression of genes involved in tumourigenesis (Lin *et al*., 2012).

Table 2. Summary of the tissue distribution, intracellular localization and possible functions of annexins in mammalian cells.

Annexin	Tissue distribution	Intracellular localization	Possible functions
A1	Ubiquitous, abundant in smooth muscle and endothelial cells	Predominantly cytosolic, but also found in plasma membrane, early endosomes, MVB and phagosomes	• Ca^{2+}-dependent dynamics of ceramide platforms • Substrate of EGFR kinase • Inward vesiculation of MVB and EGFR inactivation • Membrane-cytoskeleton linkages • Inward vesiculation of phagosomes and their Interaction with actin • Autophagy induction, possibly by controlling amphisome formation
A2	Ubiquitous, abundant in smooth muscle and endothelial cells	CLATHRIN coated pits, early and late endosomes	• Membrane-cytoskeleton linkages • Intracellular Ca^{2+}-sensor of muscle contraction • Intracellular movements of early and late endosomes • MVB formation
A3	Abundant in neutrophils and placenta Present in hepatocytes and prostate tissues	Plasma membrane, membranes of intracellular granules	• Regulation of hepatocytes regeneration
A4	Ubiquitous, abundant in smooth muscle cells and cardiomyocytes and present in polarized cells and hepatocytes	Plasma membrane, endosomes	• Apoptosis, cell cycling and anticoagulation • Regulation of the expression of cancer-related genes
A5	Ubiquitous, abundant in cardiomyocytes and endothelial cells	Plasma membrane, endocytic vesicles, endoplasmic/sarcoplasmic reticulum, Golgi complex and nucleus	• Anti-coagulant activity • Protein kinase C inactivation • Membrane-cytoskeleton linkages • Vesicle aggregation • Cell membrane repair

A6	Ubiquitous, abundant in cardiomyocytes, endothelial and smooth muscle cells	Apical membranes, sarcolemma of smooth muscle, synaptic vesicles, plasma membrane, CLATHRIN-coated vesicles, late endosomes and lysosomes	• Membrane-cytoskeleton linkages • Contraction of cardiomyocytes • Regulation of programmed cell death in neurons • Regulation of CLATHRIN-mediated endocytosis • Cholesterol accumulation in late endosomes • Vesicle fusions and endocytic traffic • Stabilization of lipid rafts at plasma membranes
A7	Ubiquitous, abundant in cardiomyocytes, and chromaffin cells and present in macrophages	Cytosol, nucleus, phagosome membranes and chromaffin granules	• Candidate tumour suppressor in prostate cancer • Autophagy induction, likely by modulating intracellular Ca^{2+} levels • Membrane fusions • Aggregation of chromaffin granules
A8	Skin, eye and tongue	Late endosomes	• Membrane-cytoskeleton linkages • Actin-dependent fusion of late endosomes
A9	Tongue, spleen and liver. Up-regulation in prostate and colon cancers	Plasma membrane of breast cancer cells under high Ca^{2+} levels	• Unknown
A10	Foetal and adult gastric mucosa	Nucleus	• Unknown
A11	Ubiquitous	Nucleus and nuclear envelope (depending on intracellular Ca^{2+} levels or cell cycle progression)	• Regulation of cell cycle progression
A13	Polarized cells, such as enterocytes	Trans-Golgi network and surface of apical cells	• Regulation of apical vesicle transport to basolateral membranes

Annexin A5 is ubiquitously expressed and is abundant in cadiomyocytes and endothelial cells (Monastyrskaya *et al*., 2009). Like other annexins, it is found at the plasma membrane and in endocytic vesicles (Rambotti *et al*., 1993; Barwise and Walker, 1996; Diakonova *et al*., 1997), but also in the endoplasmic and sarcoplasmic reticulum, in the Golgi complex (Giambanco *et al*., 1993; Rambotti *et al*., 1993; Barwise and Walker, 1996) and within the nucleus (Mohiti *et al*., 1997). However, its intracellular function is poorly understood, apart from an anti-coagulant activity (Rothhut *et al*., 1989), an involvement in the inactivation of PKC (Dubois *et al*., 1998), an *in vitro* ability to aggregate vesicles in a pH-dependent manner (Hoekstra *et al*., 1993) and a role in cell membrane repair (Bouter *et al*., 2011). It should be also mentioned here that annexin A5 is extensively used to measure apoptosis, because it binds to phosphatidylserine exposed on the outer leaflet of the plasma membrane, an event that occurs in apoptotic cells.

Annexin A6 is one of the more ubiquitous annexins. It is abundant in smooth muscle and endothelial cells (Monastyrskaya *et al*., 2009) and in cardiomyocytes, where it regulates contraction processes (Mishra *et al*., 2011). It has a wide range of intracellular localizations, including the apical surface of plasma membrane (Ortega *et al*., 1998), synaptic vesicles (Inui *et al*., 1994) and sarcolemma of smooth muscle cells (Hazarika *et al*., 1991b; Hazarika *et al*., 1991a), where it organizes microdomains enriched in lipid rafts (Babiychuk *et al*., 2000), late endosomal and pre-lysosomal compartments (Grewal *et al*., 2000; Pons *et al*., 2000) in which it induces the accumulation of cholesterol (Cubells *et al*., 2007) and the budding of CLATHRIN coated pits (Lin *et al*., 1992). Its various intracellular localizations confer to this protein several functions, ranging from the regulation of vesicle fusion and CLATHRIN-mediated endocytosis (Futter and White, 2007) to the regulation of programmed cell death in neurons (Wang *et al*., 1997).

Annexin A7 is especially abundant in cardiomyocytes (Monastyrskaya *et al*., 2009). It was initially found in chromaffin cells, where it promotes the aggregation of their granules (Zaks and Creutz, 1990). Its presence has also been documented in macrophages, where it binds to phagosome membranes (Pittis and Garcia, 1999). It has been found in the cytosol and in the nucleus (Rick *et al*., 2005) and, since it inhibits prostate cell migration, it is considered a possible tumour suppressor in prostate cancer, (Srivastava *et al*., 2007). Also, this protein is proposed to play a role in membrane fusions (Gerelsaikhan *et al*., 2012). It was recently shown to induce autophagy and to decrease the intracellular Ca^{2+} concentration (Wang *et al*., 2010). However, whether this effect on intracellular Ca^{2+} modulates autophagy or not, remains to be elucidated.

Annexin A8 is localized in late endosomes where it plays a role in the binding of the membranes of these organelles with actin filaments (Goebeler *et al*., 2008).

Annexin A9 is an atypical member of the annexin family, because it lacks its type II Ca^{2+}-binding domain (Morgan and Fernandez, 1998). Its intracellular distribution and function remain to be studied, albeit its expression was found to be up-regulated in prostate and colon cancers (Gerke and Moss, 2002). Rise of intracellular Ca^{2+} was shown to translocate this protein to the cell surface in breast cancer cells (Bode *et al*., 2008).

Annexin A10 is a nuclear annexin specifically expressed in foetal and adult gastric mucosa (Lu *et al*., 2011). It is down-regulated in gastric carcinoma (Kim *et al*., 2010).

Annexin A11 resides in the nucleus of a wide range of cell lines. Its translocation to the nuclear envelope can be regulated by elevation of intracellular Ca^{2+} levels or by the progression of cell cycle (Tomas and Moss, 2003). It is a substrate of mitogen activated protein kinase (Furge *et al*., 1999) and this has been associated with the regulation of the progression of the cell cycle (Tomas and Moss, 2003). One of its interactors

is ALG-2 (Satoh *et al*., 2002), a Ca^{2+}-sensor for later fusion events in the endolysosomal system (see p. 27) that also binds *in vitro* to copine 1 (see Table 3).

Finally, **Annexin A13** is considered the original progenitor of the 11 other members of vertebrate annexins (Turnay *et al*., 2005). It binds to intracellular lipid microdomains to regulate apical vesicle transport in certain polarized epithelial cells (Lafont *et al*., 1998).

3.2. The copines

3.2.1. The origins of the family

The first copine was discovered, almost two decades ago, while identifying proteins involved in membrane trafficking in the ciliate *Paramecium tetraurelia* (Creutz *et al*., 1998). This novel 55 kDa protein had similar properties to the annexins, with two Ca^{2+} and phospholipid-binding regions and a unique core domain responsible of the interaction with other proteins in a Ca^{2+} or Mg^{2+}-dependent manner. These binding properties confer to the protein their exclusive biochemical characteristics and since it was identified by a French group it was named copine (the French translation of “companion”). In this pioneering work, two closely related genes were identified (*CPN1* and *CPN2*) and databases revealed the presence of various copine homologues in green plants and nematodes. In humans, five genes (*CPNI, II, III, IV* and *V)* were identified (Creutz *et al*., 1998), but soon, two others (*CPNVI, also called N-CPN,* and *CPNVII*) were found in the hippocampus (Nakayama *et al*., 1998) and in breast cancer tissues (Savino *et al*., 1999), respectively. The *CPNI* gene, whose expression is the highest, shares 60, 78, 53 and 56% of sequence identities with *CPNII-V*, respectively, and 40, 40 and 33% identities with the copine genes from the nematode *Caenorhabditis elegans*, the green plant *Arabidopsis thaliana* and the ciliate *Paramecium tetraurelia*, respectively

(Creutz *et al*., 1998). Thus, copines are a family of highly conserved Ca^{2+}-binding proteins present in many eukaryotic organisms.

3.2.2. Structure and function of copines

The copines contain two C2 domains at the N-terminal region and a core "A domain" at the C-terminal region (Fig. 11A) (Creutz *et al*., 1998).

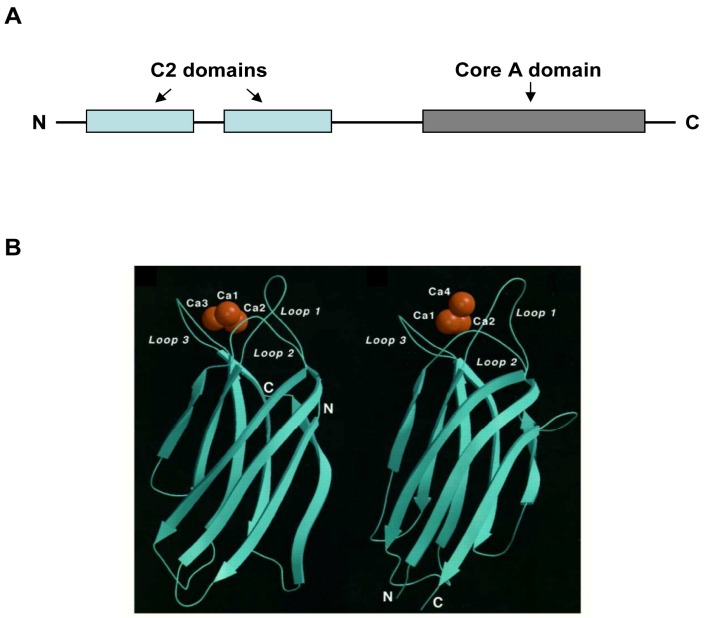

Figure 11. Representations of the domains of copines. (**A**) Schematic representation of the two types of domains, C2 and A, present in all copines. (**B**) Three-dimensional structure of the C2 domain from synaptotagmin I (left) and phospholipase C δ1 (right) (Rizo and Sudhof, 1998). The N- and C- termini are indicated. Each of the three Ca^{2+}-binding loops at the top of the C_2-domains are shown bound to a Ca^{2+} ion (orange sphere). In the C2 domain of synaptotagmin I, loops 1 and 3 contain three Ca^{2+}-binding sites (*Ca1*, *Ca2,* and *Ca3*). The C2 domain of phospholipase C δ1 shares two of the Ca^{2+}-binding sites of the synaptotagmin I C2 domain (Ca1 and Ca2), but contains a distinct third Ca^{2+}-binding site (Ca4).

The C2 domain, one of the most abundant Ca^{2+}-binding motifs, consists in three Ca^{2+}-binding loops located at the end of an eight-stranded antiparallel β sandwich and confers to the proteins a Ca^{2+}-dependent phospholipid-binding property (Fig. 11B). It was initially identified in protein kinase C and is also present in proteins involved in membrane trafficking,

such as synaptotagmin, phospholipase C, double C2 protein, rabphilin and chromobindin (Cho and Stahelin, 2006). Moreover, in a human kidney cell line, the C2 domain was found to be crucial for the Ca^{2+}-dependent translocation of some copines (1, 2, 3, 6 and 7) to the plasma membrane and to the membranes of different vesicles, suggesting a role of copines in vesicular trafficking (Perestenko *et al*., 2010).

As for the core A domain of copines, its primary structure does not share high similarity with other proteins (Creutz *et al*., 1998), suggesting an exclusive biological function. Nevertheless, this domain is reminiscent of the one responsible for the Ca^{2+}, Mg^{2+} or Mn^{2+}-dependent protein-binding characteristic of integrins and of some extracellular matrix proteins, such as collagen, matrilin, cochlin/vitrin and von Willebrand factor (Lee *et al*., 1995; Whittaker and Hynes, 2002). However, although native copine has been reported to bind Ca^{2+}, Mg^{2+}, and Mn^{2+} (Tomsig and Creutz, 2000), a yeast double hybrid screening analysis, using the A domain sequence as a bait, identified various proteins that interacted with copines 1, 2 and 4 in a Mg^{2+}-independent way (Tomsig *et al*., 2003). Therefore, the A domain probably binds proteins without the need of Mg^{2+}. The interactors of copine 1 identified in this screening analysis frequently contain a characteristic coiled-coil domain (with the consensus sequence E....R..R.L.E..EQ.RK.LELR..KQR...EL.QLD.E.E) that binds to the A domain of copine 1 (Tomsig *et al*., 2003). They are mainly proteins involved in intracellular signalling, including Ca^{2+}-binding proteins and proteins related with protein phosphorylation, ubiquitination/NEDDylation, cytoskeletal organization, exocytosis and mitosis (Table 3).

Table 3. List of interactors with the A domain of copine 1 identified in two-hybrid screening and pull-down experiments (Tomsig *et al.*, 2003). 5 proteins have been confirmed by both techniques. Interaction levels are ranged from – (null) to + (low) and ++ (high). MEK1 is a predicted interactor because it buries an α coiled-coil domain that binds to the A domain of copine 1.

Protein subgroup	Protein	Two-hybrid	Pull-down
Protein phosphorylation	Protein phosphatase 5	+ +	+ +
	Cdc42-binding kinase	-	+ +
	MAP kinase kinase (MEK1)	Predicted	+ +
Transcription	*Myc* binding protein	+	+ +
	SNO proto-oncogene	-	+
	Octamer binding protein	-	+ +
	BCL-6 co-repressor (BCOR)	-	+
	Wilm's tumour 1 associating protein (WTAP)	-	+ +
Ca^{2+}-binding proteins	Copine 1	-	+ +
	Apoptosis linked gene-2 (ALG-2)	-	+
Ubiquitination/ NEDDylation	UBC12 homolog (NEED8 conjugating enzyme)	-	+ +
	Ubiquitin conjugating enzyme (E2-230K)	+	+ +
Cytoskeleton	Radixin	+ +	+
	β-actin	+	+ +
	β-spectrin	-	+
	Collagen V α	-	+ +
Exocytosis	K1AA1217 protein (homolog of SNIP: SNAP25 interacting protein)	-	+ +
Mitosis	Kinetochore-binding protein, mitosin homolog (LEK1)	-	+ +
Others	DXImx40e protein (JM1 protein)	-	++
	PYK2 N-terminal domain-interacting receptor (NIR3)	-	++

As copines bind phospholipid membranes in a Ca^{2+}-dependent manner by the two C2 domains, and associate to other proteins *via* the A domain, it is possible that copines recruit proteins involved in membrane trafficking pathways. Support for this hypothesis was later provided by the involvement of copine 1 in the tumour necrosis factor-α receptor signalling (Tomsig *et al*., 2004).

An atomic force microscopy study has shown that copine 1 binds through its C2 domains to specific membrane areas created by annexin A1 (a member of another class of proteins involved in Ca^{2+}-dependent signal transduction at the cell membrane) and enriched in acidic phospholipids (phosphatidylserine and phosphatidylcholine) (Creutz and Edwardson, 2009). The formation of a copine scaffold in these areas may be important for the assembly of signalling molecules that bind to its A domain in membranes and, therefore, it will be interesting to determine the molecular structure of these complexes.

A more recent study postulates that C2 domains do not suffice for the association of copines to membranes and that a conserved 22 amino acid motif after the C2 domains is indispensable for the translocation of copines to the intracellular membranes (Perestenko *et al*., 2010). Moreover, this same study showed that the A domain of copines modulates both their Ca^{2+} response and their intracellular targeting. Therefore, a mutual regulation between the C2 and A domains is likely to occur in the targeting of copines to specific intracellular membranes and possibly in their interaction with other proteins.

Overall, the C2 domains followed by a conserved 22 amino acid motif enable copines to bind to intracellular membranes in a Ca^{2+}-dependent manner. Whereas the A domain confers to these proteins the property of recruiting other proteins, mainly involved in intracellular signalling. An interplay between these domains seems to coordinate the localization of copines and their functions in membrane trafficking.

3.2.3. Tissue distribution and intracellular localization of copines

Copine 1, the first protein of the copine family whose distribution was described, is ubiquitously expressed (Nakayama *et al*., 1998; Tomsig and Creutz, 2000, 2002). In mammalian cells, and in contrast to *Paramecium* whose major Ca^{2+}-dependent phospholipid-binding proteins are the two copine isoforms 1 and 2 (Creutz *et al*., 1998), copine 1 is a minor component of the Ca^{2+}-dependent phospholipid-binding proteins (Tomsig and Creutz, 2000). In rats, the highest copine 1 levels are found in the spleen (Tomsig and Creutz, 2000). However, a screening of different mouse and bovine tissues outlined an ubiquitous expression of copines 2-7 (Tomsig and Creutz, 2002). In humans, copine 2 and 3 are also ubiquitously expressed, while copine 4 expression is limited to brain, heart and prostate and copine 6 is specific to brain (Nakayama *et al*., 1998).

In HEK-293 cells (a human embryonic kidney cell line), an increase in intracellular levels of Ca^{2+} causes the translocation of copines 1-7 to the plasma membrane and also of copines 1, 2, 3 and 7 to the nucleus (Perestenko *et al*., 2010). In *Dictyostelium discoideum*, the distribution of copine A, homologous of human copine 1 and the most abundant of the six copines (A-F) of this organism, was mainly cytosolic (Damer *et al*., 2005). However, under starvation, copine A transiently localizes to the plasma membrane and intracellular vacuoles, including contractile vacuoles, endolysosomal compartments and phagosomes, by a mechanism that requires Ca^{2+} (Damer *et al*., 2005). Since copine 1 was found on autophagosomal membranes from rat liver (Overbye *et al*., 2007) and on lysosomal membranes from mouse fibroblasts (Ghislat *et al*., 2012b), this protein appears to have a possible role in endocytosis and in autophagy.

In summary, since the discovery of the first annexin in 1978 and the first copine in 1998, many studies -more *in vitro* than *in vivo*- have revealed various biochemical and biological functions of the members of these two families. Although *in vitro* analysis attribute to annexin and copine family members the same or similar Ca^{2+}-related features, *in vivo* outcomes show their involvement in a great range of cellular activities. Thus, ascribing credit for a specific physiological role to these two families of proteins becomes an ever-increasing challenge. In general, common consensus concerning annexins and copines seems to reside in their translocation to intracellular membranes under Ca^{2+} stimuli, their involvement in the traffic of vesicular membranes, especially those related with the endolysosomal system and their participation in the organization of lipid microdomains and cytoskeleton-membrane interactions. With regard to autophagy, three proteins of these two families were hitherto related to this process: copine 1 was identified as a protein associated to autophagosomal membranes in a proteomic study (Overbye *et al*., 2007). Annexins A1 (Kang *et al*., 2011) and A7 (Wang *et al*., 2010) were shown to induce the formation of autophagosomes, likely by controlling amphisome formation and intracellular Ca^{2+} levels, respectively. In this doctoral thesis, on the basis of a proteomic analysis (see Results, Chapter1), we will mainly focus on the roles of annexin A5, but also of annexin A1 and copine 1, in the autophagic and endocytic processes.

2. OBJECTIVES

Three Ca^{2+}-binding proteins, whose levels increase in lysosomal membranes of NIH3T3 mouse fibroblasts under high proteolysis conditions, especially under amino acid starvation, were identified in a proteomic analysis. On the basis of these results, the general aim of this thesis was to investigate the involvement of Ca^{2+} and of these Ca^{2+}-binding proteins in the regulation of autophagy.

More specifically, we have tried here to answer two main questions:

1. What is the Ca^{2+}-signalling pathway triggered by amino acid starvation that leads to autophagy induction?

2. What are the roles of the Ca^{2+}-binding proteins identified in the proteomic study, annexin A1, annexin A5 and copine 1 in autophagy?

3. RESULTS: CHAPTER 1

Identification of proteins associated to lysosomal membranes under different proteolytic conditions

Abstract

Lysosomes are key organelles for the breakdown of material delivered to these organelles by endocytosis or autophagy. Whereas acid hydrolases in their matrixes take charge of the cargo clearance, the proteins on their membranes play multiple roles, including, among others, the acidification of the lysosomal lumen, the separation of the hydrolytic enzymes from the cytosol, the exit of the degradation products to the cytosol and the participation in a dynamic series of fusion and fission processes in conjunction with the endocytic and autophagic machinery. These functions frequently require cytosolic proteins, some of them not yet known, for interaction with lysosomal membranes. To identify some of these proteins, here we report a proteomic analysis of lysosomal membranes from cells incubated in various media that affect intracellular proteolysis. Twelve proteins whose levels in these membranes clearly change between high and low proteolysis conditions were identified. They include subunits of the vacuolar ATPase and proteins related with Ca^{2+}-dependent signalling, carbohydrate metabolism, vesicle trafficking and protein synthesis. The possible roles of these proteins in lysosomal membranes are discussed.

Introduction

Lysosomes are the main degradative organelles in the cell. They are especially active in challenging stress situations, for example when nutrients are scarce and an intracellular supply of energy and building blocks becomes indispensable for cell homeostasis.

Lysosomes receive the cargo destined for degradation mostly *via* autophagic and endocytic pathways (Saftig and Klumperman, 2009) and its catabolism takes place inside the lysosomes by the action of hydrolases with an optimal acid pH. The catabolic enzymes of lysosomes are preserved from leaking into the cytosol by membranes that allow the transfer of the degraded material from the lysosomal lumen to the cytosol for either

resynthesis of complex molecules or energy supply. These limiting membranes consist of a lipid bilayer and various transmembrane and membrane-binding proteins. Although several integral and peripheral membrane proteins from lysosomes have been identified in various proteomic studies (*e.g.* (Bagshaw *et al*., 2005; Schroder *et al*., 2007; Nylandsted *et al*., 2011)), the functions of most of them in these organelles are still not well understood.

Lysosomal degradation depends on the nutritional and hormonal state of the cell. In early studies, nutritional or hormonal factors, such as amino acids or insulin, were shown to reduce the proteolytic activity of lysosomes (reviewed in (Kadowaki and Kanazawa, 2003; Lavallard *et al*., 2012)). Thus, it is probable that the availability of these factors in the extracellular medium affects the lysosomal membrane proteome to adapt the lysosomal activity to the environmental situation. Therefore, we intended here to identify lysosomal membrane proteins, whose levels change under high and low proteolysis conditions, by using a proteomic analysis of lysosomal membranes from mouse fibroblasts subjected to starvation (KH: Krebs-Henseleit medium) without or with insulin and amino acids (separately or together) that, respectively, produce high, intermediate or low proteolysis in these cells. Comparisons of the lysosomal membrane proteome under the various conditions revealed changes in the levels of proteins, some of them well-known members of lysosomal membranes but some others not yet identified in this compartment. We have classified these proteins according to their biochemical properties and discuss their possible roles in lysosomal proteolysis.

Materials and Methods

Materials

Dulbecco's modified Eagle's medium (DMEM), human insulin, and NH_4Cl were purchased from Sigma Chemical Co. MEM essential amino

acids 50x, foetal bovine serum, penicillin and streptomycin were supplied by Invitrogen Life Technologies. Metrizamide was from Nycomed and Percoll from Amersham Pharmacia Biotech Inc. Other reagents, purchased from Sigma Chemical Co, Invitrogen Life Technologies or Calbiochem, were of analytical grade.

Cell culture

NIH3T3 mouse embryonic fibroblasts were obtained from the European Collection of Animal Cell Cultures. Cells were grown at 37°C in a humidified atmosphere of 5% CO_2/air (v/v) in DMEM containing 10% foetal bovine serum and 1% penicillin–streptomycin. Normal human skin fibroblasts were obtained from the Coriell Institute for Medical Research (Camden, NJ, USA) and were grown as described (Esteban *et al.*, 2007). KH (118.4 mM NaCl, 4.75 mM KCl, 1.19 mM KH_2PO4, 2.54 mM $MgSO_4$, 2.44 mM $CaCl_2{\cdot}2H_2O$, 28.6 mM $NaHCO_3$, 20 mM glucose) with 10 mM 4-(2-hydroxyethyl)-1-piperazineethanesulfonic acid (Hepes), pH 7.4, was used for high proteolysis (starvation) conditions. For intermediate or low proteolysis conditions, insulin 0.1 μM, essential amino acids at two times the concentration present in MEM or both were added to KH.

Protein degradation experiments

To label proteins, NIH3T3 were incubated at 37°C for 48 h in fresh full medium with 1 μCi/ml ^{3}H-valine (Hartmann Analytic). Before the proteolysis experiments were started, the cells were washed once with full medium, containing 10 mM L-valine, and chased for 24 h at 37ºC in this medium to eliminate short-lived proteins. Proteolysis experiments and measurements of intracellular protein degradation were carried out as described previously (Fuertes *et al.*, 2003b; Fuertes *et al.*, 2003a). NH_4Cl (20 mM) plus leupeptin (0.1 mM) were used to inhibit lysosomal proteolytic activity. Although NH_4Cl has been shown to stimulate autophagosome formation (Eng *et al.*, 2010), similar results were obtained with other lysosomal inhibitors (such as bafilomycin A1 and, in some cases, chloroquine or E64d + pepstatin A). The

contribution of the lysosomal pathways to intracellular protein degradation was calculated by the inhibition obtained with NH_4Cl + leupeptin. Protein degradation was analysed 1 h after the addition of the different inhibitors and for a period of only 3 additional h to ensure optimal inhibition and to avoid possible secondary effects of the inhibitors. All experiments were performed with duplicate or triplicate samples.

Subcellular fractionation

NIH3T3 cells were incubated in KH without or with insulin, amino acids or both of them, washed with phosphate-buffered saline (PBS) and pooled in ice-cold homogenisation buffer (250 mM sucrose, 20 mM Hepes, 1 mM EDTA, pH 7.4). Then, cells were homogenised at 4°C in two steps, first in a nitrogen cavitation pump (2.41×10^5 Pa, 7 min) and then with a tight-fitting Dounce homogeniser (10 strokes). A lysosomal fraction was prepared following a procedure described elsewhere (Storrie and Madden, 1990). Briefly, homogenates were centrifuged at 3,000 g for 10 min at 4°C and the post nuclear supernatant was applied to a Percoll–metrizamide gradient (from top to bottom: 6% Percoll; 17% and 35% metrizamide) and centrifuged at 53,000 g for 35 min at 4°C in an SW41Ti rotor (Beckman). To separate lysosomes from mitochondria, the 6% Percoll/17% metrizamide interface was brought to 35% metrizamide and placed on the bottom of a second gradient of sucrose–metrizamide (from top to bottom: 0.25 M sucrose with 5%, 17% and 35% metrizamide). After centrifugation at 53,000 g for 30 min, 4°C, lysosomes were collected from the 5%/17% metrizamide interface, and incubated 15 min at 37ºC to digest the sequestered material. Subsequently, lysosomes were diluted in 0.025 M sucrose and disrupted by freezing and thawing, ten times. The pelleted lysosomal membranes were obtained by centrifugation at 105,000 g for 20 min at 4°C, in a Beckman Airfuge (rotor A-100), and washed three times in water with protease inhibitors (100 µM leupeptin, 10 µM pepstatin A, 1 mM phenylmethanesulfonylfluoride, 2 mM

EDTA and 2 mM dithiothreitol). Lysosomal membranes were then resuspended in water with the same inhibitor cocktail.

Two-dimensional electrophoresis and mass spectroscopy (MS)

Two dimensional-difference gel electrophoresis (2D-DIGE) of lysosomal membranes was carried out essentially as previously described (Bernal *et al*., 2006). Lysosomal membranes, purified as above, were solubilised in 7 M urea, 2 M thiourea, 4% (w/v) CHAPS, 20 mM dithiothreitol, 2% (v/v) Biolytes 3-10 and Bromophenol Blue (all chemicals from Bio-Rad). Samples of 100 µg protein were subjected in gel strips to isoelectric focusing generated on a Bio-Rad PROTEAN® IEF Cell at 20°C. Subsequently, the strips were reduced and alkylated (using in succession 2.5% iodoacetamide and 2% dithiothreitol) in equilibration buffer containing 6 M urea, 0.375 M Tris pH 8.8, 2% sodium dodecyl sulfate and 20% glycerol. Polyacrylamide gels (10%) were employed for the second dimension. The spots observed in the gel were manually excised, washed twice in double distilled water and digested with sequencing grade trypsin (Promega) as described previously (Andresen *et al*., 1989). Proteins were identified by MS in a 4700 Proteomics analyser (Applied Biosystems). A MASCOT search engine (Matrix-Science, London, UK) was used for a search on SwissProt and NCBI® databases. The accuracy of the protein identifications was considered when at least three peptides were detected with an overall MASCOT score>50. The significance threshold for a change in protein levels in the various conditions was set to $P \leq 0.05$ and the values were determined by factorial ANOVA tests using STATVIEW v4.53 (Abacus Concepts).

Electron microscopy and morphometric analysis

Cells were washed with ice-cold PBS and fixed for 15 min in the dishes by direct addition of a mixture of 2% (v/v) glutaraldehyde and 1% formaldehyde (EM grade; Polysciences, Warrington, PA, U.S.A.) buffered with 0.05 M sodium cacodylate (pH 7.4). The cells were detached from the dishes by gentle scraping with a rubber policeman and further fixed as

above for 45 min. Then, the cells were washed three times for 30 min in 0.05 M sodium cacodylate buffer, postfixed in a mixture of 1% osmium tetroxide (Polysciences) and 1% potassium ferrocyanide for 60 min, incubated for 1 min in 0.15% tannic acid in 0.1 M sodium cacodylate buffer and washed overnight in 0.1 M sodium cacodylate buffer. All these treatments were performed at 0–4ºC and under iso-osmolar conditions by adding sucrose when needed. The following day, the fixed cells were stained with 2% (w/v) uranyl acetate for 2 h at 20ºC and dehydrated, embedded in Poly/Bed 812 resin (Polysciences) and polymerized according to the manufacturer's instructions. Ultrathin sections of approximately 60–70 nm were cut with an LKB 4801A from LKB-Microtomy Systems (Leica Cambridge Ltd., Cambridge, UK) and were observed with a Philips CM-10 transmission electron microscope (Eindhoven, Netherlands) at 60 kV. Morphometric analysis of lysosomes was performed as previously described (Knecht *et al*., 1984), in randomly selected electron micrographs (18×24 cm^2) at a final magnification of ×10,500. For each measurement, the fractional volume of lysosomes was estimated by a point counting method using Weibel's multipurpose test system in 30 electron micrographs from three different experiments. Sediments from subcellular fractions were fixed and embedded as described above.

Measurements of lysosomal pH

To measure the pH within lysosomes, cells previously seeded in 6-well plates were loaded with 0.5 mg/ml fluorescein isothiocyanate (FITC)-dextran for 18 h. Cells were then washed five times with PBS and incubated for 4 h in KH without or with insulin, amino acids or both of them to chase the dextran conjugate from endosomes. Control samples were incubated in KH supplemented with 20 mM NH_4Cl. Subsequently, cells were transferred to a 96-well plate and were immediately placed in a SpectraMax M5 multimode plate reader for measurement of FITC (excitation: 495 nm for pH-dependent (λ1) and 450 nm for pH independent (λ2), emission: 525 nm) fluorescence emissions. The λ1/λ2 ratios of fluorescence emission were calculated and

calibration of these ratios *versus* pH was obtained using a standard curve prepared with McIlvaine's buffers (pHs ranging from 4.0 to 6.0), containing sodium azide (50 mM), 2-deoxyglucose (50 mM), nigericin (10 mM) and monensin (20 mM).

Quantification and statistics

P-values were determined by factorial ANOVA tests using GraphPad Prism Software and are indicated in all figures by asterisks: ****P*<0.0005, ***P*<0.005 and **P*<0.05.

Results and Discussion

High and low proteolysis conditions alter the proteome of lysosomal membranes

The incubations of NIH3T3 cells in KH without or with insulin, amino acids or both of them cause, as expected, respectively high, intermediate and low cellular proteolytic activity, as judged by the rate of total and lysosomal degradation of long lived proteins (Fig. 1A). As expected also, insulin and amino acids decrease the fractional volume of early (Av_i) and late (Av_d) autophagic vacuoles (Fig. 1B), confirming in NIH3T3 cells the negative effect of these factors on autophagy.

To identify proteins involved in the regulation of lysosomal proteolytic pathways, we purified lysosomes from NIH3T3 cells incubated in KH without and with insulin, amino acids or both of them, following the experimental procedures described in Materials and Methods. The purity of the lysosomal fraction obtained (yield was about 5%) was verified by electron microscopy (Fig. 1C) and by calculating the enrichment in β-*N*-acetyl-glucosaminidase and β-hexosaminidase (28.1 ± 1.5). Also, contamination of any of the fractions with mitochondria (based on the activity of succinate dehydrogenase) or cytosol (based on the activity of lactate dehydrogenase and glyceraldehyde 3-phosphate dehydrogenase) was negligible.

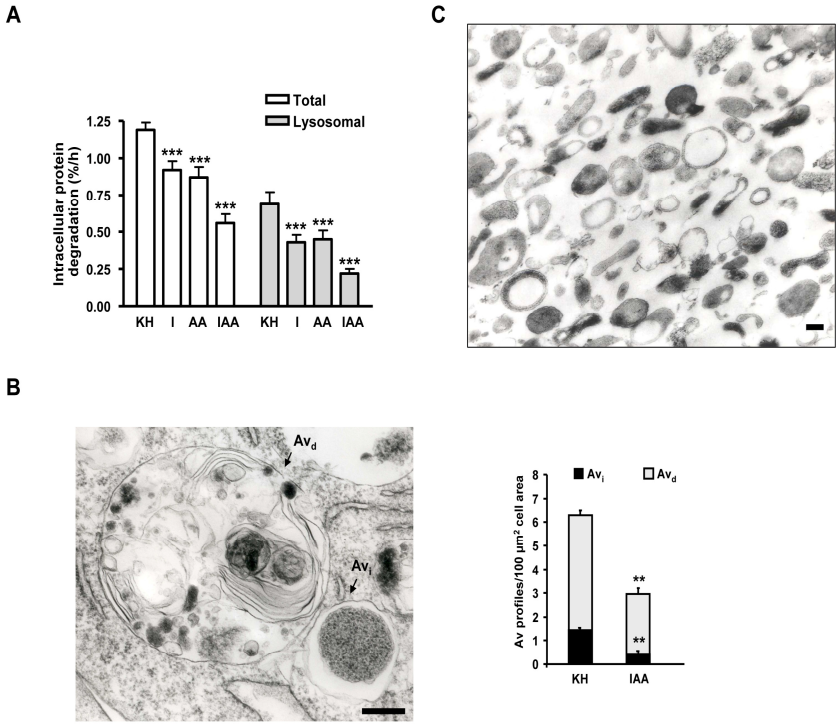

Figure 1. (**A**) Exponentially growing NIH3T3 cells were metabolically labelled with ^{3}H-valine for 48 h, chased for 24 h and then switched for 4 h to KH without (KH) or with insulin (I), amino acids (AA) or both of them (IAA). Total and lysosomal protein degradation were calculated as described in Materials and Methods. Results from three separate experiments with duplicated samples are shown as the percentage of the labelled proteins that were degraded per h under the different conditions. Differences were found to be statistically significant at ****P*<0.0005. (**B**) Representative electron micrograph of NIH3T3 incubated in KH for 4 h showing early (Avi) and late (Avd) autophagic vacuoles. The histogram on the right shows the amounts of Avi and Avd in medium in the presence (IAA) or not (KH) of insulin and amino acids, measured by electron microscopic morphometry. Each value is the mean and S.D. from two separate experiments. Differences were found to be statistically significant at ***P*<0.005. (**C**) Representative electron micrograph of a purified lysosomal fraction of cells incubated in KH. Scale bars: 0.5 µm.

Next, lysosomes were disrupted and their membranes were purified and analysed by 2D-DIGE (Fig. 2), which showed variations in the levels of some proteins under high, intermediate and low proteolysis conditions

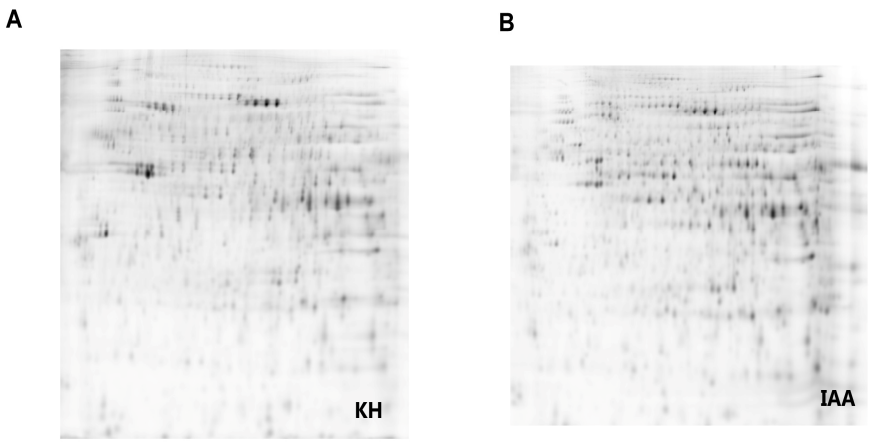

Figure 2. 2D-DIGE gels of proteins (100 µg) from lysosomal membranes isolated from NIH3T3 cells incubated for 4 h under conditions that produce high (**A**, KH) and low (**B**, IAA) proteolysis.

Identification of proteins with altered levels on lysosomal membranes under the different proteolysis conditions

Twelve proteins, whose levels in lysosomal membranes change under the different conditions were identified and grouped into four classes, according to their biochemical characteristics (Table 1). Four of these proteins were subunits of the vacuolar-type H^+-ATPase (V-ATPase). This is a well-known lysosomal membrane complex responsible for the acidification of lysosomes, composed of 14 subunits distributed in a cytosolic ATP-hydrolyzing sector (V_1) and a transmembranal H^+-translocating sector (V_0) (Mindell, 2012). The proteomic analysis showed that at least some of the subunits of V_1 (A, B, C, and E) decrease their levels in the presence of amino acids with and without insulin (Fig. 3A, C-E). In these experiments, no subunits of V_0 were detected, probably because their high hydrophobicity complicates their solubilisation and consequently their detection. Amino acids also cause a mild increase in lysosomal pH, whereas insulin does not affect it (Fig. 4), indicating that amino acids may change lysosomal pH by altering the activity of V-ATPase or perhaps by the ammonia produced in the catabolism of amino acids. This result is in agreement with an earlier study

suggesting that amino acids can inhibit lysosomal proteolysis by increasing lysosomal pH (Luiken *et al*., 1996). Interestingly, part of the A subunit of V_1, with a higher isoelectric point, increases its levels in the presence of amino acids with and without insulin (Fig. 3B and Fig. 5). This higher isoelectric point suggests a possible phosphorylation of subunit A and, in fact, subunit A of V_1 was already reported to be phosphorylated *via* PKA in the V-ATPase located at the plasma membrane (Alzamora *et al*., 2010). Unlike mammalian cells, the assembly of the V-ATPase has been extensively studied in yeast, where subunit A appears to be important for V_0/V_1 assembly (Kane, 2006). If this also occurs in mammalian cells, it is possible that phosphorylation of subunit A by amino acids leads to a disassembly of the complex and to a reduction of the lysosomal acidity, which is also important for the lysosomal fusion with autophagosomes (Kawai *et al*., 2007).

Amino acids also decreased the levels on lysosomal membranes of three proteins known to bind to phospholipids in a Ca^{2+}-dependent manner, annexin A5 (Ghislat *et al*., 2012a), annexin A1 and copine 1 (Fig. 3F and G). We previously reported that annexin A5 facilitates the fusion of lysosomes with autophagosomes (Ghislat *et al*., 2012a) (see Results, Chapter 3) and proposed, on the basis of various experiments, that copine 1 and annexin A1 participate in the completion of this event (Ghislat and Knecht, 2012) (see Results, Chapter 4). Moreover, another report showed that annexin A1 promotes autophagy and suggested that this protein plays a role in the formation of amphisomes, organelles that result from the fusion of autophagosomes with late endosomes (Kang *et al*., 2011). Since amino acids starvation raises intracellular Ca^{2+} (Ghislat *et al*., 2012b) (see Results, Chapter 2), this effect may induce the binding of these proteins to the lysosomal membrane in order to control the fusion of lysosomes with other organelles, such as autophagosomes. Furthermore, we found that annexin A5 inhibits certain types of endocytosis (especially macropinocytosis) (Ghislat *et al*., 2012a) (see Results, Chapter 3). However, further work is required to know whether the involvement of annexin A5 in endocytosis is

Ca^{2+}-dependent and whether this role depends on its localization on lysosomal membranes.

Two proteins involved in carbohydrate metabolism, NADP-dependent isocitrate dehydrogenase (IDH) and malate dehydrogenase (MDH), were found to increase their levels on lysosomal membranes in the presence of amino acids with and without insulin (Fig. 3H and I). Although these two enzymes possess cytosolic and mitochondrial isoforms and at least the cytosolic isoform of MDH was identified in a proteomic study of autophagosomal membranes (Overbye *et al*., 2007), the proteins identified here correspond to the mitochondrial isoforms on the basis of their isoelectric point (see Table 1). Therefore, at first glance these proteins appear to be mitochondrial contaminants of the lysosomal fraction. However if these contaminants derive from the autophagy of mitochondria, it is surprising that they increase under conditions that decrease autophagy (*e.g.* in the presence of amino acids).

Other proteins were also identified in the proteomic analysis. One of them is the α-soluble N-ethylmaleimide-sensitive factor attachment protein (α-SNAP), which is a well-known component of the vesicle trafficking machinery that mediates intermembrane fusion by interacting with SNAREs (Winter *et al*., 2009). Their lower levels on lysosomal membranes in the presence of amino acids (Fig. 3J) support again that amino acids may compromise the fusogenic ability of lysosomes with other organelles such as autophagosomes.

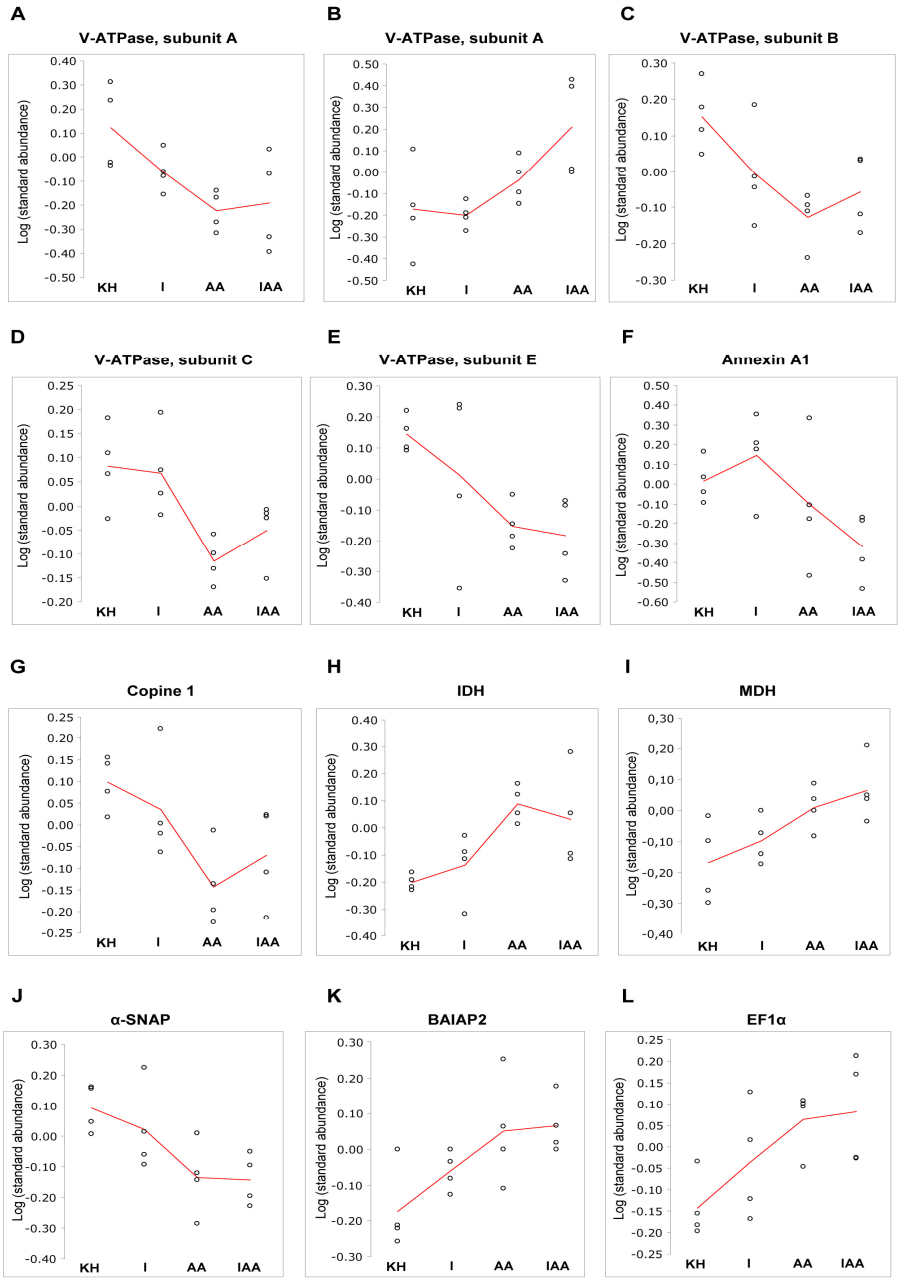

Figure 3. (**A-L**) Proteins that change their levels on lysosomal membranes isolated from cells incubated in KH without (KH) or with insulin (I), amino acids (AA) or both (IAA). Each dot corresponds to an individual experiment similar to that shown in Fig. 2. The lines join the mean values.

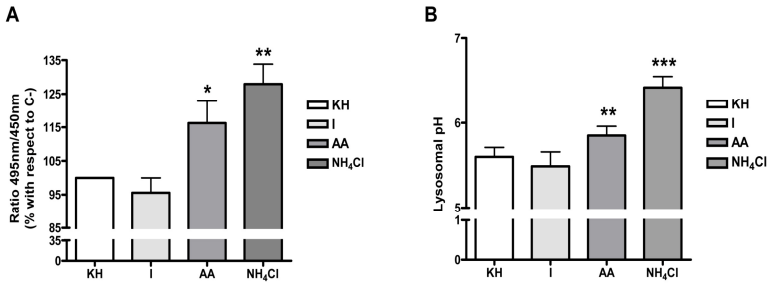

Figure 4. Amino acids, but not insulin, increase lysosomal pH. (**A**) Human fibroblasts were loaded with 0.5 mg/ml FITC-dextran for 18 h. Subsequently, cells were washed with PBS and incubated for 4 h in KH without (KH) or with insulin (I), amino acids (AA) or both of them (IAA) and, as a control, with NH_4Cl. Fluorescence intensity emitted by the dextran conjugate was assessed and λ1/λ2 ratios were measured as described in Materials and Methods. (**B**) Lysosomal pH measured as described in Materials and Methods in the different conditions. Means and SD from at least six different experiments are shown. Differences were found to be statistically significant at **P*<0.05, ***P*<0.005 and ****P*<0.0005.

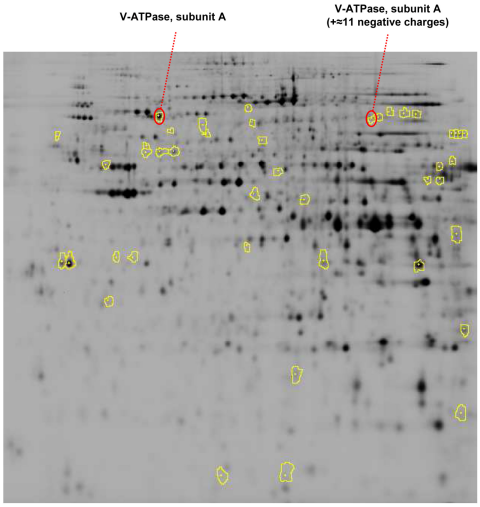

Figure 5. 2D gel with proteins (100 µg) from lysosomal membranes isolated from NIH3T3 cells incubated for 4 h under conditions that produce high (KH) proteolysis. The spots corresponding to the A subunit of V_1 with two different isoelectric points are indicated.

Another protein identified in this analysis, involved in endocytosis rather than in autophagy, is the brain specific angiogenesis inhibitor 1-associated protein 2 (BAIAP2). Its levels on lysosomal membranes were higher in the presence of amino acids (Fig. 3K). BAIAP2 was proposed to regulate actin dynamics and to generate the membrane curvature of

endocytic vesicles (Scita *et al*., 2008; Veltman *et al*., 2011). Although amino acids are well-known inhibitors of autophagy, we observed an enhanced fluid phase endocytic uptake in the presence of amino acids (see Results, Chapter 4). In agreement with our findings, amino acids, in addition to inhibit the class III phosphatidylinositol 3-kinase complex I (PI_3KI) that triggers autophagy, are thought to activate PI_3K complex II (PI_3KII), important for vesicle sorting during endocytosis and containing BIF-1, a curvature-sensing positive regulator (Ktistakis *et al*., 2012). Thus, it is possible that BAIAP2 association to lysosomal membranes in the presence of amino acids is related to the activation of the endocytosis in this condition.

The increased levels of the translation elongation factor EF1α in lysosomal membranes in the presence of amino acids (Fig. 3L) reminds the translocation of the well-known nutrient sensor and activator of protein synthesis, the mammalian target of rapamycin that, in the presence of amino acids, associates to lysosomal membranes, where it inhibits autophagy (Korolchuk and Rubinsztein, 2011). EF1α was previously reported to localize on lysosomal membranes (Bagshaw *et al*., 2005; Bandyopadhyay *et al*., 2010). This protein was shown to stabilize in these membranes the translocation complex of chaperone mediated autophagy, a selective autophagy that degrades cytosolic proteins in lysosomes (Bandyopadhyay *et al*., 2010). However, we found that the EF1α levels on lysosomal membranes increase under conditions where this autophagic pathway would be less active. Interestingly, amino acids activate Rag guanosine triphosphatases (GTPases) at lysosomal membranes (Zoncu *et al.*, 2011) and GTP seems to release EF1α from lysosomal membranes under starvation (Bandyopadhyay *et al*., 2010). Thus, the availability of amino acids may decrease GTP concentration in the proximity of the lysosome, avoiding in this way EF1α release from lysosomal membranes. Although a recent study showed that amino acids induce GTP loading of RagB on lysosomal membranes (Duran *et al.*, 2012), the levels of available free GTP for EF1 α release are unknown.

Table 1. Proteins identified in the proteomic analysis of lysosomal membranes, grouped into different categories according to their biochemical characteristics. The Swiss Prot access number of each protein is indicated. The theoretical isoelectric points and mass values were extracted from PhosphoSitePlus® (Hornbeck *et al*., 2012). Either increase (↑) or decrease (↓) of the protein levels on lysosomal membranes in the presence of insulin and amino acids (IAA) are indicated.

Protein category and description	SwissProt access nº	Theoretical isoelectric point	Observed isoelectric point	Theoretical mass (KDa)	Observed mass (KDa)	Changes in the presence of IAA
Lysosomal pH						
Vacuolar-type H^+-ATPase, subunit A, isoform 1	P50516	5.42	5.41	68.3	68.8	↓
Vacuolar-type H^+-ATPase , subunit B, isoform 2	P62814	5.57	5.57	56.7	56.8	↓
Vacuolar-type H^+-ATPase , subunit C	Q9Z1G3	7.02	6.28	43.9	41.9	↓
Vacuolar-type H^+-ATPase , subunit E	P50518	8.44	9.28	26.2	26.7	↓
Ca^{2+}-binding proteins						
Annexin A1	P10107	6.97	6.97	38.7	39.1	↓
Annexin A5	P48036	4.83	4.99	35.7	33.9	↓
Copine 1	Q8C166	5.40	5.34	58.9	50.2	↓
Carbohydrate metabolism						
NADP-dependent Isocitrate dehydrogenase	P54071	8.88	8.88	50.9	51.3	↑
Malate dehydrogenase	P08249	8.93	8.92	35.6	35.9	↑
Others						
Alpha-soluble N-ethylmaleimide-sensitive factor attachment protein	Q9DB05	5.30	5.26	33.2	39.2	↓
Brain specific angiogenesis inhibitor 1-associated protein 2	Q80Y61	9.51	8.97	58.4	57.7	↑
Elongation factor 1-alpha	P27706	9.10	9.10	50.4	50.4	↑

Concluding remarks

Overall, twelve proteins were identified in this proteomic study. The criteria for protein selection were restrictive and various proteins (keratins, plasma proteins, etc.) that are usually considered contaminants in MS analysis were discarded. In addition, it is clear that some proteins, such as transmembrane, low-abundance, high molecular weight and strongly alkaline proteins (Chevalier, 2010), were lost in this analysis.

Taking together, the results show that amino acids, more than insulin, affect the association of various proteins to lysosomal membranes, whereas the presence of both regulators may exert in some cases an enhanced effect on this association. We found, for the first time, annexin A5 associated to lysosomal membranes and identified its role in lysosomal fusion with autophagosomes (see Results, Chapter 3). Also, previously identified proteins in other proteomic analysis were found here to change their levels on lysosomal membranes, mainly depending on the presence or not of amino acids. They comprise, for example, several subunits of the V_0 and V_1 domains of V-ATPase (Bagshaw *et al*., 2005; Schroder *et al*., 2007), annexin A1 (Kang *et al*., 2011), and EF1α (Bagshaw *et al*., 2005; Bandyopadhyay *et al*., 2010). In relationship with autophagy, three proteins identified here were formerly found on autophagosomal membranes (copine 1 and MDH (Overbye *et al*., 2007)) and in a proteomic analysis of the autophagy interaction network (annexin A1 (Behrends *et al*., 2010)).

Depending on the protein, either an increase or a decrease of its levels on lysosomal membranes was observed. Proteins related to lysosomal pH, Ca^{2+}-signalling and the protein α-SNAP involved in vesicle trafficking decrease their levels in lysosomal membranes in the presence of amino acids with and without insulin. This indicates that most likely amino acids restrain lysosomal proteolysis by exerting an inhibitory effect on lysosomal pH, Ca^{2+}-signalling and vesicle traffic. In contrast, the roles in lysosomal function of the proteins with higher levels on lysosomal

membranes in the presence of amino acids remain to be elucidated. These proteins are related to lysosomal fusion/fission events during endocytosis (BAIAP2) and protein synthesis (EF1α).

In summary, at least some of these proteins could represent new regulators of lysosomal degradation, as we have shown for annexin A5 (Ghislat *et al*., 2012a) (see Results, Chapter 3), annexin A1 and copine 1 (see Results, Chapter 4), but further investigations are required to describe the molecular mechanisms by which they are involved in lysosomal proteolysis.

References

Alzamora R, Thali RF, Gong F, Smolak C, Li H, Baty CJ, Bertrand CA, Auchli Y, Brunisholz RA, Neumann D, Hallows KR, Pastor-Soler NM (2010) PKA regulates vacuolar H+-ATPase localization and activity via direct phosphorylation of the a subunit in kidney cells. J Biol Chem 285:24676-24685.

Andresen K, Simonsen PE, Andersen BJ, Birch-Andersen A (1989) Echinostoma caproni in mice: shedding of antigens from the surface of an intestinal trematode. Int J Parasitol 19:111-118.

Bagshaw RD, Mahuran DJ, Callahan JW (2005) A proteomic analysis of lysosomal integral membrane proteins reveals the diverse composition of the organelle. Mol Cell Proteomics 4:133-143.

Bandyopadhyay U, Sridhar S, Kaushik S, Kiffin R, Cuervo AM (2010) Identification of regulators of chaperone-mediated autophagy. Mol Cell 39:535-547.

Behrends C, Sowa ME, Gygi SP, Harper JW (2010) Network organization of the human autophagy system. Nature 466:68-76.

Bernal D, Carpena I, Espert AM, De la Rubia JE, Esteban JG, Toledo R, Marcilla A (2006) Identification of proteins in excretory/secretory extracts of Echinostoma friedi (Trematoda) from chronic and acute infections. Proteomics 6:2835-2843.

Chevalier F (2010) Highlights on the capacities of "Gel-based" proteomics. Proteome Sci 8:23.

Duran RV, Oppliger W, Robitaille AM, Heiserich L, Skendaj R, Gottlieb E, Hall MN (2012) Glutaminolysis activates Rag-mTORC1 signaling. Mol Cell 47:349-358.

Eng CH, Yu K, Lucas J, White E, Abraham RT (2010) Ammonia derived from glutaminolysis is a diffusible regulator of autophagy. Sci Signal 3:ra31.

Esteban I, Aguado C, Sanchez M, Knecht E (2007) Regulation of various proteolytic pathways by insulin and amino acids in human fibroblasts. FEBS Lett 581:3415-3421.

Fuertes G, Villarroya A, Knecht E (2003a) Role of proteasomes in the degradation of short-lived proteins in human fibroblasts under various growth conditions. Int J Biochem Cell Biol 35:651-664.

Fuertes G, Martin De Llano JJ, Villarroya A, Rivett AJ, Knecht E (2003b) Changes in the proteolytic activities of proteasomes and lysosomes in human fibroblasts produced by serum withdrawal, amino-acid deprivation and confluent conditions. Biochem J 375:75-86.

Ghislat G, Knecht E (2012) New Ca(2+)-dependent regulators of autophagosome maturation. Commun Integr Biol 5:308-311.

Ghislat G, Aguado C, Knecht E (2012a) Annexin A5 stimulates autophagy and inhibits endocytosis. J Cell Sci 125:92-107.

Ghislat G, Patron M, Rizzuto R, Knecht E (2012b) Withdrawal of essential amino acids increases autophagy by a pathway involving Ca2+/calmodulin-dependent kinase kinase-beta (CaMKK-beta). J Biol Chem 287:38625-38636.

Hornbeck PV, Kornhauser JM, Tkachev S, Zhang B, Skrzypek E, Murray B, Latham V, Sullivan M (2012) PhosphoSitePlus: a comprehensive resource for investigating the structure and function of experimentally determined post-translational modifications in man and mouse. Nucleic Acids Res 40:D261-270.

Kadowaki M, Kanazawa T (2003) Amino acids as regulators of proteolysis. J Nutr 133:2052S-2056S.

Kane PM (2006) The where, when, and how of organelle acidification by the yeast vacuolar H+-ATPase. Microbiol Mol Biol Rev 70:177-191.

Kang JH, Li M, Chen X, Yin XM (2011) Proteomics analysis of starved cells revealed Annexin A1 as an important regulator of autophagic degradation. Biochem Biophys Res Commun 407:581-586.

Kawai A, Uchiyama H, Takano S, Nakamura N, Ohkuma S (2007) Autophagosome-lysosome fusion depends on the pH in acidic compartments in CHO cells. Autophagy 3:154-157.

Knecht E, Hernandez-Yago J, Grisolia S (1984) Homogeneity among mitochondria revealed by a constant proportion of their enzymes. Histochemistry 80:359-362.

Korolchuk VI, Rubinsztein DC (2011) Regulation of autophagy by lysosomal positioning. Autophagy 7:927-928.

Ktistakis NT, Manifava M, Schoenfelder P, Rotondo S (2012) How phosphoinositide 3-phosphate controls growth downstream of amino acids and autophagy downstream of amino acid withdrawal. Biochem Soc Trans 40:37-43.

Lavallard VJ, Meijer AJ, Codogno P, Gual P (2012) Autophagy, signaling and obesity. Pharmacol Res 66:513-525.

Luiken JJ, Aerts JM, Meijer AJ (1996) The role of the intralysosomal pH in the control of autophagic proteolytic flux in rat hepatocytes. Eur J Biochem 235:564-573.

Mindell JA (2012) Lysosomal acidification mechanisms. Annu Rev Physiol 74:69-86.

Nylandsted J, Becker AC, Bunkenborg J, Andersen JS, Dengjel J, Jaattela M (2011) ErbB2-associated changes in the lysosomal proteome. Proteomics 11:2830-2838.

Overbye A, Fengsrud M, Seglen PO (2007) Proteomic analysis of membrane-associated proteins from rat liver autophagosomes. Autophagy 3:300-322.

Saftig P, Klumperman J (2009) Lysosome biogenesis and lysosomal membrane proteins: trafficking meets function. Nat Rev Mol Cell Biol 10:623-635.

Schroder B, Wrocklage C, Pan C, Jager R, Kosters B, Schafer H, Elsasser HP, Mann M, Hasilik A (2007) Integral and associated lysosomal membrane proteins. Traffic 8:1676-1686.

Scita G, Confalonieri S, Lappalainen P, Suetsugu S (2008) IRSp53: crossing the road of membrane and actin dynamics in the formation of membrane protrusions. Trends Cell Biol 18:52-60.

Storrie B, Madden EA (1990) Isolation of subcellular organelles. Methods Enzymol 182:203-225.

Veltman DM, Auciello G, Spence HJ, Machesky LM, Rappoport JZ, Insall RH (2011) Functional analysis of Dictyostelium IBARa reveals a conserved role of the I-BAR domain in endocytosis. Biochem J 436:45-52.

Winter U, Chen X, Fasshauer D (2009) A conserved membrane attachment site in alpha-SNAP facilitates N-ethylmaleimide-sensitive factor (NSF)-driven SNARE complex disassembly. J Biol Chem 284:31817-31826.

Zoncu R, Bar-Peled L, Efeyan A, Wang S, Sancak Y, Sabatini DM (2011) mTORC1 senses lysosomal amino acids through an inside-out mechanism that requires the vacuolar H(+)-ATPase. Science 334:678-683.

4. RESULTS: CHAPTER 2

Withdrawal of essential amino acids increases autophagy by a pathway involving Ca^{2+}/calmodulin-dependent kinase kinase-β (CaMKK-β)

Ghislat G, Patron M, Rizzuto R, Knecht E (2012) J Biol Chem 287:38625-38636.

Withdrawal of essential amino acids increases autophagy by a pathway involving CaMKK-β

Ghita Ghislat[a], Maria Patron[b], Rosario Rizzuto[b] and Erwin Knecht[a*]

[a]*Laboratorio de Biología Celular, Centro de Investigación Príncipe Felipe, Avda. Autopista del Saler 16, 46012-Valencia, Spain and CIBERER, Valencia, Spain*
[b] *Department of Biomedical Sciences, University of Padua, Via G. Colombo 3, 35131 Padua, Italy*

* Running title: *CaMKK-β regulates autophagy in response to amino acid starvation*

**Corresponding author*. Centro de Investigación Príncipe Felipe, Avda. Autopista del Saler 16, 46012-Valencia, Spain, Tel.: +34-96-3289680; fax: +34-96-3289701
E-mail: knecht@cipf.es

Key words: AMPK; Autophagy; Ca^{2+}; CaMKK-β; mTORC1; ULK1

Background: Amino acids and cell Ca^{2+} are potent regulators of autophagy that are thought to act independently of each other.
Results: Withdrawal of essential amino acids increases cytosolic Ca^{2+}, and subsequently activates autophagy *via* a CaMKK-β-AMPK pathway to ULK1 and mTORC1.
Conclusion: A Ca^{2+}-dependent pathway regulates autophagy under amino acid starvation.
Significance: This new pathway would contribute to better understand autophagy regulation.

SUMMARY

Autophagy is the main lysosomal catabolic process that becomes activated under stress conditions, such as amino acid starvation and cytosolic Ca^{2+} upload. However, the molecular details on how both conditions control autophagy are still not fully understood. Here we link essential amino acid starvation and Ca^{2+} in a signaling pathway to activate autophagy. We show that withdrawal of essential amino acids leads to an increase in cytosolic Ca^{2+}, arising from both extracellular medium and intracellular stores, which induces the activation of adenosine monophosphate activated protein kinase (AMPK) *via* Ca^{2+}/calmodulin-dependent kinase kinase-β (CaMKK-β). Furthermore, we show that autophagy induced by amino acid starvation requires AMPK, because this induction is attenuated in its absence. Subsequently, AMPK activates UNC-51 like kinase (ULK1), a mammalian autophagy-initiating kinase, through phosphorylation at S-555 in a process that requires CaMKK-β. Finally, the mammalian target of rapamycin complex 1 (mTORC1), a negative regulator of autophagy downstream of AMPK, is inhibited by amino acid starvation in a Ca^{2+} sensitive manner, and CaMKK-β appears to be important for mTORC1 inactivation, especially in the absence of extracellular Ca^{2+}. Consequently, this mTORC1 inhibition contributes to the activation of ULK1 by eliminating its phosphorylation at S-757. All these results highlight that amino acid starvation up-regulates autophagy through an increase in cellular Ca^{2+} that activates a CaMKK-β-AMPK pathway and inhibits mTORC1 to stimulate ULK1.

Cellular homeostasis is maintained by the proper balance between the biosynthesis and the degradation of macromolecules and organelles. Macroautophagy, hereafter simply called autophagy, is a main catabolic process for the clearance of intracellular components in lysosomes (1). Under full nutrient conditions, autophagy remains at a low basal levels in most cells, while under starvation and other stress conditions it rises to play a main role in cell survival by delivering nutrients and damaged cell components to lysosomes (2, 3). The most important negative regulators of autophagy are hormonal (*e.g.* insulin) and nutritional (*e.g.* amino acids) (1, 4). The serine-threonine kinase mammalian target of rapamycin complex C1 (mTORC1) is to date the best known sensor for the availability of energy and nutrients. For example, it is negatively and positively regulated, respectively, by the adenosine monophosphate activated protein kinase (AMPK) and the insulin signaling pathways. AMPK is activated by various kinases, including the Ca^{2+}/calmodulin-dependent kinase kinase-β (CaMKK-β) (5),

and its inhibitory effect on mTORC1 occurs *via* phosphorylation of TSC2 in the tuberous sclerosis complex TSC1/2, which has GTPase-activating protein activity towards its substrate ras-family GTP binding protein Rheb (6). Even though the involvement of AMPK in the inhibition of mTORC1 is now well established, its direct role inducing autophagy has been only recently described by reporting its involvement in the phosphorylation of ULK1 (UNC-51 Like Kinase), a mammalian ortholog of the yeast protein kinase Atg1 that is required to initiate autophagy (7). In the presence of nutrients, mTORC1 has also the ability to prevent ULK1 activation by phosphorylating this protein at a residue that is different from those phosphorylated by AMPK, disrupting in this way the interaction between ULK1 and AMPK (8).

Ca^{2+} ion is a major intracellular second messenger regulating many physiological functions in the cells, such as secretion, contraction, metabolism, gene transcription, death, etc., and also involved in some pathological processes (9, 10). Although the spatial and temporal distribution of Ca^{2+} in the cytosol, mitochondria, endoplasmic reticulum (ER) and nucleus determines one of the most commonly recognized and well studied intracellular signals (11, 12), its role in autophagy is hitherto poorly understood. A pioneering study demonstrated the importance of Ca^{2+} storage within intracellular compartments, rather than cytosolic Ca^{2+}, for autophagy stimulation (13). However, another report provided evidence that, at least under certain conditions, autophagy is inhibited when cytosolic Ca^{2+} increases (14), whereas others reported that rises in cytosolic Ca^{2+} stimulate autophagy (5). It is believed that the positive effects of Ca^{2+} on autophagy occur *via* activation of AMPK and are mTORC1-dependent (5), whereas the inhibition of autophagy by Ca^{2+} does not require AMPK and is independent of mTORC1 (14). Thus, apparently, conflicting results exist concerning the role of cytosolic Ca^{2+} and intracellular stores of Ca^{2+} in autophagy.

We have recently found that three Ca^{2+} binding proteins, copine 1, annexin A1 and annexin A5, translocate under essential amino acid starvation to lysosomal membranes. This translocation occurs in a Ca^{2+}-dependent manner, at least for annexin A5, which was also shown to stimulate autophagy (15). This led us to consider a possible link between autophagy induction under this condition and intracellular Ca^{2+}. Thus, we investigated in this work the dependence on cellular Ca^{2+} of autophagy induced by essential amino acid starvation. We demonstrate, for the first time, that withdrawal of amino acids provokes an increase of cytosolic Ca^{2+}, which originates from both extracellular and, to a larger extent, intracellular stores. We also describe a pathway by which amino acid starvation could activate autophagy through Ca^{2+} signaling.

2. EXPERIMENTAL PROCEDURES

2.1. Materials

Minimum Essential medium (MEM), Dulbecco's Modified Eagle´s Medium (DMEM), human insulin, 3-methyladenine, EGTA (ethylene glycol tetra-acetic acid), ionomycin, insulin and NH_4Cl were purchased from Sigma Chemical Co. MEM amino acids 50x, foetal bovine serum (FBS), fura-2AM and fluo-3AM were supplied by Molecular Probes, Invitrogen Life Technologies. Leupeptin was from Peptide Institute, Inc. and rapamycin from Calbiochem. The following antibodies were used: anti-microtubule-associated protein1 light chain 3 (anti-LC3) from Nanotools, anti-CaMKK-β and anti-CaMKK-α from Santa Cruz Biotechnology, anti-AMPK/P-AMPK (T-172), anti-p70S6K/P-p70S6K (T-389) and anti-ULK1/P-ULK1 (S-555)/P-ULK (S-757) and anti-mTOR from Cell Signaling and anti-β-actin and horseradish peroxidase-labeled secondary antibodies from Sigma Chemical Co. Radioisotopes were obtained from Amersham Pharmacia Biotech. The CaMKK-α/β inhibitor STO-609 and BAPTA-AM (1,2-bis(2-aminophenoxy) ethane-*N,N,N,N*-tetraacetic acid tetrakis(acetoxymethyl ester)) were from Tocris Bioscience. Other reagents, purchased from Sigma Chemical Co, Invitrogen Life Technologies or Calbiochem, were of analytical grade.

2.2. Cell culture, treatments and transfections

NIH3T3 mouse embryonic fibroblasts and HeLa cells, obtained from the European Collection of Animal Cell Cultures, were grown at 37ºC in a humidified atmosphere of 5% (v/v) CO_2/air in DMEM or MEM with 10% heat-inactivated FBS and 1% penicillin and streptomycin. Normal human skin fibroblasts 3349B were obtained from the Coriell Institute for Medical Research (Camden, NJ, USA) and were grown as described (4). Mouse embryonic fibroblasts (MEFs) double knockout (KO) for AMPKα1/2 subunits (α1-/- and α2-/-) and wild type controls, kindly provided by Dr. B. Viollet (Institut Cochin, INSERM U1016, CNRS UMR 8104, Université Paris Descartes, Dept. of

Endocrinology, Metabolism and Cancer, 24 rue du Faubourg Saint Jacques, 75014 Paris), were grown as described previously (16). Krebs-Henseleit medium (KH, 118.4 mM NaCl, 4.75 mM KCl, 1.19 mM KH_2PO_4, 2.54 mM $MgSO_4$, 2.44 mM $CaCl_2 \cdot 2H_2O$, 28.6 mM $NaHCO_3$, 20 mM glucose), with 10 mM Hepes, pH 7.4, was used for high proteolysis (starvation) conditions. For low proteolysis conditions, insulin (0.1 µM) and essential amino acids (at two times the concentration present in the growth media (4)) were added to KH. Incubations without extracellular Ca^{2+} were carried out in the same KH, but without $CaCl_2$ and supplemented with 100 µM EGTA.

For RNAi-mediated inhibition of the expression of *CaMKK-β, CaMKK-α* and *AMPK* genes, cells were transfected, 72 h before analysis, with small interfering RNAs (siRNAs), using X-tremeGENE siRNA Transfection Reagent (Roche Applied Science) according to the manufacturer's instructions. The siRNAs that target mouse CaMKK-β mRNA and the negative controls were purchased from Ambion Inc., whereas those that target AMPK were purchased from Santa Cruz Biotechnology. All of them were tested and used at a final concentration of 15 nM.

2.3. Measurements of intracellular Ca^{2+}

For cytosolic [Ca^{2+}] imaging, cells were loaded with 5 µM fura-2AM for 30 min at 37°C in KH. Fura-2AM fluorescence was measured at 340 nm and 380 nm excitation, and emission was detected with a 520 emission filter at intervals of 5 seconds. Analysis was done using Hamamatsu or MetaMorph/MetaFluor Analyst (Universal Imaging Corporation, Downingtown, PA). Assays were carried out on a Zeiss Axiovert 200 inverted microscope equipped either with cooled CCD digital cameras or as part of a Zeiss LSM 510 confocal microscope (Carl Zeiss, Jena, Germany).

For [Ca^{2+}] measurements by flow cytometry, cells were loaded with 5 µM fluo-3AM for 30 min, detached with trypsin–EDTA, washed once and resuspended (10^6 cells/ml) in the appropriate medium. In each experiment, 10,000 cells were analyzed by Fluorescence-activated cell sorting (FACS) using a 488±20 nm band-pass filter and a Cytomics FC 500 flow cytometer (Beckman Coulter).

2.4. Measurement of intracellular protein degradation

NIH3T3 cells were incubated for 48 h in fresh full medium with 2 µCi/ml [^{3}H]valine, followed by a 24 h chase in fresh full medium containing 10 mM L-valine to degrade short-lived proteins (17). Then, degradation of long-lived proteins was measured for 4 h with the indicated treatments. Total and autophagic protein degradation were calculated as previously described (17).

2.5. General procedures

The immunoblotting procedures were carried out as before (17). Phospho-specific antibodies were always used in the first round. After treating the membranes with stripping buffer (0.25 M glycine, pH 2.3), they were probed using the antibodies that recognize the total amount of the protein of interest. Detection of low signals was carried out with the Amersham ECL Prime Western Blotting Detection Reagent. Comparisons between different conditions, after calculating mean and S.D. values, were by Student's *t*-test. *P* values were considered significant at ***p<0.0005; **p<0.005 and *p<0.05.

3. RESULTS

3.1. Withdrawal of amino acids increases intracellular Ca^{2+} levels

To test whether cytosolic Ca^{2+} levels ($[Ca^{2+}]_c$) vary under conditions that produce high (KH alone) and low (KH plus insulin and amino acids) proteolysis, we measured their kinetic changes under these conditions in fura-2AM-loaded NIH3T3 cells. We found that in the cells incubated with KH, $[Ca^{2+}]_c$ are significantly higher without insulin and amino acids than in the presence of both proteolytic regulators (Fig. 1A and table 1). The KH-induced $[Ca^{2+}]_c$ increase is characterized by a rapid initial rise that quickly becomes stabilized. We also measured, separately, the effects of insulin and amino acids: amino acids induce a decrease in $[Ca^{2+}]_c$, while insulin does not provoke any change (Fig. 1B and C and table 1).

To examine whether the increase in $[Ca^{2+}]_c$ observed under high proteolysis conditions (KH alone) was due to extracellular Ca^{2+} influx or to release of Ca^{2+} from an intracellular store, cells were incubated in KH without extracellular Ca^{2+} and containing the cell-impermeant Ca^{2+} chelator EGTA. As shown in Fig. 1D, addition or withdrawal of amino acids from a Ca^{2+}-free medium produce changes in $[Ca^{2+}]_c$ that are similar to those observed in the presence of extracellular Ca^{2+} (see Fig. 1A and table 1), but that occur at a lower extent. The same effects were observed, with and without extracellular Ca^{2+}, in HeLa cells (Fig. S1A, B) and in 3349B human fibroblasts (Fig. S1C,

D). Moreover, a second round of amino acid challenge still depletes to some extent the intracellular stores of Ca^{2+} (Fig. 1E and Fig. S1A, B).

These data indicate that although the observed rise in $[Ca^{2+}]_c$ when the cells are incubated without essential amino acids depends in part on Ca^{2+} entry from the extracellular medium, this increase mainly comes from an intracellular Ca^{2+} store.

3.2. Withdrawal of amino acids activates AMPK in a CaMKK-β-dependent way

Amino acid removal activates autophagy by complex mechanisms still not fully understood (1, 18). In addition, it is also known that both extracellular- and ER-derived Ca^{2+} induce autophagy through the activation of AMPK by Ca^{2+}/CaMKK (5). Therefore, we asked if this signaling pathway was also implicated in the observed effects of amino acid starvation on Ca^{2+} levels or, in other words, if both groups of separate observations could be related.

First, we determined in our experimental system whether or not amino acid starvation activates AMPK, analysing its T-172 phosphorylation. Under amino acid starvation, phosphorylation of AMPK is slightly lower in the absence ($-CaCl_2$) of extracellular Ca^{2+} than in its presence ($+CaCl_2$) (Fig. S2B and C). This is in agreement with the observed effects of amino acid starvation on $[Ca^{2+}]_c$ in cells incubated in a Ca^{2+}-free medium (Fig. 1D), and also with previous reports showing that Ca^{2+} plays a crucial role in the activation of this kinase (5, 19). Furthermore, withdrawal of amino acids, with and without extracellular Ca^{2+}, activates AMPK (Fig. 2A, see the two last bands in $+CaCl_2$ and $-CaCl_2$). To analyze the possibility of a Ca^{2+}-dependent activation of AMPK by withdrawal of amino acids, we used the intracellular Ca^{2+} chelator BAPTA-AM. Chelation of intracellular Ca^{2+} by BAPTA-AM diminishes this activation in the presence of extracellular Ca^{2+} and eliminates it in its absence, indicating a Ca^{2+}-dependent activation of AMPK by amino acid starvation (Fig. 2A). Activation of AMPK can be mainly accomplished *via* its phosphorylation by the tumour suppressor kinase LKB1 (when energy levels are low), and by CaMKK-β and to a lesser extent by CaMKK-α (in response to an increase in $[Ca^{2+}]_c$) (19, 20). As demonstrated above, withdrawal of amino acids increases $[Ca^{2+}]_c$. Thus, we speculated that this effect could activate AMPK in NIH3T3 cells through CaMKK-α/β. In order to test this hypothesis, we first treated the cells with a CaMKK-α/β inhibitor (STO-609) (21). As shown in Fig. 2B (see last two bands in $+CaCl_2$ and $-CaCl_2$), STO-609 abolishes the activation of AMPK produced in the absence of amino acids and with and without extracellular Ca^{2+}. To further confirm these effects, we carried out the same experiments, but now using CaMKK-β specific siRNAs. The observed AMPK phosphorylations in CaMKK-β silenced cells (Fig. 2C) are fully consistent with the results obtained with STO-609 (Fig. 2B). To distinguish between the involvement of CaMKK-β and CaMKK-α in this pathway, we compared the silencing effect of each one. A possible higher expression of one CaMKK in response to the knockdown of the other is ruled out in Fig. S2A. In general, CaMKK-α knockdown produces less effect than that of CaMKK-β (Fig. S2B and C). In contrast to CaMKK-β, silencing of CaMKK-α does not fully abolish the activation of AMPK produced by amino acid starvation. Under CaMKK-α silencing, this activation persists in the absence of extracellular Ca^{2+} and is abrogated in its presence. This suggests that the activation of AMPK under amino acid starvation by CaMKK-α depends on extracellular Ca^{2+} and not on Ca^{2+} derived from intracellular stores. Taken together, these results show that, in NIH3T3 cells, withdrawal of amino acids activates AMPK by a signaling pathway involving Ca^{2+} and the CaMKKs, mainly the β isoform and to a lesser extent the α.

3.3. AMPK is involved in the induction of autophagy by amino acid starvation

To elucidate a possible role of AMPK in the inhibition of autophagy by amino acids, we took advantage of the availability of AMPK KO MEFs (see Experimental Procedures). Autophagy was first assessed by the levels of LC3-II, the processed and lipidated form of LC3-I that is recruited to autophagosomes (22). As LC3-II is degraded in autolysosomes, a well established procedure to investigate autophagosome formation is based on the inhibition with various agents of lysosomal proteases and/or of the fusion process between lysosomes/endosomes and autophagosomes (23). Under these conditions, the levels of LC3-II are indicative of the formation rate of autophagosomes *i.e.* the autophagic flux (2, 24, 25). Here, we used leupeptin and ammonium chloride (17, 26, 27), but similar results were obtained with 500 nM bafilomycin A (data not shown). Since LC3-I is reported to be less stable and less immunoreactive than LC3-II (28), we used the LC3-II/actin ratio to assess autophagy (28,

29). Fig. 3A shows that in WT (wild type) MEFs under amino acid starvation, LC3-II levels increase 3 times in the presence of extracellular Ca^{2+} and slightly less (2.7 times) in its absence. These values are reduced in AMPK KO MEFs to 2.3 (23% reduction) and 1.4 (48% reduction) times, respectively. These data suggest that AMPK is involved in the activation of autophagy by amino acid starvation, especially in the absence of extracellular Ca^{2+}. To further confirm these results, we carried out pulse-chase experiments to analyse the degradation of long-lived proteins by autophagy, using its inhibitor 3-methyladenine (17, 25). Similar rates of autophagic degradation under amino acid starvation were observed in AMPK WT and KO cells, possibly because of mechanisms that compensate for the lack of AMPK in order to assure the survival of the cells under this stress condition. Results show that the inhibitory effect of amino acids on autophagy is greater in WT than in KO cells (Fig. 3B), confirming a requirement of AMPK in the regulation of autophagy by amino acids. Thus, in WT MEFs, in the presence and absence of extracellular Ca^{2+}, withdrawal of amino acids increases autophagy 11.3 and 9.1 times respectively, while in AMPK KO MEFs, these increases are only 2.7 and 2.3 times. Moreover, and consistent with the findings that Ca^{2+} induces autophagy in an AMPK-dependent way (5), only WT, but not AMPK KO, MEFs show a moderate increase in the rate of autophagic degradation when extracellular Ca^{2+} is present (Fig. 3B).

Next we tested whether AMPK silencing by specific siRNAs has similar effects on autophagy induction by amino acid starvation. We found that AMPK downregulation considerably decreases the levels of LC3-II in the absence and particularly in the presence of inhibitors of lysosomal proteases (Fig. 3C), in agreement with its well established role in the activation of autophagy (7, 8). Furthermore, and in accordance with the previous results, the induction of autophagy by withdrawal of amino acids is attenuated under AMPK silencing both in the presence (2.2 times in C-siRNA transfected cells *vs* 1.6 times in silenced cells) and in the absence (1.8 times in C- siRNA transfected cells *vs* 1.1 times in silenced cells) of extracellular Ca^{2+} (Fig. 3C).

Although results were qualitatively similar in AMPK silenced cells and AMPK KO MEFs, the autophagic responses were milder in the latter cells. In this regard, AMPK is known to inhibit the activity of mTORC1, a complex with a well known inhibitory function in autophagy. Therefore, we compared the effects of AMPK silencing and KO on mTORC1 activity, measured by the T-389 phosphorylation of the ribosomal protein S6 kinase 1 (p70S6K) (30). The results show that, with or without extracellular Ca^{2+} and in contrast to AMPK silenced cells, mTORC1 activity is almost abolished in AMPK KO MEFs (Fig. 3D), which could explain the lower autophagy response in these cells. Fig. 3D also shows that these differences are not due to variations of mTORC1 levels. Therefore, AMPK KO MEFs have apparently developed a compensatory mechanism for the permanent lack of AMPK, based on a decrease of the mTORC1 activity. This assures a high level of autophagy for the survival of the cells under stress conditions such as amino acid starvation.

In summary, all these data show that withdrawal of amino acids, with or without extracellular Ca^{2+}, induces autophagy in an AMPK-dependent way.

3.4. Withdrawal of amino acids activates autophagy in a CaMKK-β-dependent way

Withdrawal of essential amino acids activates AMPK via CaMKK-β (see Fig. 2) and the induced autophagy requires, at least in part, AMPK (Fig. 3). Therefore, we next investigated whether CaMKK-β alters autophagosome formation under this stimulus. Results show that the rise of LC3-II levels under amino acid starvation considerably diminishes when CaMKK-β is inhibited with STO-609 or silenced with specific siRNAs, both in the presence and absence of extracellular Ca^{2+} (Fig. 4A and B). This indicates that withdrawal of amino acids activates autophagy *via* a CaMKK-β-dependent pathway. Interestingly, the effects are greater after CaMKK-β downregulation than after AMPK KO and silencing (see Fig. 3). Therefore, it is possible that CaMKK-β mediates the activation of autophagy by amino acid starvation following other pathways independent of AMPK. Anyway, these findings show that CaMKK-β remains as an important sensor of the withdrawal of amino acids that mediates in the activation of AMPK and of autophagy under these conditions.

3.5. Withdrawal of amino acids phosphorylates ULK1 in a CaMKK-β-dependent way

The results described above show that amino acid starvation induces autophagy by an AMPK-dependent mechanism (see Fig. 3).

Since AMPK has been shown to activate autophagy by S-555 phosphorylation of ULK1 (7), we analyzed the effect of the withdrawal of amino acids on this phosphorylation. Under these conditions, the S-555 phosphorylation of ULK1 increases both in the presence and absence of extracellular Ca^{2+} (Fig. 5A, see two first bands in $+CaCl_2$ and $-CaCl_2$). This phosphorylation is Ca^{2+}-dependent insofar as it is abrogated by BAPTA-AM (Fig. 5B, see two last bands in $+CaCl_2$ and $-CaCl_2$). Next, and given that withdrawal of amino acids activates AMPK in a CaMKK-β-sensitive manner (see Fig. 2), and that CaMKK-β is important for autophagy induction by amino acid starvation (see Fig. 4), we investigated the effect of CaMKK-β in the phosphorylation of ULK1 at S-555. Interestingly, when CaMKK-β is inhibited with STO-609 or downregulated with specific siRNAs (Fig. 5B and C, see two last bands in $+CaCl_2$ and $-CaCl_2$), the effect of amino acid starvation on S-555 phosphorylation of ULK1 is abolished. These findings, together with those shown before, indicate that Ca^{2+}-CaMKK-β-dependent activation of AMPK by withdrawal of amino acids correlates with the phosphorylation at S-555 of ULK1, a modification that induces autophagy.

3.6. Inactivation of mTORC1 by withdrawal of amino acids involves intracellular Ca^{2+} and CaMKK-β

Since ULK1 activation is positively and negatively regulated by AMPK and mTORC1 respectively (8, 31), we decided to determine if mTORC1 is also involved in the activation of the Ca^{2+}-CaMKK-β-AMPK pathway under withdrawal of amino acids by analyzing the phosphorylation of its substrate p70S6K at T-389. Amino acid removal inactivates mTORC1 in the presence and absence of extracellular Ca^{2+} (Fig. 6A, see two first bands in $+CaCl_2$ and $-CaCl_2$). This inactivation of mTORC1 was abrogated when intracellular Ca^{2+} was previously chelated with BAPTA-AM during 2 h (Fig. 6A, two last bands), which supports that inactivation of mTORC1 by withdrawal of amino acids is Ca^{2+}-dependent. Of note, the raise of intracellular Ca^{2+} levels under amino acid starvation occurs upstream of mTORC1, since this effect was insensitive to rapamycin, as shown by both cytosolic $[Ca^{2+}]$ imaging in fura-2AM loaded cells (Fig. 6B) and FACS analysis in fluo-3AM loaded cells (Fig. 6C).

In accordance with the previous results (Fig. 1D), the increase of $[Ca^{2+}]_c$ under amino acid withdrawal was also observed in fluo-3AM loaded cells analysed by FACS. BAPTA-AM cancels these effects as expected (Fig. 6C).

Moreover, when CaMKK-β was inhibited with STO-609 or downregulated with specific siRNAs, the differences in p70S6K phosphorylation with or without amino acids are attenuated in the presence of extracellular Ca^{2+} (Fig. 6D and E, see two last bands in $+CaCl_2$) and almost fully abolished in its absence (Fig. 6D and E, two last bands in $-CaCl_2$). Therefore, the CaMKK-β-AMPK signaling pathway is also involved here in mTORC1 inactivation. However, there is a difference in the effects with or without extracellular Ca^{2+}. In the latter case, the Ca^{2+}-CaMKK-β-AMPK pathway is essential for the amino acid effects on mTORC1, while when extracellular Ca^{2+} is present other pathways are also involved. Since mTORC1 has been recently reported to prevent ULK1 activation by phosphorylating it at S-757 (8), the effects of amino acid withdrawal on ULK1 phosphorylation by mTORC1 were also analyzed. As expected, phosphorylation of ULK1 at S-757 diminishes under amino acid starvation, both with and without extracellular Ca^{2+}, and BAPTA-AM restores this rapamycin-dependent phosphorylation (Fig. 6A). Taken together, these data support a model where amino acid starvation inhibits mTORC1 in a Ca^{2+}-dependent manner, which leads to ULK1 activation and consequently to autophagy induction.

4. DISCUSSION

Despite the well established role of amino acids in the regulation of autophagy, the detailed molecular mechanisms are still not fully understood (1, 32, 33). Activation of autophagy by amino acid starvation is the subject of a complex regulation *via* several signaling pathways (18). The hitherto most important step in the induction of autophagy by deprivation of amino acids is the inhibition of mTORC1. This kinase, when inactivated, dissociates from an important complex that initiates autophagy, containing, among other proteins, the AuTophagy related Gene 13 (Atg13), the Focal adhesion kinase Interacting Protein 200 (FIP200) and the kinase ULK1/2, which has been recently identified as a substrate of AMPK (7, 8, 31). Under these conditions, autophagy becomes stimulated (34, 35). However, how amino acid starvation inactivates mTORC1 is still poorly understood. This is in part due to the diversity of amino acids and to the variety of their metabolisms in different cells (4, 32, 36, 37). Examples of the pathways involved in mTORC1 inhibition by amino acid starvation

are the PI3K-Akt-mTORC1 (34, 35), and the Ras-Raf-MEK-ERK signaling cascades (38-40). In addition, mTORC1-independent pathways in the regulation of autophagy by amino acid starvation have been also postulated (reviewed in (18, 33)). The findings presented in this work support that a Ca^{2+}-dependent pathway is operative in the activation of autophagy by essential amino acid starvation. This pathway involves CaMKK-β-AMPK-ULK1 and also mTORC1 signaling.

The results reported herein show, for the first time, that the withdrawal of essential amino acids induces a rise in $[Ca^{2+}]_c$. This Ca^{2+} originates from extracellular and intracellular stores. Although the intracellular stores responsible of this Ca^{2+} release are unknown, it is possible that the ER is implicated, since it is the most important organelle that supplies Ca^{2+} to the cell (12). In fact, it has been reported that amino acid starvation causes the release of Bcl-2 from ER to induce autophagy (41) and that the association of Bcl-2 to the ER decreases the exit of Ca^{2+} from ER and inhibits autophagy. Another study showed that amino acids increase $[Ca^{2+}]_c$, which enhance the binding of Ca^{2+}/Calmodulin to hVps34. This results in a rise in PI(3)P levels and in an enhanced signaling by the mTORC1 complex (42). Since we observed the same increase in $[Ca^{2+}]_c$ when the amino acids were added to the medium without adjusting the pH to physiological conditions (data not shown), it is possible that the Ca^{2+} increase observed in that study is a physiological response to a low pH. Moreover, a more recent report in HEK293 cells suggests that the described interaction of Ca^{2+}/Calmodulin with hVps34 does not directly affect hVps34 activity (43). Therefore, the mechanisms by which amino acids control intracellular Ca^{2+} homeostasis remain to be studied.

AMPK inhibits the mTORC1 complex (6), and Ca^{2+} activates AMPK *via* CaMKK-β (5, 19). Based on these premises, we propose that the well established activation of autophagy by amino acid starvation occurs in part *via* the Ca^{2+}-CaMKK-β-AMPK pathway. This model (Fig. 7) is supported by the results showing that, under amino acid starvation, Ca^{2+} and CaMKK-β are required for the activation of AMPK and for the inhibition of mTORC1, stimulating in this way ULK1 for an increased formation of autophagosomes.

Another important output for CaMKK-β-dependent activation of AMPK by amino acid starvation is the S-555 phosphorylation of ULK1, which is required for the initiation of autophagy. Active CaMKK-β is fully required for the phosphorylation of ULK1 at S-555 produced by amino acid withdrawal. This is in accordance with the results showing the involvement of CaMKK-β in the activation of autophagosome formation by amino acid starvation. However, CaMKK-β inactivation does not fully abolish the autophagy induced by withdrawal of amino acids. This indicates that this condition also induces autophagy by pathways independent of ULK1.

mTORC1 is also involved in the Ca^{2+}-CaMKK-β-AMPK pathway stimulated by amino acid starvation. In the presence of extracellular Ca^{2+}, CaMKK-β seems to be partially involved in the inhibition of mTORC1 mediated by amino acid starvation, which suggests the involvement of other pathways in this inhibition. In fact and as mentioned above, several mTORC1-dependent pathways have been already reported for the regulation of autophagy by amino acid starvation (38-40). However, in the absence of extracellular Ca^{2+}, CaMKK-β becomes fully indispensable. It is then conceivable that Ca^{2+} provided by the extracellular medium contributes to the effect of amino acid starvation on mTORC1 activity independently of Ca^{2+}-CaMKK-β-AMPK. In contrast, Ca^{2+} provided by intracellular stores acquires an exclusive role in the regulation of mTORC1 by amino acid starvation *via* CaMKK-β.

In summary, this study proposes a pathway for the regulation of autophagy by amino acid starvation involving Ca^{2+}, CaMKK-β, AMPK, ULK1 and mTORC1. Thus, intracellular Ca^{2+} levels remain an important signal in the cell response to the availability of amino acids. As amino acids have different metabolisms, it would be important to identify those that change intracellular Ca^{2+} levels as well as the possible existence of an intra- or extracellular Ca^{2+}-dependent sensor for these amino acids.

The abbreviations used are: AMPK, adenosine monophosphate activated protein kinase; $[Ca^{2+}]_c$, cytosolic Ca^{2+} levels; CaMKK-β, Ca^{2+}/calmodulin-dependent kinase kinase-β; ER, endoplasmic reticulum; LC3, microtubule-associated protein1 light chain 3; MEFs, Mouse embryonic fibroblasts; mTORC1, mammalian target of rapamycin complex 1; ULK1, UNC-51 Like Kinase; WT, wild type.

FIGURES

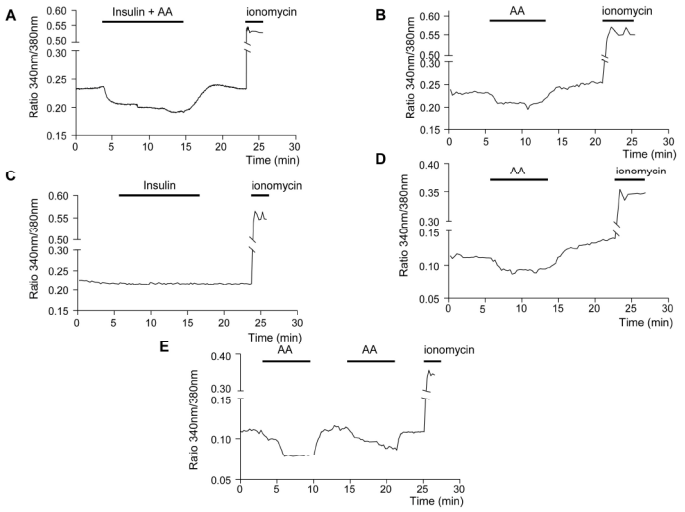

FIGURE 1. Withdrawal of amino acids raises cytosolic Ca^{2+}, derived from both extracellular and intracellular stores. For Ca^{2+} measurements, fura-2AM-loaded NIH3T3 cells were imaged as described in Experimental Procedures. The mean values from ≥40 cells from eight independent experiments are shown. The $[Ca^{2+}]_c$ are compared in cells incubated, as indicated, in KH, with and without amino acids (AA) and 0.1 µM insulin, either together (**A**) or separately (**B** and **C**, respectively). In **D** the effect of amino acids on $[Ca^{2+}]_c$ was measured in cells incubated in KH without $CaCl_2$ and containing 100 µM EGTA. Panel **E** shows a representative experiment where a second round of amino acid addition and withdrawal was carried out. To assess the viability of the cells, ionomycin (1 µM) was used as a positive control in each experiment.

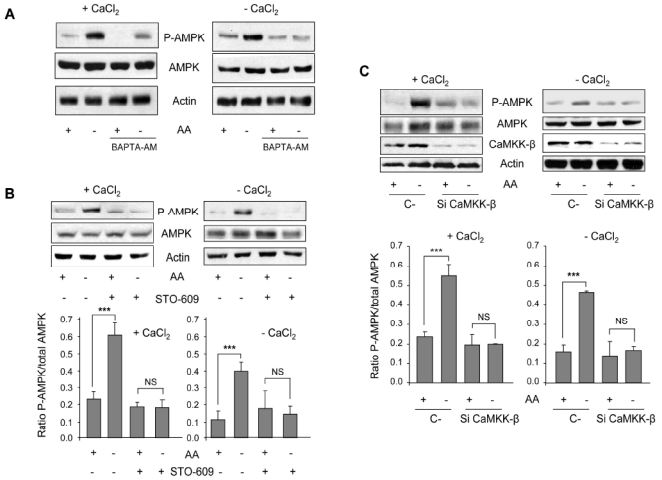

FIGURE 2. Withdrawal of amino acids activates AMPK phosphorylation in a CaMKK-β-dependent way. A. NIH3T3 cells were grown for 60 min in KH and amino acids (AA), with (+$CaCl_2$) or without $CaCl_2$ and supplemented with 100 µM EGTA (-$CaCl_2$) in the presence or absence of 500 nM BAPTA-AM. In the last 30 min of incubation, AA were removed or not as indicated. Cell extracts (75 µg protein) were analyzed by immunoblot using anti-AMPK, anti-P-AMPK (T-172) and, as a loading control, anti-actin antibodies. Low and high exposure (exp.) gels are shown. **B.** NIH3T3 cells were grown for 60 min in KH and amino acids (AA), with (+$CaCl_2$) or without $CaCl_2$ and supplemented with 100 µM EGTA (-$CaCl_2$) in the presence or absence of 25 µM STO-609. In the last 30 min of incubation, AA were removed or not as indicated. Cell extracts (75 µg protein) were analyzed by immunoblot using anti-AMPK, anti-P-AMPK (T-172) and, as a loading control, anti-actin antibodies. **C.** NIH3T3 cells were transfected with CaMKK-β (+) or with negative control (-) siRNAs. After 72 h, cells were incubated as above and analyzed by immunoblot using the same antibodies from A, plus anti-CaMKK-β. Densitometric measurements of the ratio of P-AMPK to total AMPK from four independent experiments in each case are shown below in (A) and (B). Differences were found to be statistically significant at ***p<0.0005. NS: no significant difference.

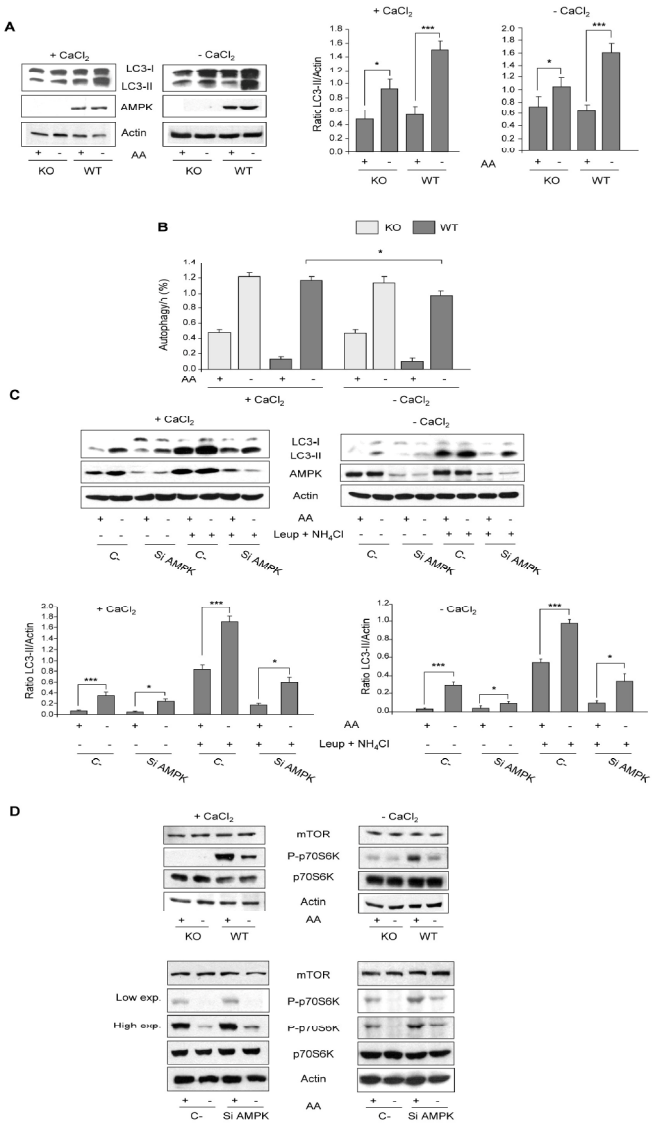

FIGURE 3. Autophagy induced by amino acid starvation is AMPK-dependent. A. AMPK KO and WT MEFs were incubated for 4 h in KH supplemented with amino acids (AA) plus 100 μM leupeptin and 20 mM NH_4Cl and in the presence (+) or not (-) of extracellular $CaCl_2$. In the last 30 min of incubation, AA were removed or not as indicated. Cell extracts (75 μg protein) were analyzed by immunoblot using anti-LC3 (-I and -II) and anti-actin antibodies. Densitometric measurements from six independent experiments are shown on the right. LC3-II bands were normalized to the corresponding actin bands. **B**. Exponentially growing AMPK KO and WT MEFs were metabolically labeled with [^{3}H]valine for 48 h, chased for 24 h and then switched to KH, with or w/o (without) $CaCl_2$ (in the last case, supplemented with 100 μM EGTA), and containing or not amino acids (AA) for 4 h. Data are from four independent experiments with duplicated samples and are expressed as the percentage of the labeled proteins that are degraded per h by autophagy in the different conditions. **C.** NIH3T3 cells were transfected with AMPK (+) or with negative control (-) siRNAs. After 72 h, cells were incubated as above (with or without 100 μM leupeptin and 20 mM NH_4Cl) and analyzed by immunoblot using the same antibodies as in (A). Densitometric measurements, as in (A), from two different blots are shown on the right. Stars indicate differences that were found to be statistically significant at ***p<0.0005 and *p<0.05. **D.** AMPK KO and WT MEFs (upper panels) and NIH3T3 cells previously transfected with AMPK (+) or with negative control (-) siRNAs (lower panels) were grown for 60 min in KH plus amino acids (AA), with (+$CaCl_2$) or without $CaCl_2$ and supplemented with 100 μM EGTA (-$CaCl_2$). In the last 30 min of incubation, AA were removed or not as indicated. Cell extracts (75 μg protein) were analyzed by immunoblot using anti-mTOR, anti-p70S6K, anti-P-p70S6K (T-389), and, as a loading control, anti-actin antibodies. In the lower panel, low and high exposure (exp.) gels are shown.

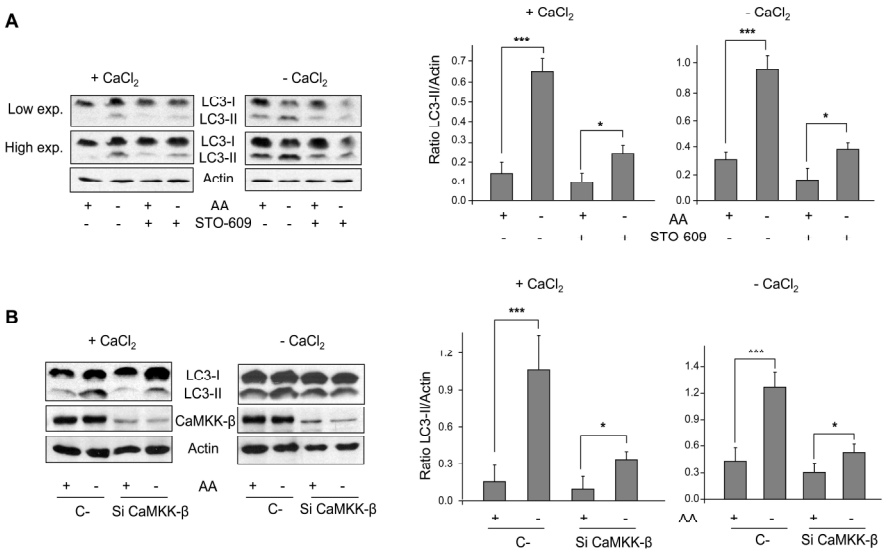

FIGURE 4. CaMKK-β is involved in the activation of autophagy by amino acid starvation. A. NIH3T3 cells were grown for 60 min in KH and amino acids (AA), with (+$CaCl_2$) or w/o $CaCl_2$ (in the last case, supplemented with 100 μM EGTA, -$CaCl_2$) plus 100 μM leupeptin and 20 mM NH_4Cl and in the presence or absence of 25 μM STO-609. In the last 30 min of incubation, AA were removed or not as indicated. Cell extracts (75 μg protein) were analyzed by immunoblot using anti-LC3 (-I and -II), and, as a loading control, anti-actin antibodies. **B.** NIH3T3 cells were transfected with CaMKK-β (+) or with negative control (-) siRNAs. After 72 h, cells were incubated as above and analyzed by immunoblot using the same antibodies from A, plus anti-CaMKK-β. In (A), low and high exposure (exp.) gels are shown. Densitometric measurements of the LC3-II/actin ratios, from three independent experiments in each case are also shown on the right of (A) and (B). Differences were found to be statistically significant at ***p<0.0005 and *p<0.05.

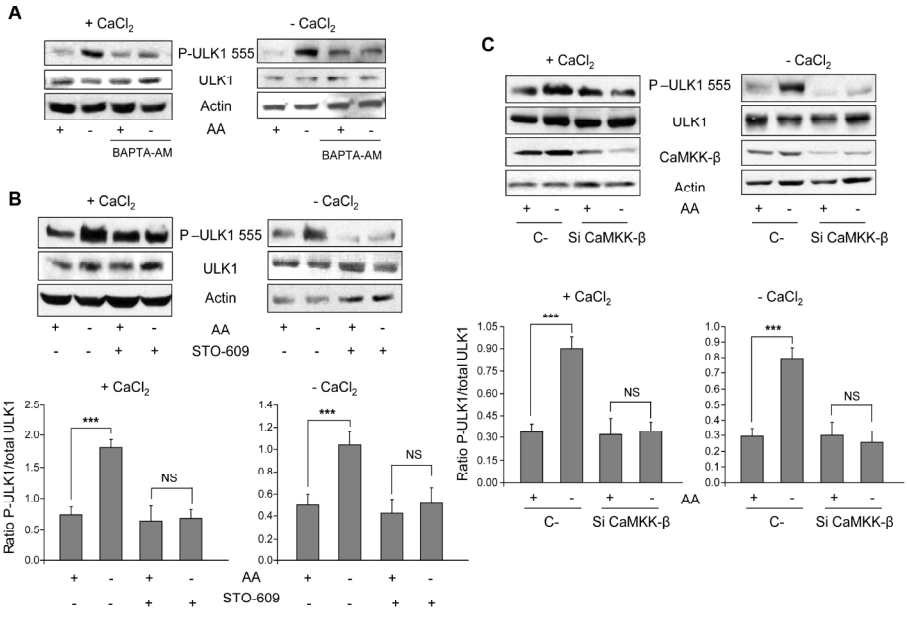

FIGURE 5. Withdrawal of amino acids increases ULK1 phosphorylation at S-555 in a CaMKK-β-dependent manner. A. NIH3T3 cells were grown and treated as described in the legend to Fig. 2A and were analyzed by immunoblot using anti-ULK1, anti-P-ULK1 (S-555) and, as a loading control, anti-actin antibodies. **B** and **C.** NIH3T3 cells were grown and treated as described in the legend to Fig. 2B and C, respectively, and were analyzed by immunoblot using the same antibodies as in (A). In (A) and (B), densitometric measurements of the ratio of P-ULK1 (S-555) to total ULK1 from four independent experiments in each case are shown below. Differences were found to be statistically significant at ***p<0.0005. NS: no significant differences.

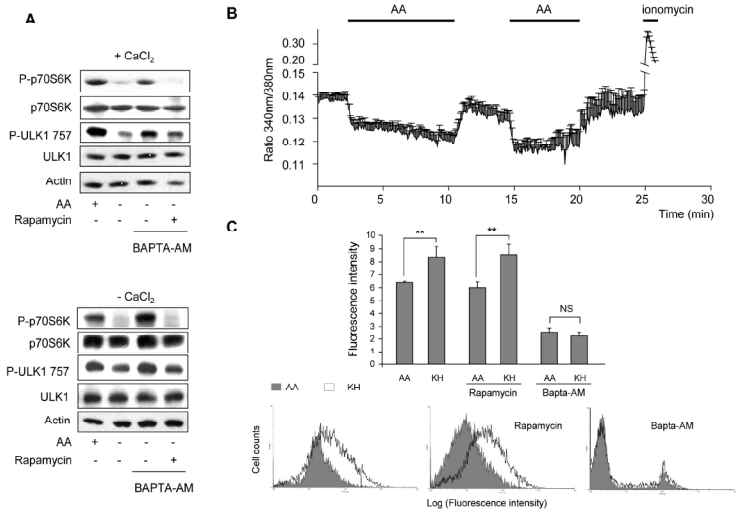

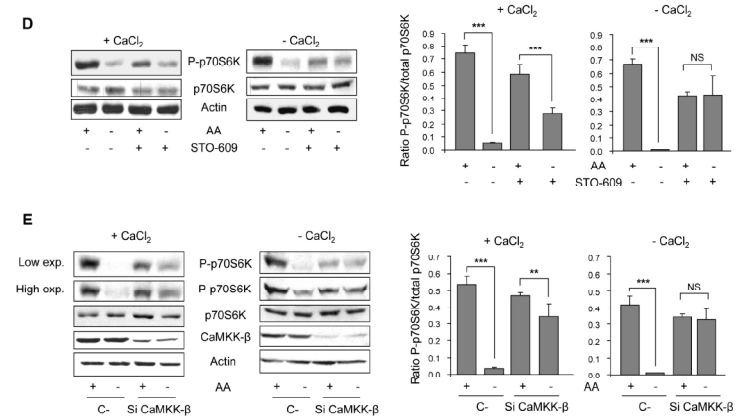

FIGURE 6. Ca^{2+} and CaMKK-β are also implicated in mTORC1 inactivation by amino acid starvation. A. NIH3T3 cells were grown for 2 h in KH plus amino acids (AA), with (+$CaCl_2$) or without $CaCl_2$ and supplemented with 100 μM EGTA (-$CaCl_2$) in the presence or absence of 10 μM BAPTA-AM. In the last 30 min of incubation, AA were removed or not as indicated. Cell extracts (75 μg protein) were analyzed by immunoblot using anti-p70S6K, anti-P-AMPK (T-172) and, as a loading control, anti-actin antibodies. **B.** Fura-2AM-loaded NIH3T3 cells incubated for 1 h with rapamycin (100 nM) were imaged as described in Experimental Procedures. The effect of AA on $[Ca^{2+}]_c$ was measured in cells incubated in KH without $CaCl_2$ and containing 100 μM EGTA. The mean values of more than 50 cells from two independent experiments are shown. **C.** NIH3T3 cells were previously incubated for 2 h in KH supplemented with AA with or without BAPTA-AM (10 μM). When indicated, rapamycin (100 nM) was used during the last hour as a control. Subsequently, AA were removed or not as indicated and cells were loaded with 5 μM fluo-3AM for 30 min. The fluorescence intensity of fluo-3AM in the cells was measured by flow cytometry. Values are the means and S.D. from two separate experiments with quadruplicated samples. Differences from AA values were found to be statistically significant at **P<0.005. The lower histograms show the fluorescence emitted by 10,000 cells in each case. **D.** NIH3T3 cells were grown and treated as described in the legend to Fig. 2B and C. Cell extracts (75 μg protein) were analyzed by immunoblot using anti-p70S6K, anti-P-p70S6K (T-389), and, as a loading control, anti-actin antibodies **E.** NIH3T3 cells were transfected with CaMKK-β (+) or with negative control (-) siRNAs. After 72 h, cells were incubated as above and analyzed by immunoblot using the same antibodies from A, plus anti-CaMKK-β. Densitometric measurements of the ratio of P-p70S6K to total p70S6K, from four independent experiments in each case, are also shown on the right of (D) and (E). In (E) low and high exposure (exp.) gels are shown. Differences were found to be statistically significant at ***p<0.0005 and **p<0.005. NS: no significant differences.

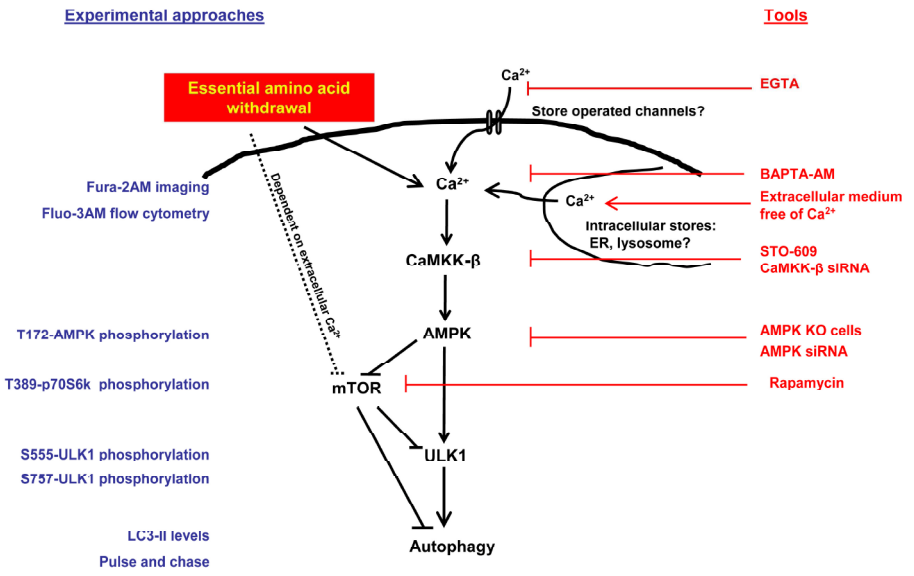

FIGURE 7. Suggested Ca^{2+}-dependent signaling cascade from amino acid starvation to autophagy. Detection methods and assays used in this study to monitor the indicated events are shown, respectively, on the left (marked in blue) and on the right (marked in red).

Table 1. Effects of insulin and/or amino acids (AA) on $[Ca^{2+}]_c$.

Stimulus	Ratio 340nm/380nm					n
	1 (2.5 min)	2 (10 min)	3 (20 min)	Addition [2.5 min-10 min]	Withdrawal [10 min-20 min]	
Insulin + AA	0.231 ± 0.009	0.198 ± 0.008	0.241 ± 0.006	-0.033 ± 0.001***	0.043 ± 0.002***	352
AA	0.240 ±0.010	0.208 ± 0.007	0.252 ± 0.009	-0.032 ± 0.003***	0.044 ± 0.002***	363
Insulin	0.228 ± 0.005	0.227 ± 0.004	0.226 ± 0.005	-0.001 ± 0.001 NS	0.001 ± 0.001 NS	349
AA†	0.121 ± 0.004	0.089 ± 0.005	0.125 ± 0.004	-0.032 ± 0.001***	0.036 ± 0.001***	365

The changes of $[Ca^{2+}]_c$ recording (ratio 340nm/380nm) upon stimulus addition (2 compared to 1) and withdrawal (3 compared to 2) were found to be statistically significant at ***p<0.0005 (NS: no significant difference). 1, 2 and 3 correspond to the time points in the time curves of Fig. 1A (for insulin +AA), Fig. 1B (for AA), Fig. 1C (for insulin) and Fig. 1D (for AA†). The data in the table rows corresponding to 1, 2 and 3 represent means ± S.D. of $[Ca^{2+}]_c$ measured at these point times. *n* corresponds to the number of analyzed cells with positive response to ionomycin from different cultures.

† Without $CaCl_2$, supplemented with 100 µM EGTA.

REFERENCES

1. Knecht E, Aguado C, Carcel J, Esteban I, Esteve JM, Ghislat G, Moruno JF, Vidal JM, Saez R. Intracellular protein degradation in mammalian cells: recent developments. Cell Mol Life Sci 2009;66(15):2427-2443.
2. Lum JJ, Bauer DE, Kong M, Harris MH, Li C, Lindsten T, Thompson CB. Growth factor regulation of autophagy and cell survival in the absence of apoptosis. Cell 2005;120(2):237-248.
3. Onodera J, Ohsumi Y. Autophagy is required for maintenance of amino acid levels and protein synthesis under nitrogen starvation. J Biol Chem 2005;280(36):31582-31586.
4. Esteban I, Aguado C, Sanchez M, Knecht E. Regulation of various proteolytic pathways by insulin and amino acids in human fibroblasts. FEBS Lett 2007;581(18):3415-3421.
5. Hoyer-Hansen M, Bastholm L, Szyniarowski P, Campanella M, Szabadkai G, Farkas T, Bianchi K, Fehrenbacher N, Elling F, Rizzuto R, Mathiasen IS, Jaattela M. Control of macroautophagy by calcium, calmodulin-dependent kinase kinase-beta, and Bcl-2. Mol Cell 2007;25(2):193-205.
6. Sarbassov DD, Ali SM, Sabatini DM. Growing roles for the mTOR pathway. Curr Opin Cell Biol 2005;17(6):596-603.
7. Egan DF, Shackelford DB, Mihaylova MM, Gelino S, Kohnz RA, Mair W, Vasquez DS, Joshi A, Gwinn DM, Taylor R, Asara JM, Fitzpatrick J, Dillin A, Viollet B, Kundu M*, et al.* Phosphorylation of ULK1 (hATG1) by AMP-activated protein kinase connects energy sensing to mitophagy. Science 2011;331(6016):456-461.
8. Kim J, Kundu M, Viollet B, Guan KL. AMPK and mTOR regulate autophagy through direct phosphorylation of Ulk1. Nat Cell Biol 2011;13(2):132-141.
9. Perez-Terzic CM, Chini EN, Shen SS, Dousa TP, Clapham DE. Ca2+ release triggered by nicotinate adenine dinucleotide phosphate in intact sea urchin eggs. Biochem J 1995;312 (Pt 3):955-959.
10. Berridge MJ, Bootman MD, Roderick HL. Calcium signaling: dynamics, homeostasis and remodelling. Nat Rev Mol Cell Biol 2003;4(7):517-529.
11. Hajnoczky G, Davies E, Madesh M. Calcium signaling and apoptosis. Biochem Biophys Res Commun 2003;304(3):445-454.
12. Pinton P, Giorgi C, Siviero R, Zecchini E, Rizzuto R. Calcium and apoptosis: ER-mitochondria Ca2+ transfer in the control of apoptosis. Oncogene 2008;27(50):6407-6418.
13. Gordon PB, Holen I, Fosse M, Rotnes JS, Seglen PO. Dependence of hepatocytic autophagy on intracellularly sequestered calcium. J Biol Chem 1993;268(35):26107-26112.
14. Williams A, Sarkar S, Cuddon P, Ttofi EK, Saiki S, Siddiqi FH, Jahreiss L, Fleming A, Pask D, Goldsmith P, O'Kane CJ, Floto RA, Rubinsztein DC. Novel targets for Huntington's disease in an mTOR-independent autophagy pathway. Nat Chem Biol 2008;4(5):295-305.
15. Ghislat G, Aguado C, Knecht E. Annexin A5 stimulates autophagy and inhibits endocytosis. J Cell Sci 2012;125(Pt 1):92-107.
16. Laderoute KR, Amin K, Calaoagan JM, Knapp M, Le T, Orduna J, Foretz M, Viollet B. 5'-AMP-activated protein kinase (AMPK) is induced by low-oxygen and glucose deprivation conditions found in solid-tumor microenvironments. Mol Cell Biol 2006;26(14):5336-5347.
17. Fuertes G, Martin De Llano JJ, Villarroya A, Rivett AJ, Knecht E. Changes in the proteolytic activities of proteasomes and lysosomes in human fibroblasts produced by serum withdrawal, amino-acid deprivation and confluent conditions. Biochem J 2003;375(Pt 1):75-86.
18. Wang RC, Levine B. Autophagy in cellular growth control. FEBS Lett 2010;584(7):1417-1426.
19. Woods A, Dickerson K, Heath R, Hong SP, Momcilovic M, Johnstone SR, Carlson M, Carling D. Ca2+/calmodulin-dependent protein kinase kinase-beta acts upstream of AMP-activated protein kinase in mammalian cells. Cell Metab 2005;2(1):21-33.
20. Hawley SA, Pan DA, Mustard KJ, Ross L, Bain J, Edelman AM, Frenguelli BG, Hardie DG. Calmodulin-dependent protein kinase kinase-beta is an alternative upstream kinase for AMP-activated protein kinase. Cell Metab 2005;2(1):9-19.
21. Tokumitsu H, Inuzuka H, Ishikawa Y, Ikeda M, Saji I, Kobayashi R. STO-609, a specific inhibitor of the Ca(2+)/calmodulin-dependent protein kinase kinase. J Biol Chem 2002;277(18):15813-15818.
22. Tanida I, Minematsu-Ikeguchi N, Ueno T, Kominami E. Lysosomal turnover, but not a cellular level, of endogenous LC3 is a marker for autophagy. Autophagy 2005;1(2):84-91.
23. Codogno P, Meijer AJ. Autophagy and signaling: their role in cell survival and cell death. Cell Death Differ 2005;12 Suppl 2:1509-1518.

24. Levine B, Klionsky DJ. Development by self-digestion: molecular mechanisms and biological functions of autophagy. Dev Cell 2004;6(4):463-477.
25. Mizushima N, Yoshimori T, Levine B. Methods in mammalian autophagy research. Cell 2010;140(3):313-326.
26. Rubinsztein DC, Cuervo AM, Ravikumar B, Sarkar S, Korolchuk V, Kaushik S, Klionsky DJ. In search of an "autophagomometer". Autophagy 2009;5(5):585-589.
27. Niemann A, Takatsuki A, Elsasser HP. The lysosomotropic agent monodansylcadaverine also acts as a solvent polarity probe. J Histochem Cytochem 2000;48(2):251-258.
28. Klionsky DJ, Abeliovich H, Agostinis P, Agrawal DK, Aliev G, Askew DS, Baba M, Baehrecke EH, Bahr BA, Ballabio A, Bamber BA, Bassham DC, Bergamini E, Bi X, Biard-Piechaczyk M*, et al*. Guidelines for the use and interpretation of assays for monitoring autophagy in higher eukaryotes. Autophagy 2008;4(2):151-175.
29. Mizushima N, Yoshimori T. How to interpret LC3 immunoblotting. Autophagy 2007;3(6):542-545.
30. Pullen N, Dennis PB, Andjelkovic M, Dufner A, Kozma SC, Hemmings BA, Thomas G. Phosphorylation and activation of p70s6k by PDK1. Science 1998;279(5351):707-710.
31. Egan D, Kim J, Shaw RJ, Guan KL. The autophagy initiating kinase ULK1 is regulated via opposing phosphorylation by AMPK and mTOR. Autophagy 2011;7(6):643-644.
32. Kim E. Mechanisms of amino acid sensing in mTOR signaling pathway. Nutr Res Pract 2009;3(1):64-71.
33. Meijer AJ. Amino acid regulation of autophagosome formation. Methods Mol Biol 2008;445:89-109.
34. Hosokawa N, Hara T, Kaizuka T, Kishi C, Takamura A, Miura Y, Iemura S, Natsume T, Takehana K, Yamada N, Guan JL, Oshiro N, Mizushima N. Nutrient-dependent mTORC1 association with the ULK1-Atg13-FIP200 complex required for autophagy. Mol Biol Cell 2009;20(7):1981-1991.
35. Jung CH, Jun CB, Ro SH, Kim YM, Otto NM, Cao J, Kundu M, Kim DH. ULK-Atg13-FIP200 complexes mediate mTOR signaling to the autophagy machinery. Mol Biol Cell 2009;20(7):1992-2003.
36. Suryawan A, Hawes JW, Harris RA, Shimomura Y, Jenkins AE, Hutson SM. A molecular model of human branched-chain amino acid metabolism. Am J Clin Nutr 1998;68(1):72-81.
37. Brosnan JT, Brosnan ME. Branched-chain amino acids: enzyme and substrate regulation. J Nutr 2006;136(1 Suppl):207S-211S.
38. Ogier-Denis E, Pattingre S, El Benna J, Codogno P. Erk1/2-dependent phosphorylation of Galpha-interacting protein stimulates its GTPase accelerating activity and autophagy in human colon cancer cells. J Biol Chem 2000;275(50):39090-39095.
39. Pattingre S, Bauvy C, Codogno P. Amino acids interfere with the ERK1/2-dependent control of macroautophagy by controlling the activation of Raf-1 in human colon cancer HT-29 cells. J Biol Chem 2003;278(19):16667-16674.
40. Shaw RJ, Cantley LC. Ras, PI(3)K and mTOR signaling controls tumour cell growth. Nature 2006;441(7092):424-430.
41. Pattingre S, Tassa A, Qu X, Garuti R, Liang XH, Mizushima N, Packer M, Schneider MD, Levine B. Bcl-2 antiapoptotic proteins inhibit Beclin 1-dependent autophagy. Cell 2005;122(6):927-939.
42. Gulati P, Gaspers LD, Dann SG, Joaquin M, Nobukuni T, Natt F, Kozma SC, Thomas AP, Thomas G. Amino acids activate mTOR complex 1 via Ca2+/CaM signaling to hVps34. Cell Metab 2008;7(5):456-465.
43. Yan Y, Flinn RJ, Wu H, Schnur RS, Backer JM. hVps15, but not Ca2+/CaM, is required for the activity and regulation of hVps34 in mammalian cells. Biochem J 2009;417(3):747-755.

FOOTNOTES:

This work was supported by the Ministerio de Educación y Ciencia (Grant BFU2011-22630), Fundació Marató TV3 (Grant number 100130). G.G. has been funded by an EMBO short-term fellowship. We thank Asunción Montaner for technical assistance and Benoit Viollet for providing the AMPK-deficient and wild-type mouse embryonic fibroblasts.

Supplementary figures

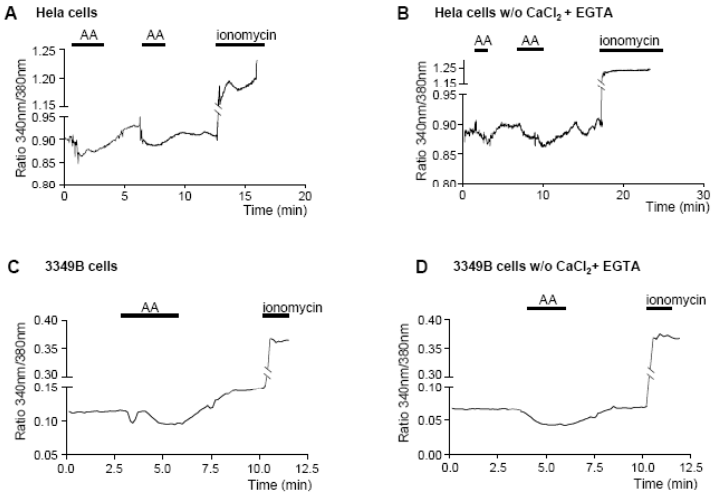

FIGURE S1. Withdrawal of amino acids raises cytosolic Ca^{2+} in HeLa cells and in 3349B fibroblasts. Fura-2AM-loaded HeLa cells (**A, B**) and 3349B normal human fibroblasts (**C, D**) were imaged as described in the Experimental Procedures. The mean values from ≥40 cells from at least 2 independent experiments are shown. The [Ca2+]c, without and with amino acids (AA) as indicated, are compared in cells incubated in KH (A, C) or in the same medium without CaCl2 and containing 100 µM EGTA (B, D). Ionomycin (1 µM) was used as a positive control.

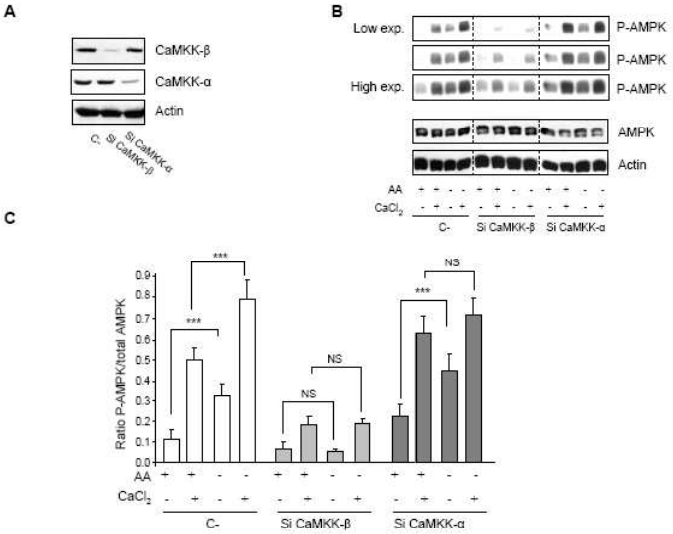

FIGURE S2. Effects of CaMKK-β or CaMKK-α silencing on AMPK activation by amino acid starvation. A. NIH3T3 cells were transfected with CaMKK-β (Si CaMKK-β), CaMKK-α (Si CaMKK-α) or with negative control (C-) siRNAs. After 72 h, cells were analyzed by immunoblot using anti-CaMKK-β, anti-CaMKK-α and, as a loading control, anti-actin antibodies. **B.** Previously transfected cells with the same siRNAs used in (A) were grown for 60 min in KH and amino acids (AA), with (+CaCl2) or without CaCl2 and supplemented with 100 µM EGTA (-CaCl2). In the last 30 min of incubation, AA were removed or not as indicated. Cell extracts (75 µg protein) were analyzed by immunoblot using anti-AMPK, anti-P-AMPK (T-172) and, as a loading control, anti-actin antibodies. Low and high exposure (exp.) blots are shown. **C.** Densitometric measurements, of the ratio of P-AMPK to total AMPK from three independent experiments. Differences were found to be statistically significant at ***p<0.0005. NS: no significant differences.

5. RESULTS: APPENDIX TO CHAPTER 2

The effect of intracellular and extracellular pH on Ca^{2+}-response to amino acids

Introduction

Chronic stress conditions, such as starvation, often alter intracellular pH (Karagiannis and Young, 2001; Korolchuk *et al*., 2011). An interplay exists between intracellular Ca^{2+} levels ($[Ca^{2+}]_c$) and pH homeostasis. This includes the activity of Ca^{2+}/H^+ antiporters and the alterations of the charge of many proteins, produced by pH modifications, which affect the affinity of Ca^{2+}-binding proteins and the activity of pumps, receptors and other channels involved in intracellular Ca^{2+} distribution (Chini *et al*., 1998; Speake and Elliott, 1998; Austin and Wray, 2000; Pernas-Sueiras *et al*., 2006; Hwang *et al*., 2011). Because our data showed a rise in $[Ca^{2+}]_c$ under amino acid depletion (Ghislat *et al*., 2012), we investigated if the Ca^{2+} response to this stress condition is dependent on extracellular and intracellular pH.

Materials and Methods

Materials

Minimum Essential medium (MEM), ionomycin, EGTA (ethylene glycol tetra-acetic acid), and nigericin were purchased from Sigma Chemical Co. MEM essential amino acids (50x), foetal bovine serum (FBS), penicillin, streptomycin 2',7'-*bis*-(carboxyethyl)-5-(and-6)-carboxyfluorescein, acetoxymethyl ester (BCECF-AM) and fura-2AM were supplied by Molecular Probes, Invitrogen Life Technologies.

Cell culture

HeLa cells, obtained from the European Collection of Animal Cell Cultures, were grown at 37ºC in a humidified atmosphere of 5% (v/v) CO_2/air in MEM with 10% heat-inactivated FBS and 1% penicillin and streptomycin. Assays were performed by incubating the cells in Krebs-Henseleit medium (KH, 118.4 mM NaCl, 4.75 mM KCl, 1.19 mM KH_2PO_4, 2.54 mM $MgSO_4$, 2.44 mM $CaCl_2 \cdot 2H_2O$, 28.6 mM $NaHCO_3$, 20 mM glucose), with 10 mM Hepes, pH 7.4. Essential amino acids were used at two times their concentration in the growth media (Esteban *et al*., 2007).

Measurements of intracellular pH

Intracellular pH was measured with 5 µM BCECF-AM as described (Tafani *et al*., 2002). Two fluorescence measurements were taken at intervals of 5 seconds at excitation wavelengths of 485 and 450 nm and an emission wavelength of 530 nm. The 485nm/450nm fluorescence ratio was used to estimate the intracellular pH. Fluorescence assays were carried out on a Zeiss Axiovert 200 inverted microscope equipped either with a cooled CCD digital camera or as part of a Zeiss LSM 510 confocal microscope (Carl Zeiss, Jena, Germany). Analysis was done using the Hamamatsu or MetaMorph/MetaFluor Analyst (Universal Imaging Corporation, Downingtown, PA).

Measurements of intracellular Ca^{2+}

Cells were loaded with 5 µM fura-2AM for 30 min at 37°C in KH and the fluorescence produced at 340 and 380 nm excitation was detected with a 520 nm emission filter at intervals of 5 seconds. The 340nm/380nm fluorescence ratio was used to estimate the intracellular Ca^{2+}. Fluorescence assays and analysis were carried out as described above for the measurement of intracellular pH.

Results

We previously found, in different cell types (NIH3T3, 3349B and HeLa cells), that withdrawal of essential amino acids increases $[Ca^{2+}]_c$, which activates autophagy by a Ca^{2+}-dependent signalling pathway (Ghislat *et al*., 2012). $[Ca^{2+}]_c$ are highly affected by extracellular pH in a wide range of cells (Negulescu and Machen, 1990; Topala *et al*., 2007; Grimm *et al*., 2012). In our experiments the starvation medium was buffered with 10 mM Hepes (see Materials and Methods), but when amino acids were added at two times their concentration in the culture medium without adjusting their pH, the pH of the incubation medium decreased to 6.0-6.5. This change of pH produces an acute increase in $[Ca^{2+}]_c$ in the presence of amino acids (Fig. 1), whereas a decrease of $[Ca^{2+}]_c$ was found after addition of essential amino acids at pH 7.4 (Ghislat *et al*., 2012).

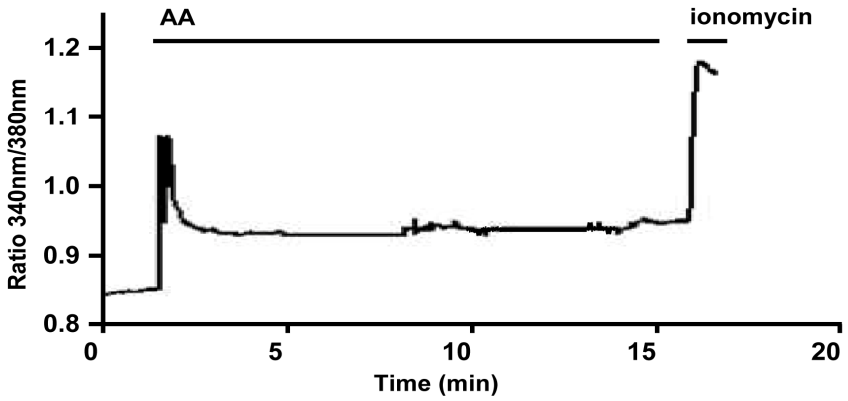

Figure 1. Addition of essential amino acids without adjusting their pH increases intracellular Ca^{2+} levels. Fura-2AM-loaded HeLa cells were imaged as described in Materials and Methods. The mean values from ≥40 cells from a representative experiment are shown. $[Ca^{2+}]_c$ are compared in cells incubated in KH without $CaCl_2$ and containing 100 µM EGTA. Where indicated, essential amino acids (AA) were added at two times their concentration in the culture medium without adjusting their pH to 7.4. To assess the viability of the cells, ionomycin (1 µM) was used in each experiment.

Therefore, in all the following experiments the amino acids added to the medium were always adjusted to physiological pH (7.4). To know whether these intracellular Ca^{2+} responses to amino acids were associated to changes in intracellular pH, which can affect $[Ca^{2+}]_c$ (Austin and Wray, 2000; Peracchia, 2004; Pernas-Sueiras *et al*., 2006), we assessed the effect of amino acids on intracellular pH, using the cell permeant fluorescent pH sensor 2',7'-*bis*-(carboxyethyl)-5-(and-6)-carboxyfluorescein, acetoxymethyl ester (BCECF-AM). The ratio of fluorescence intensities, measured at 485 and 450 nm excitation wavelengths (see Materials and Methods) is proportional to pH values, in such a way that when pH increases, higher values are obtained (Ozkan and Mutharasan, 2002). As shown in Fig. 2, essential amino acids cause a quick decrease of intracellular pH that subsequently recuperates its initial levels within approximately 2-3 min.

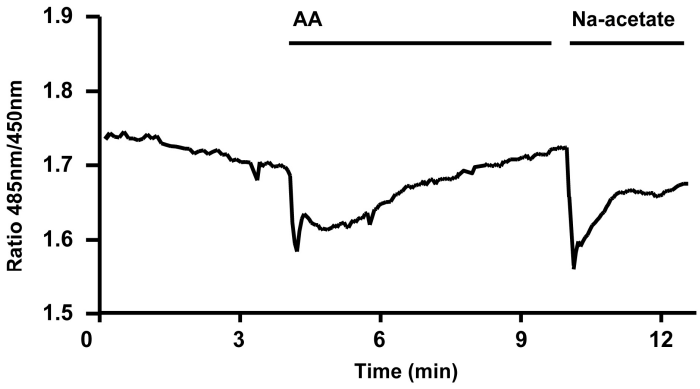

Figure 2. Essential amino acids decrease intracellular pH. BCECF-AM loaded Hela cells were imaged as described in Materials and Methods. A Representative experiment with the mean values from ≥40 cells is shown. The intracellular pH levels are compared in cells incubated, as indicated, in KH without $CaCl_2$ and containing 100 µM EGTA, with and without essential amino acids (AA). 20 mM sodium acetate (Na-acetate) was used as a control in each experiment.

Nigericin is a ionophore that equilibrates intra- and extracellular pHs and, therefore, when the incubation medium is at pH 7.4 it should cancel the intracellular acidification produced by essential amino acids. We found that when nigericin was added under these conditions, the decrease in $[Ca^{2+}]_c$ persisted (Fig. 3). This result suggests that the intracellular Ca^{2+} response to essential amino acids at pH 7.4 is independent of intracellular pH.

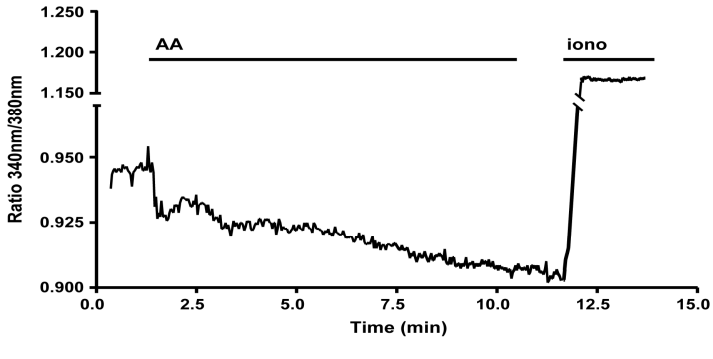

Figure 3. In the presence of nigericin, essential amino acids still decrease intracellular Ca^{2+} levels. Cells previously incubated with 20 µM nigericin were analyzed for $[Ca^{2+}]_c$ measurement in KH without $CaCl_2$ and containing 100 µM EGTA, with and without essential amino acids (AA). The mean values from ≥40 cells from a representative experiment are shown. Ionomycin (1 µM) was used as a control in each experiment.

Discussion

Fluctuations in cytosolic ion concentrations in response to various signals trigger many intracellular processes and pathways. The Ca^{2+} levels and the extracellular pH, which also affects intracellular pH (Casey *et al*., 2009), are relevant in the cell response to stress conditions, because of their importance to maintain and restore the basal metabolic activity, and they do not act independently of each other (Austin and Wray, 2000; Henrich and Buckler, 2009; Krizaj *et al.*, 2011).

The results reported herein highlight the importance of the extracellular pH in the Ca^{2+} response to amino acids. It is possible that the amino acid-dependent rise in $[Ca^{2+}]_c$ reported by others (Gulati *et al*., 2008) is related to the acidification of the medium by amino acids. Moreover, under an extracellular pH 7.4, essential amino acids decrease the intracellular pH of the cells. In accordance with this result, an increase of intracellular pH produced by amino acid starvation was reported by others in HeLa cells (Korolchuk *et al*., 2011). However, Ca^{2+} response to essential amino acids seems to be independent of this cytosolic acidification. Thus, whereas the extracellular acidification by amino acids changes their effect on cytosolic Ca^{2+}, the intracellular acidification does not affect the Ca^{2+} response to essential amino acids at pH 7.4.

Therefore, under a neutral extracellular pH, Ca^{2+} response to essential amino acids, and probably the Ca^{2+}-dependent induction of autophagy by amino acid starvation described in Chapter 3 of Results, is independent of intracellular pH.

References

Austin C, Wray S (2000) Interactions between Ca(2+) and H(+) and functional consequences in vascular smooth muscle. Circ Res 86:355-363.

Casey JR, Grinstein S, Orlowski J (2009) Sensors and regulators of intracellular pH. Nat Rev Mol Cell Biol 11:50-61.

Chini EN, Liang M, Dousa TP (1998) Differential effect of pH upon cyclic-ADP-ribose and nicotinate-adenine dinucleotide phosphate-induced Ca2+ release systems. Biochem J 335:499-504.

Esteban I, Aguado C, Sanchez M, Knecht E (2007) Regulation of various proteolytic pathways by insulin and amino acids in human fibroblasts. FEBS Lett 581:3415-3421.

Ghislat G, Patron M, Rizzuto R, Knecht E (2012) Withdrawal of essential amino acids increases autophagy by a pathway involving Ca2+/calmodulin-dependent kinase kinase-beta (CaMKK-beta). J Biol Chem 287:38625-38636.

Grimm C, Jors S, Guo Z, Obukhov AG, Heller S (2012) Constitutive activity of TRPML2 and TRPML3 channels versus activation by low extracellular sodium and small molecules. J Biol Chem 287:22701-22708.

Gulati P, Gaspers LD, Dann SG, Joaquin M, Nobukuni T, Natt F, Kozma SC, Thomas AP, Thomas G (2008) Amino acids activate mTOR complex 1 via Ca2+/CaM signalling to hVps34. Cell Metab 7:456-465.

Henrich M, Buckler KJ (2009) Acid-evoked Ca2+ signalling in rat sensory neurones: effects of anoxia and aglycaemia. Pflugers Arch 459:159-181.

Hwang SM, Koo NY, Jin M, Davies AJ, Chun GS, Choi SY, Kim JS, Park K (2011) Intracellular acidification is associated with changes in free cytosolic calcium and inhibition of action potentials in rat trigeminal ganglion. J Biol Chem 286:1719-1729.

Karagiannis J, Young PG (2001) Intracellular pH homeostasis during cell-cycle progression and growth state transition in Schizosaccharomyces pombe. J Cell Sci 114:2929-2941.

Korolchuk VI, Saiki S, Lichtenberg M, Siddiqi FH, Roberts EA, Imarisio S, Jahreiss L, Sarkar S, Futter M, Menzies FM, O'Kane CJ, Deretic V, Rubinsztein DC (2011) Lysosomal positioning coordinates cellular nutrient responses. Nat Cell Biol 13:453-460.

Krizaj D, Mercer AJ, Thoreson WB, Barabas P (2011) Intracellular pH modulates inner segment calcium homeostasis in vertebrate photoreceptors. Am J Physiol Cell Physiol 300:C187-197.

Negulescu PA, Machen TE (1990) Lowering extracellular sodium or pH raises intracellular calcium in gastric cells. J Membr Biol 116:239-248.

Ozkan P, Mutharasan R (2002) A rapid method for measuring intracellular pH using BCECF-AM. Biochim Biophys Acta 1572:143-148.

Peracchia C (2004) Chemical gating of gap junction channels; roles of calcium, pH and calmodulin. Biochim Biophys Acta 1662:61-80.

Pernas-Sueiras O, Alfonso A, Vieytes MR, Orfao A, Escribano L, Francisca SJ, Botana LM (2006) Calcium-pH crosstalks in the human mast cell line HMC-

1: intracellular alkalinization activates calcium extrusion through the plasma membrane Ca2+-ATPase. J Cell Biochem 99:1397-1408.

Sandoval AJ, Riquelme JP, Carretta MD, Hancke JL, Hidalgo MA, Burgos RA (2007) Store-operated calcium entry mediates intracellular alkalinization, ERK1/2, and Akt/PKB phosphorylation in bovine neutrophils. J Leukoc Biol 82:1266-1277.

Speake T, Elliott AC (1998) Modulation of calcium signals by intracellular pH in isolated rat pancreatic acinar cells. J Physiol 506:415-430.

Tafani M, Cohn JA, Karpinich NO, Rothman RJ, Russo MA, Farber JL (2002) Regulation of intracellular pH mediates Bax activation in HeLa cells treated with staurosporine or tumor necrosis factor-alpha. J Biol Chem 277:49569-49576.

Topala CN, Bindels RJ, Hoenderop JG (2007) Regulation of the epithelial calcium channel TRPV5 by extracellular factors. Curr Opin Nephrol Hypertens 16:319-324.

Zaun HC, Shrier A, Orlowski J (2012) N-Myristoylation and Ca2+ Binding of Calcineurin B Homologous Protein CHP3 Are Required to Enhance Na+/H+ Exchanger NHE1 Half-life and Activity at the Plasma Membrane. J Biol Chem 287:36883-36895.

6. RESULTS: CHAPTER 3

Annexin A5 stimulates autophagy and inhibits endocytosis

Ghislat G, Aguado C, Knecht E (2012) J Cell Sci 125: 92-107

Annexin A5 stimulates autophagy and inhibits endocytosis

Ghita Ghislat[a], Carmen Aguado[a,b], Erwin Knecht[a,b*]

[a]*Laboratorio de Biología Celular, Centro de Investigación Príncipe Felipe, Avda. Autopista del Saler 16, 46012-Valencia, Spain and* [b]*CIBERER, Valencia, Spain*

[*] *Corresponding author*. Centro de Investigación Príncipe Felipe, Avda. Autopista del Saler 16, 46012-Valencia, Spain, Tel.: +34-96-3289680; fax: +34-96-3289701
E-mail: knecht@cipf.es

SUMMARY

In macroautophagy, a major lysosomal catabolic process especially activated under starvation in eukaryotic cells, a new organelle, the autophagosome, engulfs cytoplasmic substrates, which are degraded after fusion with endosomes and/or lysosomes. During a shotgun proteome analysis of purified lysosomal membranes from mouse fibroblasts, a Ca^{2+}-dependent phospholipid binding protein, annexin A5, increased its levels on lysosomal membranes under starvation. This suggests a role of this protein, an abundant annexin with a still unknown intracellular function, in starvation-induced lysosomal degradation. Transient overexpression and silencing experiments showed that, in fact, annexin A5 increased lysosomal protein degradation, and colocalization experiments, based on GFP sensitivity to lysosomal acidic pH, indicated that this was mainly the result of inducing autophagosome-lysosome fusion. Annexin A5 also inhibited the endocytosis of a fluid-phase marker and of cholera toxin, but not receptor mediated endocytosis. Therefore, we propose a double and opposite role of annexin A5 regulating the endocytic and autophagic pathways and the fusion of autophagosomes with lysosomes and endosomes.

Key words: Annexin A5 / Autophagy / Endocytosis / Lysosomes

INTRODUCTION

In eukaryotic cells, macroautophagy (hereafter referred to as autophagy) is an important catabolic process for the clearance of intracellular components, including whole organelles, long-lived proteins and other cytosolic molecules (Knecht et al., 2009). The first step in autophagy involves the formation of a flat membrane sac, called in yeast the phagophore that in mammalian cells has a still controversial origin. This structure surrounds cytoplasmic substrates and eventually closes, generating thereby a double-membrane organelle, the autophagosome (Levine and Klionsky, 2004). Several compartments, including endoplasmic reticulum (ER) mainly (Axe et al., 2008; Hayashi-Nishino et al., 2009; Yla-Anttila et al., 2009), but also mitochondria (Hailey et al., 2010; Mari et al., 2010) and plasma membrane (Ravikumar et al., 2010), appear to contribute proteins and lipids to the forming autophagosome under various situations (Cuervo, 2010). Lysosomes and/or late endosomes are the eventual target of autophagosomes for fusion events, to form autolysosomes containing lysosomal hydrolases that degrade the engulfed material and recycle the breakdown products. The power of yeast genetics has allowed to clarify several steps of the molecular mechanism of this process, and more than thirty evolutionarily conserved autophagy-related proteins (Atg proteins) have been identified by complementation screening (Klionsky et al., 2003). Some of these proteins are also present in mammalian cells (Knecht et al., 2009), while there are also mammalian-specific proteins involved in autophagy.

Stress conditions, such as starvation, growth factor deprivation or protein aggregation upregulate autophagy to compensate for the lack of amino acids and energy and for other cell stresses and defects (Douglas and Dillin, 2010; Lum et al., 2005; Onodera and Ohsumi, 2005). However, mammalian cells sustain autophagy at a low basal level for the turnover of normally occurring misfolded proteins and damaged molecules and organelles. In mammalian cells, the main autophagy regulators are nutritional and hormonal (Meijer and Codogno, 2006). Thus, in early studies, insulin and amino acids were shown to inhibit autophagy, whereas glucagon activates it. In addition, glucose (which, in contrast to yeast, increases autophagy in mammalian cells), vitamins, various growth factors, Ca^{2+}, etc. have been also implicated in autophagy regulation.

Ca^{2+} is a universal messenger regulating many physiological functions in the cells, such as secretion, contraction, metabolism, gene transcription and death, and implicated in some pathological processes too (Berridge et al., 2003; Perez-Terzic et al., 1995). Regarding its role in autophagy, a pioneering study, exploring the contribution of Ca^{2+} to autophagy, established that stimulation of autophagy depends, rather than on cytoplasmic Ca^{2+}, on its presence within intracellular Ca^{2+}-storage compartments (Gordon et al., 1993). More recently, it was reported that Ca^{2+} derived from extracellular sources and from ER is a signal for autophagy induction, based on the activation of AMP-activated protein kinase by Ca^{2+}/calmodulin dependent kinase kinase-beta (Hoyer-Hansen et al., 2007). However, other studies have provided evidence that, at least under certain conditions, an increase in cytosolic Ca^{2+} should inhibit autophagy (Williams et al., 2008). In addition to these conflicting conclusions on autophagy regulation, Ca^{2+} has a more well-established role in another closely related lysosomal function, endocytosis, where it is required for efficient fusion events among late endosomes with lysosomes and autophagosomes (Luzio et al., 2007; Pryor et al., 2000).

While investigating the regulation of the lysosomal degradation of proteins, we carried out a 2-Dimensional Differential Gel Electrophoresis (2D-DIGE) proteomic study of lysosomal membranes isolated from mouse fibroblasts, to identify proteins whose levels change under conditions of high or low proteolysis in the cells. The proteins whose levels on lysosomal membranes increased under high proteolysis included at least three subunits of the vacuolar ATPase (Esteban et al., 2007) and three Ca^{2+}-dependent phospholipid binding proteins (annexin A1, annexin A5 and copine 1). In this study, we have concentrated on one of these Ca^{2+}-binding proteins, annexin A5, because it is an abundant annexin with a still unknown intracellular function, and analysed its possible role in lysosomal protein degradation.

RESULTS

Under starvation, annexin A5 translocates from Golgi to lysosomal membranes in a Ca^{++}-dependent way

To identify proteins involved in the regulation of lysosomal proteolytic pathways, we investigated, by 2-D DIGE complemented with mass spectrometry analysis, lysosomal membranes isolated from NIH3T3 cells incubated in Krebs Henseleit medium (KH) without (starvation) and with insulin (I), amino acids (AA) or both (IAA). Among other proteins whose levels changed on the lysosomal membranes under conditions that produce high (KH), low (IAA) and intermediate (I or AA) proteolysis in the cells, a spot was identified that corresponded to the phospholipid binding protein annexin A5 (Fig. 1A). As shown in Fig. 1B, levels of annexin A5 in KH (high proteolysis) decreased after addition of amino acids (AA) or insulin plus amino acids (IAA), but apparently not after addition of insulin alone (I). This was confirmed in western blot experiments of subcellular fractions enriched in nuclei, mitochondria and lysosomes from NIH3T3 cells incubated under conditions that produce high (KH) and low (IAA) proteolysis. Annexin A5 was localized in mitochondrial and lysosomal fractions, and its levels were higher in lysosomes and, with less difference, in mitochondria isolated from cells incubated in KH (Fig. 1C). Consistent with these results, we also found that colocalization of annexin A5 with a lysosomal protein, cathepsin B (Fig. 1D, see also Fig. 3B, KH and IAA in the histogram), and with LysoTracker Red (see Fig. 3A, two upper panels and KH and IAA in the histogram below), a membrane-diffusible probe accumulating in acidic organelles, especially in lysosomes (Kornhuber et al., 2010), was higher in KH than in IAA. Interestingly, the cellular localization of annexin A5 is different in both media. In IAA, annexin A5 yielded a perinuclear pattern that becomes more dispersed and punctate in KH, consistent with its translocation to a lysosomal localization under starvation. Experiments with various markers (Fig. 2) indicate colocalization of annexin A5 with Golgi complex and late endosomes, but not with ER and early endosomes. In KH, colocalization of annexin A5 with the Golgi complex strongly decreases, while colocalization with late endosomes slightly increases.

In addition, and because annexin A5 is a Ca^{2+}-dependent binding protein and unpublished results from our laboratory show a rise in intracellular Ca^{2+} levels under starvation (KH) in comparison with fed cells (IAA), we investigated if the translocation of annexin A5 to lysosomal membranes in starved cells was Ca^{2+}-dependent. Thus, an intracellular Ca^{2+} chelator, BAPTA-AM, reduced the colocalization of annexin A5 with lysosomal markers in the cells incubated in KH medium, while in the cells incubated in IAA medium with a Ca^{2+} ionophore, ionomycin, increased this colocalization (Fig. 3). Taken together,

these data suggest that under starvation conditions (KH) annexin A5 partially translocates from Golgi to lysosomal membranes in a Ca^{2+}-dependent way.

Annexin A5 increases lysosomal protein degradation

In eukaryotic cells under starvation, lysosomes represent the main catabolic compartment. Under these conditions, annexin A5 apparently translocates to lysosomal membranes. Therefore, we investigated its possible role in stimulating lysosomal protein degradation. Since the levels of annexin A5 after overexpression were lower in NIH3T3 than in HEK293T cells, we analyzed wild type (WT) and transiently transfected HEK293T cells with A5 (overexpression) or C- (negative controls) vectors. Pulse-chase experiments were carried out to analyze the degradation of long lived proteins by established procedures (Fuertes et al., 2003a; Mizushima et al., 2010). As shown in Fig. 4, overexpression of annexin A5 increased total (Fig. 4A) and especially lysosomal (Fig. 4B) protein degradation under both high (KH) and low (IAA) proteolysis. This supports a role of annexin A5 in the activation of lysosomal protein degradation. This conclusion was further confirmed by measurements in these cells of the levels of p62, a multifunctional protein that binds LC3-II and is destroyed in lysosomes (Moscat and Diaz-Meco, 2009). As shown in Fig. 4C, overexpression of annexin A5 clearly decreases p62 levels, even in the cells incubated in IAA medium, which contain more of p62 because its lower degradation, consistent with annexin A5 increasing lysosomal protein degradation. This decrease in p62 levels was prevented when the cells were incubated with bafilomycin A1 (hereafter called bafilomycin), indicating that it depends on lysosomal degradation.

We also investigated, in similar experiments, the effects of silencing annexin A5 with two different (si1, si2) siRNAs that target annexin A5 (siA5), using now NIH3T3 cells because they express higher levels of this protein. Both siA5 produced a similar silencing of the protein (Fig. S1A and B, upper panels) and, therefore, in most of the following assays we show results with one of both, but the average of the two. Silencing of annexin A5 produced the opposite effect to overexpression; it moderately decreased total (Fig. 4D) and especially lysosomal (Fig. 4E) intracellular protein degradation, and this was more evident under high proteolysis conditions (KH). In KH, decreased autophagy was also observed with its inhibitor 3-methyladenine (Fig. 4F), but this could not be investigated in IAA because under these conditions autophagy is very low and 3-methyladenine has some secondary effect increasing protein degradation, as already observed before by us and by others (Fuertes et al., 2003a; Williams et al., 2008; Wu et al., 2010). The relatively low inhibition of intracellular protein degradation by annexin A5 silencing (14.6 ± 2.3% in KH) can perhaps be explained by redundancy, because, for example, cosilencing of annexin A5 and copine 1 increased considerably (about 40.5 ± 6.5% in KH) this inhibition (our unpublished results). In addition, we found that in IAA and also in KH, silencing of annexin A5 raised p62 levels (Fig. 4G). However, in bafilomycin treated cells, in which p62 levels increased, annexin A5 knockdown caused no further increase. This indicates that the decrease in the levels of p62 depends on lysosomal degradation and that this process is partially defective under annexin A5 silencing. Therefore, all these results are consistent with annexin A5 increasing lysosomal protein degradation.

Annexin A5 enhances autophagosome maturation

Under starvation, autophagy is activated to maintain amino acids and energy levels in the cell and becomes the main lysosomal degradation pathway (Knecht et al., 2009; Levine and Klionsky, 2004). Therefore, we investigated more specifically the effect of annexin A5 on autophagy with its well-established marker LC3-II. For overexpression experiments we used, as above, transiently transfected HEK293T cells with A5 or C- vectors. Overexpression of annexin A5 decreases LC3-II levels (Fig. 5A, high exposure blot). This was also observed using HEK293T cells with stable expression of eGFP-LC3: overexpression of annexin A5 decreased the number of fluorescent puncta under high (KH) and low (IAA) proteolysis conditions (Fig. 5B). Since overexpression of annexin A5 increases lysosomal proteolysis, the observed decrease in LC3-II levels can not be due to a reduced autophagosome formation and should reflect an enhanced conversion of autophagosomes into autolysosomes. Under inhibition, with various treatments (Codogno and Meijer, 2005), of the degradation of LC3-II in autolysosomes, the levels of LC3-II are indicative of the formation rate of autophagosomes (Levine and Klionsky, 2004; Lum et al., 2005; Mizushima et al., 2010). Using leupeptin and ammonium chloride, a treatment with the same effects as bafilomycin (Esteve et al., 2010), to inhibit lysosomal degradation, we found that overexpression of annexin A5 not only does not decrease LC3-II levels, but it even produces a significant increase (Fig. 5A, low exposure blot). Thus, annexin A5 probably also increases autophagosome formation, but this effect should be less important, since in the absence of lysosomal inhibitors LC3-II levels decrease.

Silencing of annexin A5 with two different siRNAs in NIH3T3 cells incubated in KH or in IAA caused accumulation of the autophagosome-associated protein LC3-II in the absence of lysosomal inhibitors (lower panel in Fig. S1A). This accumulation most probably indicates a decreased degradation of LC3-II in the absence of annexin A5 due to an inhibition of autophagosome-lysosome fusion, as suggested in the overexpression experiments. However, the accumulation of LC3-II was also observed in the presence of lysosomal inhibitors (especially in IAA, lower panel in Fig. S1B). This was not a cell type-specific effect, since similar results were obtained with both siRNAs in HEK293T cells (Fig. S1C and D). Fig. 6A includes, on the right, the densitometric analysis of various experiments similar to the silencing experiment shown on the left. The observed increase in autophagic vacuoles in the cells incubated without lysosomal inhibitors was further confirmed using NIH3T3 cells that stably express eGFP-LC3 (Fig. 6B). Also, knockdown of annexin A5 increased the fractional volume of early (Av_i) and late (Av_d) autophagic vacuoles (Fig. 6C), and this increase was proportionally higher for Av_i (1.42x in KH and 2.16x in IAA) than for Av_d (1.08x in KH and 1.13x in IAA). These results suggest again a role of annexin A5 in autophagosome maturation. However, it remains to be explained the observed accumulation of LC3-II after silencing of annexin A5 in the presence of lysosomal inhibitors. This is later discussed.

Annexin A5 induces autophagosome delivery to lysosomes

To confirm with a different procedure that annexin A5 increases autophagic flux, as suggested in the above experiments, we used a flow cytometric assay based on the loss of eGFP fluorescence when eGFP-LC3 bound to autophagosomal membranes is delivered to lysosomes for degradation (Shvets and Elazar,

2009). As expected, if lower eGFP-LC3 fluorescence is due to an increased autophagic flux, fluorescence was lower in starvation medium (KH) than in IAA, and this decrease was blocked with wortmannin, which inhibits autophagy (Fig. 7A). Annexin A5 overexpression induces a decay in eGFP-LC3 fluorescence (Fig. 7B), supporting an enhanced delivery of eGFP-LC3 to the lysosomal compartment, while annexin A5 silencing increased this fluorescence (Fig. 7C). These results are in agreement with the LC3 western blot experiments and support the involvement of annexin A5 in the delivery of autophagosomes to lysosomes.

To further confirm the effect of annexin A5 on autophagosome maturation, we used HEK293T and NIH3T3 cells stably expressing an mRFP-GFP/LC3 tandem reporter that has been found to be useful to trace autophagosome maturation (Kimura et al., 2007). Hence, within lysosomes eGFP-LC3 fluorescence is quenched due to GFP sensitivity to acidic environments, whereas mRFP-LC3 fluorescence is more stable upon acidification. Thus, autophagosomes with a physiological pH deliver both red and green fluorescence, while the latter is lost in autolysosomes with an acidic pH. Overexpression of annexin A5 in HEK293T cells led to a rise in vesicles with red fluorescence in both KH and IAA media (Fig. 8A), indicating increased autophagosome maturation. In contrast, the relative proportion of vesicles with yellow fluorescence increased in annexin A5 silenced NIH3T3 cells incubated in both media (Fig. 8B). These results suggest again a role of annexin A5 in autophagosome maturation. Moreover, changing the endogenous levels of annexin A5 (by overexpression or silencing) neither affected the proteolytic activities of extracts from cells within a wide range of pHs (3.0 to 8.0), including those that are optimal for lysosomes (Fig. S2A and B), nor the intralysosomal pH (Table S1). Therefore, and although we cannot totally exclude that annexin A5 slightly affects also the lysosomal degradative capacity, most data support a major role in increasing the fusion of autophagosomes with lysosomes.

Since annexin A5 does not change intralysosomal pH, we also quantified the LysoTracker Red labelling by flow cytometry. Annexin A5 overexpression (Fig. 9A) slightly increased LysoTracker Red staining, especially in IAA. Therefore, it appears that annexin A5 is involved in the maturation of autophagosomes. However, silencing of annexin A5 produced the same effect (Fig. 9B) and this remains to be explained.

Annexin A5 is a negative regulator of endocytosis and of amphisome formation

Since annexin A5 appears to increase autophagy, it is surprising that its silencing also increases lysosomal mass. Lysosomes are ubiquitous degradation organelles that receive their substrates through either endocytosis or autophagy. Thus, we considered the possibility that the raise in LysoTracker Red staining under annexin A5 silencing was due to enhanced endocytic flux. Therefore, we measured the effect of annexin A5 on the internalisation of FITC-dextran, a fluid phase endocytosis marker. Overexpression of annexin A5 reduced FITC-dextran uptake (Fig. 10A), while silencing strongly increased FITC-dextran uptake (Fig. 10B). These results indicate that annexin A5 is a negative regulator of fluid phase endocytosis. Similar, but less evident, effects were obtained with cholera toxin: overexpression and silencing of annexin A5 decreased (Fig. 10C) and increased (Fig. 10D), respectively, its endocytosis. In contrast, annexin A5 has apparently no significant effect on receptor-mediated endocytosis (Fig. S3). Therefore, since annexin A5 increases autophagosome delivery to lysosomes,

decreasing at the same time endocytosis, these effects can probably account for the enhanced lysosomal mass observed under both overexpression (increased autophagic maturation) and knockdown (increased endocytic uptake) of this protein.

A last observation that remains to be explained is why annexin A5 silencing increases LC3-II levels in the presence of lysosomal inhibitors. Since annexin A5 silencing also increases endocytosis, we considered that the accumulation of LC3-II could be a secondary effect produced by an enhanced fusion of autophagosomes with late endosomes. Therefore, a colocalization analysis was carried out in NIH3T3 using antibodies that recognise LC3, as marker of autophagosomes, and LBPA, as a marker of late endosomes. The use of eGFP-LC3 was not possible here because the low pH quenches the fluorescent signal of GFP (Kimura et al., 2007). As shown in Fig. 11A-C, annexin A5 silencing increases in fact the colocalization of lysobisphosphatidic acid (LBPA) with LC3 and, thus, the formation of the so-called amphisomes, which do not degrade LC3-II as efficiently as autolysosomes (Pillay et al., 2002). This could explain the relatively low effect of annexin A5 knockdown in the pulse and chase experiments shown in Fig. 4D-F and the observed accumulation of LC3-II in annexin A5 silenced cells in the presence of lysosomal inhibitors.

Interestingly, the quantification of LBPA stained area showed a significant increase under annexin A5 knockdown (Fig. 11D), in agreement with the negative involvement of this protein in the endocytic pathway.

In summary, all the results presented here support new intracellular roles of annexin A5. First, annexin A5 facilitates the autophagic flux, increasing the fusion of autophagosomes with lysosomes but not with late endosomes. Second, annexin A5 is a negative regulator of some endocytic pathways and, therefore, its silencing increases while its overexpression decreases them.

DISCUSSION

Although in the last years numerous contributions have produced a better understanding of the mechanisms of autophagy, critical questions remain unanswered. In autophagy, formation of autophagosomes and fusion at later stages with lysosomes/endosomes are both important for autophagic flux (Noda et al., 2009; Xie and Klionsky, 2007). Our results demonstrate the involvement of annexin A5, a Ca^{2+}-binding protein, in this process. This annexin belongs to a superfamily of structurally related, Ca^{2+}-sensitive proteins that bind to negatively charged phospholipids, establishing specific interactions with other lipid microdomains. They are present in all eukaryotic cells and share a common folding motif, the "annexin core", with Ca^{2+}- and lipid-binding sites. Annexins participate in a variety of intracellular processes, ranging from the regulation of membrane dynamics to cell migration, proliferation, and apoptosis (Monastyrskaya et al., 2009). Annexin A5, one of the most abundants annexins in mammalian cells, has a hitherto unknown function within the intracellular environment, although it has been found to modulate the activities of protein kinase C as well as phospholipase A by interfering with their binding to negatively charged phospholipids and Ca^{2+} (Russo-Marie, 1999). Furthermore, an antithrombotic property has been proposed for annexin A5 by shielding phospholipids, especially phosphatidylserine, and blocking thereby their availability for coagulation reactions (Cederholm and Frostegard, 2007).

The results shown here indicate that annexin A5 migrates to lysosomal membranes under starvation and, since this is one of the best characterized stimuli of autophagy (Knecht et al., 2009), we hypothesized a possible involvement of annexin A5 in this process. Our data revealed that starvation provokes a translocation of this protein from the Golgi complex to lysosomes and, to a much lesser extent, to late endosomes. Several reports have associated annexin A5 with the Golgi complex and the ER (Barwise and Walker, 1996; Rambotti et al., 1993), late endosomal membranes (Diakonova et al., 1997; Rambotti et al., 1993) and also with the nucleus (reviewed in (Monastyrskaya et al., 2009)). Our results do not show a significant nuclear localization of annexin A5, probably because our experiments were carried out in the absence of serum, which appears to contain factors necessary for this nuclear localization (Barwise and Walker, 1996; Mohiti et al., 1997). We also do not find in our cells colocalization of annexin A5 with the ER, probably because it is cell-specific, since annexin A5 was located at the ER and Golgi complex in Langhans cells (Rambotti et al., 1993), but only at the Golgi complex in hepatoma cells (Gao et al., 2005).

We hypothesized that translocation of annexin A5 to the lysosomal membranes under starvation represents an important mechanism in the control of autophagy/lysosomal degradation. This was evidenced in pulse-chase experiments and in measurements of p62 levels after overexpressing or silencing annexin A5. These data, combined with results from LC3 western blots and eGFP-LC3 experiments, without lysosomal inhibitors and under both annexin A5 overexpression and silencing, suggest a main role of annexin A5 in autophagosome clearance. Fluorescence decay experiments together with mRFP-GFP-LC3 reporter data further support the implication of annexin A5 in the fusion of autophagosomes with lysosomes rather than in modifying the lysosomal degradative capacity, since no changes in lysosomal pH or in proteolytic activity at acid pHs were detected under knockdown and overexpression of this protein. This role of annexin A5 is compatible with previous indications that Ca^{2+}, together with the acid intralysosomal pH, are essential for autophagosome/lysosome fusion (Koga et al., 2010), and also with experiments showing that annexin A5 induces *in vitro* fusion and aggregation of vesicles in a Ca^{2+}- and acidic pH-dependent manner (Hoekstra et al., 1993). Indeed, annexin A5 binds to phospholipids in a Ca^{2+}-sensitive manner (Walker et al., 1992) and, since unpublished data from our laboratory show a rise of intracellular Ca^{2+} under starvation in mouse and human fibroblasts, it seems possible that it is this rise in Ca^{2+} what induces annexin A5 translocation to lysosomal membranes. In fact, colocalization of annexin A5 with lysosomes increases with ionomycin treatment in IAA, whereas the well established Ca^{2+} chelator BAPTA-AM, prevents this colocalization in KH medium. Also and since amino acids decrease intracellular Ca^{2+} levels while insulin not (our unpublished results), this may explain why, in contrast to amino acids, insulin does not reduce the binding of annexin A5 to lysosomal membranes. Hence, all these data are compatible with a requirement of Ca^{2+} for the translocation of annexin A5 to the lysosomal membranes. Moreover, annexin A5 shows a cholesterol-mediated enhancement of its Ca^{2+}-dependent binding to membranes (Ayala-Sanmartin, 2001), and another report supports the importance of membrane cholesterol levels in the fusion of lysosomes with autophagosomes (Massey et al., 2008). Thus, annexin A5 could induce autophagosome-lysosome fusion through cholesterol rich domains in their membranes in a pH- and Ca^{2+}-dependent way. However, the precise molecular mechanisms that drive these fusion events remain to be investigated.

The results obtained after annexin A5 silencing in the cells incubated with lysosomal inhibitors appear to be contradictory, since they still indicate higher levels of LC3-II. A possible explanation could be provided by the negative role of annexin A5 in both fluid phase and cholera toxin endocytosis. We propose that annexin A5 knockdown enhances both internalisation and convergence of endocytosis with the autophagic pathway. In fact, our data indicate a significant rise in autophagosome-late endosome fusion to form amphisomes under the low levels of annexin A5 remaining after silencing. Previous reports have shown increased accumulation of amphisomes when fusion between autophagosomes and lysosomes is impaired (Eskelinen et al., 2002; Koga et al., 2010; Massey et al., 2008), which is consistent with our results. It is known that late endosomes have proteolysis competence, although less efficiently than lysosomes (Pillay et al., 2002). Consistent with these observations, annexin A5 silencing will make degradation of LC3 in amphisomes less efficient, and this could explain the higher levels of the LC3-II autophagic marker observed under these conditions in the presence of protease inhibitors. Thus, we propose that the impairment of autophagosome fusion with lysosomes by annexin A5 knockdown is partially compensated by an enhanced formation of amphisomes.

If this is so, an obvious question is how annexin A5 could regulate negatively the fusion of autophagosomes with late endosomes, while promoting the fusion with lysosomes. Our data show colocalization of annexin A5 with lysosomes but also with late endosomes. Interestingly, a recent study suggests that, despite their similarities, fusion of autophagosomes with lysosomes or endosomes may be distinctly governed, since both types of fusion have different nucleotide requirements (Koga et al., 2010). Annexin A5 could distinctly affect the fusion of the different organelles, enhancing the fusion of certain lipids and blocking others. The identification of the precise mechanisms by which annexin A5 is involved in the fusion machinery of autophagosomes with endosomes or with lysosomes will require further work, but one possibility is that the observed differences are due to distinct intrinsic properties of the membranes of these compartments determined by their lipid composition. Relevant to this study, annexin A1, another Ca^{2+} binding protein with a significant degree of biological and structural homology to annexin A5, has been recently related to autophagy regulation (Kang et al., 2011), and the authors propose that this may occur by controlling the formation of amphisomes. In our 2D-DIGE proteomic study, this protein was one of the three Ca^{2+}-dependent phospholipid binding proteins (annexin A1, annexin A5 and copine 1) whose levels increased on lysosomal membranes from human fibroblasts under conditions of high proteolysis. Therefore, it is possible that there is some redundancy among these proteins in their effects on lysosomal degradation. In fact, we found that although cosilencing of annexin A5 and annexin A1 does not further increase the inhibition of lysosomal degradation produced by annexin A5 (~15%), cosilencing of annexin A5 and of copine I produces an important increase (~40%) in this inhibition.

In summary, our findings propose novel functions for annexin A5, promoting delivery of autophagosomes to lysosomes and inhibiting endocytosis. Therefore, annexin A5 emerges as a possible key positive regulator of autophagy and negative regulator of endocytosis through Ca^{2+} and phospholipid signalling pathways. It will be important to further investigate the molecular details of these mechanisms.

MATERIALS AND METHODS

Reagents

Minimum Essential medium (MEM), Dulbecco's Modified Eagle´s Medium (DMEM), human insulin, fluorescein isothiocyanate (FITC)-dextran, azoalbumin, ionomycin, bafilomycin, 3-methyladenine and NH_4Cl were purchased from Sigma Chemical Co. MEM amino acids 50x, foetal bovine serum, penicillin, streptomycin, LysoTracker Red, Alexa Fluor 488-cholera toxin subunit B and Alexa Fluor 488-EGF (the last three from Molecular Probes) were supplied by Invitrogen Life Technologies. Leupeptin was from Peptide Institute, Inc., saponin was from Merck and bovine serum albumin (BSA) from Roche Applied Science. Bapta-AM was from Tocris. Metrizamide was from Nycomed and Percoll from Amersham Pharmacia Biotech Inc. The following antibodies were used: anti-annexin A5 and anti-cathepsin B from Santa Cruz Biotechnology, anti-LC3B from Nanotools, anti-LBPA from Echelon Biosciences Inc., anti-lamin A, anti-p62 and anti-lamp 1 from Abcam, anti-β-actin and horseradish peroxidase-labelled secondary antibodies from Sigma Chemical Co., and anti-mitochondrial complex II (succinate-ubiquinol oxidoreductase, 70 kDa subunit) and Alexa Fluor 488 and 633 conjugated anti-rabbit and anti-mouse secondary antibodies from Molecular Probes (Invitrogen Life Technologies). Cell light-ER, Cell light-Golgi and Organelle light-early endosomes were purchased from Invitrogen Life Technologies. Radioisotopes were obtained from Amersham Pharmacia Biotech. Other reagents, purchased from Sigma Chemical Co, Invitrogen Life Technologies or Calbiochem, were of analytical grade.

Cell culture and general procedures

NIH3T3 (a mouse embryonic fibroblast cell line) and HEK293T (a human embryonic kidney cell line) cells were obtained from the European Collection of Animal Cell Cultures. Cells were grown at 37ºC in a humidified atmosphere of 5% (v/v) CO_2/air in MEM or DMEM, respectively, containing 10% foetal bovine serum and 1% penicillin/streptomycin. Krebs-Henseleit medium (KH, 118.4 mM NaCl, 4.75 mM KCl, 1.19 mM KH_2PO4, 2.54 mM $MgSO_4$, 2.44 mM $CaCl_2.2H_2O$, 28.6 mM $NaHCO_3$, 20 mM glucose) with 10 mM Hepes, pH 7.4, was used for high proteolysis (starvation) conditions. For low proteolysis conditions, insulin 0.1 μM (I) and (IAA)/or (AA) essential amino acids at two times the concentration present in the growth media were added on KH medium. Cell viability and growth curves were determined in parallel for each culture.

For immunoblotting, we followed a standard procedure previously described (Fuertes et al., 2003a). Protein bands were quantified by densitometric analysis with an Image Quant ECL (GE Healthcare). Electron microscopic morphometry and identification of Av_i and Av_d were carried out as described before (Esteban et al., 2007; Knecht et al., 1984). Proteolytic activity in cell extracts was measured by a standard endopeptidase assay with azoalbumin (Sarath et al., 2001). Proteolysis under *in vitro* conditions was also determined in radioactively labelled cell extracts as described before (Vargas et al., 1989). Protein concentration was measured by a modification, with sodium deoxycholate, of the Lowry procedure, using bovine serum albumin as the standard.

Subcellular fractionation

After incubation in KH or in IAA, NIH3T3 cells were washed with phosphate-buffered saline (PBS) and pooled in ice-cold homogenisation buffer (250 mM sucrose, 20 mM Hepes, 1 mM EDTA, pH 7.4). Then, cells were homogenized at 4°C, first with a nitrogen cavitation pump (2.41 bar, 7 minutes), and then with a tight fitting Dounce homogeniser (10 strokes). A lysosomal fraction was prepared following a procedure described elsewhere (Storrie and Madden, 1990). Briefly, homogenates were centrifuged at 3,000 g for 10 minutes, 4°C, the pellet was saved as nuclear fraction and the post nuclear supernatant was applied to a Percoll/metrizamide gradient (from top to bottom: 6% Percoll; 17% and 35% metrizamide) and centrifuged at 53,000 g for 35 minutes, 4°C in an SW41Ti rotor (Beckman). To separate lysosomes from mitochondria, the 6% Percoll/17% metrizamide interface material was brought to 35% metrizamide and placed on the bottom of a second gradient of sucrose/metrizamide (from top to bottom: 0.25 M sucrose plus 5%, 17% and 35% metrizamide). After centrifugation at 53,000 g for 30 minutes, 4°C, mitochondria and lysosomes were collected from the 17/35% and the 5/17% metrizamide interfaces, respectively, and were disrupted by freezing and thawing, ten times. Lysosomal membranes were obtained by centrifugation at 105,000 g for 20 minutes, 4ºC, in a Beckman Airfuge (rotor A-100), and washed three times.

Two-dimensional electrophoresis and mass spectroscopy

2D-DIGE of lysosomal membranes was carried out essentially as previously described (Bernal et al., 2006), solubilising protein samples purified as above in 7 M urea, 2 M thiourea, 4% (w/v) CHAPS, 20 mM dithiothreitol (DTT) and 2% (v/v) Biolytes 3–10 and bromophenol blue (all chemicals from Bio-Rad). Samples of 100 μg protein were subjected to isoelectric focusing generated on a Bio-Rad PROTEAN® IEF Cell at 20°C. Subsequently, the strips were reduced and alkylated (using 2.5% iodoacetamide and 2% DTT in succession) in equilibration buffer containing 6 M urea, 0.375 M Tris pH 8.8, 2% sodium dodecyl sulfate (SDS) and 20% glycerol. 10% polyacrylamide gels were employed for the second dimension. The spots observed in the 2-Dimension Electrophoresis gel were manually excised, washed twice with double distilled water and digested with trypsin of sequencing grade (Promega, Madison, WI) as described (Andresen et al., 1989). Protein identification by mass spectrometry was performed using a 4700 Proteomics analyser (Applied Biosystems, Foster City, CA). A MASCOT search engine (Matrix-Science, London, UK) was used for database search on Swiss-Prot and NCBInr. The accuracy of proteins identification was considered when at least three peptides were identified with a minimum overall MASCOT score >50. Significant threshold of p values, for the consideration of proteins that significantly change their levels in the various conditions, was set to ≤ 0.05 and were determined by factorial ANOVA test using STATVIEW v4.53 (Abacus Concepts).

Measurements of intracellular protein degradation

Cells were incubated 48 h in full medium containing 2 μCi/ml ^{3}H-valine, washed and incubated for 24 h in fresh full medium containing 10 mM L-valine to eliminate radiolabelled short-lived proteins (Fuertes et al., 2003b). Then, cells were incubated for the indicated times in KH and IAA media. Total,

lysosomal and autophagic protein degradations were measured and calculated as previously described (Fuertes et al., 2003a; Fuertes et al., 2003b).

Annexin A5 overexpression and small interfering RNAs suppresion

HEK293T cells were transiently transfected with An5-pCMV-Sport6 (annexin A5 overexpression vector, hereafter A5), obtained from Open Biosystems, and empty pCMV-Sport6 or pCMV-GFP (negative control vectors, hereafter C-), obtained from Molecular Probes, Invitrogen Life Technologies. Transfections were carried out using Fugene HD (Roche Applied Science), according to the manufacturer's instructions. Experimental analyses of overexpression were started 48 h after transfections. For RNAi-mediated inhibition of annexin A5 gene expression, cells were transfected, 72 h before analysis, with small interfering RNAs (siRNAs), using X-tremeGENE siRNA Transfection Reagent (Roche Applied Science) for NIH3T3 cells and siLentFect Lipid Reagent (Bio-Rad) for NIH3T3 cells stably expressing eGFP-LC3 or mRFP-GFP/LC3, according to the manufacturer's instructions. NIH3T3 and HEK293 cells stably expressing eGFP-LC3 were generated by transfection with eGFP-LC3 (construct received as a kind gift of Tamotsu Yoshimori) and subsequent selection of eGFP-LC3 stable transformants in the presence of 1 mg/ml geneticin (GIBCO).

Isolation of NIH3T3 and HEK293 cells stably expressing the mRFP-GFP/LC3 reporter (Kimura et al., 2007) was accomplished by transfecting the cells with mRFP-GFP/LC3 (purchased from Addgene), and submitting the resistant clones to two sequential cycles of cell sorting using a MoFlo High Speed Cell Sorter (Beckman-Coulter). The steady-state expression level was then confirmed by fluorescence-activated cell sorting (FACS), immunoblotting and confocal microscope analyses. These cells were grown in the same conditions as reported above (in the presence of 1 mg/ml geneticin). Two different siRNAs (1 and 2), purchased from Ambion Inc., that target mouse annexin A5 mRNA (hereafter siA5) were used at a final concentration of 25 nM, for NIH3T3 and HEK293T cells (in these human cells, annexin A5 knockdown was successful with mouse siRNA), and of 15 nM, for NIH3T3 with a stable expression of eGFP-LC3. A scrambled, non-targeting siRNA obtained from Ambion was used as a negative control (hereafter C-). Silencing efficiency was estimated at protein levels by western blot.

Fluorescence microscopy

Cells were cultured on coverslips in 12-well plates. After the different treatments (KH or IAA), lysosomes were stained by incubating the cells with 75 nM Lysotracker Red for 30 minutes at 37ºC. Then, cells were rinsed with PBS, fixed with 3.7% paraformaldehyde/PBS for 20 minutes at room temperature, washed with PBS, and mounted using Fluor-Save reagent (Calbiochem). For immunofluorescence staining, cells were fixed as above, blocked with 0.1% BSA in PBS for 10 minutes and permeabilized with saponin (0.05%, w/v, in PBS) for 10 minutes. Then, cells were incubated with antibodies against annexin A5 (dilution 1:100), cathepsin B (dilution 1:100), LC3 (dilution 1:50), or LBPA (dilution 1:50). Bound antibodies were subsequently detected by incubation, as appropriate, with Alexa Fluor 488, 633 or 647 conjugated rabbit/mouse/goat secondary antibodies (dilution 1:200). ER, Golgi and early endosomes fluorescent signals were obtained by transfecting the cells, following the manufacturer's instructions, with Cell light-ER (endoplasmic signal sequence of calreticulin and KDEL-

RFP), Cell light-Golgi (N-acetylgalactosaminyl-transferase 2-RFP) and Organelle light-early endosomes (Rab5a-RFP). Preparations were observed with a fluorescence microscope Leica DM6000 B and images were acquired with a Leica TC5 Confocal Laser Scanning Microscope. Laser lines were 488 nm (eGFP-LC3, RFP/GFP-LC3 and Alexa Fluor 488), 561 nm (RFP/GFP-LC3) and 633 and 647 nm (Alexa Fluor 633 and 647). The JaCoP plug-in (Bolte and Cordelieres, 2006) in ImageJ software was used for the quantification of the various colocalizations. The eGFP-LC3 (autophagosomes) and LysoTracker Red (lysosomes) stained areas were quantified using LCS Lite software. Number of eGFP-LC3 puncta was counted using Top Hat algorithm of MetaMorph version 7.0.

Measurement of lysosomal pH

To measure the pH within lysosomes, cells were allowed to endocytose FITC-conjugated dextran, following a procedure described elsewhere (Nilsson et al., 2003). Briefly, 72 or 48 h after annexin A5 knockdown or overexpression respectively, cells seeded in 12-well plates were treated with FITC-dextran of 40 kDa (0.5 mg/ml) for 18 h. Cells were then washed 5 times with PBS and incubated in KH and IAA media for 4 h to chase FITC-dextran from endosomes. Positive control samples were incubated with NH_4Cl (20 mM). Cells were then resuspended and washed 3 times in fresh KH and IAA media after being transferred to FACS tubes. Cell pellets were kept on ice and resuspended immediately before FACS analysis. FITC was excited at 488 nm argon laser and the resulting emission was detected using a 530 ± 28 nm (FL1) and a 610 ± 20 nm (FL3) filter. The FL1/FL3 ratios were measured for 5000 collected cells, and pH was calculated using a standard curve prepared with McIlvaine´s buffers (pHs ranging from 4.0 to 6.0), containing sodium azide (50 mM), 2-deoxyglucose (50 mM), nigericin (10 μM) and monensin (20 μM).

Flow cytometry

Lysosomal mass was determined by incubating the cells in suspension (10^6 cells/ml) with 75 nM LysoTracker Red for 30 minutes at 37ºC, and the emitted red fluorescence (620 ± 20 nm band-pass filter) was analyzed (Poot, 2001). For detection of fluid phase endocytosed cargo, using flow cytometry, cells were treated with FITC-dextran (1 mg/ml) for 30, 60 and 120 minutes at 37ºC. For detection of endocytosis of cholera toxin B or epidermal growth factor (EGF), cells were treated with Alexa Fluor 488-cholera toxin subunit B (1.5 μg/ml) or with Alexa Fluor 488-EGF (2 μg/ml) for 5, 15, 30, 60 and 90 minutes at 37ºC. Previously, cells were also incubated as above for 5 sec at 4ºC to evaluate the membrane bound marker. At the different times, cells were detached with trypsin-EDTA, washed four times, resuspended in PBS (10^6 cells/ml), and the emitted red (620 ± 20 nm band-pass filter) or green (488 ± 20 nm band-pass filter) fluorescences were analyzed by flow cytometry. In each experiment, 10,000 cells were collected and analyzed using a Cytomics FC 500 Flow cytometer (Beckman Coulter). Autophagy quantification by flow cytometry was determined by a procedure described elsewhere (Shvets and Elazar, 2009).

Quantitation and statistics

P values were determined by factorial ANOVA test using GraphPad Prism software. *P* values have been considered in all figures as: ***$p< 0.0005$; **$p< 0.005$; and *$p< 0.05$.

Acknowledgements

We thank Asunción Montaner for technical assistance, Diego Di Stefani for help with informatics and the Cytomics Laboratory, the Confocal Microscopy Technological Service and the Proteomics Unit for advice with the flow cytometry, confocal and proteomic studies, respectively. This work was supported by the Ministerio de Educación y Ciencia (Grant BFU2008-00186) and the Generalitat Valenciana (ACOMP09-157 and AP-046-10).

Conflicts of interest

The authors declare that they have no conflict of interest.

REFERENCES

Andresen, K., Simonsen, P. E., Andersen, B. J. and Birch-Andersen, A. (1989). Echinostoma caproni in mice: shedding of antigens from the surface of an intestinal trematode. *Int J Parasitol* **19**, 111-8.

Axe, E. L., Walker, S. A., Manifava, M., Chandra, P., Roderick, H. L., Habermann, A., Griffiths, G. and Ktistakis, N. T. (2008). Autophagosome formation from membrane compartments enriched in phosphatidylinositol 3-phosphate and dynamically connected to the endoplasmic reticulum. *J Cell Biol* **182**, 685-701.

Ayala-Sanmartin, J. (2001). Cholesterol enhances phospholipid binding and aggregation of annexins by their core domain. *Biochem Biophys Res Commun* **283**, 72-9.

Barwise, J. L. and Walker, J. H. (1996). Subcellular localization of annexin V in human foreskin fibroblasts: nuclear localization depends on growth state. *FEBS Lett* **394**, 213-6.

Bernal, D., Carpena, I., Espert, A. M., De la Rubia, J. E., Esteban, J. G., Toledo, R. and Marcilla, A. (2006). Identification of proteins in excretory/secretory extracts of Echinostoma friedi (Trematoda) from chronic and acute infections. *Proteomics* **6**, 2835-43.

Berridge, M. J., Bootman, M. D. and Roderick, H. L. (2003). Calcium signalling: dynamics, homeostasis and remodelling. *Nat Rev Mol Cell Biol* **4**, 517-29.

Bolte, S. and Cordelieres, F. P. (2006). A guided tour into subcellular colocalization analysis in light microscopy. *J Microsc* **224**, 213-32.

Cederholm, A. and Frostegard, J. (2007). Annexin A5 multitasking: a potentially novel antiatherothrombotic agent? *Drug News Perspect* **20**, 321-6.

Codogno, P. and Meijer, A. J. (2005). Autophagy and signaling: their role in cell survival and cell death. *Cell Death Differ* **12 Suppl 2**, 1509-18.

Cuervo, A. M. (2010). The plasma membrane brings autophagosomes to life. *Nat Cell Biol* **12**, 735-7.

Diakonova, M., Gerke, V., Ernst, J., Liautard, J. P., van der Vusse, G. and Griffiths, G. (1997). Localization of five annexins in J774 macrophages and on isolated phagosomes. *J Cell Sci* **110 (Pt 10)**, 1199-213.

Douglas, P. M. and Dillin, A. (2010). Protein homeostasis and aging in neurodegeneration. *J Cell Biol* **190**, 719-29.

Eskelinen, E. L., Illert, A. L., Tanaka, Y., Schwarzmann, G., Blanz, J., Von Figura, K. and Saftig, P. (2002). Role of LAMP-2 in lysosome biogenesis and autophagy. *Mol Biol Cell* **13**, 3355-68.

Esteban, I., Aguado, C., Sanchez, M. and Knecht, E. (2007). Regulation of various proteolytic pathways by insulin and amino acids in human fibroblasts. *FEBS Lett* **581**, 3415-21.

Esteve, J. M., Armengod, M. E. and Knecht, E. (2010). BRCA1 negatively regulates formation of autophagic vacuoles in MCF-7 breast cancer cells. *Exp Cell Res* **316**, 2618-29.

Fuertes, G., Martin De Llano, J. J., Villarroya, A., Rivett, A. J. and Knecht, E. (2003a). Changes in the proteolytic activities of proteasomes and lysosomes in human fibroblasts produced by serum withdrawal, amino-acid deprivation and confluent conditions. *Biochem J* **375**, 75-86.

Fuertes, G., Villarroya, A. and Knecht, E. (2003b). Role of proteasomes in the degradation of short-lived proteins in human fibroblasts under various growth conditions. *Int J Biochem Cell Biol* **35**, 651-64.

Gao, C. X., Miyoshi, E., Uozumi, N., Takamiya, R., Wang, X., Noda, K., Gu, J., Honke, K., Wada, Y. and Taniguchi, N. (2005). Bisecting GlcNAc mediates the binding of annexin V to Hsp47. *Glycobiology* **15**, 1067-75.

Gordon, P. B., Holen, I., Fosse, M., Rotnes, J. S. and Seglen, P. O. (1993). Dependence of hepatocytic autophagy on intracellularly sequestered calcium. *J Biol Chem* **268**, 26107-12.

Hailey, D. W., Rambold, A. S., Satpute-Krishnan, P., Mitra, K., Sougrat, R., Kim, P. K. and Lippincott-Schwartz, J. (2010). Mitochondria supply membranes for autophagosome biogenesis during starvation. *Cell* **141**, 656-67.

Hayashi-Nishino, M., Fujita, N., Noda, T., Yamaguchi, A., Yoshimori, T. and Yamamoto, A. (2009). A subdomain of the endoplasmic reticulum forms a cradle for autophagosome formation. *Nat Cell Biol* **11**, 1433-7.

Hoekstra, D., Buist-Arkema, R., Klappe, K. and Reutelingsperger, C. P. (1993). Interaction of annexins with membranes: the N-terminus as a governing parameter as revealed with a chimeric annexin. *Biochemistry* **32**, 14194-202.

Hoyer-Hansen, M., Bastholm, L., Szyniarowski, P., Campanella, M., Szabadkai, G., Farkas, T., Bianchi, K., Fehrenbacher, N., Elling, F., Rizzuto, R. et al. (2007). Control of macroautophagy by calcium, calmodulin-dependent kinase kinase-beta, and Bcl-2. *Mol Cell* **25**, 193-205.

Kang, J. H., Li, M., Chen, X. and Yin, X. M. (2011). Proteomics analysis of starved cells revealed Annexin A1 as an important regulator of autophagic degradation. *Biochem Biophys Res Commun* **407**, 581-6.

Kimura, S., Noda, T. and Yoshimori, T. (2007). Dissection of the autophagosome maturation process by a novel reporter protein, tandem fluorescent-tagged LC3. *Autophagy* **3**, 452-60.

Klionsky, D. J., Cregg, J. M., Dunn, W. A., Jr., Emr, S. D., Sakai, Y., Sandoval, I. V., Sibirny, A., Subramani, S., Thumm, M., Veenhuis, M. et al. (2003). A unified nomenclature for yeast autophagy-related genes. *Dev Cell* **5**, 539-45.

Knecht, E., Aguado, C., Carcel, J., Esteban, I., Esteve, J. M., Ghislat, G., Moruno, J. F., Vidal, J. M. and Saez, R. (2009). Intracellular protein degradation in mammalian cells: recent developments. *Cell Mol Life Sci* **66**, 2427-43.

Knecht, E., Hernandez-Yago, J. and Grisolia, S. (1984). Regulation of lysosomal autophagy in transformed and non-transformed mouse fibroblasts under several growth conditions. *Exp Cell Res* **154**, 224-32.

Koga, H., Kaushik, S. and Cuervo, A. M. (2010). Altered lipid content inhibits autophagic vesicular fusion. *FASEB J* **24**, 3052-65.

Kornhuber, J., Henkel, A. W., Groemer, T. W., Stadtler, S., Welzel, O., Tripal, P., Rotter, A., Bleich, S. and Trapp, S. (2010). Lipophilic cationic drugs increase the permeability of lysosomal membranes in a cell culture system. *J Cell Physiol* **224**, 152-64.

Levine, B. and Klionsky, D. J. (2004). Development by self-digestion: molecular mechanisms and biological functions of autophagy. *Dev Cell* **6**, 463-77.

Lum, J. J., Bauer, D. E., Kong, M., Harris, M. H., Li, C., Lindsten, T. and Thompson, C. B. (2005). Growth factor regulation of autophagy and cell survival in the absence of apoptosis. *Cell* **120**, 237-48.

Luzio, J. P., Bright, N. A. and Pryor, P. R. (2007). The role of calcium and other ions in sorting and delivery in the late endocytic pathway. *Biochem Soc Trans* **35**, 1088-91.

Mari, M., Griffith, J., Rieter, E., Krishnappa, L., Klionsky, D. J. and Reggiori, F. (2010). An Atg9-containing compartment that functions in the early steps of autophagosome biogenesis. *J Cell Biol* **190**, 1005-22.

Massey, A. C., Follenzi, A., Kiffin, R., Zhang, C. and Cuervo, A. M. (2008). Early cellular changes after blockage of chaperone-mediated autophagy. *Autophagy* **4**, 442-56.

Meijer, A. J. and Codogno, P. (2006). Signalling and autophagy regulation in health, aging and disease. *Mol Aspects Med* **27**, 411-25.

Mizushima, N., Yoshimori, T. and Levine, B. (2010). Methods in mammalian autophagy research. *Cell* **140**, 313-26.

Mohiti, J., Caswell, A. M. and Walker, J. H. (1997). The nuclear location of annexin V in the human osteosarcoma cell line MG-63 depends on serum factors and tyrosine kinase signaling pathways. *Exp Cell Res* **234**, 98-104.

Monastyrskaya, K., Babiychuk, E. B. and Draeger, A. (2009). The annexins: spatial and temporal coordination of signaling events during cellular stress. *Cell Mol Life Sci* **66**, 2623-42.

Moscat, J. and Diaz-Meco, M. T. (2009). p62 at the crossroads of autophagy, apoptosis, and cancer. *Cell* **137**, 1001-4.

Nilsson, C., Kagedal, K., Johansson, U. and Ollinger, K. (2003). Analysis of cytosolic and lysosomal pH in apoptotic cells by flow cytometry. *Methods Cell Sci* **25**, 185-94.

Noda, T., Fujita, N. and Yoshimori, T. (2009). The late stages of autophagy: how does the end begin? *Cell Death Differ* **16**, 984-90.

Onodera, J. and Ohsumi, Y. (2005). Autophagy is required for maintenance of amino acid levels and protein synthesis under nitrogen starvation. *J Biol Chem* **280**, 31582-6.

Perez-Terzic, C. M., Chini, E. N., Shen, S. S., Dousa, T. P. and Clapham, D. E. (1995). Ca2+ release triggered by nicotinate adenine dinucleotide phosphate in intact sea urchin eggs. *Biochem J* **312 (Pt 3)**, 955-9.

Pillay, C. S., Elliott, E. and Dennison, C. (2002). Endolysosomal proteolysis and its regulation. *Biochem J* **363**, 417-29.

Poot, M. (2001). Analysis of intracellular organelles by flow cytometry or microscopy. *Curr Protoc Cytom* **Chapter 9**, Unit 9 4.

Pryor, P. R., Mullock, B. M., Bright, N. A., Gray, S. R. and Luzio, J. P. (2000). The role of intraorganellar Ca(2+) in late endosome-lysosome heterotypic fusion and in the reformation of lysosomes from hybrid organelles. *J Cell Biol* **149**, 1053-62.

Rambotti, M. G., Spreca, A. and Donato, R. (1993). Immunocytochemical localization of annexins V and VI in human placentae of different gestational ages. *Cell Mol Biol Res* **39**, 579-88.

Ravikumar, B., Moreau, K., Jahreiss, L., Puri, C. and Rubinsztein, D. C. (2010). Plasma membrane contributes to the formation of pre-autophagosomal structures. *Nat Cell Biol* **12**, 747-57.

Russo-Marie, F. (1999). Annexin V and phospholipid metabolism. *Clin Chem Lab Med* **37**, 287-91.

Sarath, G., Zeece, M.G., and Penheiter, A.R. 2001. Protease assay methods. *In* Proteolytic Enzymes:A Practical Approach (R. Benyon and J.S. Bond, eds.) pp. 45-76. Oxford University Press, Oxford.

Shvets, E. and Elazar, Z. (2009). Flow cytometric analysis of autophagy in living mammalian cells. *Methods Enzymol* **452**, 131-41.

Storrie, B. and Madden, E. A. (1990). Isolation of subcellular organelles. *Methods Enzymol* **182**, 203-25.

Vargas, J. L., Aniento, F., Cervera, J. and Knecht, E. (1989). Vanadate inhibits degradation of short-lived, but not of long-lived, proteins in L-132 human cells. *Biochem J* **258**, 33-40.

Walker, J. H., Boustead, C. M., Koster, J. J., Bewley, M. and Waller, D. A. (1992). Annexin V, a calcium-dependent phospholipid-binding protein. *Biochem Soc Trans* **20**, 828-33.

Williams, A., Sarkar, S., Cuddon, P., Ttofi, E. K., Saiki, S., Siddiqi, F. H., Jahreiss, L., Fleming, A., Pask, D., Goldsmith, P. et al. (2008). Novel targets for Huntington's disease in an mTOR-independent autophagy pathway. *Nat Chem Biol* **4**, 295-305.

Wu, Y. T., Tan, H. L., Shui, G., Bauvy, C., Huang, Q., Wenk, M. R., Ong, C. N., Codogno, P. and Shen, H. M. (2010). Dual role of 3-methyladenine in modulation of autophagy via different temporal patterns of inhibition on class I and III phosphoinositide 3-kinase. *J Biol Chem* **285**, 10850-61.

Xie, Z. and Klionsky, D. J. (2007). Autophagosome formation: core machinery and adaptations. *Nat Cell Biol* **9**, 1102-9.

Yla-Anttila, P., Vihinen, H., Jokitalo, E. and Eskelinen, E. L. (2009). 3D tomography reveals connections between the phagophore and endoplasmic reticulum. *Autophagy* **5**, 1180-5.

Sarath, G.; Zeece, M. G.; and Penheiter, A. R.

FIGURES

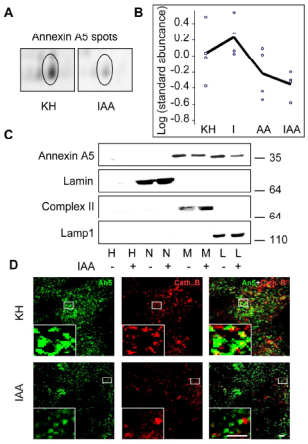

Fig. 1. Under starvation, annexin A5 translocates to lysosomal membranes. A. Representative area corresponding to annexin A5 (encircled spots) from 2D-gels with proteins (100 µg) from lysosomal membranes isolated from NIH3T3 cells incubated for 4 h under conditions that produce low (IAA) and high (KH) proteolysis. **B**. Levels of annexin A5 on lysosomal membranes isolated from cells incubated in Krebs-Henseleit medium without (KH) or with insulin (I), amino acids (AA) or both (IAA). Data are from four independent experiments similar to that shown in A. The line binds the corresponding mean values. **C**. Subcellular fractions were isolated as described in Materials and Methods from NIH3T3 cells incubated 4 h in KH (-) or IAA (+). 25 µg protein from each fraction were subjected to SDS-polyacrylamide gel electrophoresis and immunoblotted with antibodies that recognise annexin A5, lamin (nuclear marker), mitochondrial complex II (succinate-ubiquinol oxidoreductase, mitochondrial marker) and lamp1 (lysosomal marker). H, homogenate; N, M, L, nuclear, mitochondrial and lysosomal fractions, respectively. **D**. Confocal images of NIH3T3 cells incubated 4 h in KH (upper panels) or in IAA (lower panels) and immunostained with cathepsin B (Cath. B, middle panels) and annexin A5 (An5, left panels) antibodies and merge of both (Cath. B+An5, right panels). Insets: high-magnification images of fusion events. Bars: 2.5 µm.

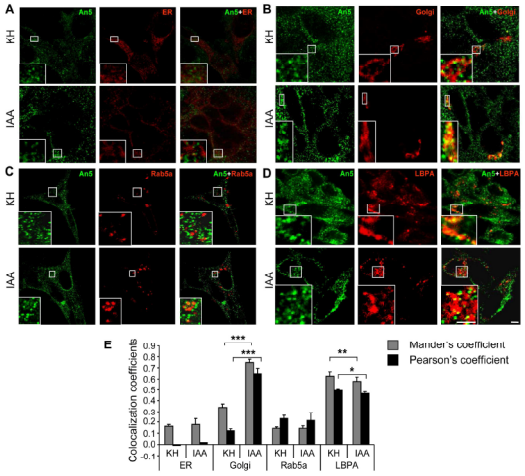

Fig. 2. The intracellular distribution of annexin A5 under high and low proteolysis conditions is different. A, B, C. Confocal images of NIH3T3 cells, previously infected with Cell light-ER (signal sequence of calreticulin and KDEL-RFP, **A**) or Cell light-Golgi (N-acetylgalactosaminyltransferase 2-RFP, **B**) or with Organelle light-early endosomes (Rab5a-RFP, **C**). After 4 h in KH (upper panels) or in IAA (lower panels) media, cells were immunostained with annexin A5 antibody. **D**. Confocal images of NIH3T3 cells incubated 4 h in KH (upper panels) or in IAA (lower panels) and immunostained with LBPA (middle panels) and annexin A5 (An5, left panels) antibodies and merge of both (LBPA+An5, right panels). Bars: 5 µm. Insets: high-magnification images of fusion events. **E**. Quantification of colocalizations. The analysis, for two independent experiments, was performed as detailed in Materials and Methods. The graph shows the Mander's colocalization coefficient (fraction of An5-positive structures overlapping ER, Golgi, Rab5a and LPBA-positive structures, grey bars) and Pearson's correlation coefficient (black bars). Differences between KH and IAA values were found to be statistically significant at *p<0.05, **p <0.005 and ***p<0.0005.

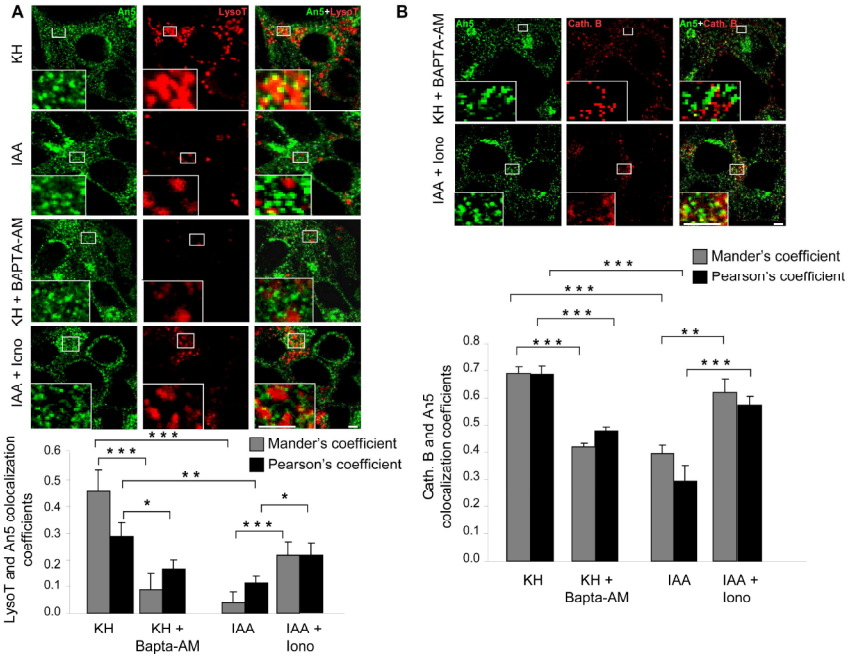

Fig. 3. Colocalization of annexin A5 with LysoTracker Red and cathepsin B is Ca^{2+}-dependent. A, B. Confocal images of NIH3T3 cells incubated 4 h in KH with and without BAPTA-AM (20 μM) or in IAA with and without ionomycin (10 μM) and stained with annexin A5 antibody (An5, left panels), LysoTracker Red (LysoT, middle panels) and merge of both (LysoT+An5, right panels)(**A**) or cathepsin B (Cath. B, middle panels), and merge of both (Cath. B+An5, right panels)(**B**). Bars: 2.5 μm. Insets: high-magnification images of fusion events. Quantifications of the colocalization of annexin A5 with lysosomal markers under the various conditions are shown below. The analysis, for two independent experiments, was performed as detailed in the legend to Fig. 2E. Differences were found to be statistically significant at *p<0.05, **p <0.005 and ***p<0.0005.

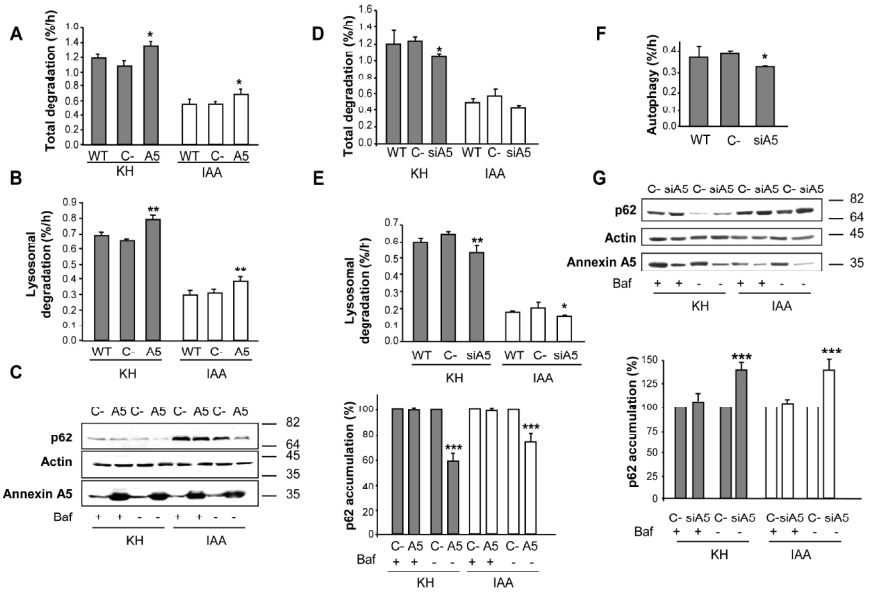

Fig. 4. Annexin A5 increases lysosomal protein degradation. A, B. Overexpression of annexin A5 raises lysosomal protein degradation. Exponentially growing HEK293T cells (WT and transiently transfected with C- or A5 vectors) were metabolically labelled with [^{3}H] valine for 48 h, chased for 24 h and then switched for 4 h to KH or IAA media. Total (**A**) and lysosomal (**B**) protein degradations were calculated as described in Materials and Methods. Results from three separate experiments with duplicated samples are shown as percentage of the labelled proteins that are degraded per hour under the different conditions. **C**. Cells treated and incubated as above, with and without bafilomycin A1 (Baf, 500 nM), were subjected to immunoblotting with p62, actin (as a loading control) and annexin A5 (to show overexpression) antibodies. Densitometric measurements of the p62 bands shown in the histogram on the right were normalized to the corresponding actin bands and expressed as % of the corresponding C- (negative control) values. **D-F**. Silencing of annexin A5 decreases lysosomal protein degradation. Exponentially growing NIH3T3 cells (WT and C- or siA5 treated) were labelled and incubated as above. Total (**D**), lysosomal (**E**) and autophagic (**F**) degradations were calculated as indicated in Materials and Methods. Results represent the mean and SD from ten independent experiments with duplicated samples. **G**. NIH3T3 cells, treated and incubated as above, were subjected to immunoblotting with p62, actin and annexin A5 antibodies. Densitometric measurements of the p62 bands were normalized to the corresponding actin bands and are shown in the histogram below. Data are expressed as in the legend to Fig. 4C and represent the mean and SD of four independent experiments. Differences from the respective C- values in the different histograms were found to be statistically significant at *p<0.05, **p <0.005 and ***p<0.0005.

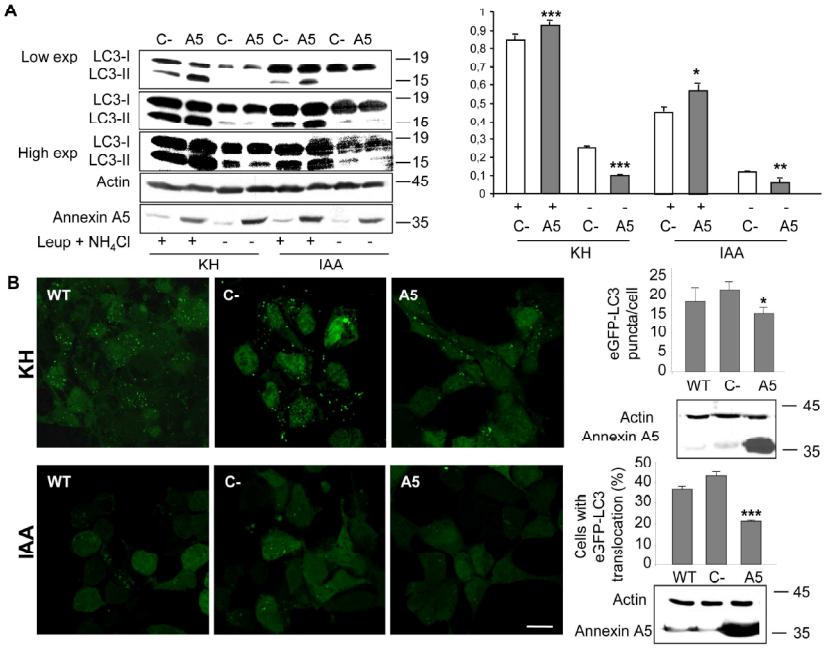

Fig. 5. Annexin A5 overexpression increases autophagic flux. A. HEK293T cells were transiently transfected with A5 or C- vectors as in Fig. 4A-C. After 48 h, the cells were incubated for 4 h in KH or IAA media with or without leupeptin (Leup, 100 μM) and NH_4Cl (20 mM). Then, the cells (75 μg protein) were subjected to immunoblotting, with various exposures (exp), using antibodies that recognise LC3 (-I and -II), actin and annexin A5. The histogram on the right shows densitometric measurements of the ratio of LC3-II to actin bands from six independent experiments. **B**. HEK293T cells with stable expression of eGFP-LC3 were transiently transfected and incubated as in A and examined in a confocal microscope. WT NIH3T3 cells are also shown. Bar: 10 μm. The number of eGFP-LC3 puncta/cell (KH) or the percentage of cells with fluorescent dots (IAA, cells containing more than 5 dots were considered positive) were determined in two independent experiments (at least 150 cells per condition) and results are shown on the right. Actin and annexin A5 levels are also shown below. Differences from negative control (C-) values in the **A** and **B** histograms were found to be statistically significant at *p<0.05, **p<0.005 and ***p<0.0005.

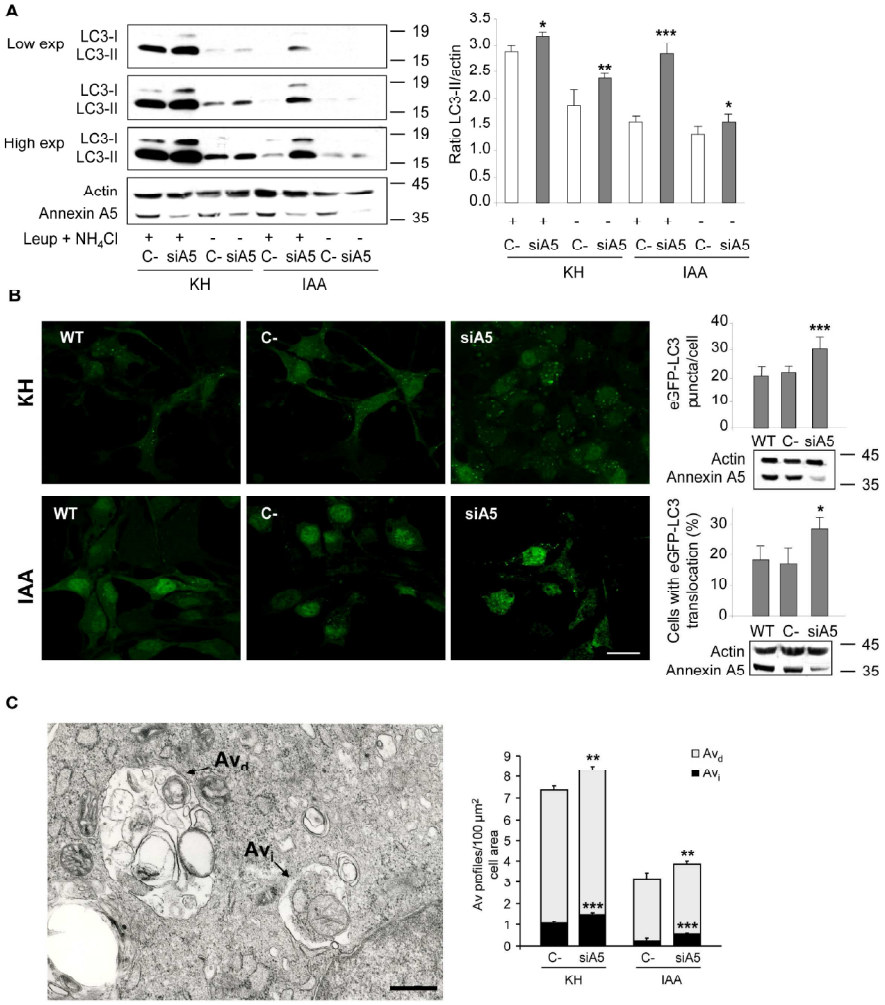

Fig. 6. Silencing of annexin A5 increases the accumulation of autophagosomes. **A**. NIH3T3 cells were transfected with annexin A5 (siA5) or a negative control (C-) siRNA. After 72 h, cells were incubated, immunoblotted and subjected to densitometric analysis as described in the legend to Fig. 5A. The histogram on the right shows the quantification of the ratio of LC3-II to actin bands from eight independent experiments. **B**. NIH3T3 cells with stable expression of eGFP-LC3 (WT) were transfected with siA5 or C- siRNA for 72 h, incubated for 4 h in KH or in IAA media and then examined in a confocal microscope. Bar: 10 µm. The number of eGFP-LC3 puncta/cell (KH) or the percentage of cells with fluorescent dots (IAA) in two different experiments were determined as described in the legend to Fig. 5B and results are shown on the right. Actin and annexin A5 levels are also shown below. **C**. Representative electron micrograph of NIH3T3 cells transfected with siA5 incubated in KH medium for 4 h showing early (Av_i) and late (Av_d) autophagic vacuoles. Bar: 0.5 µm. The histograms on the right show the amounts of Av_i and Av_d, in C- and siA5 transfected cells incubated in KH or in IAA media, determined by morphometry in two different experiments. Differences from negative control (C-) values in the A, B and C histograms were found to be statistically significant at *p<0.05, **p <0.005 and ***p<0.0005.

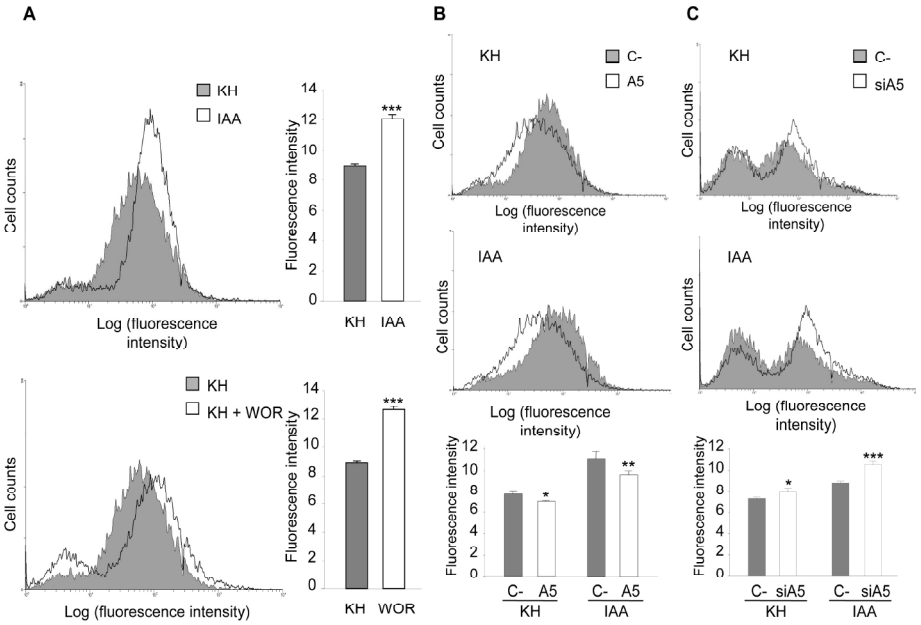

Fig. 7. Annexin A5 promotes autophagosome delivery to lysosomes. NIH3T3 cells stably expressing eGFP-LC3 were incubated under the indicated conditions and the fluorescence intensity of eGFP in the cells was measured by flow cytometry. Histograms indicate the mean values of each measurement. **A**. Cells were incubated for 4 h under conditions that produce low (IAA) or high (KH) proteolysis, without or with (Pillay et al., 2002) 100 nM wortmannin (+ WOR). **B, C**. HEK293T and NIH3T3 cells stably expressing eGFP-LC3 were, respectively, transfected with C- or A5 (overexpression of annexin A5) vectors (**B**) or C- or siA5 (silencing of annexin A5) siRNAs (**C**). Results are the mean and SD from at least four separate experiments with duplicated samples. Differences from negative control (C-) values were found to be statistically significant at *p<0.05, **p <0.005 and ***p<0.0005.

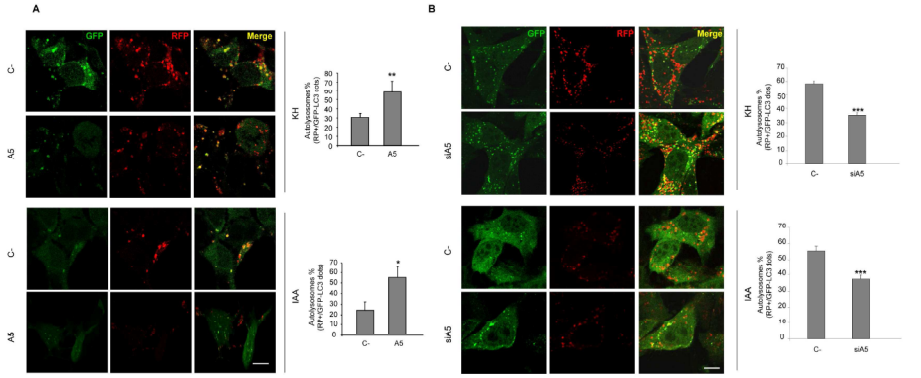

Fig. 8. Annexin A5 promotes autophagosome maturation. A. HEK293T or NIH3T3 cells stably expressing an mRFP-GFP/LC3 construct were seeded on glass coverslips and transfected for 48 h with A5 or C- plasmids (**A**) or for 72 h with siA5 or C- siRNAs (**B**). Then, the cells were incubated for 4 h in KH or in IAA media and subsequently fixed and analysed by confocal microscopy. The histograms on the right show percentage of autolysosomes in the cells incubated under the various conditions calculated from three different experiments. Differences from negative control (C-) values were found to be statistically significant at *p<0.05, **p <0.005 and ***p<0.0005. Bars: 5 µm.

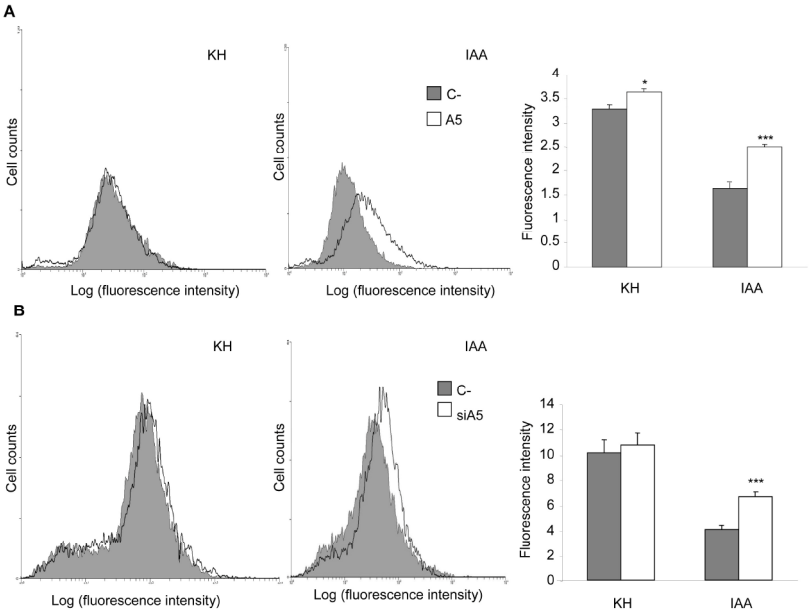

Fig. 9. Both silencing and overexpression of annexin A5 increase lysosomal mass. NIH3T3 cells transfected with C- or A5 vectors (**A**) or HEK293T cells transfected with C- or siA5 siRNAs (**B**) were incubated 4 h in KH or IAA media in the presence of LysoTracker Red (75 nM). LysoTracker Red fluorescence was analyzed by quantitative flow cytometric analysis (10,000 events). In the histograms on the right, the results shown are the mean and SD from two separate experiments. Differences from negative control values (C-) were found to be statistically significant at $*p<0.05$ and $***p<0.0005$.

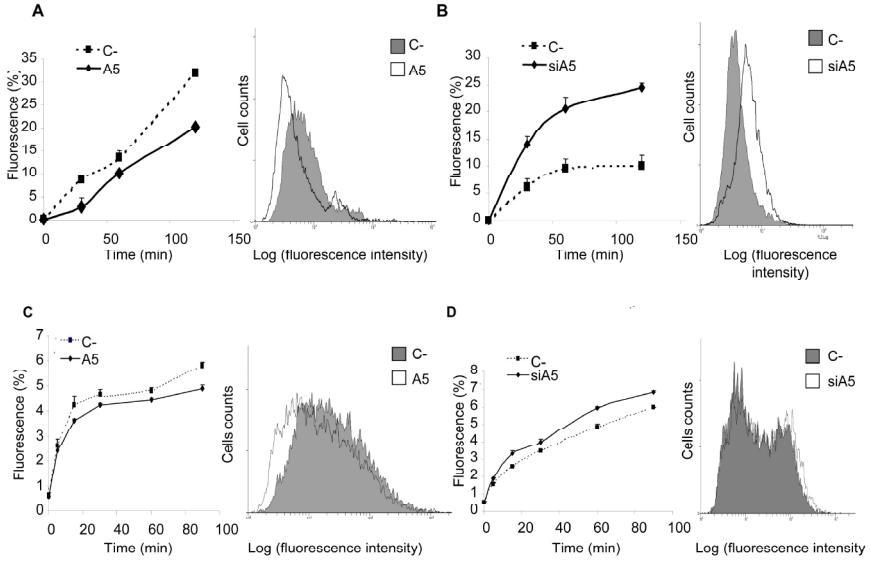

Fig. 10. Annexin A5 inhibits fluid phase and cholera toxin endocytosis. A, B. Quantitative flow cytometric analysis (10,000 events) of FITC-dextran (1 mg/ml) internalization in HEK293T cells transfected with C- or A5 vectors (**A**) and in NIH3T3 cells transfected with C- or siA5 siRNAs (**B**). **C, D**. Similar experiments were carried out with Alexa Fluor 488-cholera toxin subunit B (1.5 μg/ml) in HEK293T cells transfected with C- or A5 vectors (**C**) and in NIH3T3 cells transfected with C- or siA5 siRNAs (**D**). All experiments were carried out for 5 sec at 4ºC (to evaluate the membrane bound marker), and for 30, 60 and 120 minutes at 37ºC for fluid phase endocytosis and for 5, 15, 30, 60 and 90 minutes at 37ºC for cholera toxin B endocytosis. In **A**, **B**, **C** and **D**, values on the *y*-axis of the left graphs indicate the percentage of fluorescence in arbitary units of viable cells assessed by propidium iodide (1 μg/ml). Results are the mean and SD from six separate experiments.

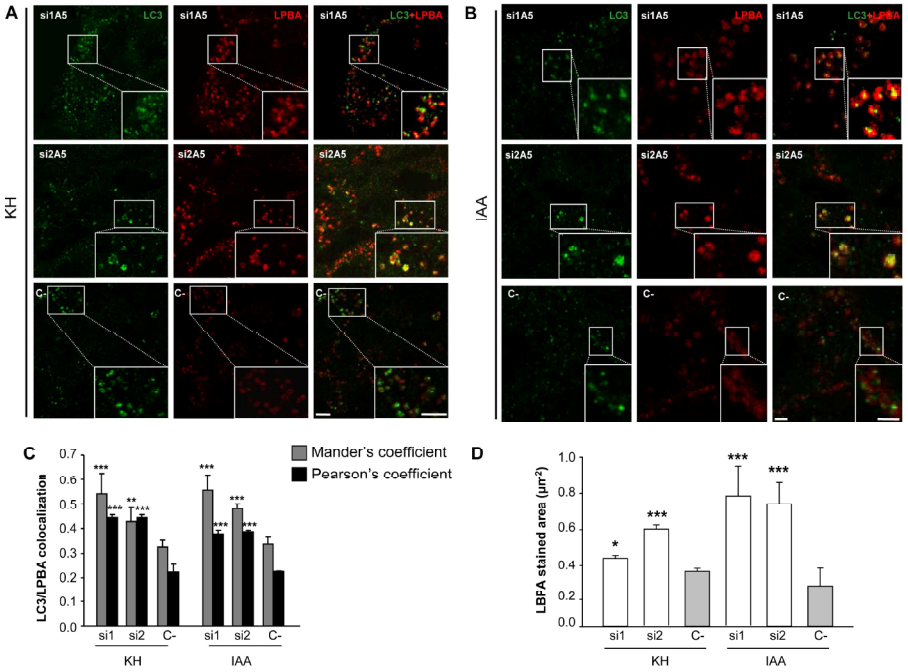

Fig. 11. Silencing of annexin A5 enhances autophagosome-endosome fusion. NIH3T3 cells were treated with two different annexin A5 siRNAs (si1A5 or si2A5) or with a negative control (C-) siRNA. After 72 h, the cells were incubated in KH (**A**) or in IAA (**B**) media for 4 h and immunostained with LBPA and LC3 antibodies. The cells were observed in a Leica confocal microscope. In **A** and **B**, first, second and third rows correspond, respectively, to cells treated with si1A5, si2A5 or C-, and right, middle and left panels show, respectively, LC3 (green fluorescence), LBPA (red fluorescence) immunostaining and the merge of both. The insets show high-magnification images of selected areas to show more clearly the colocalizations. Bars: 5 (**A**) and 2.5 (**B**) µm. **C.** Quantification of LC3 colocalization with LBPA. The analysis, for two independent experiments, was performed as detailed in the legend to Fig. 2E with the Mander's colocalisation coefficient (grey bars) corresponding to the fraction of LC3 containing vesicles overlapping LBPA positive structures. **D.** Quantification of LBPA (late endosomes) stained areas in two independent experiments, using LCS Lite software under the conditions cited above. Differences from negative control (C-) values in **C** and **D** were found to be statistically significant at *p<0.05, **p<0.005 and ***p<0.0005.

SUPPLEMENTARY FIFURES

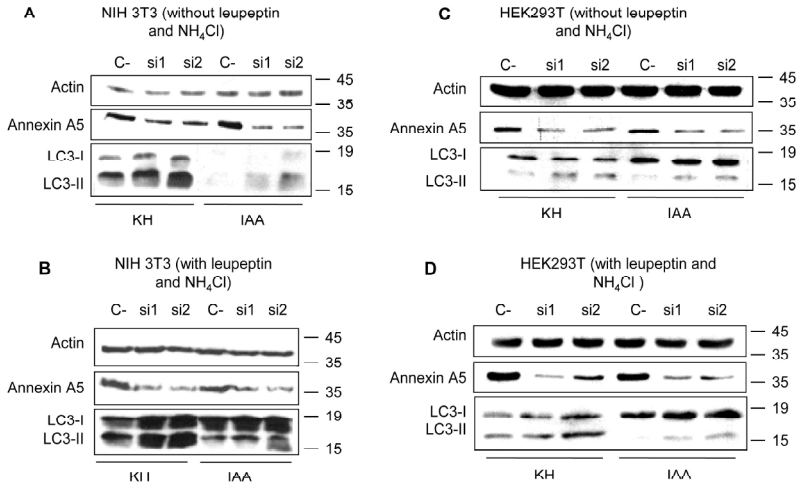

Fig. S1. Silencing of annexin A5 with two different siRNAs leads to LC3-II accumulation in both NIH3T3 and HEK293T cells. A, B. NIH3T3 cells were treated with two different annexin A5 siRNAs (si1 or si2) or with a negative control siRNA (C-). 72 h later, LC3-II levels were measured by immunoblot after 4 h in high (KH) or low (IAA) proteolysis media in the presence (**B**) or in the absence (**A**) of lysosomal inhibitors (100 μM leupeptin and 20 mM NH_4Cl). **C, D**. The same experiments than in A and B, respectively, were carried out with HEK293T cells. In all experiments, annexin A5 and actin (as a loading control) levels are also provided.

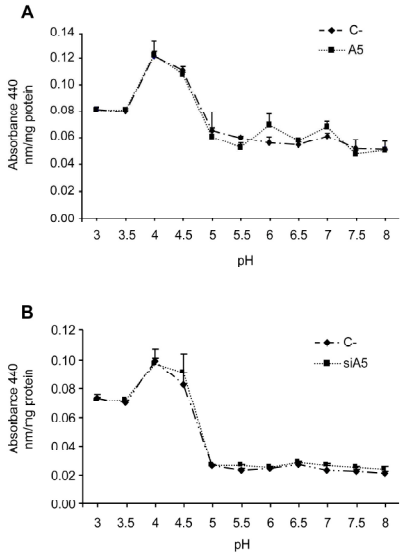

Fig. S2. Annexin A5 does not affect the lysosomal degradation capacity. Proteolysis of azoalbumin at different pHs by extracts of HEK293T cells transfected 48 h with A5 or C- plasmids (**A**) or by extracts of NIH3T3 cells previously transfected 72 h with siA5 or C- siRNAs (**B**). Error bars and data are from three independent experiments. Similar results were obtained, at the different pHs, using radioactively labelled cell extracts (see Materials and Methods).

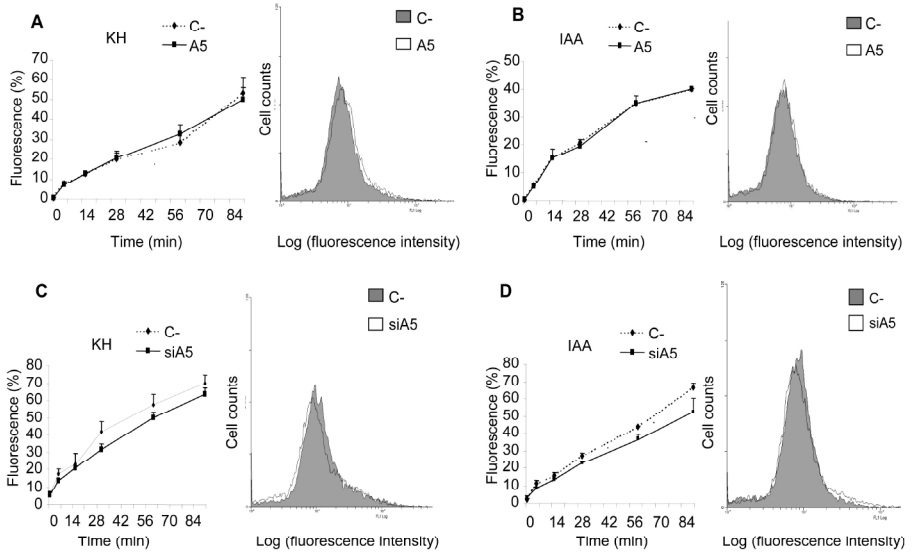

Fig. S3. Annexin A5 does not affect receptor mediated endocytosis. Quantitative flow cytometric analysis (10,000 events) of the internalization by HEK293T cells of Alexa Fluor 488-EGF (2 μg/ml) transfected with C- or A5 vectors (**A**, **B**) or with C- or siA5 siRNAs (**C**, **D**) and incubated in KH (**A**, **C**) or in IAA (**B**, **D**). All experiments were carried out for 5 sec at 4ºC (to evaluate membrane bound marker), and for 5, 15, 30, 60 and 90 minutes at 37ºC. In **A**, **B**, **C** and **D**, values on the *y*-axis of the left graphs indicate the same as in Fig. 10. Results are the mean and SD from 6 different experiments.

Table S1. Lysosomal pH under annexin A5 overexpression and silencing

		Overexpression		Silencing
KH	C-	5.52 ± 0.02	C-	5.66 ± 0.08
	A5	5.58 ± 0.10	siA5	5.64 ± 0.02
	NH_4Cl	6.64 ± 0.05	NH_4Cl	6.40 ± 0.03
IAA	C-	5.23 ± 0.07	C-	5.39 ± 0.07
	A5	5.27 ± 0.04	siA5	5.42 ± 0.05
	NH_4Cl	6.38 ± 0.11	NH_4Cl	6.49 ± 0.14

HEK293T cells were transfected with C- or A5 vectors (for overexpression) or C- and siA5 (for silencing). After 48 or 72 h, respectively, lysosomal pH was measured in cells incubated in KH or IAA media for 4 h as described in Materials and Methods. NH_4Cl (20 mM) was used as positive control and pH values are shown as mean and SD from three different experiments. Differences were found not to be statistically significant.

7. RESULTS: CHAPTER 4

Annexin A1 and mostly copine 1 cooperate with annexin A5 to the enhancement of autophagy and copine 1 promotes endocytosis

Abstract

In a previous work we found that three Ca^{2+}-dependent phospholipid-binding proteins, annexin A1, annexin A5 and copine 1, increased their levels on isolated lysosomal membranes from mouse fibroblasts under starvation and also that annexin A5 is involved in autophagosome maturation. Therefore, we analysed now the effect of the knockdown and overexpression of the two other Ca^{2+}-binding proteins, annexin A1 and copine 1, in autophagic degradation. We found that they also induce autophagosome maturation and that their co-silencing with annexin A5 increase the inhibitory effect produced by annexin A5 knockdown, especially in the case of copine 1. Therefore, all these proteins promote autophagosome fusion with lysosomes. Moreover, we found that copine 1 induces endocytosis. Because we previously found an inhibitory effect of annexin A5 on this process and copine 1 increases its levels under annexin A5 knockdown, it is possible that annexin A5 and copine 1 regulate endocytosis in a coordinated way.

Introduction

Lysosomes are highly specialized acidic organelles that degrade extracellular and intracellular material through endocytosis and autophagy, respectively (Saftig and Klumperman, 2009). The most important form of autophagy is macroautophagy, hereafter simply called autophagy. Its earlier stage involves the formation of a double lipid bilayer called phagophore, whose components probably derive from several intracellular compartments (Axe *et al*., 2008; Hayashi-Nishino *et al*., 2009; Yla-Anttila *et al*., 2009; Hailey *et al*., 2010; Mari *et al*., 2010; Ravikumar *et al*., 2010; Longatti and Tooze, 2012; Yamamoto *et al*., 2012). Once the autophagic cargo is sequestered and the autophagosome is formed, it matures by fusing with late endosomes/lysosomes to acquire proteolytic competence (Noda *et al*., 2009). More than 30 different and evolutionarily conserved autophagy-

related genes that participate in all these steps have been identified in yeast (Klionsky *et al*., 2003). Most of them are conserved in mammalian cells, although some mammalian-specific autophagy related genes also exist (Knecht *et al*., 2009).

Autophagy is physiologically regulated by various hormonal and nutritional agents and in mammalian cells the most studied negative regulators of this process are insulin and amino acids (Lavallard *et al*., 2012). In the last years, the second messenger Ca^{2+} has gained importance in the regulation of autophagy. However, conflicting results exist concerning the role of this cation in the signalling and trafficking steps of autophagy (Ghislat and Knecht, 2012a). We previously identified in a proteomic analysis of lysosomal membranes higher levels of three Ca^{2+}-dependent phospholipid-binding proteins under amino acid starvation (Ghislat and Knecht, 2012b). Since we found that annexin A5, one of these proteins promotes autophagosome maturation and inhibits endocytosis (Ghislat *et al*., 2012a), we analysed here the possible role of the two other identified Ca^{2+}-dependent membrane-binding proteins, annexin A1 and copine 1, in lysosomal protein degradation, with particular emphasis in autophagy.

Materials and methods

Materials

Minimum essential medium (MEM), Dulbecco's modified Eagle's medium (DMEM), human insulin, fluorescein isothiocyanate (FITC)–dextran, 3-methyladenine and NH_4Cl were purchased from Sigma Chemical Co. Leupeptin was from Peptide Institute, Inc. Radioisotopes and Percoll were obtained from Amersham Pharmacia Biotech Inc. MEM amino acids 50x, foetal bovine serum (FBS), penicillin, streptomycin and LysoTracker Red were from Molecular Probes (Invitrogen Life Technologies). Saponin was from Merck and bovine serum albumin (BSA) from Roche Applied Science, BAPTA-AM was from Tocris and metrizamide was from Nycomed. The

following antibodies were used: anti-annexin A5, anti-annexin A1, anti-copine 1 and anti-cathepsin D (Santa Cruz Biotechnology); anti-LC3B (Nanotools); anti-lamin A, anti-early endosome antigen 1 (EAA1), anti-calnexin, anti-p62 and anti-lamp 1 (Abcam); anti-glyceraldehyde-3-phosphate dehydrogenase (GAPDH) (Trevigen); anti-β-actin and horseradish-peroxidase labelled secondary antibodies (Sigma Chemical Co.); anti-mitochondrial complex II (succinate-ubiquinol oxidoreductase, 70 kDa subunit), Alexa-Fluor-488- and Alexa-Fluor-633-conjugated anti-rabbit and anti-mouse secondary antibodies (Molecular Probes, Invitrogen Life Technologies). Other reagents, purchased from Sigma Chemical Co, Invitrogen Life Technologies or Calbiochem, were of analytical grade.

Cell culture and general methods

Mouse fibroblasts NIH3T3 and the human embryonic kidney cell line HEK293T were obtained from the European Collection of Animal Cell Cultures. Cells were grown at 37ºC in a humidified atmosphere of 5% (v/v) CO_2/air in MEM or DMEM with 10% heat-inactivated FBS and 1% penicillin and streptomycin. Krebs–Henseleit medium (KH; 118.4 mM NaCl, 4.75 mM KCl, 1.19 mM KH_2PO_4, 2.54 mM $MgSO_4$, 2.44 mM $CaCl_2{\cdot}2H_2O$, 28.6 mM $NaHCO_3$, 20 mM glucose) with 10 mM Hepes, pH 7.4, was used for high proteolysis (starvation) conditions. For intermediate proteolysis conditions, 0.1 μM insulin or essential amino acids at two times the concentration present in MEM were added to the KH. For low proteolysis conditions, both of them were present. For immunoblotting, we followed our standard procedure previously described (Fuertes *et al*., 2003b). Protein bands were quantified by densitometric analysis with an Image Quant ECL (GE Healthcare). Electron microscope morphometry and identification of Av_i and Av_d were carried out as previously described (Esteban *et al*., 2007).

Proteomic analysis and subcellular fractionation

Isolation of highly purified lysosomal membranes from NIH3T3, the two-dimensional differential gel electrophoresis (2D-DIGE) and mass

spectroscopy (MS) analysis were performed as previously described (Ghislat *et al*., 2012a).

For subcellular fractionation by differential centrifugation, HEK293T cells were homogenised in 0.25 M sucrose at 4°C, first with a nitrogen cavitation pump ($2.41x10^5$ Pa, 7 minutes), and then with a tight-fitting Dounce homogeniser (10 strokes). Next, homogenates in 0.25 M sucrose were centrifuged at 1000 g for 10 min at 4°C, the pellet was saved as a fraction enriched in nuclei and the post-nuclear supernatant was applied to a second centrifugation (7000 g; 10 min) where the pellet was saved as a mitochondrial/lysosomal fraction 1. After a centrifugation (25,000 g; 10 min) of the supernatant, a mitochondrial/lysosomal fraction 2 was collected in the pellet. A subsequent centrifugation (105,000 g; 1h) of the supernatant allowed the collection of a pellet and a new supernatant saved, respectively, as microsomal and cytosolic fractions. Each pellet was washed and centrifuged again three times in 0.25M sucrose.

Measurement of intracellular protein degradation

Pulse and chase experiments were carried out as previously described (Fuertes *et al*., 2003a). Briefly, cells were incubated for 48 h in fresh full medium with 2 µCi/ml [^{3}H]valine, followed by a 24 h chase in fresh full medium containing 10 mM L-valine to degrade short-lived proteins. Then, and to measure the degradation of long-lived proteins, all cultures were incubated for 4 h in KH without or with insulin and amino acids. Total and lysosomal protein degradation were measured and calculated as previously described (Fuertes *et al*., 2003b).

Overexpressions and small interfering RNA suppressions

Recombinant DNA— Mouse annexin A1 and copine 1 cDNA clones were isolated from a mouse liver cDNA library (Invitrogen Life Technologies). The coding regions were amplified by a polymerase chain reaction and produced 1.39- and 2.02-kilobase cDNA fragments corresponding,

respectively, to annexin A1 and copine 1. Then, PCR products were purified with the High Pure Template Preparation Kit (Roche Applied Science), digested with BamH1 and Xho1 (New England Biolabs) and subsequently cloned into the mammalian expression vector pcDNA3.1 (Invitrogen Life Technologies) using a T4 DNA ligase (New England Biolabs) to generate An1-pcDNA3.1 and Cp1-pcDNA3.1. Plasmids were transformed into chemically competent bacteria, which were grown overnight at 37ºC in a shaking incubator in lactulose breath test (LBT) broth (10 mg/ml NaCl, 10 mg/ml Bacto-tryptone, 5 mg/ml yeast extract and 40 mg/ml thymine) with the appropriate selective antibiotic (50 µg/ml ampicillin). Plasmids were then purified using Plasmid Mini, Midi or Maxi kits (Qiagen), depending on the volume of culture grown. A glycerol stock stored at -80ºC was made by adding 0.25 ml of glycerol to 0.75 ml of bacterial culture. The purified plasmids were quantified by absorbance readings in a Nanodrop ND-1000 spectrophotometer (Thermo Scientific).

Transfections— HEK293T cells were transiently transfected with An1-pcDNA3.1 (annexin A1 overexpression vector; referred to as An1 vector), Cp1-pcDNA3.1 (copine 1 overexpression vector; referred to as Cp1 vector) and empty pcDNA3.1 (negative control vectors: C- vector). Transfections were carried out using Fugene HD (Roche Applied Science), according to the manufacturer's instructions. Experimental analyses of overexpression were started 48 h after transfections. NIH3T3 and HEK293 cells stably expressing eGFP–LC3 were generated by transfection with eGFP–LC3 (the construct was a kind gift from Tamotsu Yoshimori, Department of Genetics, Osaka University, Japan) and subsequent selection of eGFP–LC3 stable transformants in the presence of 1 mg/ml geneticin (Gibco). Isolation of NIH3T3 stably expressing the mRFP–GFP–LC3 reporter (Kimura *et al*., 2007) was accomplished as previously described (Ghislat *et al*., 2012a). These cells were grown in the same conditions as reported above (in the presence of 1 mg/ml geneticin). For the knockdown of annexin A1, annexin A5 and copine 1, NIH3T3 cells were transfected, 72 h before analysis, with

small interfering RNAs (siRNAs) using siLentFect Lipid Reagent (Bio-Rad). Two different siRNAs (1 and 2), purchased from Ambion Inc., that target mouse annexin A5 mRNA, annexin A1 and copine 1 mRNAs were used at a final concentration of 25 nM. As a negative control (C-), scrambled, non-targeting siRNAs obtained from Ambion Inc. were used. Silencing efficiency was estimated at the protein level by western blotting.

Fluorescence microscopy

Immunofluorescence staining was performed as previously described (Ghislat *et al*., 2012a). Briefly, cells were cultured on coverslips in 12-well plates. After the different treatments, cells were fixed with 3.7% paraformaldehyde-PBS for 20 min at room temperature, blocked with 0.1% BSA-PBS for 10 min and permeabilised with 0.05% saponin-PBS for 10 min. Then, cells were incubated with antibodies against lamp 1 (dilution 1:100), annexin A1 (dilution 1:100), and copine 1 (dilution 1:50) and mounted using Fluor-Save reagent (Calbiochem). Bound antibodies were subsequently detected by incubation, as appropriate, with Alexa-Fluor-488-, or -633-conjugated rabbit, or mouse secondary antibodies (dilution 1:200). Laser lines were 488 nm (eGFP–LC3, mRFP–GFP–LC3 and Alexa Fluor 488), 561 nm (mRFP–GFP–LC3) and 633 nm (Alexa Fluor 633). Preparations were observed and images were acquired with a Leica DM6000 B fluorescence microscope equipped with a Leica TC5 confocal laser scanning system or with a Zeiss Axiovert 200 inverted microscope equipped with Apotome system.

Flow cytometry

Lysosomal mass was determined by incubating the cells in suspension (~10^6 cells/ml) with 75 nM LysoTracker Red for 30 min at 37°C, and the emitted red fluorescence (620±20 nm band-pass filter) was analysed (Poot, 2001). For measurements of fluid phase endocytosis, using flow cytometry, cells were incubated with FITC–dextran (1 mg/ml) for 30, 60, 120, or 240 min at 37°C. Previously, cells were also incubated as above, but for 5

s at 4°C to evaluate the membrane-bound marker. At the different times, cells were detached with trypsin–EDTA, washed four times, resuspended in PBS (10^6 cells/ml), and the emitted red (620±20 nm band-pass filter) fluorescence was analysed by flow cytometry. In each experiment, 10,000 cells were collected and analysed using a Cytomics FC 500 flow cytometer (Beckman Coulter). Autophagy quantification by flow cytometry was determined by a procedure described elsewhere (Shvets and Elazar, 2009), but washing the cells with PBS containing 0.05% saponin, previously to flow cytometry, to eliminate eGFP-LC3-I from the cells (Eng *et al*., 2010).

Quantification and statistics

P-values were determined by factorial t-test student using GraphPad Prism software. *P*-values were considered significant at ***$P \leq 0.0005$, **$P \leq 0.005$ and *$P \leq 0.05$.

Results

Under amino acid starvation, annexin A1 and copine 1 translocate to lysosomal membranes

We analysed by 2D-DIGE and MS lysosomal membranes isolated from NIH3T3 cells incubated under conditions of high (KH alone: starvation), intermediate (KH with insulin or amino acids) and low (KH with insulin and amino acids) proteolysis to identify proteins that could regulate lysosomal protein degradation. Like annexin A5 (Ghislat *et al*., 2012a) (see Results, Chapter 3), the levels of annexin A1 and copine 1 on the lysosomal membranes under high proteolysis conditions (Fig. 1A), significantly decreased after addition of amino acids with or without insulin, but not after addition of insulin alone (Fig. 1B). This was confirmed by western blot analysis of subcellular fractions from HEK293T cells: the association of both proteins to the mitochondrial/lysosomal fractions observed under starvation decreases under conditions of low proteolysis (Fig. 1C). Finally, an

enhanced colocalization of annexin A1 and copine 1 with the lysosomal marker lamp 1 under high proteolysis conditions was evidenced by immunofluorescence microscopy (Fig. 1D). Since the total levels of both proteins under all these conditions do not change (Fig. S1), we conclude that annexin A1 and copine 1 translocate to lysosomal compartments under high proteolysis conditions.

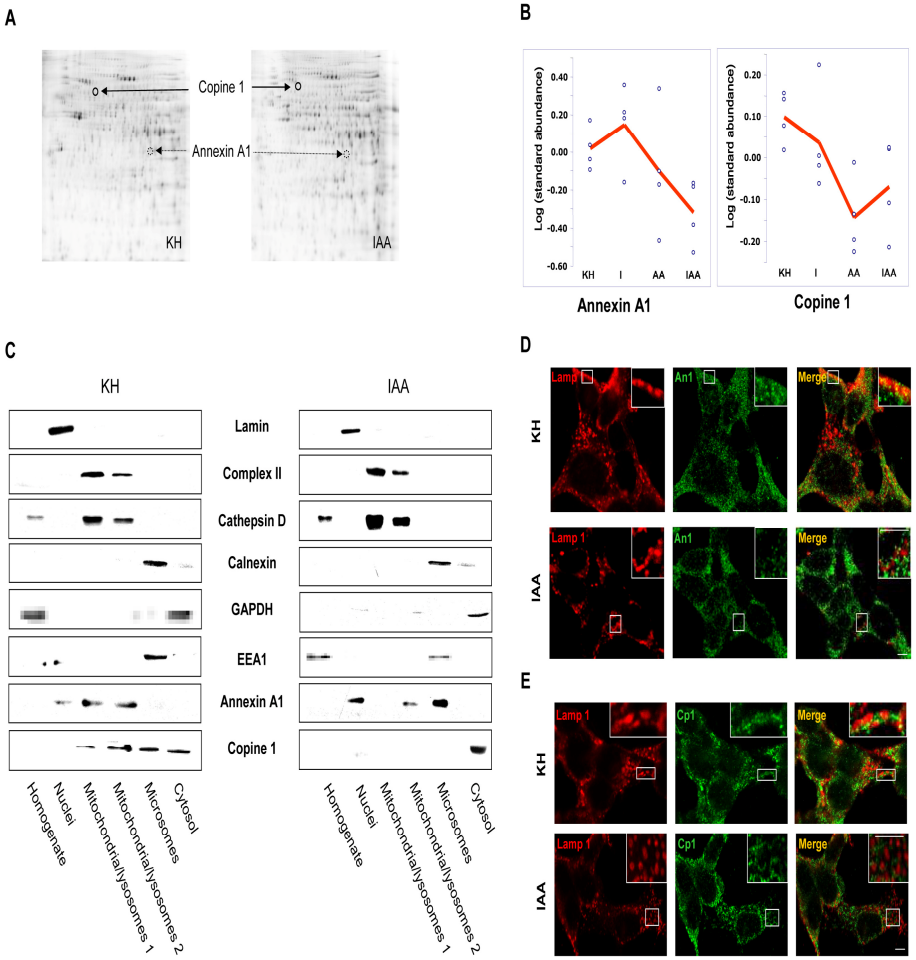

Figure 1. Annexin A1 and copine 1 translocate to lysosomal membranes under starvation. (**A**) Lysosomal membrane proteins (100 µg) from NIH3T3 cells incubated for 4 h in KH without (KH) or with insulin and amino acids (IAA), were separated in 2D-DIGE gels. Representative gels showing annexin A1 and copine 1 (encircled spots). (**B**) Levels of annexin A1 and copine 1 on lysosomal membranes isolated from NIH3T3 cells incubated in KH without (KH) or with insulin (I), amino acids (AA) or both (IAA). Data are from four independent experiments similar to that shown in A. The line joins the mean values of each experiment. (**C**) Subcellular fractions were isolated, as described in Materials and Methods, from HEK293T cells incubated for 4 h in KH or in IAA. 25 µg protein from each fraction were subjected to SDS-polyacrylamide gel electrophoresis and immunoblotted with antibodies that recognise lamin (nuclear marker), complex II of mitochondria (succinate-ubiquinol oxidoreductase; mitochondrial marker), cathepsin D (lysosomal marker), calnexin (microsomal marker), GAPDH (glyceraldehyde-3-phosphate dehydrogenase; cytosolic marker), EAA1 (Early endosome antigen 1; marker for early endosomes), annexin A1 and copine 1. (**D, E**) Confocal images of NIH3T3 cells immunostained with annexin A1 (An1) (D) or copine 1 (Cp1) (E) and with lamp 1. Cells were previously incubated for 4 h in KH (upper panels) or in IAA (lower panels). Merged images are shown in the right panels. Insets: high-magnification images of selected areas. Scale bars: 5 µm.

Annexin A1 and copine 1 promote lysosomal protein degradation

Under starvation (high proteolysis conditions), lysosomes represent the main catabolic compartment for intracellular material in eukaryotic cells (Fuertes *et al*., 2003b). Therefore, we investigated a possible role of annexin A1 and copine 1 in lysosomal protein degradation measured by procedures previously described (Fuertes *et al*., 2003b; Mizushima *et al*., 2010). Two different short-interfering RNAs (siRNAs) for each protein (s1An; s2An for annexin A1 and s1Cp; s2Cp for copine 1) were used in NIH3T3 cells, which produced a similar reduction (75-85%) in protein expression (Fig. 2A). Silencing of annexin A1 or copine 1 slightly decreased the total degradation of long-lived proteins (Fig. 2B), a reduction that was more evident when the lysosomal degradation was analysed (Fig. 2C) using NH_4Cl and leupeptin as described (Fuertes *et al*., 2003b; Mizushima *et al*., 2010). Furthermore, under high proteolysis conditions, the levels of p62, a multifunctional protein that binds LC3-II and ubiquitinated proteins for their destruction in lysosomes (Moscat and Diaz-Meco, 2009), increased after annexin A1 or copine 1 silencing and this effect was dependent on lysosomal degradation, since it was prevented by the inhibition of lysosomal degradation with NH_4Cl and leupeptin (Fig. 2D). Conversely, the overexpression of these two proteins (Fig. 2E) in HEK293T cells (which have a higher overexpression efficiency in

comparison with NIH3T3 cells) increased total and lysosomal degradation of long-lived proteins under low (Fig. 2F) but not under high proteolysis conditions (Fig. 2G), probably because under the latter conditions the levels of these two proteins in lysosomal membranes and lysosomal proteolysis are already high.

Overall, these results are consistent with a role of annexin A1 and copine 1 in lysosomal protein degradation.

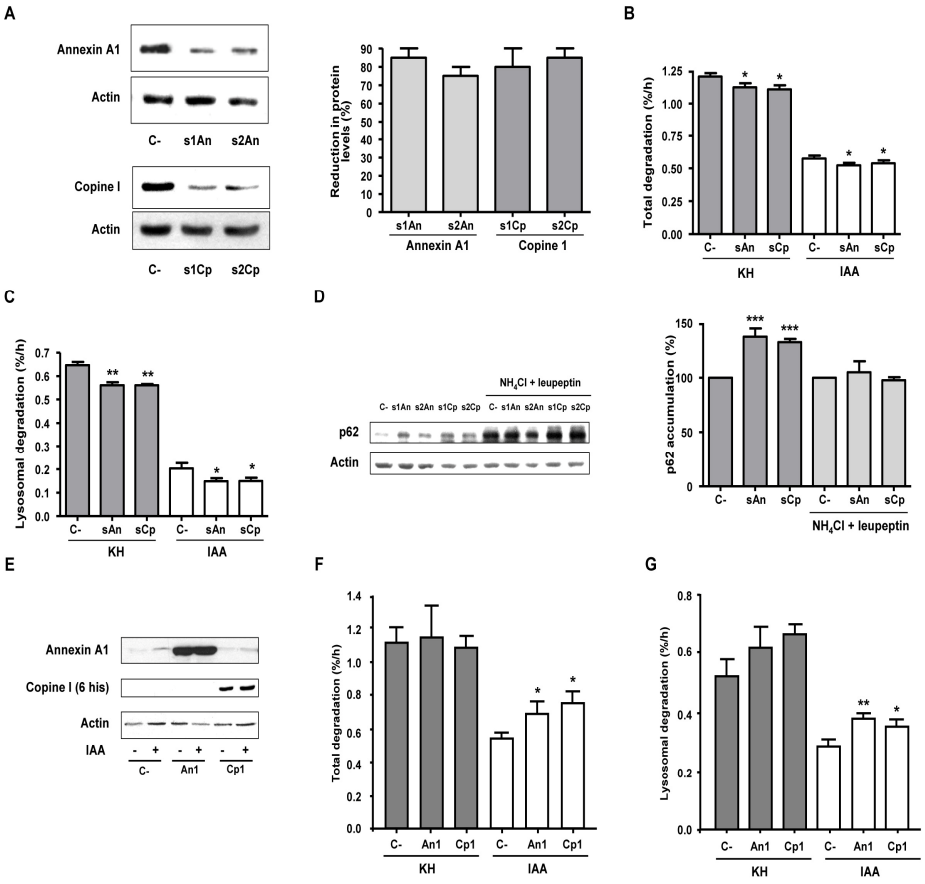

Figure 2. Annexin A1 and copine 1 promote lysosomal protein degradation. (**A**) NIH3T3 cells were transfected with non-targeting siRNAs (negative control, C-), and with two different annexin A1 (s1An and s2An) and copine 1 (s1Cp and s2Cp) siRNAs. Then, the cells were grown for 72 h. Left: Immunoblot using antibodies that recognize annexin A1, copine 1 and actin (as a loading control). Right: Quantification of the reduction in annexin A1 and copine 1 levels produced by the different siRNAs (in percentage). (**B, C**) NIH3T3 cells previously transfected with C-, s1An, s2An, s1Cp, or s2Cp siRNAs were metabolically labelled with [^{3}H]valine for 48 h, chased for 24 h and then switched for 4 h to KH without (KH) or with insulin and amino acids (IAA). Total (B) and lysosomal (C) protein degradations were calculated as indicated in Materials and Methods. The average of the means obtained with s1An and s2An for annexin A1 knockdown and s1Cp and s2Cp for copine 1 knockdown are indicated (sAn and sCp, respectively). (**D**) NIH3T3 cells transfected as in B and C, treated in KH for 4 h without or with NH_4Cl (20 mM) and leupeptin (Leup, 100 μM) were subjected to immunoblotting with p62 and actin antibodies. Densitometric measurements of the p62 bands shown in the histogram on the right were normalised to the corresponding actin bands and are expressed as a percentage of the corresponding negative control (C-) values. (**E-G**) HEK293T cells, transiently transfected with C-, An1 or Cp1 vectors, were labelled and incubated as above (F, G). Total (F) and lysosomal (G) protein degradations in low (IAA) and high (KH) proteolysis conditions were calculated as described in the Materials and Methods. Data represent the mean and SD from 3 (A, D, F, G) and 8 (B, C) independent experiments (with duplicated samples in B, C, F and G). Differences from the respective control values in the histograms were found to be statistically significant at ***P<0.0005, **P<0.005 and *P<0.05.

Annexin A1 and copine 1 promote autophagy

Based on the results shown in Fig. 1 and 2, and given that annexin A5, another protein with the same Ca^{2+}-related characteristics as annexin A1 and copine 1, enhances autophagy (Ghislat *et al*., 2012a) (see Results, Chapter 3), we investigated the effect of annexin A1 and copine 1 knockdown on starvation-induced autophagy. It is known that LC3-II, the processed and lipidated form of the protein LC3-I, is recruited to autophagosomes (Tanida *et al*., 2005). When its degradation in autolysosomes is inhibited (Codogno and Meijer, 2005), its levels (relative to actin or tubulin and not to LC3-I, which is reported to be less stable and less immunoreactive than LC3-II (Mizushima and Yoshimori, 2007; Klionsky *et al*., 2008)) are indicative of the rate of autophagosome formation (Levine and Klionsky, 2004; Lum *et al*., 2005; Mizushima *et al*., 2010). Using NH_4Cl and leupeptin to inhibit lysosomal degradation, a treatment with the same effect on LC3-II accumulation than bafilomycin A1 (Esteve *et al*., 2010), we found that silencing of annexin A1 caused an increase in the LC3-II/actin ratio in the absence, but not in the presence of inhibitors of lysosomal degradation (Fig. 3A). As for copine 1 knockdown, it caused an accumulation of LC3-II

both in the absence and presence of inhibitors of lysosomal degradation, an increase which was more evident in the former (about 2.44 times) than in the latter (about 1.28 times) condition (Fig. 3B).

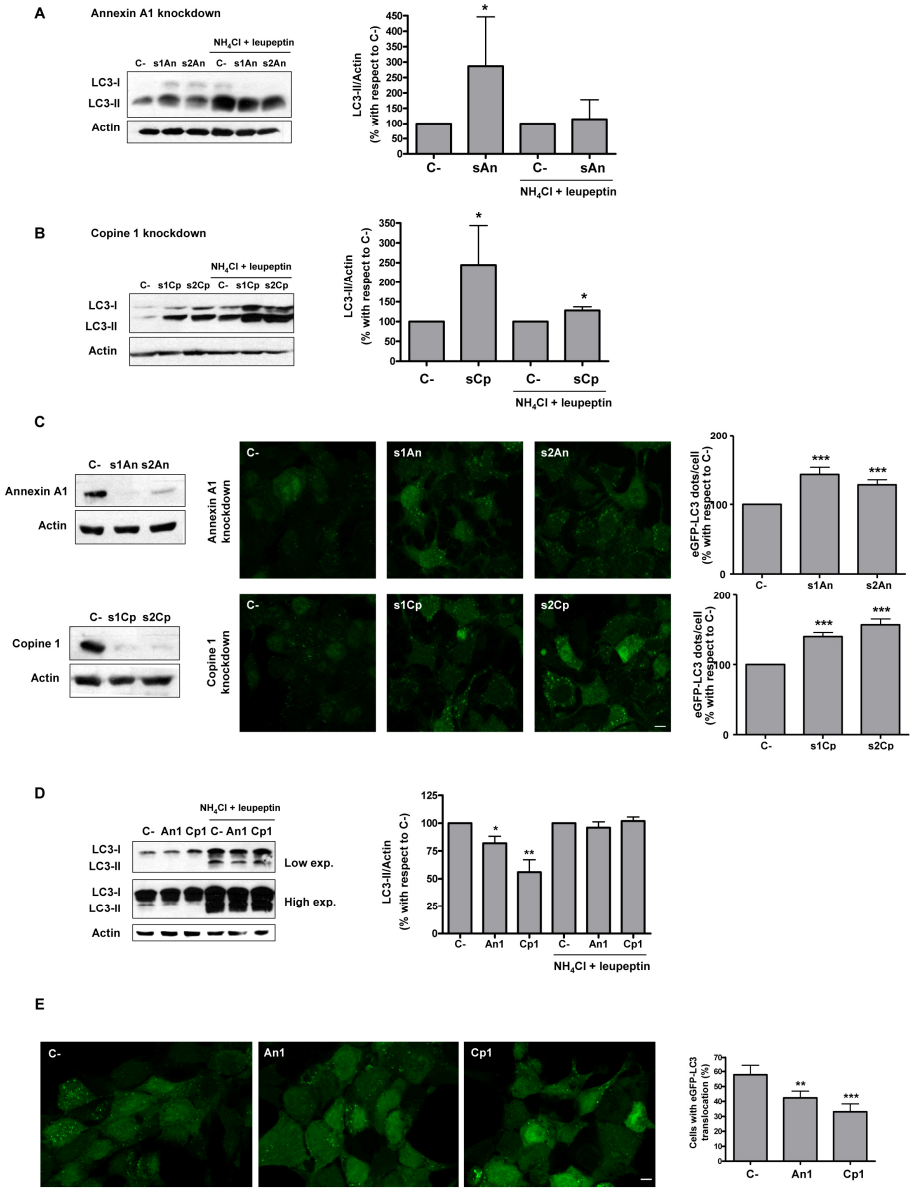

Figure 3. Annexin A1 and copine 1 promote autophagy. (**A, B**) NIH3T3 cells were transfected with C-, s1An, s2An, s1Cp or s2Cp siRNAs. After 72 h, cells were incubated in KH for 4 h without or with NH_4Cl (20 mM) and leupeptin (Leup, 100 µM) and were subjected to immunoblotting with LC3 and actin antibodies. Densitometric measurements of the LC3-II bands were normalised to the corresponding actin bands and are shown in the histogram on the right. Data are expressed as percentage of an average of the two siRNAs targeted to annexin A1 (sAn) and to copine 1 (sCp) with respect to the corresponding C- values. (**C**) NIH3T3 cells stably expressing eGFP–LC3 were transfected for 72 h with the same siRNAs than A and B, incubated for 4 h in KH and then examined using a fluorescence microscope equipped with Apotome system. The number of eGFP–LC3 puncta per cell was determined in at least 100 cells per condition and results are shown on the right. Actin, annexin A1 and copine 1 levels are shown on the left. (**D**) HEK293T cells were transiently transfected with C-, An1 or Cp1 vectors, and were incubated for 3.5 h in KH and subsequently switched to KH with insulin and amino acids for 30 min. Then, the cells were subjected to immunoblotting, with various exposures (exp), using antibodies that recognise LC3 (-I and -II) and actin. The histogram on the right shows densitometric measurements of the ratio of LC3-II to actin bands. (**E**) HEK293T cells with stable expression of eGFP–LC3 were transiently transfected and incubated as in (D). Cells were then examined using a confocal microscope. The percentage of cells with eGFP–LC3 translocation (cells containing more than five dots were considered positive) was determined (at least 100 cells per condition) and results are shown on the right. Data represent the mean and SD from 8 (A, B), 3 (C), 6 (D), and 2 (E) independent experiments. Differences from the respective control values in the different histograms were found to be statistically significant at ***P<0.0005. **P<0.005 and *P<0.05. Scale bars: 5 µm.

In addition, in NIH3T3 cells with stable expression of eGFP–LC3, annexin A1 and copine 1 knockdown augmented the number of fluorescent puncta under high proteolysis conditions (Fig. 3C). Because silencing of annexin A1 and copine 1 decreased lysosomal proteolysis (Fig. 2C), the observed raise in LC3-II levels cannot be due to an increased formation of autophagosomes and instead could reflect an accumulation of autophagosomes not converted into autolysosomes. Moreover, we compared in similar experiments the effect of annexin A1 and copine 1 overexpressions on LC3-II levels. We used, as above, transiently transfected HEK293T cells with An1, Cp1 or C- vectors. As the overexpressions of copine 1 and annexin A1 promote lysosomal degradation under low rather than high proteolysis condition (Fig. 2F and G), we assessed autophagosome levels under the former condition. Because LC3-II is difficult to detect under this condition (due to its low levels) especially in the absence of inhibitors of lysosomal degradation, we incubated the cells for 3.5 h in KH to induce autophagosome formation, and switched the cells for 30 min in KH with insulin and amino acids. LC3-II levels decreased under annexin A1 overexpression, and this decrease was more evident under copine 1

overexpression (Fig. 3D, high exposure blot). These effects were only observed in the absence of inhibitors of lysosomal degradation (NH_4Cl and leupeptin) indicating that autophagosome formation was not affected by these overexpressions. Furthermore, overexpression of annexin A1 and copine 1 in HEK293T cells with stable expression of eGFP–LC3 decreased the number of fluorescent puncta (Fig. 3E). Since overexpression of these two proteins increases lysosomal proteolysis (Fig. 2F and G), the observed decrease in LC3-II levels may be explained, as was the case with annexin A5 (Ghislat *et al*., 2012a) by an enhanced conversion of autophagosomes into autolysosomes.

Annexin A1 and copine 1 increase the activation of lysosomal protein degradation by annexin A5

Since these three proteins share common properties such as binding to phospholipids in a Ca^{2+}-dependent way, we investigated their combined effect on lysosomal degradation. Therefore, we co-transfected the cells with siRNAs directed to annexin A1/annexin A5 (An1/An5), annexin A1/copine 1 (An1/Cp1) or annexin A5/copine 1 (An5/Cp1) (Fig. 4A). Co-silencings of annexin A1/annexin A5 and annexin A5/copine 1, but not of annexin A1/copine 1, decreased total and lysosomal degradation under starvation more than their separate individual silencings (Fig. 4B and C). Because annexin A5 is one of the most abundant annexins in mammalian cells (Russo-Marie, 1999), and its knockdown inhibited lysosomal protein degradation more than annexin A1 and copine 1 silencing (Fig. 4B) this protein may counterbalance the effect of the knockdown of annexin A1 and copine 1 on lysosomal protein degradation. This could explain the moderate inhibitory effect of the transfections with siRNAs targeted to annexin A1 and copine 1 (Fig. 2B and C).

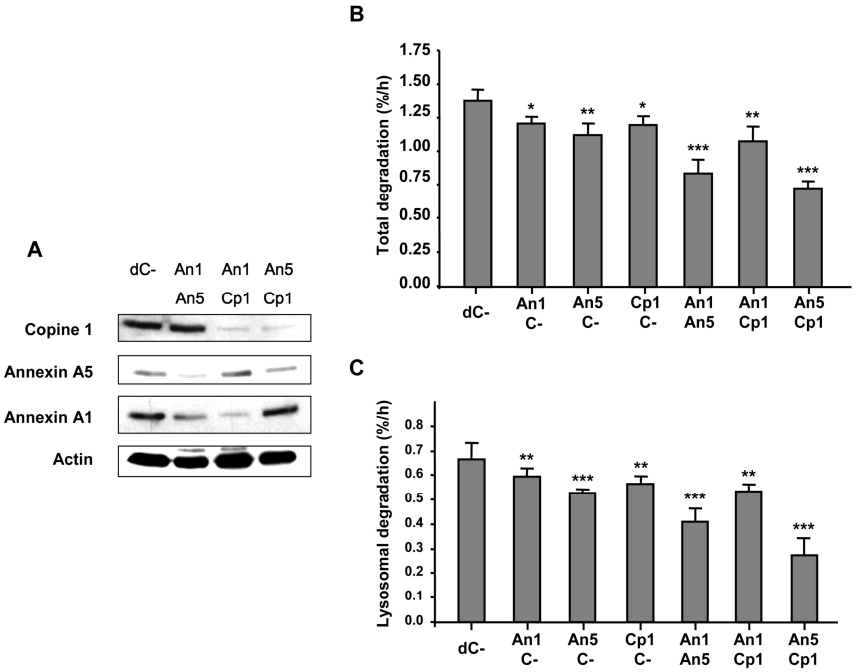

Figure 4. Inhibitory effects of annexin A1, annexin A5 and copine 1 co-silencings on lysosomal protein degradation (**A**) NIH3T3 cells were co-transfected with double concentration of C- siRNAs (dC-) or two siRNAs targeted to annexin A1/annexin A5 (An1/An5), annexin A1/copine 1 (An1/Cp1) or annexin A5/copine 1 (An5/Cp1). 72 h later, cells were subjected to immunoblotting with antibodies that recognize copine 1, annexin A5, annexin A1 and actin (as a loading control). (**B, C**) NIH3T3 cells previously co-transfected as in (A) or with annexin A1/C- siRNAs (An1/C-), or with annexin A5/C- siRNAs (An5/C-) or with copine 1/C- siRNAs (Cp1/C-) were metabolically labelled with [^{3}H]valine for 48 h, chased for 24 h and then switched for 4 h to KH. Total (B) and lysosomal (C) degradations were calculated as indicated in Materials and Methods. Values are the means and SD from three independent experiments with duplicated samples. Differences from the respective control values in the histograms were found to be statistically significant at ***P<0.0005, **P<0.005 and *P<0.05.

From the three silencing combinations, the highest inhibition of lysosomal degradation in starved cells was obtained when annexin A5 and copine 1 were co-silenced. Therefore, we investigated the possible role of these two proteins in autophagy. When both proteins were silenced, we observed an increased accumulation of LC3-II and p62 (Fig. 5A) and also in cells stably expressing eGFP-LC3 of autophagosomes (Fig. 5B).

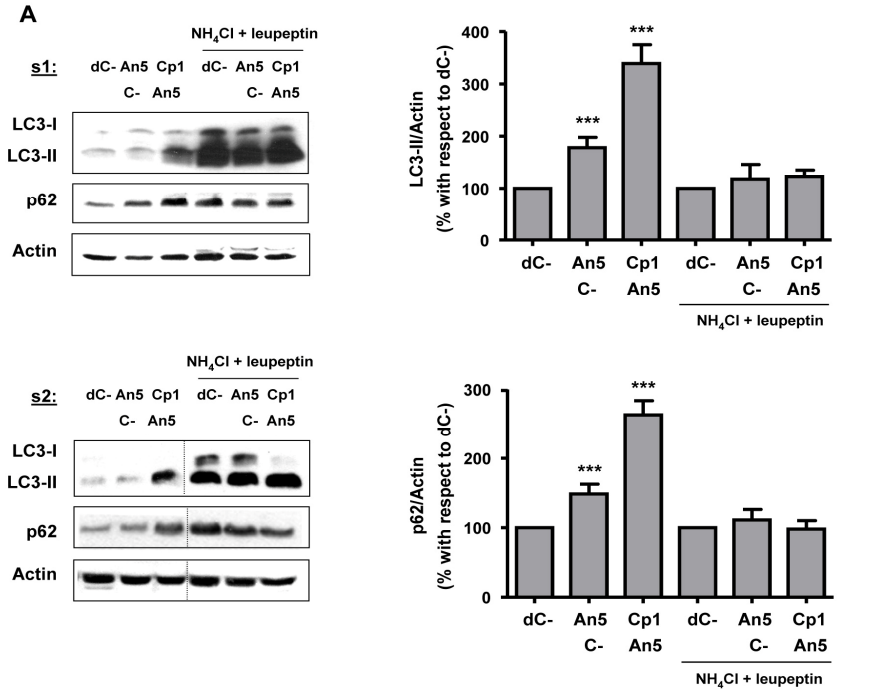
A
NH4Cl + leupeptin
s1:
dC- An5 C- Cp1 An5
dC- An5 C- Cp1 An5
LC3-I
LC3-II
p62
Actin
LC3-II/Actin (% with respect to dC-)
400
300
200
100
0
***
***
dC- An5 C- Cp1 An5 dC- An5 C- Cp1 An5
NH4Cl + leupeptin
s2:
p62/Actin (% with respect to dC-)
300
200
100
0

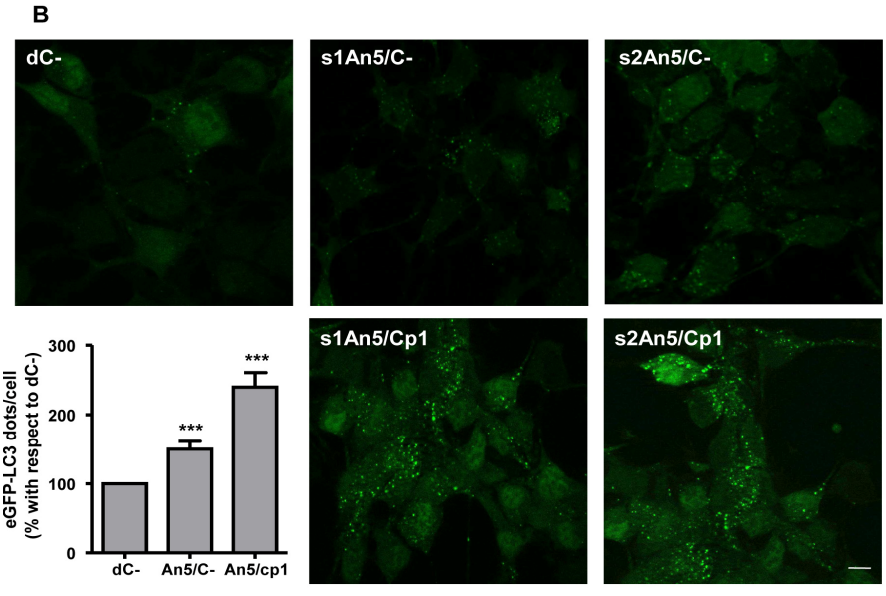
B
dC-
s1An5/C-
s2An5/C-
s1An5/Cp1
s2An5/Cp1
eGFP-LC3 dots/cell (% with respect to dC-)
300
200
100
0
***
***
dC- An5/C- An5/cp1

Figure 5. Annexin A5 and copine 1 co-silencing causes a higher accumulation of autophagosomes. (**A**) NIH3T3 cells were co-transfected with double concentration of C- siRNAs (dC-), with C- siRNAs plus one of the two different siRNAs targeted to annexin A5 (s1 and s2) or with copine 1 and annexin A5 siRNAs together (using a combination of s1Cp with s1An5 or with s2An5). After 72 h, cells were incubated in KH for 4 h without or with leupeptin (100 μM) and NH_4Cl (20 mM) and were subjected to immunoblotting with p62, LC3 and actin antibodies. The discontinuous lines indicate that intervening lanes have been cut off from the blot. The densitometric measurements of the p62 and LC3-II bands shown in the two histograms on the right were normalized to the corresponding actin bands and are expressed as a percentage of an average of the two siRNAs with respect to the corresponding negative control (dC-) values. (**B**) NIH3T3 cells stably expressing eGFP-LC3 were transfected for 72 h with the same siRNAs than in A, incubated for 4 h in KH and then observed in a fluorescence microscope equipped with Apotome system. Scale bar: 5 μm. The number of eGFP-LC3 puncta per cell was determined in at least 100 cells per condition and results are expressed as a percentage of an average of the two siRNAs with respect to the corresponding negative control (dC-) values, shown at the bottom, left. Data represent the mean and SD from 3 (A) and 2 (B) independent experiments. Differences from negative control (dC-) values in all the histograms were found to be statistically significant at ***P<0.0005. Scale bar: 5 μm.

Since in these experiments LC3-II and p62 did not accumulate when lysosomal degradation was inhibited with NH_4Cl and leupeptin (Fig 5A), we further analysed whether autophagic flux was disrupted using a flow cytometric assay based on the loss of eGFP fluorescence when eGFP-LC3 bound to autophagosomal membranes is delivered to lysosomes for degradation (Shvets and Elazar, 2009). As expected, higher eGFP-LC3 fluorescence due to accumulation of autophagosomes is observed in the presence of NH_4Cl because it rises the lysosomal pH and consequently inhibits autophagosome delivery to lysosomes (Kawai *et al*., 2007). The individual knockdowns of annexin A5 and copine 1 caused a slight increase in eGFP-LC3, whereas their co-silencing accentuated this increase (Fig. 6A), supporting the requirement of both proteins for autophagosome delivery to lysosomes.

To further confirm that annexin A5 and copine 1 induce the maturation of autophagosomes, we used NIH3T3 cells stably expressing an mRFP-GFP-LC3 tandem reporter, a useful tool to trace autophagosome maturation (Kimura *et al*., 2007). The eGFP-LC3 fluorescence within lysosomes is quenched because of the sensitivity of GFP to acidic environments, whereas mRFP–LC3 fluorescence is more stable upon acidification. Thus, autophagosomes with a neutral pH show both red and green fluorescence,

whereas the latter is lost in autolysosomes with an acidic pH and this allows to calculate the percentage of the autolysosomes. We found that the knockdown of annexin A5 (as previously reported (Ghislat *et al*., 2012a)) or copine 1 slightly decreased the formation of autolysosomes, whereas co-silencing of both proteins produced a stronger effect (Fig. 6B). This finding shows that in cells lacking annexin A5 and copine 1, autophagosomal vesicles not converted into autolysosomes accumulate, sustaining the involvement of both proteins in autophagosome maturation.

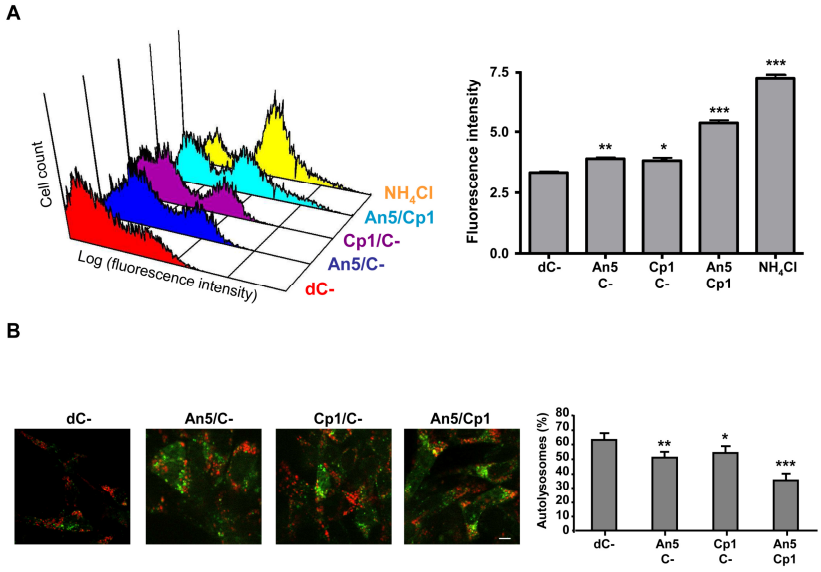

Figure 6. Annexin A5 and copine 1 co-silencing disrupts autophagosome maturation. (**A**) NIH3T3 cells stably expressing eGFP–LC3 were transfected with double concentration of C-siRNAs (dC-), annexin A5/C- siRNAs (An5/C-), copine 1/C- siRNAs (Cp1/C-) or both annexin A5 and copine 1 siRNAs (An5/Cp1). 72 h later, cells were incubated for 4 h in KH. As a control, wild type cells were incubated in KH containing 20 mM NH_4Cl (NH_4Cl). Next, cells were briefly washed with PBS containing 0.05% saponin and the fluorescence intensity of eGFP in the cells was measured by flow cytometry (10,000 events). The histogram on the right shows the mean values of each measurement. (**B**) NIH3T3 cells stably expressing an mRFP–GFP–LC3 construct were seeded on glass coverslips and transfected as in (A). Then, cells were incubated for 4 h in KH and subsequently fixed and analysed using a microscope equipped with Apotome system. The histogram on the right shows the percentage of autolysosomes in the cells incubated under the various conditions. Data represent the mean and SD from 2 (A) and 3 (B) independent experiments (with triplicated samples in A). Differences from negative control (dC-) values in the two histograms were found to be statistically significant at ***P<0.0005, **P<0.005 and *P<0.05. Scale bar: 5 μm.

Copine 1 and annexin A5 have opposite roles in endocytosis

Quantification of the lysosomal mass with LysoTracker Red by flow cytometry showed either a decrease or a moderate increase, respectively, after copine 1 or annexin A5 silencing, and no effect when both proteins were co-silenced (Fig. 7A). The rise in LysoTracker Red staining when annexin A5 is silenced was explained in Chapter 3 of Results by the previously reported inhibition of endocytosis by this protein (Ghislat *et al*., 2012a). The decrease in lysosomal mass under copine 1 silencing can then be explained by an opposite effect of this protein on endocytosis. In fact, the co-silencing of annexin A5 and copine 1 leads to an intermediate effect in LysoTracker Red staining. According to this reasoning, copine 1 would enhance endocytosis. However, a direct role of copine 1 in endocytosis, to the best of our knowledge, has not yet been explored in mammalian cells. Therefore, we measured the effect of its silencing on the internalization of fluorescein-isothiocyanate (FITC)–dextran, a fluid phase endocytosis marker. Results showed that copine 1 silencing significantly reduced this endocytosis (by ≈ 42%) (Fig. 7B), suggesting a positive role of this protein in this process. Thus, this effect can probably account for the decreased lysosomal mass observed under copine 1 silencing (Fig. 7A). Because annexin A5 and copine 1 silencing have opposite effects on endocytic uptake, we further analysed the expression of each of these two proteins when the other is knocked-down. Copine 1 silencing did not change annexin A5 levels (Fig. 8A), whereas annexin A5 silencing raises copine 1 levels in the presence of insulin and amino acids but not in their absence (Fig. 8B). This finding suggests that annexin A5 acts upstream of copine 1 in a cellular process that gains more importance in the presence of extracellular nutrients. Since autophagy is not active under the latter condition, we examined whether endocytosis is induced by the presence of nutrients. We found that the uptake of FITC–dextran is enhanced in the presence of insulin and amino acids (Fig. 8C). Thus, it is possible that under conditions where endocytosis is active, such as in the presence of insulin and amino acids,

annexin A5 may down-regulate the levels of copine 1 to control the endocytic uptake.

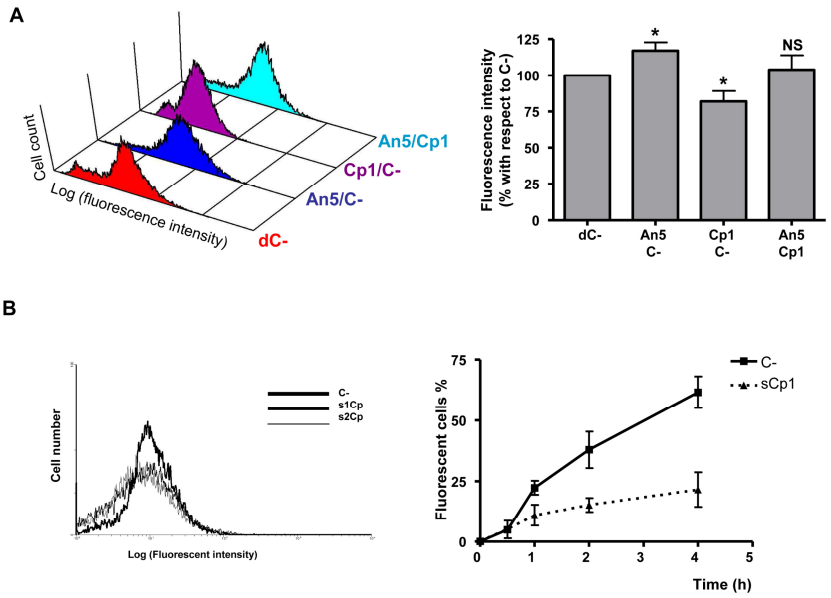

Figure 7. Copine 1 silencing decreases lysosomal mass and fluid phase endocytic uptake. (**A**) NIH3T3 cells were co-transfected with double concentration of C- siRNAs (dC-), annexin A5/C- siRNAs (An5/C-), copine 1/C- siRNAs (Cp1/C-) or with annexin A5/copine 1 siRNAs (An5/Cp1). 72 h later, cells were incubated for 4 h in KH in the presence of LysoTracker Red (75 nM). LysoTracker Red fluorescence was analysed by quantitative flow cytometry (10,000 events). Differences from negative control values (dC-) were found to be statistically significant at **P*<0.05. NS: no significant differences. (**B**) Quantitative flow cytometry (10,000 events) of FITC–dextran (1 mg/ml) internalization in NIH3T3 cells transfected with C-, s1Cp or s2Cp siRNAs. In all experiments, control samples were carried out for 5 s at 4°C (to evaluate the membrane bound marker) and the remaining samples for 30 min, 1, 2 and 4 h at 37°C. The average of values obtained using both siRNAs are indicated in the graph on the right (sCp1). Values on the y-axis indicate the fluorescence percentage in arbitrary units of viable cells, as assessed by propidium iodide staining (1 µg/ml). The histogram on the left is reprentative of the fluorescence obtained in the cells incubated with FITC–dextran for 4 h. Data represent the mean and SD from 3 (A, with quadruplet samples) and 2 (B, with duplicated samples) independent experiments.

In summary, our findings confer to copine 1 a similar function as annexin A5 in autophagosome maturation and an opposite role in endocytosis.

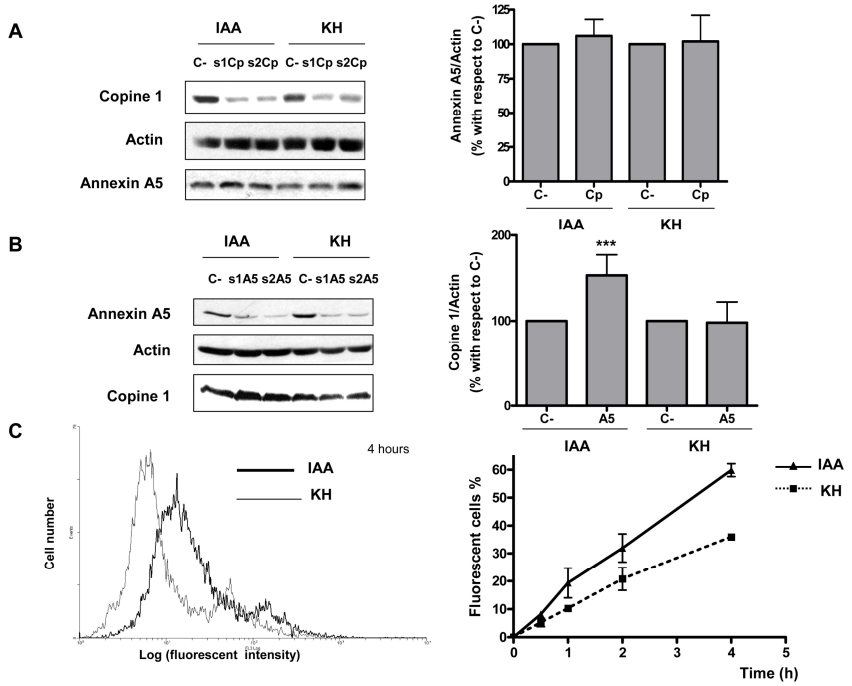

Figure 8. Copine 1 is upregulated under annexin A5 silencing in conditions that promote fluid phase endocytosis. NIH3T3 cells were transfected with C-, s1Cp, or s2Cp siRNAs (**A**) and C-, s1An5, or s2An5 siRNAs (**B**). After 72 h cells were incubated for 4 h in KH without or with insulin and amino acids (IAA) and were subjected to immunoblotting with copine 1, annexin A5 and actin antibodies. Densitometric measurements of the annexin A5 (A) and copine 1 (B) bands were normalised to the corresponding actin bands and are shown in the histograms on the right. Data are expressed as a percentage of an average of the two siRNAs (Cp or A5) with respect to the corresponding negative control (C-) values. The difference from the control values in the histogram was found to be statistically significant at ****P*<0.0005. (**C**) Quantitative flow cytometry (10,000 events) of FITC–dextran (1 mg/ml) internalization in NIH3T3 cells incubated in either KH or IAA. All experiments were carried out for 5 s at 4°C (to evaluate the membrane bound marker) and for 30 min, 1, 2 and 4 h at 37°C. The averages of values obtained in both conditions at the different times are indicated in the graph on the right. Values on the y-axis indicate the fluorescence percentage in arbitrary units of viable cells, as assessed by propidium iodide staining (1 µg/ml). Data represent the mean and SD from 4 (A, B) and 2 (C, with duplicated samples) independent experiments.

Discussion

Although in the last years numerous details on the mechanism of autophagy have been elucidated, many questions still remain unsolved. In this process, both formation and maturation of autophagosomes are important but, comparatively to the earlier steps, less attention has been given in these last years to the late stages of autophagy (Noda *et al*., 2009).

Here, we have shown the involvement of two new Ca^{2+}-dependent phospholipid binding proteins, annexin A1 and copine 1, in the autophagosome delivery to lysosomes. They, respectively, belong to the annexin and copine superfamilies that enclose structurally related Ca^{2+}-sensitive proteins able to bind negatively charged phospholipids to establish specific interactions with other lipid microdomains (Creutz *et al*., 1998; Monastyrskaya *et al*., 2009).

Annexin A1 was previously reported to translocate, in a Ca^{2+}-dependent way, from predominantly cytosolic areas to the plasma membrane, where it was shown to regulate its lipid architecture by binding to ceramide platforms (Babiychuk *et al*., 2008), and also to intracellular membranes (Monastyrskaya *et al*., 2007). Here we found that this protein associates to lysosomal membranes under starvation, a condition that we previously associated with high intracellular Ca^{2+} levels (Ghislat *et al*., 2012b). Therefore, and although we have not investigated this here, it is possible then that this translocation occurs in a Ca^{2+}-dependent way. Another report showed that under stimulation by the epidermal growth factor (EGF), annexin A1 accumulates inside multivesicular bodies (MVB) where it was proposed to mediate the formation of its vesicles (White *et al*., 2006). Therefore, annexin A1 may be differently located (membranes from MVB or lysosomes) depending on the extracellular stimulus (EGF or starvation) to produce different effects (inward vesiculation or autophagosome delivery to lysosomes). Further support for a role of annexin A1 in lysosomal membranes is provided by the localization on these membranes of S100A1, a small dimeric Ca^{2+}-binding protein that can form a complex with annexin A1 (Nylandsted *et al*., 2011). Finally, a proteomic study identified also annexin A1 in lysosomal membranes under starvation and the authors suggested that it induces autophagy possibly by promoting amphisome formation (Kang *et al*., 2011).

Several studies (reviewed in (Monastyrskaya *et al*., 2009)) suggested Ca^{2+}-dependent association to specific endo-lysosomal compartments of annexin A1 (early endosomes, multivesicular bodies) and annexin A5 (late endosomes). Since Ca^{2+} was shown to promote *in vitro* the fusion of autophagosomes with lysosomes (Koga *et al*., 2010), both annexins may be involved in Ca^{2+}-regulated interactions of the autophagosomal and lysosomal membranes that finally lead to their fusion and to the delivery of the autophagosomal content into the lysosome. Another interesting association of annexin A1 with autophagy was revealed in studies that identified an interaction of annexin A1 with Atg4B (Behrends *et al*., 2011). However, this interaction requires confirmation by more direct experimental procedures.

Concerning copine 1, its presence in autophagosomal, phagosomal and lysosomal membranes, has been previously reported (Damer *et al*., 2005; Overbye *et al*., 2007). Interestingly, an *in vitro* study has shown that annexin A1 forms suitable phosphatidylserine domains for the recruitment of copine 1 aggregates that possibly provide a scaffold to cluster signalling proteins in the presence of Ca^{2+} (Creutz and Edwardson, 2009). Also, annexin A5 is known to bind with high specificity to phosphatidylserine (Gerke and Moss, 2002), which is known to be distributed in all cellular membranes, but it only confers a negative charge (ideal for Ca^{2+} binding) at the cytosolic face of late endosomes and lysosomes (Yeung *et al*., 2008). It is possible then, that annexin A5, like annexin A1, also forms suitable domains for copine 1 recruitment on the lysosomal membranes to facilitate their fusion with autophagosomes. Since annexin A5 levels are higher than those of annexin A1, at least in our cells (NIH3T3 and HEK293 cells), this may explain the lower inhibitory effect of annexin A1/copine 1 co-silencing on autophagy compared to annexin A5/copine 1 co-silencing.

In the present study, we also showed for the first time an involvement of copine 1 in endocytosis in mammalian cells. The opposite roles of copine

1 and annexin A5 in endocytosis are possibly associated with the up-regulation of copine 1 observed under annexin A5 silencing, since this occurs in the presence of nutrients when the endocytic uptake is increased. In accordance with our results, insulin and amino acids were previously reported to induce endocytosis (Pitterle *et al*., 1999; Fagerholm *et al*., 2009) (Ktistakis *et al*., 2012). Thus, it is possible that in the presence of insulin and amino acids, annexin A5 downregulates copine 1 to maintain low levels of endocytosis.

Overall, annexin A1, annexin A5, and copine 1, emerge as regulators of autophagosome maturation. The identification of other proteins and the specific lipids that interact with them at the cytosolic surface of the endo-lysosomal membranes may help to identify their specific mechanisms, which most probably require Ca^{2+} and phospholipid rearrangements.

References

Axe EL, Walker SA, Manifava M, Chandra P, Roderick HL, Habermann A, Griffiths G, Ktistakis NT (2008) Autophagosome formation from membrane compartments enriched in phosphatidylinositol 3-phosphate and dynamically connected to the endoplasmic reticulum. J Cell Biol 182:685-701.

Babiychuk EB, Monastyrskaya K, Draeger A (2008) Fluorescent annexin A1 reveals dynamics of ceramide platforms in living cells. Traffic 9:1757-1775.

Behrends C, Sowa ME, Gygi SP, Harper JW (2011) Network organization of the human autophagy system. Nature 466:68-76.

Codogno P, Meijer AJ (2005) Autophagy and signaling: their role in cell survival and cell death. Cell Death Differ 12 Suppl 2:1509-1518.

Creutz CE, Edwardson JM (2009) Organization and synergistic binding of copine I and annexin A1 on supported lipid bilayers observed by atomic force microscopy. Biochim Biophys Acta 1788:1950-1961.

Creutz CE, Tomsig JL, Snyder SL, Gautier MC, Skouri F, Beisson J, Cohen J (1998) The copines, a novel class of C2 domain-containing, calcium-dependent, phospholipid-binding proteins conserved from Paramecium to humans. J Biol Chem 273:1393-1402.

Damer CK, Bayeva M, Hahn ES, Rivera J, Socec CI (2005) Copine A, a calcium-dependent membrane-binding protein, transiently localizes to the plasma membrane and intracellular vacuoles in Dictyostelium. BMC Cell Biol 6:46.

Eng KE, Panas MD, Karlsson Hedestam GB, McInerney GM (2010) A novel quantitative flow cytometry-based assay for autophagy. Autophagy 6:634-641.

Esteban I, Aguado C, Sanchez M, Knecht E (2007) Regulation of various proteolytic pathways by insulin and amino acids in human fibroblasts. FEBS Lett 581:3415-3421.

Esteve JM, Armengod ME, Knecht E (2010) BRCA1 negatively regulates formation of autophagic vacuoles in MCF-7 breast cancer cells. Exp Cell Res 316:2618-2629.

Fagerholm S, Ortegren U, Karlsson M, Ruishalme I, Stralfors P (2009) Rapid insulin-dependent endocytosis of the insulin receptor by caveolae in primary adipocytes. PLoS One 4:e5985.

Fuertes G, Villarroya A, Knecht E (2003a) Role of proteasomes in the degradation of short-lived proteins in human fibroblasts under various growth conditions. Int J Biochem Cell Biol 35:651-664.

Fuertes G, Martin De Llano JJ, Villarroya A, Rivett AJ, Knecht E (2003b) Changes in the proteolytic activities of proteasomes and lysosomes in human fibroblasts produced by serum withdrawal, amino-acid deprivation and confluent conditions. Biochem J 375:75-86.

Gerke V, Moss SE (2002) Annexins: from structure to function. Physiol Rev 82:331-371.

Ghislat G, Knecht E (2012a) Ca2+-sensor proteins in the autophagic and endocytic traffic. Curr Protein Pept Sci. *In press.*

Ghislat G, Knecht E (2012b) New Ca2+-dependent regulators of autophagosome maturation. Commun Integr Biol 5.

Ghislat G, Aguado C, Knecht E (2012a) Annexin A5 stimulates autophagy and inhibits endocytosis. J Cell Sci 125:92-107.

Ghislat G, Patron M, Rizzuto R, Knecht E (2012b) Withdrawal of essential amino acids increases autophagy by a pathway involving Ca2+/calmodulin-dependent kinase kinase-beta (CaMKK-beta). J Biol Chem 287:38625-38636.

Hailey DW, Rambold AS, Satpute-Krishnan P, Mitra K, Sougrat R, Kim PK, Lippincott-Schwartz J (2010) Mitochondria supply membranes for autophagosome biogenesis during starvation. Cell 141:656-667.

Hayashi-Nishino M, Fujita N, Noda T, Yamaguchi A, Yoshimori T, Yamamoto A (2009) A subdomain of the endoplasmic reticulum forms a cradle for autophagosome formation. Nat Cell Biol 11:1433-1437.

Kang JH, Li M, Chen X, Yin XM (2011) Proteomics analysis of starved cells revealed Annexin A1 as an important regulator of autophagic degradation. Biochem Biophys Res Commun 407:581-586.

Kawai A, Uchiyama H, Takano S, Nakamura N, Ohkuma S (2007) Autophagosome-lysosome fusion depends on the pH in acidic compartments in CHO cells. Autophagy 3:154-157.

Kimura S, Noda T, Yoshimori T (2007) Dissection of the autophagosome maturation process by a novel reporter protein, tandem fluorescent-tagged LC3. Autophagy 3:452-460.

Klionsky DJ, Cregg JM, Dunn WA, Jr., Emr SD, Sakai Y, Sandoval IV, Sibirny A, Subramani S, Thumm M, Veenhuis M, Ohsumi Y (2003) A unified nomenclature for yeast autophagy-related genes. Dev Cell 5:539-545.

Klionsky DJ, Abeliovich H, Agostinis P, Agrawal DK, Aliev G, Askew DS, Baba M, Baehrecke EH, Bahr BA, Ballabio A, Bamber BA, Bassham DC, Bergamini E, Bi X, Biard-Piechaczyk M, Blum JS, Bredesen DE, Brodsky JL, Brumell JH, Brunk UT, Bursch W, Camougrand N, Cebollero E, Cecconi F, Chen Y, Chin LS, Choi A, Chu CT, Chung J, Clarke PG, Clark RS, Clarke SG, Clave C, Cleveland JL, Codogno P, Colombo MI, Coto-Montes A, Cregg JM, Cuervo AM, Debnath J, Demarchi F, Dennis PB, Dennis PA, Deretic V, Devenish RJ, Di Sano F, Dice JF, Difiglia M, Dinesh-Kumar S, Distelhorst CW, Djavaheri-Mergny M, Dorsey FC, Droge W, Dron M, Dunn WA, Jr., Duszenko M, Eissa NT, Elazar Z, Esclatine A, Eskelinen EL, Fesus L, Finley KD, Fuentes JM, Fueyo J, Fujisaki K, Galliot B, Gao FB, Gewirtz DA, Gibson SB, Gohla A, Goldberg AL, Gonzalez R, Gonzalez-Estevez C, Gorski S, Gottlieb RA, Haussinger D, He YW, Heidenreich K, Hill JA, Hoyer-Hansen M, Hu X, Huang WP, Iwasaki A, Jaattela M, Jackson WT, Jiang X, Jin S, Johansen T, Jung JU, Kadowaki M, Kang C, Kelekar A, Kessel DH, Kiel JA, Kim HP,

Kimchi A, Kinsella TJ, Kiselyov K, Kitamoto K, Knecht E, *et el*. (2008) Guidelines for the use and interpretation of assays for monitoring autophagy in higher eukaryotes. Autophagy 4:151-175.

Knecht E, Aguado C, Carcel J, Esteban I, Esteve JM, Ghislat G, Moruno JF, Vidal JM, Saez R (2009) Intracellular protein degradation in mammalian cells: recent developments. Cell Mol Life Sci 66:2427-2443.

Koga H, Kaushik S, Cuervo AM (2010) Altered lipid content inhibits autophagic vesicular fusion. Faseb J 24:3052-3065.

Ktistakis NT, Manifava M, Schoenfelder P, Rotondo S (2012) How phosphoinositide 3-phosphate controls growth downstream of amino acids and autophagy downstream of amino acid withdrawal. Biochem Soc Trans 40:37-43.

Lavallard VJ, Meijer AJ, Codogno P, Gual P (2012) Autophagy, signaling and obesity. Pharmacol Res 66:513-525.

Levine B, Klionsky DJ (2004) Development by self-digestion: molecular mechanisms and biological functions of autophagy. Dev Cell 6:463-477.

Longatti A, Tooze SA (2012) Recycling endosomes contribute to autophagosome formation. Autophagy 8:1682-1683.

Lum JJ, Bauer DE, Kong M, Harris MH, Li C, Lindsten T, Thompson CB (2005) Growth factor regulation of autophagy and cell survival in the absence of apoptosis. Cell 120:237-248.

Mari M, Griffith J, Rieter E, Krishnappa L, Klionsky DJ, Reggiori F (2010) An Atg9-containing compartment that functions in the early steps of autophagosome biogenesis. J Cell Biol 190:1005-1022.

Mizushima N, Yoshimori T (2007) How to interpret LC3 immunoblotting. Autophagy 3:542-545.

Mizushima N, Yoshimori T, Levine B (2010) Methods in mammalian autophagy research. Cell 140:313-326.

Monastyrskaya K, Babiychuk EB, Draeger A (2009) The annexins: spatial and temporal coordination of signaling events during cellular stress. Cell Mol Life Sci 66:2623-2642.

Monastyrskaya K, Babiychuk EB, Hostettler A, Rescher U, Draeger A (2007) Annexins as intracellular calcium sensors. Cell Calcium 41:207-219.

Moscat J, Diaz-Meco MT (2009) p62 at the crossroads of autophagy, apoptosis, and cancer. Cell 137:1001-1004.

Noda T, Fujita N, Yoshimori T (2009) The late stages of autophagy: how does the end begin? Cell Death Differ 16:984-990.

Nylandsted J, Becker AC, Bunkenborg J, Andersen JS, Dengjel J, Jaattela M (2011) ErbB2-associated changes in the lysosomal proteome. Proteomics 11:2830-2838.

Overbye A, Fengsrud M, Seglen PO (2007) Proteomic analysis of membrane-associated proteins from rat liver autophagosomes. Autophagy 3:300-322.

Pitterle DM, Sperling RT, Myers MG, Jr., White MF, Blackshear PJ (1999) Early biochemical events in insulin-stimulated fluid phase endocytosis. Am J Physiol 276:E94-E105.

Poot M (2001) Analysis of intracellular organelles by flow cytometry or microscopy. Curr Protoc Cytom Chapter 9:Unit 9 4.

Ravikumar B, Moreau K, Jahreiss L, Puri C, Rubinsztein DC (2010) Plasma membrane contributes to the formation of pre-autophagosomal structures. Nat Cell Biol 12:747-757.

Russo-Marie F (1999) Annexin V and phospholipid metabolism. Clin Chem Lab Med 37:287-291.

Saftig P, Klumperman J (2009) Lysosome biogenesis and lysosomal membrane proteins: trafficking meets function. Nat Rev Mol Cell Biol 10:623-635.

Shvets E, Elazar Z (2009) Flow cytometric analysis of autophagy in living mammalian cells. Methods Enzymol 452:131-141.

Tanida I, Minematsu-Ikeguchi N, Ueno T, Kominami E (2005) Lysosomal turnover, but not a cellular level, of endogenous LC3 is a marker for autophagy. Autophagy 1:84-91.

White IJ, Bailey LM, Aghakhani MR, Moss SE, Futter CE (2006) EGF stimulates annexin 1-dependent inward vesiculation in a multivesicular endosome subpopulation. Embo J 25:1-12.

Yamamoto H, Kakuta S, Watanabe TM, Kitamura A, Sekito T, Kondo-Kakuta C, Ichikawa R, Kinjo M, Ohsumi Y (2012) Atg9 vesicles are an important membrane source during early steps of autophagosome formation. J Cell Biol 198:219-233.

Yeung T, Gilbert GE, Shi J, Silvius J, Kapus A, Grinstein S (2008) Membrane phosphatidylserine regulates surface charge and protein localization. Science 319:210-213.

Yla-Anttila P, Vihinen H, Jokitalo E, Eskelinen EL (2009) 3D tomography reveals connections between the phagophore and endoplasmic reticulum. Autophagy 5:1180-1185.

A Supplementary figure

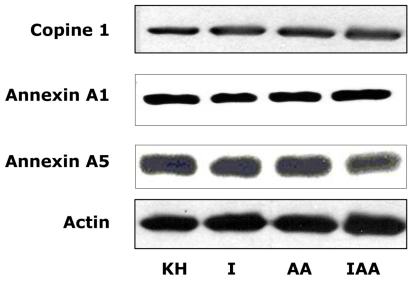

Figure S1. Annexin A1 and copine 1 expressions do not change between high, intermediate and low proteolysis conditions. Extracts from NIH3T3 cells, incubated in KH without (KH) or with insulin (I), amino acids (AA) or both (IAA), were subjected to immunoblotting with annexin A1, copine 1 and actin (as a loading control) antibodies.

8. GENERAL DISCUSSION

How nutrient availability regulates lysosomal catabolism is critical to fully understand this process. Because lysosomes represent the “last station” to receive the cargo destined for degradation *via* several pathways, nutrient sensing is thought to occur in most cases upstream of these organelles.

To the best of our knowledge, the proteomic analysis of lysosomal membranes described here is the first one that has analysed, separately and together, the effects of nutritional (amino acids) and hormonal (insulin) factors. Curiously, amino acids increased or decreased the levels of some proteins at the lysosomal membranes, whereas insulin does not appear to strongly affect the proteome of these membranes. This observation is perhaps related to the intracellular sensing of amino acids, probably positioned in a prelysosomal area, although an amino acid receptor on the plasma membrane was recently reported (Wauson *et al*., 2012) and the sensing of insulin that occurs at the cell surface (Lavallard *et al*., 2012).

The possible functions of the identified proteins in lysosomal degradation were discussed in Chapter 1 of Results on the basis of their biochemical properties and of the effects of amino acids on autophagy (inhibition) and on endocytosis (induction) (Results, Chapter 4). Briefly, the proteins with lower levels on lysosomal membranes in the presence of amino acids were related to the maintenance of lysosomal pH (subunits A, B, C and E of the vacuolar ATPase), Ca^{2+}-dependent binding to lysosomal membranes (annexin A1, annexin A5 and copine 1) and facilitation of vesicle trafficking (α-Soluble N-ethylmaleimide-sensitive factor attachment protein (α-SNAP)). Considering that these properties can stimulate autophagy (Results, Chapter 1), the observed decrease of these proteins on lysosomal membranes in the presence of essential amino acids may be relevant to their well-established inhibition of this process (See Fig. 1).

The proteins with higher levels on lysosomal membranes are either possible inhibitors of autophagy (*e.g.* EF1α) (See Fig. 1) or possible

activators of endocytosis (e.g. BAIAP2) (Results, Chapter 1), indicating that amino acids may inhibit autophagy or induce endocytosis by associating these proteins to the lysosomal membranes.

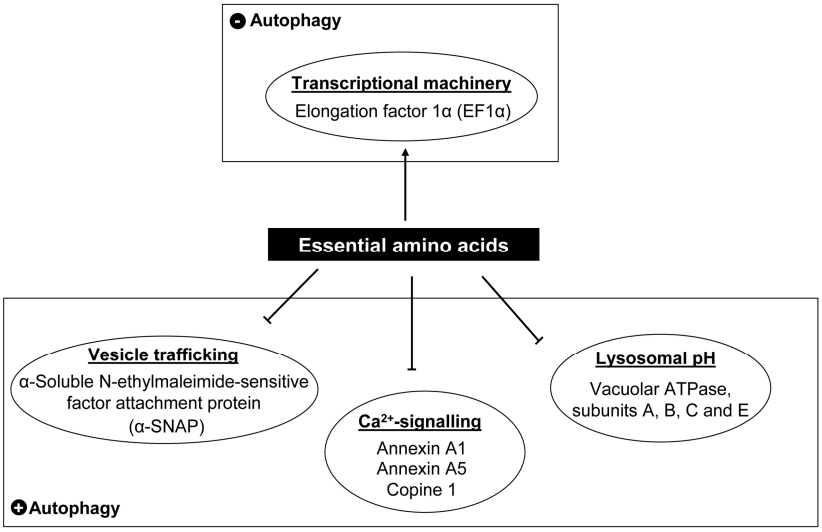

Figure 1. Possible involvement of the proteins indentified in the proteomic analysis of lysosomal membranes in the regulation of autophagy by amino acids. Amino acids decrease (blunted lines) the levels in lysosomal membranes of proteins associated with vesicle trafficking, Ca^{2+}-signalling and lysosomal pH, which may lead to autophagy induction (⊕ Autophagy). The proteins with higher levels in lysosomal membranes when amino acids are added (arrows) are related to the transcriptional machinery. Their possible involvement in the inhibition of autophagy (⊖Autophagy) is indicated. See text for further details.

Among all these proteins, here we have focused on the analysis of the three proteins that bind to phospholipid membranes in a Ca^{2+}-dependent manner, annexin A1, annexin A5 and copine 1. Since their levels on lysosomal membranes increase under withdrawal of amino acids but not of insulin, we analysed the effect of amino acid starvation on: i) intracellular Ca^{2+} levels, and ii) the Ca^{2+}-dependent activation of the major lysosomal degradative pathway, macroautophagy.

Starvation of essential amino acids is a well-known inducer of macroautophagy *via* several signalling pathways, whose detailed molecular

mechanisms are still not fully understood (Knecht *et al*., 2009; Wang and Levine, 2010; Lavallard *et al*., 2012). This is in part due to the diversity of amino acids and to the variety of their metabolisms in different cells (Suryawan *et al*., 1998; Brosnan and Brosnan, 2006; Esteban *et al*., 2007; Kim, 2009). The findings presented in Chapter 2 of Results support that a Ca^{2+}-dependent pathway is operative in autophagy activation under starvation of essential amino acids. This pathway involves the sequence CAMKK-β→AMPK→ULK1 and also mTORC1 signalling.

The rise of cytosolic Ca^{2+} caused by amino acid starvation originates from extracellular and intracellular stores. It is possible that lysosomes are the intracellular store responsible of this Ca^{2+} release, given that Ca^{2+} derived from these organelles is required for their fusion with autophagosomes (Coen *et al*., 2012). In this respect, a release of luminal Ca^{2+} from endolysosomal compartments, and not from other sources, is thought to trigger fusion between their membranes, because cytosolic Ca^{2+} possesses a slow diffusion rate (Pryor *et al.*, 2000; Hay, 2007; Luzio *et al.*, 2007a; Luzio *et al.*, 2007b). Therefore, it is possible that the translocation, to lysosomal membranes, of the three Ca^{2+}-dependent phospholipid binding proteins, involved in autophagosome fusion with lysosomes, annexin A1, annexin A5 and copine 1 (Results, Chapter 3 and 4) requires Ca^{2+} provided from lysosomes.

However, the contribution of other Ca^{2+} sources, such as the ER, which is the most important organelle that supplies Ca^{2+} to the cell, cannot be excluded. This is supported by reports showing that the association of BCL-2 to the ER, which decreases the exit of Ca^{2+} from ER and inhibits autophagy (Chen *et al*., 2004; Palmer *et al*., 2004; Hanson *et al*., 2008; Rong *et al*., 2008), is disrupted under amino acid starvation to induce autophagy (Pattingre *et al*., 2005). Therefore, further investigations are required to insure whether the observed increase of Ca^{2+} from intracellular sources is provided from lysosomes, ER or other organelles.

Another study in HeLa cells showed the opposite results to those shown here, namely that amino acids increase intracellular Ca^{2+} levels (Gulati *et al*., 2008). Because we obtained the same result when the amino acids were added to the medium without adjusting the pH to 7.4 (Results, Appendix to Chapter 2), it is possible that the extracellular pH is crucial for a Ca^{2+} response to cell stimuli (Austin and Wray, 2000; Peracchia, 2004; Pernas-Sueiras *et al*., 2006). Thus, a physiological neutral pH is important for the Ca^{2+}-dependent signalling triggered by amino acid starvation, which leads to the activation of autophagy.

Under amino acid starvation CAMKK-β links the Ca^{2+} signal to AMPK, which inhibits mTORC1. A previous report described the same pathway when intracellular Ca^{2+} levels were raised with pharmacological compounds (Hoyer-Hansen *et al*., 2007). In addition to the finding that amino acid starvation can activate this Ca^{2+}-dependent pathway, we have described here that ULK1 is also involved. This is an important protein in the initiation of autophagy that has been recently reported to be activated by AMPK and inhibited by mTORC1 through multi-site phosphorylation (Egan *et al*., 2011; Kim *et al*., 2011). Under amino acid starvation, ULK1 is activated *via* an increase of AMPK-mediated phosphorylation at Ser-555, and a decrease of mTORC1-mediated phosphorylation at Ser-757. Other AMPK specific phosphorylation sites of ULK1 were also reported, such as Ser-317, Ser-777 (Kim *et al*., 2011), Ser-637 and Ser-467 (Egan *et al*., 2011; Shang *et al*., 2011). Thus, although we have not addressed this point here, it is possible that amino acid starvation also results in ULK1 phosphorylation at these sites.

Fig. 2 summarizes the pathway by which amino acid starvation regulates autophagy *via* Ca^{2+}-mediated activation of AMPK by CAMKK-β.

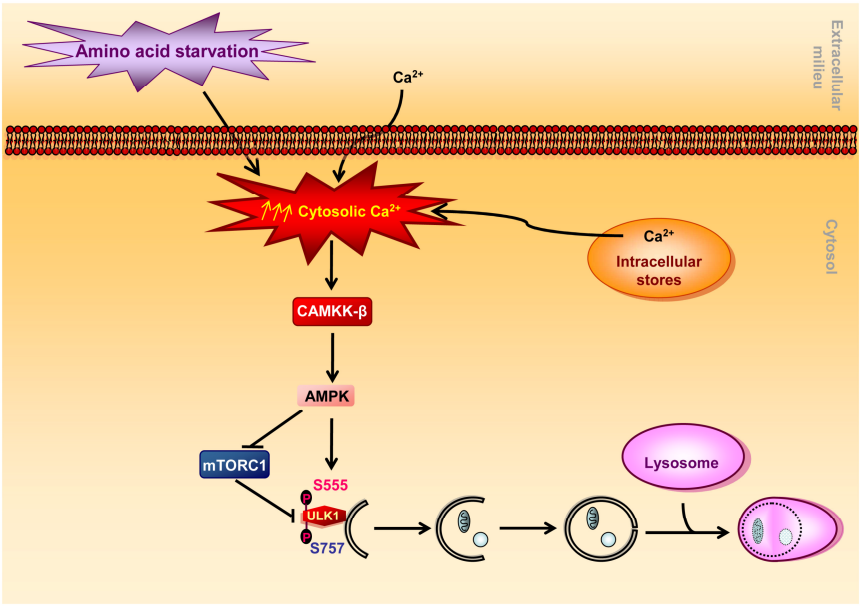

Figure 2. Ca^{2+}-dependent signalling pathway by which amino acid starvation activates autophagy. A rise of cytosolic Ca^{2+}, from both extracellular and intracellular stores, is triggered by amino acid starvation. Subsequently, CAMKK-β activates AMPK that inhibits mTORC1. Finally, ULK1 is positively and negatively regulated by AMPK and mTORC1, respectively, through phosphorylation at two different sites. See text for further details.

It is important to note that the pathway described above is part of a complex signalling network, since autophagy is induced by amino acid starvation through several mechanisms (Wang and Levine, 2010). Our results showed that Ca^{2+} and CAMKK-β are fully required for ULK1 activation, whereas their contribution in autophagy induction by withdrawal of amino acids is only partial. Therefore, apart from this Ca^{2+}-dependent pathway to ULK1, additional pathways that do not require this protein should probably be involved in autophagy activation by amino acid starvation. The regulation of ULK1 by a multisite phosphorylation-dependent mechanism was for the first time reported to occur under serum (Egan *et al*., 2011) and glucose (Kim *et al*., 2011) starvation. In this latter report, AMPK involvement in ULK1 activation by amino acid starvation was shown to be moderate compared to glucose starvation. In our study, there was a good correlation between the activation of AMPK by amino acid starvation and ULK1

phosphorylation at Ser-555, and both of them were fully dependent of CAMKK-β. However, since the knockdown and knockout of AMPK did not fully abolish the autophagy activation produced by starvation of amino acids, it is possible then that autophagy is activated by CAMKK-β in this stress condition *via* AMPK and other kinases. In fact, it has been reported that Ca^{2+} can also induce autophagy by an alternative pathway downstream of CAMKK-β that activates Ca^{2+}/CALMODULIN-dependent protein kinase I (CAMKI) and bypasses AMPK (Pfisterer *et al*., 2011).

Another important output for CAMKK-β-dependent activation of autophagy is the relevance of intracellular Ca^{2+} for mTORC1 inhibition. In the presence of extracellular Ca^{2+}, CAMKK-β seems to be partially involved in the inhibition of mTORC1 mediated by amino acid starvation. However, in the absence of extracellular Ca^{2+}, CAMKK-β becomes fully indispensable. It is then plausible that the Ca^{2+} provided by the extracellular medium contributes to the effect of amino acid starvation on mTORC1 activity independently of the Ca^{2+}→CAMKK-β→AMPK signalling pathway. In contrast, Ca^{2+} provided by intracellular stores acquires an exclusive role in the regulation of mTORC1 by amino acid starvation *via* CAMKK- β.

Overall, Chapter 2 of Results proposes a pathway for the regulation of autophagy by amino acid starvation involving Ca^{2+}, CAMKK-β, AMPK, ULK1, and mTORC1. Thus, intracellular Ca^{2+} levels remain an important signal in the cell response to the availability of amino acids. It would be important to identify the specific amino acids that change intracellular Ca^{2+} levels, as well as the possible existence of an intracellular Ca^{2+}-dependent sensor for them.

From the findings of Chapters 3 and 4 of Results, amino acid starvation appears as a stimulus for the early steps of autophagy and also for the fusion of autophagosomes with lysosomes through the action of the three Ca^{2+}-binding proteins discussed below.

Annexins and Copines are two families of ubiquitous Ca^{2+}-dependent membrane-binding proteins whose intracellular functions are associated with

their ability to attach to specific lipid microdomains. Three proteins of these families, annexin A5, annexin A1 and copine 1 were identified in our proteomic study with lower levels in lysosomal membranes under low proteolysis conditions, caused by the presence of amino acids. Chapters 3 and 4 of Results show the involvement of these three proteins in autophagosome maturation, a later stage in autophagy crucial for autophagic flux (Hayashi-Nishino *et al*., 2009). The model proposed in our study is illustrated in Fig. 3 and the molecular mechanisms by which these proteins may affect this process are discussed below.

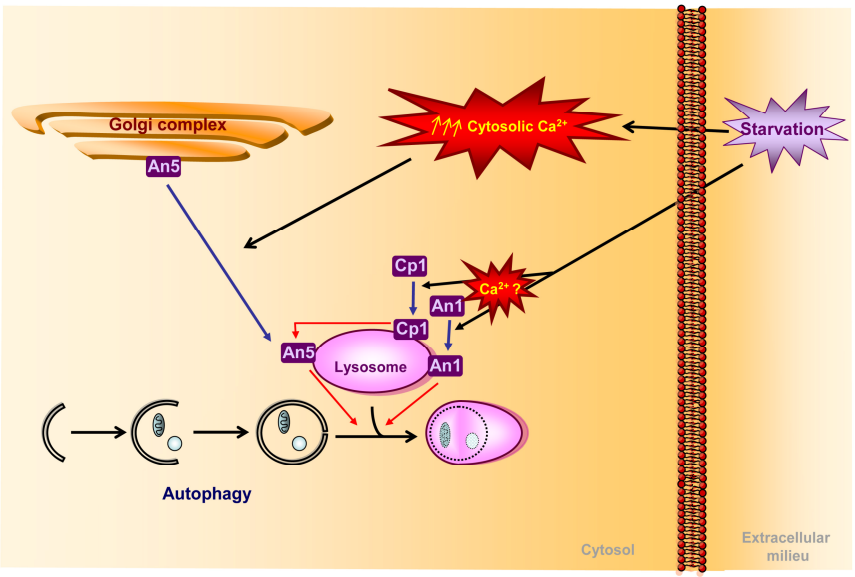

Figure 3. Proposed model by which annexin A5, annexin A1 and copine1 regulate autophagy in starved cells. Starvation induces annexin A5 translocation from Golgi complex to lysosomal membranes in a Ca^{2+}-dependent way. This protein induces autophagosome fusion with lysosomes. Likewise, annexin A1 and copine 1 are localized on lysosomal membranes under starvation and enhance autophagosome fusion with lysosomes. copine1 enhances the effect of annexin A5 in this process. It is likely that, akin to annexin A5, the translocation of annexin A1 and copine 1 to lysosomal membranes occurs in a Ca^{2+}-dependent manner. Blue and red arrows indicate, respectively, the intracellular migration of the three proteins under starvation and their involvement in autophagosome maturation. See text for further details.

Chapters 3 and 4 of Results indicate that starvation provokes the translocation of annexin A1, annexin A5 and copine 1 to lysosomal membranes. This may be due to the rise of intracellular Ca^{2+} levels observed

under amino acids starvation (Results, Chapter 2), since these three proteins share the property of binding to phospholipid membranes in a Ca^{2+}-dependent manner (Creutz *et al*., 1998; Monastyrskaya *et al*., 2009) and annexin A5 translocates to lysosomal membranes under starvation in a Ca^{2+}-dependent way (Results, Chapter 3). Given that insulin does not decrease intracellular Ca^{2+} levels (Results, Chapter 2), this could explain why, in contrast to amino acids, insulin does not reduce the binding of annexin A1, annexin A5 and copine 1 to lysosomal membranes in the proteomic analysis.

Mounting evidences support that, in spite of their lack of transmembrane domains, various members of the annexin family can induce membrane fusions. In fact, several studies (reviewed in (Monastyrskaya *et al*., 2009)) described a Ca^{2+}-dependent role of some of these proteins in the traffic of specific endo-lysosomal compartments. Moreover, annexin A1 was previously associated to early endosomes and multivesicular bodies and annexin A5 to late endosomes (Monastyrskaya *et al*., 2009). These two annexins may be involved then in Ca^{2+}-regulated interactions of the autophagosomal and endolysosomal membranes that finally lead to their fusion and to the delivery of the autophagosomal content to the lysosome.

Annexin A5 was previously reported to induce the *in vitro* fusion and aggregation of vesicles in a Ca^{2+}-dependent manner (Hoekstra *et al*., 1993). Moreover, the Ca^{2+}-dependent binding of annexin A5 to membranes increases when they are enriched in cholesterol (Ayala-Sanmartin, 2001). Since the levels of this lipid on lysosomal membranes seem to be important for the fusion of autophagosomes with lysosomes (Koga *et al*., 2010), annexin A5 could induce autophagosome–lysosome fusion through cholesterol-rich domains in their membranes in a Ca^{2+}-dependent way. In contrast, cholesterol has been reported to inhibit autophagosome formation (Zhang *et al.*, 2013). Therefore, it is possible that cholesterol exerts different roles in early and late steps of autophagy.

Moreover, we found that whereas annexin A5 knockdown inhibits autophagosome fusion with lysosomes, it enhances in contrast the formation of amphisomes, organelles produced by autophagosome fusion with late endosomes. This may facilitate the degradation of the autophagic cargo, but only to some extent, since these hybrid organelles do not degrade it as efficiently as autolysosomes. In fact, previous reports have shown increased accumulation of amphisomes when fusion between autophagosomes and lysosomes is compromised (Eskelinen *et al*., 2002; Massey *et al*., 2008; Koga *et al*., 2010). This is consistent with the enhanced endocytic activity observed under annexin A5 knockdown, that we will discuss later. If this is so, an obvious question is how annexin A5 negatively regulates the fusion of autophagosomes with late endosomes while promoting their fusion with lysosomes. In this regard, it has been suggested that the fusion of autophagosomes with lysosomes or endosomes is distinctly governed, because they require different nucleotides (Koga *et al*., 2010). Thus, annexin A5 could differentially affect the fusion of these organelles, through different mechanisms.

Somewhat related to our finding concerning annexin A1 association to lysosomal membranes and its involvement in autophagosome maturation, other authors have reported additional results. A small dimeric Ca^{2+}-binding protein that can form a complex with annexin A1, S100A11, was also identified as a component of lysosomal membranes (Nylandsted *et al*., 2011) and annexin A1 was found, in another study, to induce autophagy by an unidentified mechanism but possibly by promoting amphisome formation (Kang *et al*., 2011). Also and interestingly, an autophagy related protein, ATG4B, was identified as a putative interactor of annexin A1 in preliminary maps of autophagy interaction network (Behrends *et al*., 2011). This protease participates in the lipidation and delipidation of LC3 (Nakatogawa *et al*., 2007). Therefore, it is tempting to speculate that annexin A1 regulates, through its interaction, the activity of ATG4B on LC3 lipidation and delipidation. However, the interaction between these two proteins should be

validated by other experimental approaches and whether this occurs when it is localized at the lysosomal membranes under conditions of amino acid starvation remains to be verified. In relationship with copine 1, its presence in autophagosomal, phagosomal and lysosomal delimiting membranes, has been previously reported (Damer *et al*., 2005; Overbye *et al*., 2007). In agreement with our results, in *Dictyostelium* and under starvation this protein transiently localizes to the membranes of intracellular vacuoles (Damer *et al*., 2005).

Interestingly, an *in vitro* study showed that annexin A1 creates membrane domains enriched in phosphatidylserine that assemble copine 1 aggregates. This provides a possible scaffold to cluster signalling proteins in the presence of Ca^{2+} (Creutz and Edwardson, 2009). It is likely then, that annexin A1 forms suitable domains for copine 1 recruitment, after its translocation under high proteolysis conditions from cytosol to lysosomal membranes. Also, annexin A5 is known to bind with high specificity to phosphatidylserine (Gerke and Moss, 2002). This lipid is known to be distributed in all cellular membranes, but it only confers a negative charge (ideal for Ca^{2+} binding) at the cytosolic face of late endosomes, lysosomes and plasma membranes. In other organelles, such as mitochondria, endoplasmic reticulum and Golgi, phosphatidylserine is mainly localized in the luminal leaflets of their membranes (Yeung *et al*., 2008). Since we found that starvation causes the translocation of annexin A5 to lysosomal and late endosomal membranes (Results, Chapter 3), it is possible that this protein together with annexin A1, form phosphatidylserine enriched domains at lysosomal membranes, suitable for copine 1 recruitment which could somehow facilitate the fusion of lysosomes with autophagosomes. Since annexin A5 levels are higher than those of annexin A1, at least in our experimental model (NIH3T3 and HEK293 cells), annexin A5 may easily substitute annexin A1, when this latter is silenced. This may explain why a higher inhibition of autophagy occurs under copine 1/annexin A5 co-silencing than under copine 1/annexin A1 co-silencing (Results, Chapter 4).

In summary, our findings indicate new functions for annexin A1, annexin A5 and copine 1 in autophagy. As they seem to act in the delivery of autophagosomes to lysosomes and all of them translocate to lysosomal membranes under conditions of high autophagic activity, these proteins emerge as possible Ca^{2+}-sensors for the fusion between autophagosomal and lysosomal membranes. In contrast to autophagy, our findings conferred opposite roles for annexin A5 and copine 1 in endocytosis. As for the role of annexin A1 in this process, its participation in the formation of multivesicular bodies was extensively studied before (reviewed in (Futter and White, 2007)). Therefore we have concentrated here only on the role of annexin A5 and copine 1 in endocytosis.

In Chapter 4 of Results, and in contrast to annexin A5 (Results, Chapter 2), we showed for the first time an involvement of copine 1 in endocytosis in mammalian cells. A previous report showed that the knockout of copine A, a copine 1 homolog in *Dictyostelium*, does not affect endocytosis (Damer *et al*., 2007). By contrast, we found that annexin A5 inhibits endocytosis. The localization of annexin A5 in late endosomes in considerably higher amounts than in early endosomes suggests that the inhibition of endocytosis probably occurs at late steps of this process. The opposite roles of copine 1 and annexin A5 in endocytosis is possibly associated with the upregulation of copine 1 under annexin A5 silencing, since this occurs in the presence of full nutrient conditions, where we observed an increased endocytic uptake. In fact, an earlier study showed that insulin stimulates fluid phase endocytosis and that this requires the insulin receptor, the insulin receptor substrate-1 and Class I phosphatidylinositol 3-kinase (Pitterle *et al*., 1999). A more recent report demonstrated that upon insulin stimulation, the autophosphorylated insulin receptor in primary adipocytes is rapidly endocytosed in a caveolae-mediated process (Fagerholm *et al*., 2009). Amino acids were also reported

to positively regulate endocytosis. Their presence was shown to activate the Class III phosphatidylinositol 3-kinase complex II involved in endoytosis whereas their removal activates the Class III phosphatidylinositol 3-kinase complex I involved in autophagy (Ktistakis *et al*., 2012). Thus, it is conceivable that insulin and amino acids play opposite roles in autophagy and endocytosis. Our findings suggest that annexin A5 maintains low levels of copine 1 in order to control the endocytic activity of the cell. However, further work is required to determine how annexin A5 controls the levels of copine 1 and by which mechanism this process may affect endocytosis.

Taken as a whole, annexin A1, annexin A5, and copine 1 emerge as regulators of autophagosome maturation, possibly by mechanisms that require Ca^{2+} and phospholipid rearrangements. To determine which of the proposed molecular mechanism are involved in this process, it will be necessary to identify other proteins and, perhaps more important, the specific lipids that interact with annexin A1 and annexin A5 and also with copine 1 at the cytosolic surface of the endo-lysosomal membranes. Whether these interactions produce phospholipid rearrangements at specific lipid domains on lysosomal membranes remains to be elucidated. In particular, it would be interesting to compare the protein and lipid interactors of copine 1 and annexin A5 in order to understand their opposite roles on endocytic uptake.

9. CONCLUSIONS

Conclusions 1:

- Starvation of amino acids produces a rise of intracellular Ca^{2+} levels and induces autophagosome formation in a Ca^{2+}-dependent way.
- The rise of intracellular Ca^{2+} triggered by amino acid starvation activates autophagy by the following signalling pathway:

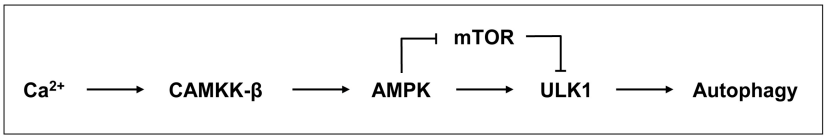

Conclusions 2:

- Annexin A1, annexin A5 and copine 1 migrate to lysosomal membranes under starvation. At least in the case of annexin A5, this translocation is Ca^{2+}-dependent.
- Annexin A1, copine 1 and mainly annexin A5 promote autophagosome fusion with lysosomes.
- Annexin A5 and copine 1 are, respectively, negative and positive regulators of endocytosis.

10. REFERENCES

Adler EM, Augustine GJ, Duffy SN, Charlton MP (1991) Alien intracellular calcium chelators attenuate neurotransmitter release at the squid giant synapse. J Neurosci 11:1496-1507.

Axe EL, Walker SA, Manifava M, Chandra P, Roderick HL, Habermann A, Griffiths G, Ktistakis NT (2008) Autophagosome formation from membrane compartments enriched in phosphatidylinositol 3-phosphate and dynamically connected to the endoplasmic reticulum. J Cell Biol 182:685-701.

Ayala-Sanmartin J, Vincent M, Sopkova J, Gallay J (2000) Modulation by Ca(2+) and by membrane binding of the dynamics of domain III of annexin 2 (p36) and the annexin 2-p11 complex (p90): implications for their biochemical properties. Biochemistry 39:15179-15189.

Babiychuk EB, Draeger A (2000) Annexins in cell membrane dynamics. Ca(2+)-regulated association of lipid microdomains. J Cell Biol 150:1113-1124.

Babiychuk EB, Monastyrskaya K, Draeger A (2008) Fluorescent annexin A1 reveals dynamics of ceramide platforms in living cells. Traffic 9:1757-1775.

Babiychuk VS, Draeger A, Babiychuk EB (2000) Smooth muscle actomyosin promotes Ca2+-dependent interactions between annexin VI and detergent-insoluble glycosphingolipid-enriched membrane domains. Acta Biochim Pol 47:579-589.

Balaban RS (2009) The role of Ca(2+) signaling in the coordination of mitochondrial ATP production with cardiac work. Biochim Biophys Acta 1787:1334-1341.

Bargal R, Cormier-Daire V, Ben-Neriah Z, Le Merrer M, Sosna J, Melki J, Zangen DH, Smithson SF, Borochowitz Z, Belostotsky R, Raas-Rothschild A (2009) Mutations in DDR2 gene cause SMED with short limbs and abnormal calcifications. Am J Hum Genet 84:80-84.

Barwise JL, Walker JH (1996) Annexins II, IV, V and VI relocate in response to rises in intracellular calcium in human foreskin fibroblasts. J Cell Sci 109 (Pt 1):247-255.

Beck A, Kolisek M, Bagley LA, Fleig A, Penner R (2006) Nicotinic acid adenine dinucleotide phosphate and cyclic ADP-ribose regulate TRPM2 channels in T lymphocytes. FASEB J 20:962-964.

Bernales S, Papa FR, Walter P (2006) Intracellular signaling by the unfolded protein response. Annu Rev Cell Dev Biol 22:487-508.

Berridge MJ (2002) The endoplasmic reticulum: a multifunctional signaling organelle. Cell Calcium 32:235-249.

Berridge MJ, Bootman MD, Roderick HL (2003) Calcium signalling: dynamics, homeostasis and remodelling. Nat Rev Mol Cell Biol 4:517-529.

Bilmen JG, Wootton LL, Godfrey RE, Smart OS, Michelangeli F (2002) Inhibition of SERCA Ca2+ pumps by 2-aminoethoxydiphenyl borate (2-APB). 2-APB reduces both Ca2+ binding and phosphoryl transfer

from ATP, by interfering with the pathway leading to the Ca2+-binding sites. Eur J Biochem 269:3678-3687.

Bode G, Luken A, Kerkhoff C, Roth J, Ludwig S, Nacken W (2008) Interaction between S100A8/A9 and annexin A6 is involved in the calcium-induced cell surface exposition of S100A8/A9. J Biol Chem 283:31776-31784.

Bonfils G, Jaquenoud M, Bontron S, Ostrowicz C, Ungermann C, De Virgilio C (2012) Leucyl-tRNA synthetase controls TORC1 via the EGO complex. Mol Cell 46:105-110.

Bouter A, Gounou C, Berat R, Tan S, Gallois B, Granier T, d'Estaintot BL, Poschl E, Brachvogel B, Brisson AR (2011) Annexin-A5 assembled into two-dimensional arrays promotes cell membrane repair. Nat Commun 2:270.

Brailoiu E, Churamani D, Cai X, Schrlau MG, Brailoiu GC, Gao X, Hooper R, Boulware MJ, Dun NJ, Marchant JS, Patel S (2009) Essential requirement for two-pore channel 1 in NAADP-mediated calcium signaling. J Cell Biol 186:201-209.

Brandt I, De Vriendt K, Devreese B, Van Beeumen J, Van Dongen W, Augustyns K, De Meester I, Scharpe S, Lambeir AM (2005) Search for substrates for prolyl oligopeptidase in porcine brain. Peptides 26:2536-2546.

Bultynck G, Vermassen E, Szlufcik K, De Smet P, Fissore RA, Callewaert G, Missiaen L, De Smedt H, Parys JB (2003) Calcineurin and intracellular Ca2+-release channels: regulation or association? Biochem Biophys Res Commun 311:1181-1193.

Burgoyne RD, Clague MJ (2003) Calcium and calmodulin in membrane fusion. Biochim Biophys Acta 1641:137-143.

Buser CA, Kim J, McLaughlin S, Peitzsch RM (1995) Does the binding of clusters of basic residues to acidic lipids induce domain formation in membranes? Mol Membr Biol 12:69-75.

Butsushita K, Fukuoka S, Ida K, Arii Y (2009) Crystal structures of sodium-bound annexin A4. Biosci Biotechnol Biochem 73:2274-2280.

Byfield MP, Murray JT, Backer JM (2005) hVps34 is a nutrient-regulated lipid kinase required for activation of p70 S6 kinase. J Biol Chem 280:33076-33082.

Calcraft PJ, Ruas M, Pan Z, Cheng X, Arredouani A, Hao X, Tang J, Rietdorf K, Teboul L, Chuang KT, Lin P, Xiao R, Wang C, Zhu Y, Lin Y, Wyatt CN, Parrington J, Ma J, Evans AM, Galione A, Zhu MX (2009) NAADP mobilizes calcium from acidic organelles through two-pore channels. Nature 459:596-600.

Camors E, Monceau V, Charlemagne D (2005) Annexins and Ca2+ handling in the heart. Cardiovasc Res 65:793-802.

Cantiello HF, Montalbetti N, Goldmann WH, Raychowdhury MK, Gonzalez-Perrett S, Timpanaro GA, Chasan B (2005) Cation channel activity of mucolipin-1: the effect of calcium. Pflugers Arch 451:304-312.

Cardenas C, Miller RA, Smith I, Bui T, Molgo J, Muller M, Vais H, Cheung KH, Yang J, Parker I, Thompson CB, Birnbaum MJ, Hallows KR, Foskett JK (2010) Essential regulation of cell bioenergetics by constitutive InsP3 receptor Ca2+ transfer to mitochondria. Cell 142:270-283.

Cereghetti GM, Stangherlin A, Martins de Brito O, Chang CR, Blackstone C, Bernardi P, Scorrano L (2008) Dephosphorylation by calcineurin regulates translocation of Drp1 to mitochondria. Proc Natl Acad Sci U S A 105:15803-15808.

Chang NC, Nguyen M, Germain M, Shore GC (2010) Antagonism of Beclin 1-dependent autophagy by BCL-2 at the endoplasmic reticulum requires NAF-1. Embo J 29:606-618.

Chasserot-Golaz S, Vitale N, Sagot I, Delouche B, Dirrig S, Pradel LA, Henry JP, Aunis D, Bader MF (1996) Annexin II in exocytosis: catecholamine secretion requires the translocation of p36 to the subplasmalemmal region in chromaffin cells. J Cell Biol 133:1217-1236.

Chen R, Valencia I, Zhong F, McColl KS, Roderick HL, Bootman MD, Berridge MJ, Conway SJ, Holmes AB, Mignery GA, Velez P, Distelhorst CW (2004) Bcl-2 functionally interacts with inositol 1,4,5-trisphosphate receptors to regulate calcium release from the ER in response to inositol 1,4,5-trisphosphate. J Cell Biol 166:193-203.

Cho W, Stahelin RV (2006) Membrane binding and subcellular targeting of C2 domains. Biochim Biophys Acta 1761:838-849.

Churchill GC, Okada Y, Thomas JM, Genazzani AA, Patel S, Galione A (2002) NAADP mobilizes Ca(2+) from reserve granules, lysosome-related organelles, in sea urchin eggs. Cell 111:703-708.

Colombo MI, Beron W, Stahl PD (1997) Calmodulin regulates endosome fusion. J Biol Chem 272:7707-7712.

Concha NO, Head JF, Kaetzel MA, Dedman JR, Seaton BA (1993) Rat annexin V crystal structure: Ca(2+)-induced conformational changes. Science 261:1321-1324.

Copetti T, Bertoli C, Dalla E, Demarchi F, Schneider C (2009) p65/RelA modulates BECN1 transcription and autophagy. Mol Cell Biol 29:2594-2608.

Creutz CE, Sterner DC (1983) Calcium dependence of the binding of synexin to isolated chromaffin granules. Biochem Biophys Res Commun 114:355-364.

Creutz CE, Snyder SL (2005) Interactions of annexins with the mu subunits of the clathrin assembly proteins. Biochemistry 44:13795-13806.

Creutz CE, Edwardson JM (2009) Organization and synergistic binding of copine I and annexin A1 on supported lipid bilayers observed by atomic force microscopy. Biochim Biophys Acta 1788:1950-1961.

Creutz CE, Pazoles CJ, Pollard HB (1978) Identification and purification of an adrenal medullary protein (synexin) that causes calcium-

dependent aggregation of isolated chromaffin granules. J Biol Chem 253:2858-2866.

Creutz CE, Tomsig JL, Snyder SL, Gautier MC, Skouri F, Beisson J, Cohen J (1998) The copines, a novel class of C2 domain-containing, calcium-dependent, phospholipid-binding proteins conserved from Paramecium to humans. J Biol Chem 273:1393-1402.

Criollo A, Maiuri MC, Tasdemir E, Vitale I, Fiebig AA, Andrews D, Molgo J, Diaz J, Lavandero S, Harper F, Pierron G, di Stefano D, Rizzuto R, Szabadkai G, Kroemer G (2007) Regulation of autophagy by the inositol trisphosphate receptor. Cell Death Differ 14:1029-1039.

Crompton MR, Moss SE, Crumpton MJ (1988) Diversity in the lipocortin/calpactin family. Cell 55:1-3.

Cubells L, Vila de Muga S, Tebar F, Wood P, Evans R, Ingelmo-Torres M, Calvo M, Gaus K, Pol A, Grewal T, Enrich C (2007) Annexin A6-induced alterations in cholesterol transport and caveolin export from the Golgi complex. Traffic 8:1568-1589.

Cuervo AM (2010a) Chaperone-mediated autophagy: selectivity pays off. Trends Endocrinol Metab 21:142-150.

Cuervo AM (2010b) The plasma membrane brings autophagosomes to life. Nat Cell Biol 12:735-737.

Damer CK, Bayeva M, Hahn ES, Rivera J, Socec CI (2005) Copine A, a calcium-dependent membrane-binding protein, transiently localizes to the plasma membrane and intracellular vacuoles in Dictyostelium. BMC Cell Biol 6:46.

De Duve C, Wattiaux R (1966) Functions of lysosomes. Annu Rev Physiol 28:435-492.

De Duve C, Pressman BC, Gianetto R, Wattiaux R, Appelmans F (1955) Tissue fractionation studies. 6. Intracellular distribution patterns of enzymes in rat-liver tissue. Biochem J 60:604-617.

De Haro L, Quetglas S, Iborra C, Leveque C, Seagar M (2003) Calmodulin-dependent regulation of a lipid binding domain in the v-SNARE synaptobrevin and its role in vesicular fusion. Biol Cell 95:459-464.

Decuypere JP, Monaco G, Bultynck G, Missiaen L, De Smedt H, Parys JB (2010) The IP(3) receptor-mitochondria connection in apoptosis and autophagy. Biochim Biophys Acta 1813:1003-1013.

Decuypere JP, Welkenhuyzen K, Luyten T, Ponsaerts R, Dewaele M, Molgo J, Agostinis P, Missiaen L, De Smedt H, Parys JB, Bultynck G (2011) IP 3 receptor-mediated Ca (2+) signaling and autophagy induction are interrelated. Autophagy 7:1472-1489.

Denisov G, Wanaski S, Luan P, Glaser M, McLaughlin S (1998) Binding of basic peptides to membranes produces lateral domains enriched in the acidic lipids phosphatidylserine and phosphatidylinositol 4,5-bisphosphate: an electrostatic model and experimental results. Biophys J 74:731-744.

Diakonova M, Gerke V, Ernst J, Liautard JP, van der Vusse G, Griffiths G (1997) Localization of five annexins in J774 macrophages and on isolated phagosomes. J Cell Sci 110 (Pt 10):1199-1213.

Diwan A, Matkovich SJ, Yuan Q, Zhao W, Yatani A, Brown JH, Molkentin JD, Kranias EG, Dorn GW, 2nd (2009) Endoplasmic reticulum-mitochondria crosstalk in NIX-mediated murine cell death. J Clin Invest 119:203-212.

Dode L, Andersen JP, Vanoevelen J, Raeymaekers L, Missiaen L, Vilsen B, Wuytack F (2006) Dissection of the functional differences between human secretory pathway Ca2+/Mn2+-ATPase (SPCA) 1 and 2 isoenzymes by steady-state and transient kinetic analyses. J Biol Chem 281:3182-3189.

Doherty GJ, McMahon HT (2009) Mechanisms of endocytosis. Annu Rev Biochem 78:857-902.

Dong XP, Shen D, Wang X, Dawson T, Li X, Zhang Q, Cheng X, Zhang Y, Weisman LS, Delling M, Xu H (2010) PI(3,5)P(2) controls membrane trafficking by direct activation of mucolipin Ca(2+) release channels in the endolysosome. Nat Commun 1:38.

Draeger A, Wray S, Babiychuk EB (2005) Domain architecture of the smooth-muscle plasma membrane: regulation by annexins. Biochem J 387:309-314.

Dubois T, Mira JP, Feliers D, Solito E, Russo-Marie F, Oudinet JP (1998) Annexin V inhibits protein kinase C activity via a mechanism of phospholipid sequestration. Biochem J 330 (Pt 3):1277-1282.

Duchen MR (2004) Mitochondria in health and disease: perspectives on a new mitochondrial biology. Mol Aspects Med 25:365-451.

Elmore SP, Qian T, Grissom SF, Lemasters JJ (2001) The mitochondrial permeability transition initiates autophagy in rat hepatocytes. FASEB J 15:2286-2287.

Emans N, Gorvel JP, Walter C, Gerke V, Kellner R, Griffiths G, Gruenberg J (1993) Annexin II is a major component of fusogenic endosomal vesicles. J Cell Biol 120:1357-1369.

Ernst JD, Hoye E, Blackwood RA, Jaye D (1990) Purification and characterization of an abundant cytosolic protein from human neutrophils that promotes Ca2(+)-dependent aggregation of isolated specific granules. J Clin Invest 85:1065-1071.

Esteban I, Aguado C, Sanchez M, Knecht E (2007) Regulation of various proteolytic pathways by insulin and amino acids in human fibroblasts. FEBS Lett 581:3415-3421.

Fader CM, Colombo MI (2009) Autophagy and multivesicular bodies: two closely related partners. Cell Death Differ 16:70-78.

Favier-Perron B, Lewit-Bentley A, Russo-Marie F (1996) The high-resolution crystal structure of human annexin III shows subtle differences with annexin V. Biochemistry 35:1740-1744.

Feng W, Huang S, Wu H, Zhang M (2007) Molecular basis of Bcl-xL's target recognition versatility revealed by the structure of Bcl-xL in complex with the BH3 domain of Beclin-1. J Mol Biol 372:223-235.

Furge LL, Chen K, Cohen S (1999) Annexin VII and annexin XI are tyrosine phosphorylated in peroxovanadate-treated dogs and in platelet-derived growth factor-treated rat vascular smooth muscle cells. J Biol Chem 274:33504-33509.

Futter CE, White IJ (2007) Annexins and endocytosis. Traffic 8:951-958.

Galione A, Morgan AJ, Arredouani A, Davis LC, Rietdorf K, Ruas M, Parrington J (2010) NAADP as an intracellular messenger regulating lysosomal calcium-release channels. Biochem Soc Trans 38:1424-1431.

Ganley IG, Wong PM, Gammoh N, Jiang X (2011) Distinct autophagosomal-lysosomal fusion mechanism revealed by thapsigargin-induced autophagy arrest. Mol Cell 42:731-743.

Gao W, Ding WX, Stolz DB, Yin XM (2008) Induction of macroautophagy by exogenously introduced calcium. Autophagy 4:754-761.

Geng D, Chura J, Roberts MF (1998) Activation of phospholipase D by phosphatidic acid. Enhanced vesicle binding, phosphatidic acid-Ca2+ interaction, or an allosteric effect? J Biol Chem 273:12195-12202.

Gerelsaikhan T, Vasa PK, Chander A (2012) Annexin A7 and SNAP23 interactions in alveolar type II cells and in vitro: A role for Ca(2+) and PKC. Biochim Biophys Acta 1823:1796-1806.

Gerke V (2001) Annexins And Membrane Organisation In The Endocytic Pathway. Cell Mol Biol Lett 6:204.

Gerke V, Moss SE (2002) Annexins: from structure to function. Physiol Rev 82:331-371.

Gerke V, Creutz CE, Moss SE (2005) Annexins: linking Ca2+ signalling to membrane dynamics. Nat Rev Mol Cell Biol 6:449-461.

Giambanco I, Verzini M, Donato R (1993) Annexins V and VI in rat tissues during post-natal development: immunochemical measurements. Biochem Biophys Res Commun 196:1221-1226.

Goebeler V, Ruhe D, Gerke V, Rescher U (2003) Atypical properties displayed by annexin A9, a novel member of the annexin family of Ca(2+) and lipid binding proteins. FEBS Lett 546:359-364.

Goebeler V, Poeter M, Zeuschner D, Gerke V, Rescher U (2008) Annexin A8 regulates late endosome organization and function. Mol Biol Cell 19:5267-5278.

Gordon PB, Holen I, Fosse M, Rotnes JS, Seglen PO (1993) Dependence of hepatocytic autophagy on intracellularly sequestered calcium. J Biol Chem 268:26107-26112.

Grewal T, Heeren J, Mewawala D, Schnitgerhans T, Wendt D, Salomon G, Enrich C, Beisiegel U, Jackle S (2000) Annexin VI stimulates endocytosis and is involved in the trafficking of low density

lipoprotein to the prelysosomal compartment. J Biol Chem 275:33806-33813.

Grimm C, Hassan S, Wahl-Schott C, Biel M (2012) Role of TRPML and Two-Pore Channels in Endolysosomal Cation Homeostasis. J Pharmacol Exp Ther 342:236-244.

Grimm C, Cuajungco MP, van Aken AF, Schnee M, Jors S, Kros CJ, Ricci AJ, Heller S (2007) A helix-breaking mutation in TRPML3 leads to constitutive activity underlying deafness in the varitint-waddler mouse. Proc Natl Acad Sci U S A 104:19583-19588.

Grotemeier A, Alers S, Pfisterer SG, Paasch F, Daubrawa M, Dieterle A, Viollet B, Wesselborg S, Proikas-Cezanne T, Stork B (2010) AMPK-independent induction of autophagy by cytosolic Ca2+ increase. Cell Signal 22:914-925.

Gurusamy N, Lekli I, Mukherjee S, Ray D, Ahsan MK, Gherghiceanu M, Popescu LM, Das DK (2010) Cardioprotection by resveratrol: a novel mechanism via autophagy involving the mTORC2 pathway. Cardiovasc Res 86:103-112.

Gwinn DM, Shackelford DB, Egan DF, Mihaylova MM, Mery A, Vasquez DS, Turk BE, Shaw RJ (2008) AMPK phosphorylation of raptor mediates a metabolic checkpoint. Mol Cell 30:214-226.

Hailey DW, Rambold AS, Satpute-Krishnan P, Mitra K, Sougrat R, Kim PK, Lippincott-Schwartz J (2010) Mitochondria supply membranes for autophagosome biogenesis during starvation. Cell 141:656-667.

Han JM, Jeong SJ, Park MC, Kim G, Kwon NH, Kim HK, Ha SH, Ryu SH, Kim S (2012) Leucyl-tRNA synthetase is an intracellular leucine sensor for the mTORC1-signaling pathway. Cell 149:410-424.

Hanson CJ, Bootman MD, Distelhorst CW, Wojcikiewicz RJ, Roderick HL (2008) Bcl-2 suppresses Ca2+ release through inositol 1,4,5-trisphosphate receptors and inhibits Ca2+ uptake by mitochondria without affecting ER calcium store content. Cell Calcium 44:324-338.

Harashima M, Harada K, Ito Y, Hyuga M, Seki T, Ariga T, Yamaguchi T, Niimi S (2008) Annexin A3 expression increases in hepatocytes and is regulated by hepatocyte growth factor in rat liver regeneration. J Biochem 143:537-545.

Harr MW, McColl KS, Zhong F, Molitoris JK, Distelhorst CW (2010) Glucocorticoids downregulate Fyn and inhibit IP(3)-mediated calcium signaling to promote autophagy in T lymphocytes. Autophagy 6:912-921.

Hay JC (2007) Calcium: a fundamental regulator of intracellular membrane fusion? EMBO Rep 8:236-240.

Hayashi-Nishino M, Fujita N, Noda T, Yamaguchi A, Yoshimori T, Yamamoto A (2009) A subdomain of the endoplasmic reticulum forms a cradle for autophagosome formation. Nat Cell Biol 11:1433-1437.

Hayes MJ, Rescher U, Gerke V, Moss SE (2004) Annexin-actin interactions. Traffic 5:571-576.

Hazarika P, Sheldon A, Kaetzel MA, Diaz-Munoz M, Hamilton SL, Dedman JR (1991a) Regulation of the sarcoplasmic reticulum Ca(2+)-release channel requires intact annexin VI. J Cell Biochem 46:86-93.

Hazarika P, Kaetzel MA, Sheldon A, Karin NJ, Fleischer S, Nelson TE, Dedman JR (1991b) Annexin VI is associated with calcium-sequestering organelles. J Cell Biochem 46:78-85.

Hoekstra D, Buist-Arkema R, Klappe K, Reutelingsperger CP (1993) Interaction of annexins with membranes: the N-terminus as a governing parameter as revealed with a chimeric annexin. Biochemistry 32:14194-14202.

Holroyd C, Kistner U, Annaert W, Jahn R (1999) Fusion of endosomes involved in synaptic vesicle recycling. Mol Biol Cell 10:3035-3044.

Hoyer-Hansen M, Jaattela M (2007) Connecting endoplasmic reticulum stress to autophagy by unfolded protein response and calcium. Cell Death Differ 14:1576-1582.

Hoyer-Hansen M, Bastholm L, Szyniarowski P, Campanella M, Szabadkai G, Farkas T, Bianchi K, Fehrenbacher N, Elling F, Rizzuto R, Mathiasen IS, Jaattela M (2007) Control of macroautophagy by calcium, calmodulin-dependent kinase kinase-beta, and Bcl-2. Mol Cell 25:193-205.

Huang KS, Wallner BP, Mattaliano RJ, Tizard R, Burne C, Frey A, Hession C, McGray P, Sinclair LK, Chow EP, et al. (1986) Two human 35 kd inhibitors of phospholipase A2 are related to substrates of pp60v-src and of the epidermal growth factor receptor/kinase. Cell 46:191-199.

Huber LA, Fialka I, Paiha K, Hunziker W, Sacks DB, Bahler M, Way M, Gagescu R, Gruenberg J (2000) Both calmodulin and the unconventional myosin Myr4 regulate membrane trafficking along the recycling pathway of MDCK cells. Traffic 1:494-503.

Iglesias JM, Morgan RO, Jenkins NA, Copeland NG, Gilbert DJ, Fernandez MP (2002) Comparative genetics and evolution of annexin A13 as the founder gene of vertebrate annexins. Mol Biol Evol 19:608-618.

Inui M, Watanabe T, Sobue K (1994) Annexin VI binds to a synaptic vesicle protein, synapsin I. J Neurochem 63:1917-1923.

Jager S, Bucci C, Tanida I, Ueno T, Kominami E, Saftig P, Eskelinen EL (2004) Role for Rab7 in maturation of late autophagic vacuoles. J Cell Sci 117:4837-4848.

Jahn R, Scheller RH (2006) SNAREs--engines for membrane fusion. Nat Rev Mol Cell Biol 7:631-643.

Kang JH, Li M, Chen X, Yin XM (2011) Proteomics analysis of starved cells revealed Annexin A1 as an important regulator of autophagic degradation. Biochem Biophys Res Commun 407:581-586.

Kanno T, Siebenlist U (1996) Activation of nuclear factor-kappaB via T cell receptor requires a Raf kinase and Ca2+ influx. Functional synergy between Raf and calcineurin. J Immunol 157:5277-5283.

Khan MT, Joseph SK (2010) Role of inositol trisphosphate receptors in autophagy in DT40 cells. J Biol Chem 285:16912-16920.

Kim HJ, Soyombo AA, Tjon-Kon-Sang S, So I, Muallem S (2009) The Ca(2+) channel TRPML3 regulates membrane trafficking and autophagy. Traffic 10:1157-1167.

Kim HJ, Li Q, Tjon-Kon-Sang S, So I, Kiselyov K, Muallem S (2007) Gain-of-function mutation in TRPML3 causes the mouse Varitint-Waddler phenotype. J Biol Chem 282:36138-36142.

Kim J, Guan KL (2011) Amino acid signaling in TOR activation. Annu Rev Biochem 80:1001-1032.

Kim J, Kundu M, Viollet B, Guan KL (2011) AMPK and mTOR regulate autophagy through direct phosphorylation of Ulk1. Nat Cell Biol 13:132-141.

Kim J, Kim YC, Fang C, Russell RC, Kim JH, Fan W, Liu R, Zhong Q, Guan KL (2013) Differential regulation of distinct Vps34 complexes by AMPK in nutrient stress and autophagy. Cell 152:290-303.

Kim JK, Kim PJ, Jung KH, Noh JH, Eun JW, Bae HJ, Xie HJ, Shan JM, Ping WY, Park WS, Lee JY, Nam SW (2010) Decreased expression of annexin A10 in gastric cancer and its overexpression in tumor cell growth suppression. Oncol Rep 24:607-612.

Klionsky DJ (2012) Look people, "Atg" is an abbreviation for "autophagy-related." That's it. Autophagy 8:1281-1282.

Klionsky DJ, Cregg JM, Dunn WA, Jr., Emr SD, Sakai Y, Sandoval IV, Sibirny A, Subramani S, Thumm M, Veenhuis M, Ohsumi Y (2003) A unified nomenclature for yeast autophagy-related genes. Dev Cell 5:539-545.

Knecht E, Aguado C, Carcel J, Esteban I, Esteve JM, Ghislat G, Moruno JF, Vidal JM, Saez R (2009) Intracellular protein degradation in mammalian cells: recent developments. Cell Mol Life Sci 66:2427-2443.

Koga H, Kaushik S, Cuervo AM (2010) Altered lipid content inhibits autophagic vesicular fusion. FASEB J 24:3052-3065.

Kojima K, Utsumi H, Ogawa H, Matsumoto I (1994) Highly polarized expression of carbohydrate-binding protein p33/41 (annexin IV) on the apical plasma membrane of epithelial cells in renal proximal tubules. FEBS Lett 342:313-318.

Kollermann J, Schlomm T, Bang H, Schwall GP, von Eichel-Streiber C, Simon R, Schostak M, Huland H, Berg W, Sauter G, Klocker H, Schrattenholz A (2008) Expression and prognostic relevance of annexin A3 in prostate cancer. Eur Urol 54:1314-1323.

Lafont F, Lecat S, Verkade P, Simons K (1998) Annexin XIIIb associates with lipid microdomains to function in apical delivery. J Cell Biol 142:1413-1427.

Lam D, Kosta A, Luciani MF, Golstein P (2008) The inositol 1,4,5-trisphosphate receptor is required to signal autophagic cell death. Mol Biol Cell 19:691-700.

Lange I, Yamamoto S, Partida-Sanchez S, Mori Y, Fleig A, Penner R (2009) TRPM2 functions as a lysosomal Ca2+-release channel in beta cells. Sci Signal 2:ra23.

LaPlante JM, Falardeau J, Sun M, Kanazirska M, Brown EM, Slaugenhaupt SA, Vassilev PM (2002) Identification and characterization of the single channel function of human mucolipin-1 implicated in mucolipidosis type IV, a disorder affecting the lysosomal pathway. FEBS Lett 532:183-187.

LaPlante JM, Ye CP, Quinn SJ, Goldin E, Brown EM, Slaugenhaupt SA, Vassilev PM (2004) Functional links between mucolipin-1 and Ca2+-dependent membrane trafficking in mucolipidosis IV. Biochem Biophys Res Commun 322:1384-1391.

Lavallard VJ, Meijer AJ, Codogno P, Gual P (2012) Autophagy, signaling and obesity. Pharmacol Res 66:513-525.

Le Cabec V, Russo-Marie F, Maridonneau-Parini I (1992) Differential expression of two forms of annexin 3 in human neutrophils and monocytes and along their differentiation. Biochem Biophys Res Commun 189:1471-1476.

Lee JO, Rieu P, Arnaout MA, Liddington R (1995) Crystal structure of the A domain from the alpha subunit of integrin CR3 (CD11b/CD18). Cell 80:631-638.

Levine B, Klionsky DJ (2004) Development by self-digestion: molecular mechanisms and biological functions of autophagy. Dev Cell 6:463-477.

Liemann S, Lewit-Bentley A (1995) Annexins: a novel family of calcium- and membrane-binding proteins in search of a function. Structure 3:233-237.

Lin HC, Sudhof TC, Anderson RG (1992) Annexin VI is required for budding of clathrin-coated pits. Cell 70:283-291.

Lin LL, Huang HC, Juan HF (2012) Revealing the molecular mechanism of gastric cancer marker annexin a4 in cancer cell proliferation using exon arrays. PLoS One 7:e44615.

Longatti A, Tooze SA (2012) Recycling endosomes contribute to autophagosome formation. Autophagy 8:Epub ahead of print.

Lu SH, Chen YL, Shun CT, Lai JN, Peng SY, Lai PL, Hsu HC (2011) Expression and prognostic significance of gastric-specific annexin A10 in diffuse- and intestinal-type gastric carcinoma. J Gastroenterol Hepatol 26:90-97.

Luecke H, Chang BT, Mailliard WS, Schlaepfer DD, Haigler HT (1995) Crystal structure of the annexin XII hexamer and implications for bilayer insertion. Nature 378:512-515.

Luzio JP, Pryor PR, Bright NA (2007a) Lysosomes: fusion and function. Nat Rev Mol Cell Biol 8:622-632.

Luzio JP, Bright NA, Pryor PR (2007b) The role of calcium and other ions in sorting and delivery in the late endocytic pathway. Biochem Soc Trans 35:1088-1091.

Malsam J, Kreye S, Sollner TH (2008) Membrane fusion: SNAREs and regulation. Cell Mol Life Sci 65:2814-2832.

Mari M, Griffith J, Rieter E, Krishnappa L, Klionsky DJ, Reggiori F (2010) An Atg9-containing compartment that functions in the early steps of autophagosome biogenesis. J Cell Biol 190:1005-1022.

Martens S, McMahon HT (2008) Mechanisms of membrane fusion: disparate players and common principles. Nat Rev Mol Cell Biol 9:543-556.

Martina JA, Lelouvier B, Puertollano R (2009) The calcium channel mucolipin-3 is a novel regulator of trafficking along the endosomal pathway. Traffic 10:1143-1156.

Massey D, Traverso V, Maroux S (1991) Lipocortin IV is a basolateral cytoskeleton constituent of rabbit enterocytes. J Biol Chem 266:3125-3130.

Mayran N, Parton RG, Gruenberg J (2003) Annexin II regulates multivesicular endosome biogenesis in the degradation pathway of animal cells. Embo J 22:3242-3253.

McBride HM, Rybin V, Murphy C, Giner A, Teasdale R, Zerial M (1999) Oligomeric complexes link Rab5 effectors with NSF and drive membrane fusion via interactions between EEA1 and syntaxin 13. Cell 98:377-386.

Meijer AJ, Codogno P (2009) Autophagy: regulation and role in disease. Crit Rev Clin Lab Sci 46:210-240.

Merrifield CJ, Moss SE, Ballestrem C, Imhof BA, Giese G, Wunderlich I, Almers W (1999) Endocytic vesicles move at the tips of actin tails in cultured mast cells. Nat Cell Biol 1:72-74.

Miedel MT, Rbaibi Y, Guerriero CJ, Colletti G, Weixel KM, Weisz OA, Kiselyov K (2008) Membrane traffic and turnover in TRP-ML1-deficient cells: a revised model for mucolipidosis type IV pathogenesis. J Exp Med 205:1477-1490.

Mijaljica D, Prescott M, Devenish RJ (2011) Microautophagy in mammalian cells: revisiting a 40-year-old conundrum. Autophagy 7:673-682.

Mills IG, Urbe S, Clague MJ (2001) Relationships between EEA1 binding partners and their role in endosome fusion. J Cell Sci 114:1959-1965.

Mishra S, Chander V, Banerjee P, Oh JG, Lifirsu E, Park WJ, Kim do H, Bandyopadhyay A (2011) Interaction of annexin A6 with alpha actinin in cardiomyocytes. BMC Cell Biol 12:7.

Missiaen L, Callewaert G, De Smedt H, Parys JB (2001) 2-Aminoethoxydiphenyl borate affects the inositol 1,4,5-trisphosphate receptor, the intracellular Ca2+ pump and the non-specific Ca2+ leak from the non-mitochondrial Ca2+ stores in permeabilized A7r5 cells. Cell Calcium 29:111-116.

Missiaen L, Callewaert G, Parys JB, Wuytack F, Raeymaekers L, Droogmans G, Nilius B, Eggermont J, De Smedt H (2000a) [Intracellular calcium: physiology and physiopathology]. Verh K Acad Geneeskd Belg 62:471-499.

Missiaen L, Robberecht W, van den Bosch L, Callewaert G, Parys JB, Wuytack F, Raeymaekers L, Nilius B, Eggermont J, De Smedt H (2000b) Abnormal intracellular ca(2+)homeostasis and disease. Cell Calcium 28:1-21.

Miwa N, Uebi T, Kawamura S (2008) S100-annexin complexes--biology of conditional association. Febs J 275:4945-4955.

Mizushima N, Yoshimori T, Ohsumi Y (2011a) The role of Atg proteins in autophagosome formation. Annu Rev Cell Dev Biol 27:107-132.

Mizushima N, Yoshimori T, Ohsumi Y (2011b) The role of Atg proteins in autophagosome formation. Annu Rev Cell Dev Biol 27:107-132.

Mohiti J, Caswell AM, Walker JH (1997) The nuclear location of annexin V in the human osteosarcoma cell line MG-63 depends on serum factors and tyrosine kinase signaling pathways. Exp Cell Res 234:98-104.

Momoi T (2006) Conformational diseases and ER stress-mediated cell death: apoptotic cell death and autophagic cell death. Curr Mol Med 6:111-118.

Monastyrskaya K, Babiychuk EB, Hostettler A, Wood P, Grewal T, Draeger A (2009) Plasma membrane-associated annexin A6 reduces Ca2+ entry by stabilizing the cortical actin cytoskeleton. J Biol Chem 284:17227-17242.

Morgan RO, Fernandez MP (1998) Expression profile and structural divergence of novel human annexin 31. FEBS Lett 434:300-304.

Moss SE, Morgan RO (2004) The annexins. Genome Biol 5:219.

Mussunoor S, Murray GI (2008) The role of annexins in tumour development and progression. J Pathol 216:131-140.

Nagata K, Zheng L, Madathany T, Castiglioni AJ, Bartles JR, Garcia-Anoveros J (2008) The varitint-waddler (Va) deafness mutation in TRPML3 generates constitutive, inward rectifying currents and causes cell degeneration. Proc Natl Acad Sci U S A 105:353-358.

Nakata T, Sobue K, Hirokawa N (1990) Conformational change and localization of calpactin I complex involved in exocytosis as revealed by quick-freeze, deep-etch electron microscopy and immunocytochemistry. J Cell Biol 110:13-25.

Nakayama T, Yaoi T, Yasui M, Kuwajima G (1998) N-copine: a novel two C2-domain-containing protein with neuronal activity-regulated expression. FEBS Lett 428:80-84.

Nara A, Mizushima N, Yamamoto A, Kabeya Y, Ohsumi Y, Yoshimori T (2002) SKD1 AAA ATPase-dependent endosomal transport is involved in autolysosome formation. Cell Struct Funct 27:29-37.

Nicklin P, Bergman P, Zhang B, Triantafellow E, Wang H, Nyfeler B, Yang H, Hild M, Kung C, Wilson C, Myer VE, MacKeigan JP, Porter JA, Wang YK, Cantley LC, Finan PM, Murphy LO (2009) Bidirectional transport of amino acids regulates mTOR and autophagy. Cell 136:521-534.

Nobukuni T, Joaquin M, Roccio M, Dann SG, Kim SY, Gulati P, Byfield MP, Backer JM, Natt F, Bos JL, Zwartkruis FJ, Thomas G (2005) Amino

acids mediate mTOR/raptor signaling through activation of class 3 phosphatidylinositol 3OH-kinase. Proc Natl Acad Sci U S A 102:14238-14243.

Noda T, Fujita N, Yoshimori T (2009) The late stages of autophagy: how does the end begin? Cell Death Differ 16:984-990.

Oberstein A, Jeffrey PD, Shi Y (2007) Crystal structure of the Bcl-XL-Beclin 1 peptide complex: Beclin 1 is a novel BH3-only protein. J Biol Chem 282:13123-13132.

Ogata M, Hino S, Saito A, Morikawa K, Kondo S, Kanemoto S, Murakami T, Taniguchi M, Tanii I, Yoshinaga K, Shiosaka S, Hammarback JA, Urano F, Imaizumi K (2006) Autophagy is activated for cell survival after endoplasmic reticulum stress. Mol Cell Biol 26:9220-9231.

Ortega D, Pol A, Biermer M, Jackle S, Enrich C (1998) Annexin VI defines an apical endocytic compartment in rat liver hepatocytes. J Cell Sci 111 (Pt 2):261-269.

Overbye A, Fengsrud M, Seglen PO (2007) Proteomic analysis of membrane-associated proteins from rat liver autophagosomes. Autophagy 3:300-322.

Palmer AE, Jin C, Reed JC, Tsien RY (2004) Bcl-2-mediated alterations in endoplasmic reticulum Ca2+ analyzed with an improved genetically encoded fluorescent sensor. Proc Natl Acad Sci U S A 101:17404-17409.

Patel DM, Ahmad SF, Weiss DG, Gerke V, Kuznetsov SA (2011) Annexin A1 is a new functional linker between actin filaments and phagosomes during phagocytosis. J Cell Sci 124:578-588.

Patterson RL, Boehning D, Snyder SH (2004) Inositol 1,4,5-trisphosphate receptors as signal integrators. Annu Rev Biochem 73:437-465.

Perestenko PV, Pooler AM, Noorbakhshnia M, Gray A, Bauccio C, Jeffrey McIlhinney RA (2010) Copines-1, -2, -3, -6 and -7 show different calcium-dependent intracellular membrane translocation and targeting. Febs J 277:5174-5189.

Peters C, Mayer A (1998) Ca2+/calmodulin signals the completion of docking and triggers a late step of vacuole fusion. Nature 396:575-580.

Peters C, Andrews PD, Stark MJ, Cesaro-Tadic S, Glatz A, Podtelejnikov A, Mann M, Mayer A (1999) Control of the terminal step of intracellular membrane fusion by protein phosphatase 1. Science 285:1084-1087.

Pfisterer SG, Mauthe M, Codogno P, Proikas-Cezanne T (2011) Ca2+/calmodulin-dependent kinase (CaMK) signaling via CaMKI and AMP-activated protein kinase contributes to the regulation of WIPI-1 at the onset of autophagy. Mol Pharmacol 80:1066-1075.

Pittis MG, Garcia RC (1999) Annexins VII and XI are present in a human macrophage-like cell line. Differential translocation on FcR-mediated phagocytosis. J Leukoc Biol 66:845-850.

12. APPENDIX 2: MATERIALS AND METHODS

Materials

1. Cell Culture

The cell lines employed in this study and their culture conditions are summarized in Table1.

Table 1. Cell lines used and culture conditions employed.

Cells	Description	Source*	Culture medium**
NIH3T3	Fibroblasts from NIH Swiss mouse embryo	European Collection of Animal Cell Cultures	DMEM, 10% FBS
HEK293	Human embryonic kidney cell line	European Collection of Animal Cell Cultures	MEM, 10% FBS
3349B	Normal human skin fibroblasts	Coriell Institute for Medical Research	MEM, Earle's salts, 2mM L-glutamine, 1x MEM amino acids, 1x MEM nonessential amino acids, 1x MEM vitamins, 20% FCS
Hela	Human cervical cancer cells	European Collection of Animal Cell Cultures	MEM, 10% FBS
MEFs (WT and AMPK KO)	Mouse embryonic fibroblasts, wild type and double knockout for AMPKa1/2 subunits (α1-/- and α2-/-)	Dr. Benoit Viollet	DMEM, 10% FBS

*European Collection of Animal Cell Cultures (Salisbury, United Kingdom); Coriell Institute for Medical Research (Camden, NJ, U.S.A.) and Dr. Benoit Viollet (Institut Cochin, INSERM U1016, CNRS UMR 8104, Université Paris Descartes, Dept. of Endocrinology, Metabolism and Cancer).

**All culture media are supplemented with 100 units/ml penicillin and 100 μg/ml streptomycin. FBS and FCS are inactivated foetal bovine and calf serums, respectively. All these reagents were provided by Probes Invitrogen Life Technologies Corporation (Carlsbad, CA, U.S.A.).

2. Antibodies

Detection of proteins by western blotting and immunofluorescence was performed by using the antibodies listed in Table 2.

Table 2. Antibodies used for immunoblotting and immunofluorescence staining.

Antigen	MW (kDa)	Host	Dilution	Source*
AMPK	62	Rabbit	1/1000	Cell signalling
P-AMPK (T-172)	62	Rabbit	1/1000	Cell signalling
ANNEXIN A1	37	Rabbit	1/1000	Abcam
ANNEXIN A5	35	Rabbit	1/1000	Santa Cruz Biotechnology
β-ACTIN	42	Rabbit	1/4000	Sigma Chemical Co.
CALNEXIN	67	Rabbit	1/2000	Abcam
CAMKK-α	65	Goat	1/500	Santa Cruz Biotechnology
CAMKK-β	65	Mouse	1/500	Santa Cruz Biotechnology
CATHEPSIN B	31	Mouse	1/500	Santa Cruz Biotechnology
CATHEPSIN D	33	Goat	1/500	Santa Cruz Biotechnology
COPINE 1	59 predicted 68 observed	Mouse	1/200	Santa Cruz Biotechnology
EEA1	50	Rabbit	1/1000	Abcam
GAPDH	37	Rabbit	1/4000	Trevigen
LAMIN A	69	Mouse	1/1000	Abcam
LAMP 1	120	Mouse	1/1000	Abcam
LBPA	95	Mouse	1/400	Echelon Biosciences Inc.
LC3B	LC3-I 16 LC3-II 18	Mouse	1/500	Nanotools
COX II: mitochondrial complex II (succinate-ubiquinol oxidoreductase)	70	Mouse	1/7000	Molecular Probes Invitrogen Life Technologies Corporation
p62	62	Mouse	1/7000	Abcam
p70S6K	70	Rabbit	1/1000	Cell signalling
P-p70S6K (T-389)	70	Rabbit	1/1000	Cell signalling
Ulk1	150	Rabbit	1/1000	Cell signalling
P-Ulk1 (S-555)	150	Rabbit	1/1000	Cell signalling
Horseradish peroxidase-labeled secondary antibodies	—	Rabbit, mouse or goat	From 1/3000 to 1/10000	Sigma Chemical Co.

*****Cell Signalling (Danvers, MA, U.S.A.); Abcam (Cambridge, United Kingdom); Santa Cruz Biotechnology Inc. (Santa Cruz, CA, U.S.A.); Sigma Chemical Co. (St. Louis, MO, U.S.A.); Trevigen Inc. (Gaithersburg, MD, U.S.A.); Echelon Biosciences Inc. (Salt Lake City, UT, U.S.A.); Nanotools (Teningen, Alemania) and Molecular Probes Invitrogen Life Technologies Corporation (Carlsbad, CA, U.S.A.).

3. siRNA transfections

Details of siRNAs used for knockdown of the corresponding proteins are summarized in Table 3.

Table 3. siRNAs used for knockdown experiments.

Target	Sequence (5´→3´)	Source*
AMPKα1/2	GCUAUCUUCUGGACUUCAAtt GACAUGCAGUGUUAUUGAAtt GAAUCCUCAUAGACCUUAUtt CCAAUCCAGUGCAUAGAAAtt	Santa Cruz Biotechnology
ANNEXIN A1	siRNA1: CUAUCAUGGUUAAAGGUGUtt siRNA2: GAUCAAGGCCGCGUACUUAtt	Ambion Inc.
ANNEXIN A5	siRNA1: GAAGAGUGUUUGACAAGUAtt siRNA2: GAAGCAUGCUCUUAAGGGAtt	Ambion Inc.
COPINE 1	siRNA1: CAAUCCCAGUAAUCCGUAUtt siRNA2: GAACCGAGGUAGUCAAGAAtt	Ambion Inc.
CAMKK-α	GGCCUACAACGAAAGUGAAtt	Ambion Inc.
CAMKK-β	GGAGAUUGCUAUCCUCAAAtt	Ambion Inc.
Negative controls	Not provided	Ambion Inc.

***** Ambion Inc. (Foster City, Ca, U.S.A.)

4. PCR primers

Details of PCR primers designed for cDNA amplification are summarized in Table 4.

Table 4. PCR primers used for annexin A1 and copine 1 cDNA amplification.

Target	Orientation	Species	Sequence
Copine	Forward	Mouse	GATAGGATCCATGGCTCATTGCGTGACCTTGGTCC
	Reverse	Mouse	GATACTCGAGCTATGCCTGTGGGGCCTGTGCGG
Annexin A1	Forward	Mouse	CGGATCCATGGCAATGGTATCAGAATTCC
	Reverse	Mouse	ACTCGAGTAGTTTCCACCACACAGAGCC

5. Vectors

The vectors used for plasmid constructions and their respective inserts are listed in Table 5.

Table 5. Vectors used and their characteristics.

Insert*	Vector	Source**
ANNEXIN A1	pcDNA3.1	cloned
ANNEXIN A5	pCMV-Sport6	Open Biosystems
COPINE 1	pcDNA3.1	cloned
eGFP-LC3	pEGFP-C1	Dr. Tamotsu Yoshimori
mRFP–GFP–LC3	pEGFP-C1+mRFP	Addgene

*enhanced Green Fluorescent Protein (eGFP) and monomeric Red Fluorescent Protein (RFP).

**Open Biosystems (Huntsville, TN, U.S.A.); Dr. Tamotsu Yoshimori (Department of Genetics, Osaka University, Japan) and Addgene (Cambridge, MA, U.S.A.).

6. Main reagents

The most important reagents used in diverse experimental assays are alphabetically ordered in Table 6. Their respective characteristics are described.

Table 5. Main reagents used for biochemical assays and their characteristics.

Reagents	Experimental conditions	Provenance*	Description
3-methyladenine	10 mM, 4 h	Sigma Chemical Co.	- Inhibits autophagy by blocking autophagosome formation *via* the inhibition of type III Phosphatidylinositol 3-kinases
Alexa-Fluor-488–EGF	2 µg/ml, 5-90 min	Molecular Probes Invitrogen Life Technologies Corporation	- A fluorescent marker of epidermal growth factor receptor mediated endocytosis.
Alexa-Fluor-488–cholera-toxin-subunit-B	1.5 µg/ml, 5-90 min	Molecular Probes Invitrogen Life Technologies Corporation	- A fluorescent marker of cholera toxin endocytosis.
Azoalbumin	2% w/v in different pH buffers	Sigma Chemical Co.	- Chromogenic derivative of albulim used as a potein substrate to measure proteolysis activity.
Bafilomycin	500 nM, 4 h	Sigma Chemical Co.	- Specific inhibitor of vacuolar-type H^+-ATPase, used to inhibit lysosomal degradation.
BAPTA-AM	20 µM, 0.5-4 h	Tocris Bioscience	- Is an intracellular chelator of Ca^{2+}
Cell light-ER	Transduce cells at a 70% confluence according to the manufacturer's instructions.	Molecular Probes Invitrogen Life Technologies Corporation	- Signal sequence of calreticulin and KDEL–RFP enclosed in a baculovirus coupled with a mammalian promoter.

Cell light-Golgi	Transduce cells at a 70% confluence according to the manufacturer's instructions.	Molecular Probes Invitrogen Life Technologies Corporation	- N-acetylgalactosaminyl-transferase-2–RFP enclosed in a baculovirus coupled with a mammalian promoter.
FITC–dextran	1 mg/ml, 0.5-2 h 0.5mg/ml, 18 h	Sigma Chemical Co.	- To measure fluid phase endocytosis. - To measure lysosomal pH.
Fura-2AM	5 µM, 30 min	Molecular Probes Invitrogen Life Technologies Corporation	- Is a membrane permeable Ca^{2+} indicator.
^{3}H-Valine	2 mCi/ml, 24 h	Invitrogen Life Technologies	- used to metabolically labell long half-life proteins.
Ionomycin	1-10 µM, 5 min-4 h	Sigma Chemical Co.	- Ionophore responsible of intracellular rise of Ca^{2+} du to formation of hydrophilic pores into the plasma membrane.
Leupeptin	100 µM, 4 h	Peptide Institute, Inc.	- *N*-acetyl-L-leucyl-L-leucyl-L-argininal, inhibitor of cystein, and thiol peptidases.
LysoTracker Red	75 nM, 4 h	Molecular Probes Invitrogen Life Technologies Corporation	- A membrane-diffusible probe that accumulates in acidic organelles, especially lysosomes.
Metrizamide	35 and 17% in a percoll/metrizamide gradient 35, 17 and 5% in a sucrose/metrizamide gradient	Nycomed	- Is a solute for density gradient centrifugation optimal for high density solutions without increasing their viscosity.
NH_4Cl	20 mM, 4 h	Sigma Chemical Co.	- lysosomotropic agent used to inhibit lysosomal degradation through lysosomal lumen alkalinisation.
Organelle light-early endosomes	Transduce cells at a 70% confluence according to the manufacturer's instructions.	Molecular Probes Invitrogen Life Technologies Corporation	- Rab5a–RFP enclosed in a baculovirus coupled with a mammalian promoter.
Percoll	17% in a percoll/metrizamide gradient	Amersham Pharmacia Biotech Inc.	- Is composed of silica sol with nondialyzable polyvinylpyrrolidone coating. It is an efficient toll for density separation.
Saponin	0.05% w/v, 10 min (in cold Phosphate Buffered Saline (PBS))	Merck	- Is a detergent used for membrane permeabilisation.
STO-609	25 µM, 1 h	Tocris Bioscience	- CaMKK-α/β inhibitor

*Tocris Bioscience (Bristol, United Kingdom); Peptide Institute, Inc. (Osaka, Japan); Nycomed (Zurich, Switzerland); Amersham Pharmacia Biotech Inc. (Piscataway, NJ, U.S.A.) and Merck (Darmstadt, Germany).

Methods

1. Cell culture

Cells were grown at 37ºC in a humidified atmosphere of 5% CO_2/air (v/v) in the indicated media (Table 1). Cell density was assessed using a Bürker hemocytometer (Brand, Wertheim, Germany). Krebs-Henseleit medium (KH, 118.4 mM NaCl, 4.75 mM KCl, 1.19 mM KH_2PO_4, 2.54 mM $MgSO_4$, 2.44 mM $CaCl_2 \cdot 2H_2O$, 28.6 mM $NaHCO_3$, 20 mM glucose), with 10 mM Hepes, pH 7.4, was used for high proteolysis (starvation) conditions. For low proteolysis conditions, insulin (0.1 µM) and essential amino acids (at two times the concentration present in the growth media) were added to KH. For intermediate proteolysis conditions, either insulin or amino acids were deleted. Incubations without extracellular Ca^{2+} were carried out in the same KH, but without $CaCl_2$ and supplemented with 100 µM ethylene glycol tetra acetic acid (EGTA). Cell viability and growth curves were determined in parallel for each culture.

2. Subcellular fractionation

Cells were washed with PBS and pooled in ice-cold homogenisation buffer (250 mM sucrose, 20 mM Hepes, 1 mM Ethylenediaminetetraacetic acid (EDTA), pH 7.4). Then, cells were homogenised at 4°C, first in a nitrogen cavitation pump (2.41 x 10^5 Pa, 7 min), and then with a tight-fitting Dounce (10 strokes). Subcellular fractions were prepared according as follows: homogenates were centrifuged at 3000 g for 10 min at 4°C, the pellet was saved as the nuclear fraction and the post nuclear supernatant was applied to a Percoll (Amersham Parmacia Biotech Inc.) metrizamide (Nycomed) gradient (from top to bottom: 6% Percoll; 17% and 35% metrizamide) and centrifuged at 53,000 g for 35 min at 4°C in an SW41Ti rotor (Beckman). To separate lysosomes from mitochondria, the 6% Percoll–17% metrizamide interface material was brought to 35% metrizamide and

placed on the bottom of a second gradient of sucrose–metrizamide (from top to bottom: 0.25 M sucrose plus 5%, 17% and 35% metrizamide). After centrifugation at 53,000 g for 30 min, 4°C, mitochondria and lysosomes were collected from the 17%/35% and the 5%/17% metrizamide interfaces, respectively, and were disrupted by freezing and thawing, ten times. Lysosomal membranes were obtained by centrifugation at 105,000 g for 20 min at 4°C, in a Beckman Airfuge (rotor A-100), and washed three times.

3. Two-dimensional electrophoresis and mass spectroscopy

2D-DIGE of lysosomal membranes was carried out by solubilising protein samples purified in 7 M urea, 2 M thiourea, 4% (w/v) CHAPS, 20 mM dithiothreitol (DTT) and 2% (v/v) Biolytes 3–10 and Bromophenol Blue (all chemicals from Bio-Rad). Samples of 100 µg protein were subjected to isoelectric focusing generated on a Bio-Rad PROTEAN® IEF Cell at 20°C. Subsequently, the strips were reduced and alkylated (using 2.5% iodoacetamide and 2% DTT in succession) in equilibration buffer containing 6 M urea, 0.375 M tris(hydroxymethyl)aminomethane (Tris) pH 8.8, 2% sodium dodecyl sulfate (SDS) and 20% glycerol. Polyacrylamide gels (10%) were employed for the second dimension. The spots observed in the gel were manually excised, washed twice with double distilled water and digested with sequencing grade trypsin (Promega, Madison, WI, U.S.A.). Proteins were identified by mass spectrometry using a 4700 Proteomics analyser (Applied Biosystems, Foster City, Ca, U.S.A.). A MASCOT search engine (Matrix-Science, London, UK) was used for a database search on SwissProt and NCBInr. The accuracy of proteins identification was considered when at least three peptides were identified with a minimum overall MASCOT score>50. The significance threshold for a change in protein levels in the various conditions was set to $P \leq 0.05$ and the values were determined by factorial ANOVA tests using STATVIEW v4.53 (Abacus Concepts, Piscataway, NJ, U.S.A.). All the proteomic studies were

performed in the Proteomics Unit of Centro de Investigación Príncipe Felipe, Valencia, Spain.

4. Measurement of intracellular Ca^{2+}

For cytosolic [Ca^{2+}] imaging, cells were preloaded for 30 min at 37°C with the membrane permeable Ca^{2+} indicator fura-2AM (Molecular Probes Invitrogen Life Technologies Corporation) at 5 µM in KH. Then, the cells were washed twice with PBS and incubated for 15 min with the assay medium. Fura-2AM fluorescence was measured at 340 nm and 380 nm excitation and emission was detected with a 520 nm emission filter in a Zeiss Axiovert 200 inverted microscope equipped with either cooled CCD digital cameras or as part of a Zeiss LSM 510 confocal microscope (Carl Zeiss, Jena, Germany).

5. Measurements of intracellular pH

Cells were preloaded for 30 min at 37°C with BCECF-AM (2',7'-*bis*-(carboxyethyl)-5-(and-6)-carboxyfluorescein, acetoxymethyl ester) (Molecular Probes Invitrogen Life Technologies Corporation) at 5 µM in KH. Then, the cells were washed twice with PBS and incubated for 15 min with the assay medium. Two fluorescence measurements were taken at intervals of 5 seconds at excitation wavelengths of 485 and 450 nm and an emission wavelength of 530 nm. The 485nm/450nm fluorescence ratio was used to estimate the intracellular pH. Fluorescence assays were carried out on a Zeiss Axiovert 200 inverted microscope equipped either with a cooled CCD digital camera or as part of a Zeiss LSM 510 confocal microscope (Carl Zeiss, Jena, Germany). Analysis was done using the Hamamatsu or MetaMorph/MetaFluor Analyst (Universal Imaging Corporation, Downingtown, PA).

6. Constructs

The polymerase chain reaction (PCR) was performed to generate inserts corresponding to annexin A1 and copine 1 cDNAs. Details of the different PCRs carried out are summarized in Table 6.

Table 6. PCR experimental details.

Conditions	Cycles**
94ºC, 3 min	1
94ºC, 30 s	30
65ºC, 30 s*	
70ºC, 1,5 min	
70ºC, 4 min	1

*Melting temperature varies between 45 and 65ºC depending on the primer.

**A 50 µl mix of 2.5 mM dNTPs, 50 mM $MgCl_2$, 10 µM primer (each one), 5-10 ng template and one unity Taq polymerase was submitted to each cycle.

PCR products were analysed by electrophoresis using ethidium bromide-containing agarose gels (0.8% w/v in Tris-acetate-EDTA buffer (89 mM Tris, 89 mM boric acid, 2 mM EDTA pH8)) and imaged using an UV Transilluminator (Alpha Innotech Corporation, San Leandro, CA, U.S.A.). Then, PCR products were purified with the High Pure Template Preparation Kit (Roche Applied Science, Basel, Switzerland), digested with BamH1 and Xho1 (New England Biolabs, Ipswich, MA, U.S.A.) and subsequently cloned into pcDNA3.1 vectors using a T4 DNA ligase (New England Biolabs). Plasmids were transformed into chemically competent bacteria and grown overnight in Lactulose breath test (LBT) broth (10 mg/ml NaCl, 10 mg/ml Bacto-tryptone, 5 mg/ml yeast extract and 40 mg/ml thymine) with the appropriate selective antibiotic (50 µg/ml ampicillin) at 37ºC in a shaking incubator. Plasmids were then purified using QIAGEN (Madrid, Spain) Plasmid Mini, Midi or Maxi kits, depending on the volume of culture grown. A glycerol stock stored at -80ºC was made by adding 0.25 ml of glycerol to 0.75 ml of bacterial culture. The purified plasmids were quantified by

absorbance readings computed by a Nanodrop ND-1000 spectrophotometer (Thermo Scientific, Wilmington, DE, U.S.A.).

7. Cell transfections

Transient transfections with plasmids were carried out using Fugene HD (Roche Applied Science), according to the manufacturer's instructions. Experimental analyses of overexpression were started 48 h after transfections.

For RNAi-mediated inhibition of the expression of the genes corresponding to the proteins of interest, cells were transfected, 72 h before analysis, with the negative control or the corresponding siRNAs using X-tremeGENE siRNA Transfection Reagent (Roche Applied Science) or siLentFect Lipid Reagent (Bio-Rad) according to the manufacturer's instructions. The final concentration range of all siRNAs tested was 15-25 nM.

Overexpression and silencing efficiencies were estimated at the protein level by western blotting.

Isolation of cells stably expressing fluorescent reporters was accomplished by transfecting the cells with the plasmids holding fluorescently tagged protein sequences and subsequent detection of stable transformants by antibiotic selection (1 mg/ml geneticin; Gibco). The resistant clones were next submitted to two sequential cycles of cell sorting, using a MoFlo high speed cell sorter (Beckman-Coulter). The steady-state expression level was then confirmed by fluorescence-activated cell sorting (FACS), immunoblotting and confocal microscope analyses.

8. Immunoblot analysis

Cells were collected using a rubber policeman in RIPA buffer (150 mM NaCl, 1% Nonidet P-40, 0.5% sodium deoxycholate, 0.1% SDS, 50 mM Tris, pH 8.0) containing 0.1 mM leupeptin and 1 mM PMSF. Cell lysates

destinated to protein phosphorylation analysis were prepared in a lysis buffer (5 mM NaCl, 1% Nonidet P-40, 1M Tris, pH 7.5 and glycerol 20%) to which 1 mM PMSF, 0.1 mM leupeptin, 50 mM EDTA, 50 mM NaF and 5 mM $Na_2P_2O_7$. After 1 h of incubation on ice with frequent agitations, cell lysates were centrifuged at 12.000 g, 10 min, the supernatants were collected and the concentration of proteins determined by Lowry´s method using an UV*/*vis spectrophotometer (Helios β, Unicom). Proteins (75 *μ*g) from the various lysates were separated on 10 to 16.5% polyacrylamide slab gels (depending on the size of the protein to be analysed) and transferred to PVDF membranes (electrophoresis grade, 0.45 *μ*m pore size; GE healthcare) for 16 h at 4ºC and at 30 V, using a blotting tank transfer cell (Bio-Rad Laboratories, Richmond, CA, U.S.A.). The membranes were stained for 2 min with 0.2% (w/v) Ponceau S (Sigma Chemical Co.) solution in 3% trichloroacetic acid (TCA), destained with PBS for 5 min, blocked with 5% (w/v) skimmed milk in Tris-buffered saline (TBS: 150 mM NaCl, 10 mM Tris-HCl, pH 7,4) for 1 h at room temperature and reacted for 16 h at 4ºC with the appropriate primary antibody. Primary and HRP-conjugated antibodies were applied in 3% (w/v) BSA in TBS, plus 0.02 % sodium azide. Incubations with secondary antibodies were for 1 h at room temperature. Membranes were rinsed between incubations for 5 min, three times, with TBS, plus 0.05 % tween-20. After the last wash, membranes were imaged using “Lumi-Light” system Roche Diagnostics Corporation following the manufacturer’s instructions. Protein bands were quantified by densitometric analysis with an Image Quant ECL.

9. Immunofluorescence analysis

Cells were cultured on coverslips in 12-well plates. After the different treatments or transfections, cells were rinsed with PBS, fixed with 3.7% paraformaldehyde–PBS for 20 min at room temperature, washed with PBS, and mounted using Fluor-Save reagent (Calbiochem). For immunofluorescence staining with antibodies, cells were fixed as above,

blocked with 0.1% BSA in PBS for 10 min and permeabilised with saponin (Merck) at 0.05% w/v in PBS for 10 min. Then, cells were incubated with antibodies against the pertinent proteins. Bound antibodies were subsequently detected by incubation, as appropriate, with Alexa-Fluor-488-, 633- or 647-conjugated rabbit, mouse or goat secondary antibodies (dilution 1:200).

ER, Golgi and early endosome fluorescent signals were obtained by transfecting the cells (following the manufacturer's instructions; Invitrogen) with Cell Light-ER (endoplasmic signal sequence of calreticulin and KDEL–RFP), Cell Light-Golgi (N-acetylgalactosaminyl-transferase 2–RFP) and Organelle Light-early endosomes (Rab5a–RFP).

Immunofluorescence preparations were observed with a Leica DM6000B fluorescence microscope equipped with AxioCam MRm (Carl Zeiss) camera and images were acquired with a Leica TC5 confocal laser scanning microscope. Laser lines were 488 nm (eGFP–LC3, RFP–GFP–LC3 and Alexa Fluor 488), 561 nm (RFP–GFP–LC3) and 633 and 647 nm (Alexa Fluor 633 and 647). The JaCoP plug-in (Bolte and Cordelieres, 2006) in ImageJ software was used for the quantification of the various colocalisations. Fluorescent stained areas were quantified using LCS Lite software. The number of eGFP–LC3 puncta was counted using the Top Hat algorithm in MetaMorph version 7.0.

10. Measurement of intracellular degradation of long-lived proteins

To label long-lived proteins, cells were incubated for 48 h in fresh full medium with 2 µCi/ml ^{3}H-valine in order to label long-lived proteins. Before starting the proteolysis measurements, the cells were washed once with full medium, containing 10 mM L-valine, and chased for 24 h at 37ºC in this medium to degrade short-lived proteins. A saturated concentration of L-valine is employed in wash and chase mediums for minimizing the reuse of labelled amino acids released by cells to the extracellular milieu. Next, all cultures were incubated in the indicated medium (depending on the

experiment) containing 10 mM L-valine for 4 h. During these 4 h chase, cells were maintained without or with a combination of 20 mM NH_4Cl and 100 μM leupeptin to inhibit lysosomal degradation or with 3-methyladenine (10 mM) to inhibit autophagy. Preliminary experiments suggested the convenience of analysing protein degradation 1 h after the addition of the different inhibitors used and for a period of only 3 additional h. This ensures optimal inhibition and should avoid possible secondary effects of the drugs, which may compromise cell viability. A 0.5 ml portion of the medium was transferred out at each chase time (1, 2.5 and 4 h), and was added to 0.5 ml ice-cold 10% (w/v) TCA (final concentration was then 5%). After 30 min in an ice bath, the samples were centrifuged for 10 min at 5000 g, and the pellet was washed with 0.5 ml of 5% TCA and centrifuged again. Supernatants from both centrifugations were pooled. The sediments were dissolved in 0.2 N NaOH. Radioactivity in supernatant and sediment was measured by liquid-scintillation counting. At the end of the chase period, final radioactivity of cells was determined after a 30 min wash of the cells with 10% ice-cold TCA followed by dissolution in 0.2 N NaOH containing 0.4% Sodium deoxycholate for 2 4h. Measurement of the β radiation emitted by ^3H in either soluble or non-soluble TCA fractions was carried out using Liquid Scintillation Analyzer Tri-Carb 3100 TR from PerkinElmer, Inc. (Boston, MA, U.S.A.). The initial radioactivity was calculated, as described previously (Vargas *et al*., 1989; Fuertes *et al*., 2003), by adding the final radioactivity in the cells to the total radioactivity released into the medium during the chase period. Radioactivity released in non-soluble TCA fractions of the medium was negligible (at all the experimental times it was always less than 0.3% h^{-1} of the initial non-soluble TCA radioactivity) and represents protein secretion and/or detachment of cells from the monolayer. Protein degradation of each chase time was calculated by dividing the total radioactivity released at this time to the medium by the initial radioactivity in the cells (calculated as described above) and expressed as percentage.

11. Electron microscopy and morphometric analysis

Cells were washed with ice-cold PBS and fixed for 15 min in the dishes by direct addition of a mixture of 2% (v/v) glutaraldehyde and 1% formaldehyde (EM grade; Polysciences,Warrington, PA, U.S.A.) buffered with 0.05 M sodium cacodylate (pH 7.4). The cells were detached from the dishes with a rubber policeman and further fixed as above for 45 min. Then, the cells were washed three times for 30 min in 0.05 M sodium cacodylate buffer, postfixed in a mixture of 1% osmium tetroxide (Polysciences) and 1% potassium ferrocyanide for 60 min, incubated for 1 min with 0.15% tannic acid in 0.1 M sodium cacodylate buffer and washed overnight in 0.1 M sodium cacodylate buffer. All these treatments were performed at 0–4ºC. The following day, the fixed cells were stained with 2% (w/v) uranyl acetate for 2 h at 20ºC and dehydrated, embedded in Poly/Bed 812 resin (Polysciences) and polymerized according to the manufacturer's instructions. Ultrathin sections of approx. 60–70 nm were cut with an LKB 4801A from LKB-Microtomy Systems (Leica Cambridge Ltd., Cambridge, UK) and were observed with a Philips CM-10 transmission electron microscope (Eindhoven, Netherlands) at 60 kV. Morphometric analysis of lysosomes was performed, as previously described (Cuervo *et al*., 1997), in randomly selected electron micrographs (18 cm ×24 cm) at a final magnification of ×10500. For each measurement, the fractional volume of lysosomes was estimated by the point counting method in 30 electron micrographs from three different experiments.

12. Measurement of lysosomal pH

To measure the pH within lysosomes, cells were allowed to endocytose FITC-conjugated dextran, following a procedure described elsewhere (Nilsson *et al*., 2003). Previously seeded cells in 12-well plates were treated with 40 kDa FITC–dextran (0.5 mg/ml) for 18 h. Cells were then washed five times with PBS and incubated in the appropriate medium for 4 h

to chase the FITC–dextran from the endosomes. Positive control samples were incubated with 20 mM NH_4Cl. Next, lysosomal pH was measured by using FACS analysis (i) or fluorometric assays (ii). (i) Cells were resuspended and washed three times in fresh medium after being transferred to FACS tubes. Cell pellets were kept on ice and resuspended immediately before FACS analysis. FITC was excited at 488 nm with an argon laser and the resulting emission was detected using a 530±28 nm (FL1) and a 610±20 nm (FL3) filter. The FL1/FL3 ratios were measured in 5000 collected cells. (ii) Cells were transferred to a 96-well plate and were immediately placed in a SpectraMax M5 multimode plate reader for measurement of FITC (excitation: 495 nm for pH-dependent (λ1) and 450 nm for pH independent (λ2), emission: 525 nm) fluorescence emissions. The λ1/λ2 ratios of fluorescence emission were calculated. Calibration of these ratios *versus* pH was obtained using a standard curve prepared with McIlvaine's buffers (pHs ranging from 4.0 to 6.0), containing sodium azide (50 mM), 2-deoxyglucose (50 mM), nigericin (10 mM) and monensin (20 mM).

13. Flow cytometry

Lysosomal mass was determined by incubating the cells in suspension (10^6 cells/ml) with 75 nM LysoTracker Red for 30 min at 37°C.

For detection of fluid phase endocytosed cargo, cells were treated with FITC–dextran (1 mg/ml) for 30, 60 or 120 min at 37ºC. For detection of endocytosis of cholera toxin B or epidermal growth factor (EGF), cells were treated with Alexa-Fluor-488–cholera-toxin-subunit-B (1.5 mg/ml) or with Alexa-Fluor-488–EGF (2 mg/ml) for 5, 15, 30, 60 or 90 min at 37°C. Previously, cells were also incubated as above for 5 s at 4°C to evaluate the membrane-bound marker.

Autophagy was quantified in eGFP-LC3 stably expressing cells, previously switched to low or high proteolysis medium, and after a quick

wash with saponin 0.1% (w/v) in order to release cytosolic eGFP-LC3 leaving only the autophagic membrane bound eGFP-LC3 signal.

After staining, the cells were detached with trypsin–EDTA, washed four times and resuspended in PBS (10^6 cells/ml). In each experiment, 10,000 cells were collected and analysed using a Cytomics FC 500 flow cytometer (Beckman Coulter). The emitted red and green fluorescences were respectively analysed by 620±20 nm and 488±20 nm band-pass filters.

14. Quantification and statistics

P-values were determined by factorial ANOVA tests using GraphPad Prism software. P-values were considered significant at ***P≤0.0005, **P≤0.005 and *P≤0.05.

References

Cuervo AM, Dice JF, Knecht E (1997) A population of rat liver lysosomes responsible for the selective uptake and degradation of cytosolic proteins. J Biol Chem 272:5606-5615.

Fuertes G, Villarroya A, Knecht E (2003) Role of proteasomes in the degradation of short-lived proteins in human fibroblasts under various growth conditions. Int J Biochem Cell Biol 35:651-664.

Nilsson C, Kagedal K, Johansson U, Ollinger K (2003) Analysis of cytosolic and lysosomal pH in apoptotic cells by flow cytometry. Methods Cell Sci 25:185-194.

Vargas JL, Aniento F, Cervera J, Knecht E (1989) Vanadate inhibits degradation of short-lived, but not of long-lived, proteins in L-132 human cells. Biochem J 258:33-40.

Pol A, Ortega D, Enrich C (1997) Identification of cytoskeleton-associated proteins in isolated rat liver endosomes. Biochem J 327 (Pt 3):741-746.

Pons M, Ihrke G, Koch S, Biermer M, Pol A, Grewal T, Jackle S, Enrich C (2000) Late endocytic compartments are major sites of annexin VI localization in NRK fibroblasts and polarized WIF-B hepatoma cells. Exp Cell Res 257:33-47.

Pryor PR, Mullock BM, Bright NA, Gray SR, Luzio JP (2000) The role of intraorganellar Ca(2+) in late endosome-lysosome heterotypic fusion and in the reformation of lysosomes from hybrid organelles. J Cell Biol 149:1053-1062.

Pryor PR, Mullock BM, Bright NA, Lindsay MR, Gray SR, Richardson SC, Stewart A, James DE, Piper RC, Luzio JP (2004) Combinatorial SNARE complexes with VAMP7 or VAMP8 define different late endocytic fusion events. EMBO Rep 5:590-595.

Puertollano R, Kiselyov K (2009) TRPMLs: in sickness and in health. Am J Physiol Renal Physiol 296:F1245-1254.

Puzianowska-Kuznicka M, Kuznicki J (2009) The ER and ageing II: calcium homeostasis. Ageing Res Rev 8:160-172.

Rambotti MG, Spreca A, Donato R (1993) Immunocytochemical localization of annexins V and VI in human placentae of different gestational ages. Cell Mol Biol Res 39:579-588.

Rasola A, Bernardi P (2007) The mitochondrial permeability transition pore and its involvement in cell death and in disease pathogenesis. Apoptosis 12:815-833.

Ravikumar B, Moreau K, Jahreiss L, Puri C, Rubinsztein DC (2010a) Plasma membrane contributes to the formation of pre-autophagosomal structures. Nat Cell Biol 12:747-757.

Ravikumar B, Sarkar S, Davies JE, Futter M, Garcia-Arencibia M, Green-Thompson ZW, Jimenez-Sanchez M, Korolchuk VI, Lichtenberg M, Luo S, Massey DC, Menzies FM, Moreau K, Narayanan U, Renna M, Siddiqi FH, Underwood BR, Winslow AR, Rubinsztein DC (2010b) Regulation of mammalian autophagy in physiology and pathophysiology. Physiol Rev 90:1383-1435.

Raynal P, Pollard HB (1994) Annexins: the problem of assessing the biological role for a gene family of multifunctional calcium- and phospholipid-binding proteins. Biochim Biophys Acta 1197:63-93.

Raynal P, Hullin F, Ragab-Thomas JM, Fauvel J, Chap H (1993) Annexin 5 as a potential regulator of annexin 1 phosphorylation by protein kinase C. In vitro inhibition compared with quantitative data on annexin distribution in human endothelial cells. Biochem J 292 (Pt 3):759-765.

Rescher U, Gerke V (2008) S100A10/p11: family, friends and functions. Pflugers Arch 455:575-582.

Rety S, Sopkova-de Oliveira Santos J, Dreyfuss L, Blondeau K, Hofbauerova K, Raguenes-Nicol C, Kerboeuf D, Renouard M,

Russo-Marie F, Lewit-Bentley A (2005) The crystal structure of annexin A8 is similar to that of annexin A3. J Mol Biol 345:1131-1139.

Rick M, Ramos Garrido SI, Herr C, Thal DR, Noegel AA, Clemen CS (2005) Nuclear localization of Annexin A7 during murine brain development. BMC Neurosci 6:25.

Rintala-Dempsey AC, Rezvanpour A, Shaw GS (2008) S100-annexin complexes--structural insights. Febs J 275:4956-4966.

Rizo J, Sudhof TC (1998) C2-domains, structure and function of a universal Ca2+-binding domain. J Biol Chem 273:15879-15882.

Rong YP, Aromolaran AS, Bultynck G, Zhong F, Li X, McColl K, Matsuyama S, Herlitze S, Roderick HL, Bootman MD, Mignery GA, Parys JB, De Smedt H, Distelhorst CW (2008) Targeting Bcl-2-IP3 receptor interaction to reverse Bcl-2's inhibition of apoptotic calcium signals. Mol Cell 31:255-265.

Roth MG (2004) Phosphoinositides in constitutive membrane traffic. Physiol Rev 84:699-730.

Rothhut B, Comera C, Cortial S, Haumont PY, Diep Le KH, Cavadore JC, Conard J, Russo-Marie F, Lederer F (1989) A 32 kDa lipocortin from human mononuclear cells appears to be identical with the placental inhibitor of blood coagulation. Biochem J 263:929-935.

Runkel F, Michels M, Franken S, Franz T (2006) Specific expression of annexin A8 in adult murine stratified epithelia. J Mol Histol 37:353-359.

Rytomaa M, Kinnunen PK (1996) Dissociation of cytochrome c from liposomes by histone H1. Comparison with basic peptides. Biochemistry 35:4529-4539.

Saftig P, Klumperman J (2009) Lysosome biogenesis and lysosomal membrane proteins: trafficking meets function. Nat Rev Mol Cell Biol 10:623-635.

Sakaki K, Wu J, Kaufman RJ (2008) Protein kinase Ctheta is required for autophagy in response to stress in the endoplasmic reticulum. J Biol Chem 283:15370-15380.

Sancak Y, Bar-Peled L, Zoncu R, Markhard AL, Nada S, Sabatini DM (2010) Ragulator-Rag complex targets mTORC1 to the lysosomal surface and is necessary for its activation by amino acids. Cell 141:290-303.

Sarbassov DD, Ali SM, Sabatini DM (2005) Growing roles for the mTOR pathway. Curr Opin Cell Biol 17:596-603.

Saris CJ, Tack BF, Kristensen T, Glenney JR, Jr., Hunter T (1986) The cDNA sequence for the protein-tyrosine kinase substrate p36 (calpactin I heavy chain) reveals a multidomain protein with internal repeats. Cell 46:201-212.

Saris CJ, Kristensen T, D'Eustachio P, Hicks LJ, Noonan DJ, Hunter T, Tack BF (1987) cDNA sequence and tissue distribution of the mRNA for bovine and murine p11, the S100-related light chain of the protein-

tyrosine kinase substrate p36 (calpactin I). J Biol Chem 262:10663-10671.

Sarkar S, Floto RA, Berger Z, Imarisio S, Cordenier A, Pasco M, Cook LJ, Rubinsztein DC (2005) Lithium induces autophagy by inhibiting inositol monophosphatase. J Cell Biol 170:1101-1111.

Satoh H, Shibata H, Nakano Y, Kitaura Y, Maki M (2002) ALG-2 interacts with the amino-terminal domain of annexin XI in a Ca(2+)-dependent manner. Biochem Biophys Res Commun 291:1166-1172.

Savino M, d'Apolito M, Centra M, van Beerendonk HM, Cleton-Jansen AM, Whitmore SA, Crawford J, Callen DF, Zelante L, Savoia A (1999) Characterization of copine VII, a new member of the copine family, and its exclusion as a candidate in sporadic breast cancers with loss of heterozygosity at 16q24.3. Genomics 61:219-226.

Scarlatti F, Maffei R, Beau I, Codogno P, Ghidoni R (2008) Role of non-canonical Beclin 1-independent autophagy in cell death induced by resveratrol in human breast cancer cells. Cell Death Differ 15:1318-1329.

Settembre C, Zoncu R, Medina DL, Vetrini F, Erdin S, Erdin S, Huynh T, Ferron M, Karsenty G, Vellard MC, Facchinetti V, Sabatini DM, Ballabio A (2012) A lysosome-to-nucleus signalling mechanism senses and regulates the lysosome via mTOR and TFEB. Embo J 31:1095-1108.

Shaw RJ, Cantley LC (2006) Ras, PI(3)K and mTOR signalling controls tumour cell growth. Nature 441:424-430.

Sopkova J, Raguenes-Nicol C, Vincent M, Chevalier A, Lewit-Bentley A, Russo-Marie F, Gallay J (2002) Ca(2+) and membrane binding to annexin 3 modulate the structure and dynamics of its N terminus and domain III. Protein Sci 11:1613-1625.

Soyombo AA, Tjon-Kon-Sang S, Rbaibi Y, Bashllari E, Bisceglia J, Muallem S, Kiselyov K (2006) TRP-ML1 regulates lysosomal pH and acidic lysosomal lipid hydrolytic activity. J Biol Chem 281:7294-7301.

Spat A, Szanda G, Csordas G, Hajnoczky G (2008) High- and low-calcium-dependent mechanisms of mitochondrial calcium signalling. Cell Calcium 44:51-63.

Srivastava M, Torosyan Y, Raffeld M, Eidelman O, Pollard HB, Bubendorf L (2007) ANXA7 expression represents hormone-relevant tumor suppression in different cancers. Int J Cancer 121:2628-2636.

Sugden MC, Holness MJ (2003) Recent advances in mechanisms regulating glucose oxidation at the level of the pyruvate dehydrogenase complex by PDKs. Am J Physiol Endocrinol Metab 284:E855-862.

Sun W, Yan Q, Vida TA, Bean AJ (2003) Hrs regulates early endosome fusion by inhibiting formation of an endosomal SNARE complex. J Cell Biol 162:125-137.

Swairjo MA, Roberts MF, Campos MB, Dedman JR, Seaton BA (1994) Annexin V binding to the outer leaflet of small unilamellar vesicles

leads to altered inner-leaflet properties: 31P- and 1H-NMR studies. Biochemistry 33:10944-10950.

Swairjo MA, Concha NO, Kaetzel MA, Dedman JR, Seaton BA (1995) Ca(2+)-bridging mechanism and phospholipid head group recognition in the membrane-binding protein annexin V. Nat Struct Biol 2:968-974.

Swanson JA (2008) Shaping cups into phagosomes and macropinosomes. Nat Rev Mol Cell Biol 9:639-649.

Szabadkai G, Duchen MR (2008) Mitochondria: the hub of cellular Ca2+ signaling. Physiology (Bethesda) 23:84-94.

Tamai K, Tanaka N, Nara A, Yamamoto A, Nakagawa I, Yoshimori T, Ueno Y, Shimosegawa T, Sugamura K (2007) Role of Hrs in maturation of autophagosomes in mammalian cells. Biochem Biophys Res Commun 360:721-727.

Tauber AI (2003) Metchnikoff and the phagocytosis theory. Nat Rev Mol Cell Biol 4:897-901.

Thastrup O, Cullen PJ, Drobak BK, Hanley MR, Dawson AP (1990) Thapsigargin, a tumor promoter, discharges intracellular Ca2+ stores by specific inhibition of the endoplasmic reticulum Ca2(+)-ATPase. Proc Natl Acad Sci U S A 87:2466-2470.

Tomas A, Moss SE (2003) Calcium- and cell cycle-dependent association of annexin 11 with the nuclear envelope. J Biol Chem 278:20210-20216.

Tomsig JL, Creutz CE (2000) Biochemical characterization of copine: a ubiquitous Ca2+-dependent, phospholipid-binding protein. Biochemistry 39:16163-16175.

Tomsig JL, Creutz CE (2002) Copines: a ubiquitous family of Ca(2+)-dependent phospholipid-binding proteins. Cell Mol Life Sci 59:1467-1477.

Tomsig JL, Snyder SL, Creutz CE (2003) Identification of targets for calcium signaling through the copine family of proteins. Characterization of a coiled-coil copine-binding motif. J Biol Chem 278:10048-10054.

Tomsig JL, Sohma H, Creutz CE (2004) Calcium-dependent regulation of tumour necrosis factor-alpha receptor signalling by copine. Biochem J 378:1089-1094.

Treusch S, Knuth S, Slaugenhaupt SA, Goldin E, Grant BD, Fares H (2004) Caenorhabditis elegans functional orthologue of human protein h-mucolipin-1 is required for lysosome biogenesis. Proc Natl Acad Sci U S A 101:4483-4488.

Turnay J, Lecona E, Fernandez-Lizarbe S, Guzman-Aranguez A, Fernandez MP, Olmo N, Lizarbe MA (2005) Structure-function relationship in annexin A13, the founder member of the vertebrate family of annexins. Biochem J 389:899-911.

Twig G, Elorza A, Molina AJ, Mohamed H, Wikstrom JD, Walzer G, Stiles L, Haigh SE, Katz S, Las G, Alroy J, Wu M, Py BF, Yuan J, Deeney JT, Corkey BE, Shirihai OS (2008) Fission and selective fusion govern

mitochondrial segregation and elimination by autophagy. EMBO J 27:433-446.
van Sluijters DA, Dubbelhuis PF, Blommaart EF, Meijer AJ (2000) Amino-acid-dependent signal transduction. Biochem J 351 (Pt 3):545-550.
Venkatachalam K, Hofmann T, Montell C (2006) Lysosomal localization of TRPML3 depends on TRPML2 and the mucolipidosis-associated protein TRPML1. J Biol Chem 281:17517-17527.
Vergarajauregui S, Martina JA, Puertollano R (2009) Identification of the penta-EF-hand protein ALG-2 as a Ca2+-dependent interactor of mucolipin-1. J Biol Chem 284:36357-36366.
Vicencio JM, Ortiz C, Criollo A, Jones AW, Kepp O, Galluzzi L, Joza N, Vitale I, Morselli E, Tailler M, Castedo M, Maiuri MC, Molgo J, Szabadkai G, Lavandero S, Kroemer G (2009) The inositol 1,4,5-trisphosphate receptor regulates autophagy through its interaction with Beclin 1. Cell Death Differ 16:1006-1017.
Vingtdeux V, Giliberto L, Zhao H, Chandakkar P, Wu Q, Simon JE, Janle EM, Lobo J, Ferruzzi MG, Davies P, Marambaud P (2010) AMP-activated protein kinase signaling activation by resveratrol modulates amyloid-beta peptide metabolism. J Biol Chem 285:9100-9113.
Wang L, Dong Z, Huang B, Zhao B, Wang H, Zhao J, Kung H, Zhang S, Miao J (2010) Distinct patterns of autophagy evoked by two benzoxazine derivatives in vascular endothelial cells. Autophagy 6:1115-1124.
Wang RC, Levine B (2010) Autophagy in cellular growth control. FEBS Lett 584:1417-1426.
Wang S, Dibenedetto AJ, Pittman RN (1997) Genes induced in programmed cell death of neuronal PC12 cells and developing sympathetic neurons in vivo. Dev Biol 188:322-336.
Wang SH, Shih YL, Ko WC, Wei YH, Shih CM (2008) Cadmium-induced autophagy and apoptosis are mediated by a calcium signaling pathway. Cell Mol Life Sci 65:3640-3652.
Wauson EM, Zaganjor E, Lee AY, Guerra ML, Ghosh AB, Bookout AL, Chambers CP, Jivan A, McGlynn K, Hutchison MR, Deberardinis RJ, Cobb MH (2012) The G protein-coupled taste receptor T1R1/T1R3 regulates mTORC1 and autophagy. Mol Cell 47:851-862.
Whittaker CA, Hynes RO (2002) Distribution and evolution of von Willebrand/integrin A domains: widely dispersed domains with roles in cell adhesion and elsewhere. Mol Biol Cell 13:3369-3387.
Williams A, Sarkar S, Cuddon P, Ttofi EK, Saiki S, Siddiqi FH, Jahreiss L, Fleming A, Pask D, Goldsmith P, O'Kane CJ, Floto RA, Rubinsztein DC (2008) Novel targets for Huntington's disease in an mTOR-independent autophagy pathway. Nat Chem Biol 4:295-305.
Xia HG, Zhang L, Chen G, Zhang T, Liu J, Jin M, Ma X, Ma D, Yuan J (2010) Control of basal autophagy by calpain1 mediated cleavage of ATG5. Autophagy 6:61-66.

Xu H, Delling M, Li L, Dong X, Clapham DE (2007) Activating mutation in a mucolipin transient receptor potential channel leads to melanocyte loss in varitint-waddler mice. Proc Natl Acad Sci U S A 104:18321-18326.

Yamamoto H, Kakuta S, Watanabe TM, Kitamura A, Sekito T, Kondo-Kakuta C, Ichikawa R, Kinjo M, Ohsumi Y (2012) Atg9 vesicles are an important membrane source during early steps of autophagosome formation. J Cell Biol 198:219-233.

Yan Q, Sun W, McNew JA, Vida TA, Bean AJ (2004) Ca2+ and N-ethylmaleimide-sensitive factor differentially regulate disassembly of SNARE complexes on early endosomes. J Biol Chem 279:18270-18276.

Yanez M, Gil-Longo J, Campos-Toimil M (2012) Calcium binding proteins. Adv Exp Med Biol 740:461-482.

Yitzhaki S, Hochhauser E, Porat E, Shainberg A (2007) Uridine-5'-triphosphate (UTP) maintains cardiac mitochondrial function following chemical and hypoxic stress. J Mol Cell Cardiol 43:653-662.

Yla-Anttila P, Vihinen H, Jokitalo E, Eskelinen EL (2009) 3D tomography reveals connections between the phagophore and endoplasmic reticulum. Autophagy 5:1180-1185.

Yu L, McPhee CK, Zheng L, Mardones GA, Rong Y, Peng J, Mi N, Zhao Y, Liu Z, Wan F, Hailey DW, Oorschot V, Klumperman J, Baehrecke EH, Lenardo MJ (2010) Termination of autophagy and reformation of lysosomes regulated by mTOR. Nature 465:942-946.

Zaks WJ, Creutz CE (1990) Annexin-chromaffin granule membrane interactions: a comparative study of synexin, p32 and p67. Biochim Biophys Acta 1029:149-160.

Zalckvar E, Berissi H, Eisenstein M, Kimchi A (2009a) Phosphorylation of Beclin 1 by DAP-kinase promotes autophagy by weakening its interactions with Bcl-2 and Bcl-XL. Autophagy 5:720-722.

Zalckvar E, Berissi H, Mizrachy L, Idelchuk Y, Koren I, Eisenstein M, Sabanay H, Pinkas-Kramarski R, Kimchi A (2009b) DAP-kinase-mediated phosphorylation on the BH3 domain of beclin 1 promotes dissociation of beclin 1 from Bcl-XL and induction of autophagy. EMBO Rep 10:285-292.

Zeevi DA, Lev S, Frumkin A, Minke B, Bach G (2010) Heteromultimeric TRPML channel assemblies play a crucial role in the regulation of cell viability models and starvation-induced autophagy. J Cell Sci 123:3112-3124.

Zhang J, Ney PA (2009) Role of BNIP3 and NIX in cell death, autophagy, and mitophagy. Cell Death Differ 16:939-946.

Zoncu R, Bar-Peled L, Efeyan A, Wang S, Sancak Y, Sabatini DM (2011) mTORC1 senses lysosomal amino acids through an inside-out mechanism that requires the vacuolar H(+)-ATPase. Science 334:678-683.

Zong X, Schieder M, Cuny H, Fenske S, Gruner C, Rotzer K, Griesbeck O, Harz H, Biel M, Wahl-Schott C (2009) The two-pore channel TPCN2 mediates NAADP-dependent Ca(2+)-release from lysosomal stores. Pflugers Arch 458:891-899.

11. APPENDIX 1

New Ca(2+)-dependent regulators of autophagosome maturation

Ghislat G, Knecht E (2012) Commun Integr Biol 5:308-11.

Ghita Ghislat[a], Erwin Knecht[a*]

[a]*Laboratorio de Biología Celular, Centro de Investigación Príncipe Felipe, Avda. Autopista del Saler 16, 46012-Valencia, Spain and CIBERER, Valencia, Spain*

**Corresponding author*. Centro de Investigación Príncipe Felipe, Avda. Autopista del Saler 16, 46012-Valencia, Spain, Tel.: +34-96-3289680; fax: +34-96-3289701
E-mail: knecht@cipf.es

Addedum to: Ghislat G, Aguado C, Knecht E. Annexin A5 stimulates autophagy and inhibits endocytosis. J Cell Sci. 2012 Jan 1;125(Pt 1):92-107.

Key words: *Annexin A1, annexin A5, copine 1, Ca^{++}, autophagosomal maturation, endosomes, lysosomes*

Abstract

Autophagy is a membrane trafficking pathway responsible for the breakdown of unwanted intracellular materials in order to assure cell healthiness and survival. In the autophagic flux, various dynamic membrane rearrangements occur from autophagosome formation and closure till its fusion with late endosomes and with lysosomes. Although Ca^{++} is a well established regulator of membrane fusions, little is known about this role with autophagosomes. Recent studies based on proteomic analyses have provided data for new directions in this field. Three proteins that bind to phospholipid membranes in a Ca^{++}-dependent manner, annexin A1, annexin A5 and copine 1, increased their levels on lysosomal membranes when nutrients are scarce, a condition that promotes autophagic degradation. Annexin A5 and annexin A1, have been already related to autophagosome maturation in two different studies. Here, we discuss the possible molecular mechanisms by which these three proteins and Ca^{++} could regulate autophagosome delivery to endosomes and lysosomes.

Background

The clearance of cell components is essential for cell welfare and survival and is mainly carried out by two different degradation pathways that direct them either to proteasomes or to the acidic milieu of lysosomes[1]. The most important way to deliver cell material to lysosomes for its breakdown is mediated by double membrane vesicles, called autophagosomes. The origin and mechanisms of autophagosome formation have been extensively analyzed and discussed in the last years. However, comparatively much less attention has been paid to later steps, when autophagosomes deliver their content to acidic compartments for degradation, which is nonetheless the final destiny of autophagy. At this stage, autophagosomes mature by fusing with different endocytic and lysosomal vesicles, hence the complexity of these fusion events.

Autophagosomal fusion machinery

Although the available information on this machinery is still fragmentary, several components have been described to be involved in the fusion of autophagosomes with endo-lysosomal compartments. For example, microtubules are thought to conduct the traffic of autophagosomes towards lysosomes and endosomes[2, 3]. Also SNAREs (Soluble N-ethylmaleimide-sensitive factor attachment protein receptors), with a well known role in tethering/docking of vesicles in the presence of Ca^{++}[4-6], induce the fusion of autophagosomes with lysosomes in association with Rab7 GTPase and the HOPS (Homotypic fusion and protein sorting) complex[7-10]. In addition, the three ESCRT (Endosomal sorting complex required for transport) complexes, I–III, originally associated with the sorting of ubiquitinated membrane proteins into multivesicular bodies[11-13], have been reported to participate in the fusion of autophagosomes with lysosomes by still unknown mechanisms[14].

Involvement of annexins in autophagy

Annexins are a family of ubiquitous Ca^{++}-dependent membrane-binding proteins whose intracellular functions are associated with their ability to attach to specific lipid microdomains. Using a proteomic approach, we recently identified annexin A5 as a regulator of autophagosome maturation, especially in the starvation response where it localizes to lysosomal membranes in a Ca^{++}-dependent way[15]. Under starvation annexin A5 translocates from the Golgi complex to lysosomes and, to a lesser extent, to late endosomes. Interestingly, this protein was found to promote autophagosome fusion with lysosomes, but to inhibit fluid phase and cholera toxin endocytosis. The localization of annexin A5 in late endosomes in considerably higher amounts than in early endosomes suggests that the inhibition of endocytosis probably occurs at late steps of this process. Moreover, whereas annexin A5 induces autophagosome fusion with lysosomes, it inhibits the formation of amphisomes, hybrid organelles produced by autophagosome fusion with late endosomes. Although it remains to be elucidated the molecular basis of these two opposite roles of annexin A5, it is possible that lysosomal and late endosomal membranes possess different properties in terms of their abilities to fuse with autophagosomes. In accordance with this concept, at least one protein, Rab7, is reported to be required for autophagosome-lysosome fusions[16] but is dispensable for fusions of autophagosomes with late endosomes[17].

Experimental findings also support the possible involvement of another protein of the same family, annexin A1, in autophagy. In fact, in the same proteomic analysis, we found that, like annexin A5, its levels on lysosomal membranes increased upon starvation[15]. Also, a different group showed that annexin A1 promotes autophagic degradation and suggested a role of annexin A1 in increasing the formation of amphisomes[18]. Somewhat complementary to these results, S100A11, a small dimeric Ca^{++}-binding protein that can form a complex with annexin A1, was identified as another component of the lysosomal membrane[19].

Mounting evidences support that annexin family members, in spite of their lack of transmembrane domains, are able to induce membrane fusions [20-22]. Thus, several studies associated various members of the annexin family to the formation and traffic of specific endo-lysosomal compartments in a Ca^{++}-dependent way[23], among them annexin A1 (early endosomes, multivesicular bodies and lysosomes), and annexin A5 (late endosomes and lysosomes). Since Ca^{++} promotes fusions between autophagosomes/lysosomes *in vitro*[24], it is reasonable to propose that the participation of these two annexins in autophagosome delivery to lysosomes mentioned above, occurs through their involvement in membrane interactions regulated by Ca^{++}.

Another interesting association of annexin A1 with autophagy was described in preliminary maps of interaction networks in autophagy based on a shotgun proteomic analysis[25]. In this study, annexin A1 emerged as a putative interactor of Atg4B. This is a crucial protease for conjugation/deconjugation of phosphoethanolamine to LC3, a mammalian orthologue of yeast Atg8 that, when lipidated, participates in the formation and maturation of autophagosomes[26, 27]. Given that the activity of Atg4B on the balance between lipidation and delipidation of LC3 controls the tethering and hemifusion during autophagic membranes closure[28], an important condition for its fusion with lysosomes[29], it is tempting to speculate that at least annexin A1 mediates the fusogenic potential of autophagosomes by regulating Atg4B activity.

Possible involvement of copine 1 in autophagy in relationship with annexins

Copine 1, another protein whose levels also increased on lysosomal membranes under high proteolysis conditions[15], shares with the annexin family of proteins the property of binding to phospholipid membranes in a Ca^{++}-dependent manner[30]. In addition, its presence in autophagosomal, phagosomal and lysosomal delimiting membranes has been previously reported[31, 32]. Interestingly, an *in vitro* study showed that annexin A1 creates membrane domains enriched in phosphatidyl serine (PS) that assemble copine 1 aggregates, thus providing a possible scaffold to cluster signalling proteins in the presence of Ca^{++}[33]. Also, annexin A5 is known to bind to PS with high specificity using Ca^{++} as a bridge between the negatively charged convex side of its C-terminal domain and this anionic phospholipid[34]. PS is known to be distributed in all cellular membranes, but it only confers a negative charge (ideal for Ca^{++} binding) at the cytosolic face of endosomes and lysosomes, probably because it is localized in the luminal leaflets of the membranes from other organelles such as mitochondria, Golgi and endoplasmic reticulum [35]. Although annexin A1 and A5 lack a coiled-coil domain, which allows copine 1 binding according to a yeast two-hybrid screening study[36], it is possible that, like annexin A1, cytosolic annexin A5 translocates to lysosomal membranes in order to form domains suitable for copine 1 recruitment.

Conclusions and future work

Annexin A1, annexin A5 and probably also copine 1 emerge as possible regulators of autophagosomes maturation by mechanisms that require Ca^{++}. The two annexins could be subjected on the lysosomal surface to interactions, regulated by phospholipid rearrangements and Ca^{++}, with copine 1 to promote autophagosome fusion with lysosomes (see Fig. 1).

To determine which of the proposed molecular mechanism are involved in this process, it will be necessary to investigate the proteins and specially the lipids interacting with annexins A1 and A5 and also with copine 1 at the cytosolic surface of the endolysosomal membranes, and to verify whether these bindings produce phospholipid rearrangements in specific lipid domains.

Acknowledgements

Work in the author´s labs was supported by the Spanish Ministry of Science and Innovation (BFU2008-00186), the
Fundación Marato TV3 (Ref. 100130) and the Centro de Investigación Biomédica en Red de Enfermedades Raras
(CIBERER).

REFERENCES

1. Knecht E, Aguado C, Carcel J, Esteban I, Esteve JM, Ghislat G, et al. Intracellular protein degradation in mammalian cells: recent developments. Cell Mol Life Sci 2009; 66:2427-43.
2. Ravikumar B, Acevedo-Arozena A, Imarisio S, Berger Z, Vacher C, O'Kane CJ, et al. Dynein mutations impair autophagic clearance of aggregate-prone proteins. Nat Genet 2005; 37:771-6.
3. Fass E, Shvets E, Degani I, Hirschberg K, Elazar Z. Microtubules support production of starvation-induced autophagosomes but not their targeting and fusion with lysosomes. J Biol Chem 2006; 281:36303-16.
4. Parlati F, McNew JA, Fukuda R, Miller R, Sollner TH, Rothman JE. Topological restriction of SNARE-dependent membrane fusion. Nature 2000; 407:194-8.
5. Atlashkin V, Kreykenbohm V, Eskelinen EL, Wenzel D, Fayyazi A, Fischer von Mollard G. Deletion of the SNARE vti1b in mice results in the loss of a single SNARE partner, syntaxin 8. Mol Cell Biol 2003; 23:5198-207.
6. Jena BP. Role of SNAREs in membrane fusion. Adv Exp Med Biol 2011; 713:13-32.
7. Zerial M, McBride H. Rab proteins as membrane organizers. Nat Rev Mol Cell Biol 2001; 2:107-17.
8. Sun Q, Westphal W, Wong KN, Tan I, Zhong Q. Rubicon controls endosome maturation as a Rab7 effector. Proc Natl Acad Sci U S A 2010; 107:19338-43.
9. Sato TK, Rehling P, Peterson MR, Emr SD. Class C Vps protein complex regulates vacuolar SNARE pairing and is required for vesicle docking/fusion. Mol Cell 2000; 6:661-71.
10. Seals DF, Eitzen G, Margolis N, Wickner WT, Price A. A Ypt/Rab effector complex containing the Sec1 homolog Vps33p is required for homotypic vacuole fusion. Proc Natl Acad Sci U S A 2000; 97:9402-7.
11. Katzmann DJ, Babst M, Emr SD. Ubiquitin-dependent sorting into the multivesicular body pathway requires the function of a conserved endosomal protein sorting complex, ESCRT-I. Cell 2001; 106:145-55.
12. Babst M, Katzmann DJ, Snyder WB, Wendland B, Emr SD. Endosome-associated complex, ESCRT-II, recruits transport machinery for protein sorting at the multivesicular body. Dev Cell 2002; 3:283-9.
13. Babst M, Katzmann DJ, Estepa-Sabal EJ, Meerloo T, Emr SD. Escrt-III: an endosome-associated heterooligomeric protein complex required for mvb sorting. Dev Cell 2002; 3:271-82.
14. Rusten TE, Stenmark H. How do ESCRT proteins control autophagy? J Cell Sci 2009; 122:2179-83.
15. Ghislat G, Aguado C, Knecht E. Annexin A5 stimulates autophagy and inhibits endocytosis. J Cell Sci 2012.
16. Ganley IG, Wong PM, Gammoh N, Jiang X. Distinct autophagosomal-lysosomal fusion mechanism revealed by thapsigargin-induced autophagy arrest. Mol Cell 2011; 42:731-43.
17. Fader CM, Sanchez D, Furlan M, Colombo MI. Induction of autophagy promotes fusion of multivesicular bodies with autophagic vacuoles in k562 cells. Traffic 2008; 9:230-50.
18. Eden ER, White IJ, Futter CE. Down-regulation of epidermal growth factor receptor signalling within multivesicular bodies. Biochem Soc Trans 2009; 37:173-7.
19. Nylandsted J, Becker AC, Bunkenborg J, Andersen JS, Dengjel J, Jaattela M. ErbB2-associated changes in the lysosomal proteome. Proteomics 2011; 11:2830-8.
20. McNeil AK, Rescher U, Gerke V, McNeil PL. Requirement for annexin A1 in plasma membrane repair. J Biol Chem 2006; 281:35202-7.
21. Rafikova ER, Melikov K, Ramos C, Dye L, Chernomordik LV. Transmembrane protein-free membranes fuse into Xenopus nuclear envelope and promote assembly of functional pores. J Biol Chem 2009; 284:29847-59.
22. Shen S, Tobery CE, Rose MD. Prm3p is a pheromone-induced peripheral nuclear envelope protein required for yeast nuclear fusion. Mol Biol Cell 2009; 20:2438-50.
23. Monastyrskaya K, Babiychuk EB, Draeger A. The annexins: spatial and temporal coordination of signaling events during cellular stress. Cell Mol Life Sci 2009; 66:2623-42.
24. Koga H, Kaushik S, Cuervo AM. Altered lipid content inhibits autophagic vesicular fusion. Faseb J 2010; 24:3052-65.

25. Behrends C, Sowa ME, Gygi SP, Harper JW. Network organization of the human autophagy system. Nature 2011; 466:68-76.
26. Satoo K, Noda NN, Kumeta H, Fujioka Y, Mizushima N, Ohsumi Y, et al. The structure of Atg4B-LC3 complex reveals the mechanism of LC3 processing and delipidation during autophagy. Embo J 2009; 28:1341-50.
27. Weidberg H, Shvets E, Shpilka T, Shimron F, Shinder V, Elazar Z. LC3 and GATE-16/GABARAP subfamilies are both essential yet act differently in autophagosome biogenesis. Embo J 2011; 29:1792-802.
28. Nakatogawa H, Ichimura Y, Ohsumi Y. Atg8, a ubiquitin-like protein required for autophagosome formation, mediates membrane tethering and hemifusion. Cell 2007; 130:165-78.
29. Rusten TE, Vaccari T, Lindmo K, Rodahl LM, Nezis IP, Sem-Jacobsen C, et al. ESCRTs and Fab1 regulate distinct steps of autophagy. Curr Biol 2007; 17:1817-25.
30. Creutz CE, Tomsig JL, Snyder SL, Gautier MC, Skouri F, Beisson J, et al. The copines, a novel class of C2 domain-containing, calcium-dependent, phospholipid-binding proteins conserved from Paramecium to humans. J Biol Chem 1998; 273:1393-402.
31. Overbye A, Fengsrud M, Seglen PO. Proteomic analysis of membrane-associated proteins from rat liver autophagosomes. Autophagy 2007; 3:300-22.
32. Damer CK, Bayeva M, Hahn ES, Rivera J, Socec CI. Copine A, a calcium-dependent membrane-binding protein, transiently localizes to the plasma membrane and intracellular vacuoles in Dictyostelium. BMC Cell Biol 2005; 6:46.
33. Creutz CE, Edwardson JM. Organization and synergistic binding of copine I and annexin A1 on supported lipid bilayers observed by atomic force microscopy. Biochim Biophys Acta 2009; 1788:1950-61.
34. Gerke V, Moss SE. Annexins: from structure to function. Physiol Rev 2002; 82:331-71.
35. Yeung T, Gilbert GE, Shi J, Silvius J, Kapus A, Grinstein S. Membrane phosphatidylserine regulates surface charge and protein localization. Science 2008; 319:210-3.
36. Tomsig JL, Creutz CE. Copines: a ubiquitous family of Ca(2+)-dependent phospholipid-binding proteins. Cell Mol Life Sci 2002; 59:1467-77.

FIGURE

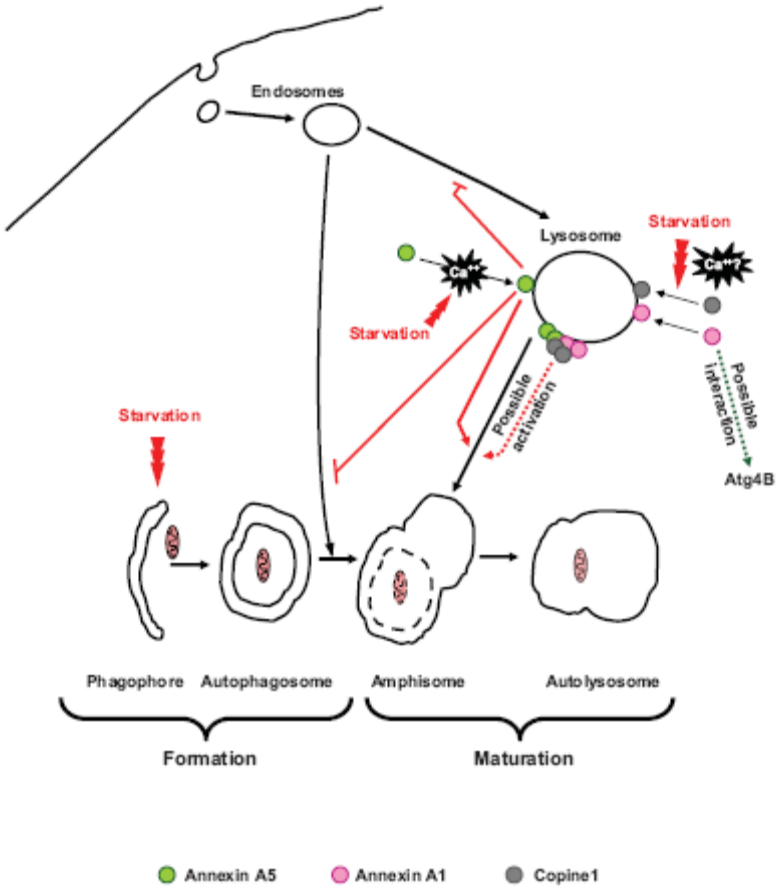

Figure 1. Possible mechanisms of the involvement of Ca^{++}-dependent phospholipid binding proteins in autophagosome maturation: Starvation induces annexin A5 translocation to lysosomal membranes in a Ca^{++} dependent way. This protein inhibits endocytic uptake and induces autophagosome fusion with lysosomes. Likewise, annexin A1 and copine 1 are localized on lysosomal membranes under starvation. It is likely that annexin A5 and annexin A1 aggregate in a Ca^{++}-dependent way on lysosomal membranes in order to form domains for the subsequent binding of copine 1, and that interaction between these and perhaps other proteins promotes the fusion of autophagosomes with lysosomes. Another possibility, at least for annexin A1, is that its interaction with Atg4B regulates somehow the activity of this protease promoting LC3 lipidation/delipidation and, thus, the eventual ability of autophagosomal membrane to fuse with lysosomes.